



저작자표시-비영리-변경금지 2.0 대한민국

이용자는 아래의 조건을 따르는 경우에 한하여 자유롭게

- 이 저작물을 복제, 배포, 전송, 전시, 공연 및 방송할 수 있습니다.

다음과 같은 조건을 따라야 합니다:



저작자표시. 귀하는 원저작자를 표시하여야 합니다.



비영리. 귀하는 이 저작물을 영리 목적으로 이용할 수 없습니다.



변경금지. 귀하는 이 저작물을 개작, 변형 또는 가공할 수 없습니다.

- 귀하는, 이 저작물의 재이용이나 배포의 경우, 이 저작물에 적용된 이용허락조건을 명확하게 나타내어야 합니다.
- 저작권자로부터 별도의 허가를 받으면 이러한 조건들은 적용되지 않습니다.

저작권법에 따른 이용자의 권리는 위의 내용에 의하여 영향을 받지 않습니다.

이것은 [이용허락규약\(Legal Code\)](#)을 이해하기 쉽게 요약한 것입니다.

[Disclaimer](#)

이학박사 학위논문

**Coastal food web structure and its function
along climatic zones: Case studies in Ganghwa salt
marsh, Saemangeum tidal flat, the mangrove forest
in Pear River Estuary, and Marian Cove
in Antarctica**

기후대에 따른 연안 먹이망 구조 및 기능:
강화 염습지, 새만금 갯벌, 주장하구 맹그로브 숲,
남극 마리안소만 사례 연구

2023년 8월

서울대학교 대학원
지구환경과학부

이 인 옥

**Coastal food web structure and its function
along climatic zones: Case studies in Ganghwa salt
marsh, Saemangeum tidal flat, the mangrove forest
in Pear River Estuary, and Marian Cove
in Antarctica**

지도 교수 김 종 성

이 논문을 이학박사 학위논문으로 제출함

2023년 5월

서울대학교 대학원

지구환경과학부

이 인 옥

이인옥의 이학박사 학위논문을 인준함

2023년 7월

위 원 장 _____(인)

부위원장 _____(인)

위 원 _____(인)

위 원 _____(인)

위 원 _____(인)

ABSTRACT

Ecologically important coastal habitats have been severely degraded and destroyed by the cumulative pressures of anthropogenic activities combined with the effects of climate change. The effects of habitat degradation can be assessed through the ecological responses of organisms in the coastal food web. Food web studies can therefore be used for the conservation and management of coastal habitats. The present study used stable isotope analysis to investigate the food web responses to natural, anthropogenic, and climate change-driven environmental changes in four coastal habitats (salt marsh; tidal flat; mangrove forest; Antarctic coast) along the three climate zones. The objectives of the present study were 1) to reveal the overall structure of the food web, 2) to determine the spatiotemporal ecological responses of coastal organisms to environmental changes, and finally, 3) to characterise the coastal food web in terms of food diversity and anthropogenic impacts by comparing the stable isotope distributions along the climate zones.

Salt marshes, tidal flats and mangrove forests have been severely degraded by reclamation projects in Korea and China over the past century. In order to better understand the food web structures and functions of such habitats, seasonal sampling was first conducted in Korean Ganghwa tidal flats with different habitat conditions (sediment bottom types and vegetation). Stable isotope analysis revealed that deposit feeders consumed more microphytobenthos (MPB) on bare sites, whereas they actively utilised ^{13}C -depleted organic matter on vegetated sites. Altogether, the results suggest that the distribution of organic matter through habitat diversity can alter the trophic function of the tidal flat at mesoscale spatial scales. Second, the food web dynamics under eutrophic water discharge from a dike were elucidated in the Korean Saemangeum tidal flat. High total nitrogen concentrations near the water gates increased the biomass and production of MPB and its subsequent utilisation by benthos, revealing the indirect effect of water discharge on the food web function. The results showed that environmental changes caused by human activities have altered the structure and function of the food web in the Saemangeum tidal flat. In the torrid zone, the seasonal food web dynamics in the Pearl River Estuary (PRE) were elucidated by analysing the stable isotope signatures of diet and consumers.

Fish had a large niche space during the monsoon summer, reflecting their increased trophic role. In contrast, benthos had consistent trophic positions across seasons. They used mainly plant organic matter in the dry season and particulate organic matter in the wet season. Literature reviews characterised the food web with a high contribution of mangrove-derived organic carbon and sewage input in the PRE.

Compared to other coastal habitats, the Antarctic coast is experiencing intense impacts of climate change. However, the long-term responses of the food web to the ice dynamics remain unresolved. Stable isotope signatures of diet and organisms in the Antarctic coast revealed the influence of glacier and sea ice dynamics on the coastal food web. The $\delta^{13}\text{C}$ enrichment near the glacier revealed environmental heterogeneity along the Marian Cove (MC) with meltwater intrusion. The primary diet of limpets shifted from microalgae to macroalgae with a decadal increase in macroalgal production due to increased light penetration and glacial nutrient input. Literature reviews revealed contrasting functional changes between the western and eastern Antarctic coasts with sea ice polarisation over a decade. These results warn of a future climate crisis in the simplified Antarctic coastal ecosystem.

Overall, this series of studies has provided the first evidence of the ecological responses of organisms to environmental change in coastal habitats along the climate zones. The large $\delta^{13}\text{C}$ distributions in the coastal food web in the torrid and frigid zones revealed the diverse origin of organic matter inputs in contrast to the temperate zone. Comparisons of the coastal food webs along the climate zones showed that spatial differences in primary production influenced the dietary priorities of consumers. In contrast, within coastal habitats, seasonal flooding strongly influenced the distribution of organic matter compared to other factors (i.e., sediment type and vegetation). Furthermore, the $\delta^{15}\text{N}$ distribution in the food webs revealed the strong influence of anthropogenic discharges in the temperate and torrid habitats, but the influence was minor on the Antarctic coast. The present study provides comprehensive insights for predicting food web dynamics under increasing human impact and climate change, which can be used for future management and conservation of coastal habitats.

Keywords: Coastal food web structure, Stable isotopes, Korea, China, Antarctica

Student Number: 2018–30803

TABLE OF CONTENTS

ABSTRACT	I–II
TABLE OF CONTENTS	III–V
LIST OF ABBREVIATIONS	VI–VII
LIST OF TABLES	VIII–XI
LIST OF FIGURES	XII– XIX

CHAPTER 1. Introduction 1–9

1.1. Backgrounds	2
1.2. Objectives	8

CHAPTER 2. Food web structure of Ganghwa salt marsh in Korea with sediment and halophyte distribution 10–40

2.1. Introduction	11
2.2. Materials and methods	13
2.2.1. Study area and data collection	13
2.2.2. Sample collection and preparation	16
2.2.3. Stable isotope analysis	19
2.2.4. Trophic level	20
2.2.5. Statistical analysis	21
2.3. Results and discussion	22
2.3.1. Spatial distribution of sedimentary organic matter	22
2.3.2. Benthic food web structure	28
2.3.3. Spatial variation in the stable isotopes of deposit feeders	35

CHAPTER 3. Food web structure of Saemangeum tidal flat in Korea with water discharge from a dike 41–97

3.1. Introduction	42
3.2. Materials and methods	45
3.2.1. Sample collection and preparation	45
3.2.2. Stable isotope analysis	48

3.2.3. Trophic level	49
3.2.4. Statistical analysis	50
3.3. Results and discussion	67
3.3.1. Water environmental conditions	67
3.3.2. Sediment environmental conditions	74
3.3.3. Food web structure	81
3.3.4. Spatiotemporal stable isotopic dynamics	87
3.3.5. Comparison of trophic characteristics to other Korean tidal flat	95
 CHAPTER 4. Food web structure of mangrove forest in Pearl River Estuary in China with seasonal flood dynamics	98–142
4.1. Introduction	99
4.2. Materials and methods	101
4.2.1. Study area	101
4.2.2. Sample collection and preparation	103
4.2.3. Stable isotope analysis	118
4.2.4. Trophic level	119
4.2.5. Statistical analysis	120
4.3. Results and discussion	121
4.3.1. Environmental conditions	121
4.3.2. Food web structure	123
4.3.3. Seasonal stable isotopic dynamics	129
4.3.4. Comparison of trophic characteristics to other Chinese coastal ecosystem.	139
 CHAPTER 5. Food web structure of Marian Cove in Antarctic peninsula with glacier retreat	143–181
5.1. Introduction	144
5.2. Materials and methods	146
5.2.1. Sample and data collection	146
5.2.2. Stable isotope analysis	159
5.2.3. Trophic level	160
5.2.4. Statistical analysis	161
5.3. Results and discussion	162
5.3.1. Environment in Marian Cove (MC), King George Island	162

5.3.2. Food web structure in MC	163
5.3.3. Spatial stable isotopic distribution of producers and consumers in MC	167
5.3.4. Decadal changes in the structure and function of Antarctic limpet in MC ..	170
5.3.5. Influence of multi-decadal changes to sea ice extent on the spatial variation of stable isotopes for producers and consumers in Antarctica	174
CHAPTER 6. Conclusions	182–192
6.1. Summary	183
6.2. Ecological implications	187
6.3. Limitations and future research directions	191
BIBLIOGRAPHY	193–217
ABSTRACT (IN KOREAN)	218–220

LIST OF ABBREVIATIONS

AN	Annelida
ANOVA	One-way analysis of variance
AR	Arthropoda
AS	Anseong
B	Barton
BR	Brachiopoda
C/N	Carbon to nitrogen ratio
CA	Carnivore
Chl- <i>a</i>	Chlorophyll- <i>a</i>
CI	Credible interval
DF	Deposit feeder
DG	Donggeom
DM	Dongmak
DO	Dissolved oxygen
Dry I	1 st dry season
Dry II	2 nd dry season
E	Echinodermata
EA-IRMS	Isotope ratio mass spectrometer connected to an elemental analyzer
ETR	Photosystem II electron transport rate
FF	Filter feeder
FPOM	Particulate organic matter in the freshwater
GR	Garyuk
HB	Herbivore
HCL	Hydrochloric acid
LOI	Loss on ignition
M	Mollusca
MC	Mud content in chapter 2–4; Marian Cove in chapter 5
MAX	Maximum
MIN	Minimum
MPB	Microphytobenthos
OC	Organic content
OM	Omnivore
P/B	Primary production/biomass

PI	Period I
PII	Period II
PK	Planktivore
POM	Particulate organic matter
PP	Primary production
PRE	Pearl River Estuary
SCF	Sea point Chlorophyll Fluorometer
SEA _b	Bayesian standard ellipse area
SEA _c	The small sample size corrected standard ellipse area
SIBER	Stable isotope bayesian ellipses in R
SIMMR	Bayesian stable isotope mixing model in R
SiO ₂	Silicon dioxide
SOM	Sediment organic matter
SPOM	particulate organic matter in the seawater
SS	Sinsi
Stdev.	Standard deviation
TEF	Trophic enrichment factor
TL	Trophic level
TN	Total nitrogen
TOC	Total organic carbon
TP	Total phosphorus
VPDB	Vienna Peedee Belemnite
W	Weaver
WC	Water content
WY	Woryeon
YC	Yeocho
YM	Yami
$\delta^{13}\text{C}$	Carbon stable isotope ratio
$\delta^{15}\text{N}$	Nitrogen stable isotope ratio

LIST OF TABLES

Table 2.1. Seasonal environmental parameters of seawater obtained from the national monitoring station near to Ganghwa Island	15
Table 2.2. The list of macrobenthos with corresponding feeding types found on Ganghwa Island, Korea	18
Table 2.3. Physicochemical parameters of sediments collected from Yeocha (YC), Dongmak (DM), and Donggeom (DG) on Ganghwa Island. All parameters are expressed as means values with standard deviations (mean±s.d.)	24
Table 2.4. Result of one-way analysis of variance (ANOVA) with Tukey post-hoc honest significant difference (HSD) test on the sediment characteristics and microalgal biomass measured at three sites (Yeocha, YC; Dongmak, DM; Donggeom, DG) on Ganghwa Island. Bold values indicate the significance at $p<0.05$	25
Table 2.5. Data on the seasonal sediment properties measured at three sites (Yeocha, YC; Dongmak, DM; Donggeom, DG) on Ganghwa Island from March 2018 to February 2019. All parameters are reported as mean with range (min.–max.)	26
Table 2.6. Stable carbon and nitrogen isotope values ($\delta^{13}\text{C}$ and $\delta^{15}\text{N}$) of food sources (sediment organic matter, SOM; particulate organic matter, POM; microphytobenthos, MPB; halophytes; meiofauna) and macrofauna collected from Yeocha (YC), Dongmak (DM), and Donggeom (DG) on Ganghwa Island from March 2018 to February 2019, with corresponding trophic level (TL). The feeding types of macrofauna are indicated (deposit feeders, Df; filter feeders, Ff; omnivores, Om; carnivores, Ca). Isotopic values are given as means with range (min.–max.)	30
Table 2.7. Seasonal stable carbon and nitrogen isotopic values ($\delta^{13}\text{C}$ and $\delta^{15}\text{N}$) of potential food sources (particulate organic matter, POM; sediment organic matter, SOM; microphytobenthos, MPB). Isotopic values are reported as mean with range (min.–max.)	31
Table 3.1. Previous studies which conducted in the Saemangeum tidal flat, Korea. The black box indicates the previous study of food web structure in the Saemangeum tidal flat	44
Table 3.2. List of benthic consumers with corresponding five functional groups (grazers; filter feeders; deposit feeders; omnivores; carnivores) collected in the Saemangeum tidal flat, Korea from 2019 to 2022	51
Table 3.3. Review of carbon and nitrogen stable isotope values ($\delta^{13}\text{C}$ and $\delta^{15}\text{N}$) of potential food sources (MPB, microphytobenthos; POM, particulate organic matter; SOM, sediment organic matter) in previous food web studies, western and southern tidal flats, Korea ...	53

Table 3.4. Review of stable carbon and nitrogen isotope values ($\delta^{13}\text{C}$ and $\delta^{15}\text{N}$) of potential diets in previous food web studies, western and southern tidal flats, Korea. Five functional groups of consumers are described by abbreviations (grazers, Gr; deposit feeders, Df; filter feeders, Ff; omnivores, Om; carnivores, Ca)	56
Table 3.5. Water environmental parameters (temperature; salinity; dissolved oxygen, DO; pH) collected in the Saemangeum tidal flat (Yami, YM; Sinsi, SS; Garyuk1, GR1) and two sites located in the tributaries (Woryeon, WY; Anseong, AS) of the Mangyeong and Dongjin Rivers. Values are expressed as annual mean with standard deviation (mean \pm s.d.). PI and PII indicate period I (2019–2020) and period II (2021–2022), respectively	71
Table 3.6. Carbon and nitrogen stable isotope values ($\delta^{13}\text{C}$ and $\delta^{15}\text{N}$) of particulate organic matter (FPOM and SPOM) collected from the Saemangeum tidal flat (Yami, YM; Sinsi, SS; Garyuk, GR1), and the two lower reaches of the Mangyeong and Dongjin Rivers (Woryeon, WY; Anseong, AS) from 2019 to 2022. Values are expressed as means with standard deviations (stdev.). PI and PII indicate period I (2019–2020) and period II (2021–2022), respectively	73
Table 3.7. Sediment physicochemical parameters (water content, WC; mud content, MC; total organic carbon, TOC; total nitrogen, TN; carbon to nitrogen ratio, C/N; carbon and nitrogen stable isotope ratios, $\delta^{13}\text{C}$ and $\delta^{15}\text{N}$) collected seasonally at three sites (Yami, YM; Sinsi, SS; Garyuk, GR1) in the Saemangeum tidal flat, Korea from 2019 to 2022. Values are expressed as annual means with standard deviations (mean \pm s.d.). PI and PII indicate period I (2019–2020) and period II (2021–2022), respectively	76
Table 3.8. Seasonally collected nutrient concentrations (total nitrogen, TN; total phosphorus, TP; silicon dioxide, SiO_2) in the sediment porewater at three sites (Yami, YM; Sinsi, SS; Garyuk1, GR1) in the Saemangeum tidal flat, Korea from 2019 to 2022. Values are expressed as annual means with standard deviations (mean \pm s.d.). PI and PII indicate period I (2019 – 2020) and period II (2021–2022), respectively	78
Table 3.9. Biomass (Chl- <i>a</i> , mg m^{-2}), primary production (PP, $\text{mg C m}^{-2}\text{h}^{-1}$), and primary productivity (P/B, $\text{mg C (mg Chl-}a)^{-1} \text{h}^{-1}$) of microphytobenthos collected at three sites (Yami, YM; Sinsi, SS; Garyuk, GR1) in the Saemangeum tidal flat, Korea from 2019 to 2022. Values are expressed as annual means with standard deviations (mean \pm s.d.). PI and PII indicate period I (2019–2020) and period II (2021–2022), respectively	80
Table 3.10. Carbon and nitrogen stable isotope values of 54 consumers with six feeding types (grazers, Gr; filter feeders, Ff; deposit feeders, Df; omnivores, Om; carnivores, Ca) and their potential diets [freshwater and seawater particulate organic matter, FPOM and SPOM; sediment organic matter, SOM; microphytobenthos, MPB] collected in the Saemangem tidal flat, Korea from 2019 to 2022. Species are listed with corresponding trophic level (TL) in descending order for each taxon (Annelida; Brachiopoda; Mollusca; Arthropoda; Chordata). Values are expressed as mean with standard deviation (stdev.). The superscript number indicates the identification of each species described in Fig. 3.8	85

Table 3.11. Seasonal niche metrics (Bayesian standard ellipse area, SEA _b ; sample size corrected ellipse area, SEA _c) of deposit- and filter-feeding consumers collected at three sites (Yami, YM; Sinsi, SS; Garyuk1, GR1) in the Saemangeum tidal flat, Korea from 2019 to 2022. PI and PII indicate period I (2019–2020) and period II (2021–2022), respectively	92
Table 4.1. Previous studies which conducted in the Pearl River Estuary, China. The black box indicates the previous study of food web structure in the Pearl River Estuary	106
Table 4.2. List of benthic and pelagic consumers with corresponding functional groups (herbivores, Hb; deposit feeders, Df; filter feeders, Ff; planktivores, Pk; omnivores, Om; carnivores, Ca) collected in the Pearl River Estuary, China	107
Table 4.3. Results of the Chi-square test performed to investigate the difference in occurrence among feeding guilds in each consumer group [benthos (herbivores; filter feeders; deposit feeders; omnivores; carnivores); fish (planktivores; carnivores)] in three seasons	108
Table 4.4. Review of the stable isotope values for carbon and nitrogen ($\delta^{13}\text{C}$ and $\delta^{15}\text{N}$) of potential diets in previous studies ($n=18$) for six provinces (Fujian, Guangdong, Guangxi, Hong Kong, Shanghai, and Zhejiang) in China. Values are expressed as mean with range (min.–max.)	109
Table 4.5. Review of the stable isotope values for carbon and nitrogen ($\delta^{13}\text{C}$ and $\delta^{15}\text{N}$) of consumers in previous studies ($n=18$) in six provinces of China (Fujian, Guangdong, Guangxi, Hong Kong, Shanghai, and Zhejiang). Six functional groups of consumers are shown with abbreviations (herbivore, Hb; deposit feeder, Df; filter feeder, Ff; planktivore, Pk; omnivore, Om; carnivore, Ca). Values are expressed as mean with range (min.–max.)	112
Table 4.6. Environmental physicochemical parameters (temperature; salinity; dissolved oxygen, DO; pH; mud content, MC; loss on ignition, LOI; total organic carbon, TOC; total nitrogen, TN; carbon to nitrogen ratio, C/N; carbon and nitrogen stable isotope ratio, $\delta^{13}\text{C}$ and $\delta^{15}\text{N}$), porewater nutrient concentrations, biomass and primary productivity of benthic microalgae (Chlorophyll- <i>a</i> , Chl- <i>a</i> ; primary productivity, PP) collected in the Pearl River Estuary during three seasons in 2019 (Dry I, February; Wet, July; Dry II, November). Variables are expressed as mean with standard deviations (mean \pm s.d.)	122
Table 4.7. C and N stable isotope values in the diets (particulate organic matter, POM; sediment organic matter, SOM; microphytobenthos, MPB; C ₄ halophytes; mangrove) and consumers collected in the Pearl River Estuary, China. Species are listed with the corresponding trophic level (TL) in descending order for each taxon (Mollusca; Arthropoda; Chordata). Values are expressed as mean with range (min.–max.)	127
Table 4.8. Pearson correlation analysis between carbon and nitrogen stable isotope values in each of the two consumer groups (benthos and fish). Significant correlation coefficient values (r) at $p<0.05$ are shown in bold italics with an asterisk (*)	128

Table 4.9. Seasonal niche metrics (Bayesian standard ellipse area, SEA _b ; sample size corrected ellipse area, SEA _c ; overlap) of consumers collected in the Pearl River Estuary, China. Isotopic niche overlap between fish and benthos is calculated in each season (Dry I, February; Wet, July; Dry II, November)	134
Table 4.10. Diet (particulate organic matter, POM; microphytobenthos, MPB; mangrove; C ₄ halophyte) contribution to the 34 consumers collected in the Pearl River Estuary, China, during the three seasons (Dry I, February; Wet, July; Dry II, November) in 2019. <i>n</i> indicates the number of samples, including replicates. Values are expressed as means with standard deviations (mean±s.d.)	138
Table 5.1. List of Antarctic consumers with corresponding feeding types (grazers, Gr; filter feeders, Ff; deposit feeders, Df; omnivores, Om; scavengers, Sc; carnivores, Ca)	153
Table 5.2. Review (<i>n</i> =16) of spatial and temporal changes in sympagic, pelagic, and benthic primary production along the Antarctic coast	158
Table 5.3. Stable carbon and nitrogen isotope ratios ($\delta^{13}\text{C}$ and $\delta^{15}\text{N}$) of food sources (POM, particulate organic matter; microalgae; macroalgae) and eight consumers collected from the five intertidal sites along the Marian Cove, King George Island during the summer of 2018 to 2019 with corresponding trophic level (TL). Isotopic values are reported as means with standard deviations (s.d.). <i>n</i> indicates the number of samples	166
Table 5.4. Decadal comparison of spatial stable isotope variability ($\delta^{13}\text{C}$ and $\delta^{15}\text{N}$) and dietary utilisation of <i>Nacella concinna</i> in Marian Cove, King George Island during summer. Isotopic values and contributions are reported as means with standard deviations (s.d.) and means with range (min.–max.), respectively	173
Table 5.5. Stable carbon and nitrogen isotope ratios ($\delta^{13}\text{C}$ and $\delta^{15}\text{N}$) of the consumers with six feeding strategies (grazers, Gr; filter feeders, Ff; deposit feeders, Df; omnivores, Om; scavengers, Sc; carnivores, Ca) in the ice extent decreased in western Antarctica and increased in eastern Antarctica during summer as reported in previous studies. Species isotopic values are reported as means with standard deviations (s.d.)	178

LIST OF FIGURES

Figure 1.1. Degraded and destroyed ecologically important coastal habitats (salt marshes, tidal flat, mangrove forests, polar coasts, etc.) which supports 80% of marine biodiversity	3
Figure 1.2. Stable carbon and nitrogen isotopes ($\delta^{13}\text{C}$ and $\delta^{15}\text{N}$) are used in coastal ecosystems to investigate the food web structure and function (1, dietary contribution; 2, trophic relationship; 3, trophic level)	6
Figure 1.3. The number of publications for coastal food web structure from 1990 to 2023 (left), the studies conducted in specific habitats (middle), and the study limitations for Korean salt marshes and tidal flats; Chinese mangrove forest; Antarctic coast based on the Scopus review (right)	7
Figure 1.4. Objectives, research framework, and general research questions of the present study (Chapters 2 to 5). Using case studies, this dissertation addresses the characteristics of the food web structure and its function in four coastal habitats (Korean salt marsh and tidal flat; Chinese mangrove forest; Antarctic coast) in three climate zones (temperate; torrid; frigid)	9
Figure 2.1. Map of the study area showing the three sites (Yeocha, YC; Dongmak, DM; Donggeom, DG) with seven sampling sites (YC 1-2, DM 1-2, and DG 1-3) around Ganghwa Island, Korea. Habitat characteristics are shown in enlarged maps, with the spatial distribution of vegetated areas and the proportion of dominant macrofauna species in the corresponding sites	14
Figure 2.2. Biplot of stable carbon and nitrogen isotope signatures ($\delta^{13}\text{C}$ and $\delta^{15}\text{N}$) of potential food sources and macrobenthos in the Ganghwa tidal flat. The values of potential food sources (halophytes [<i>Phragmites australis</i> and <i>Suaeda japonica</i>]; particulate organic matter, POM; sediment organic matter, SOM; microphytobenthos, MPB; meiofauna) represent the total means with standard deviations (black line). The values of macrobenthos represent the mean of each species collected in four seasons (spring, summer, autumn, and winter). An asterisk indicates statistical significance among four functional groups (filter feeders, Ff; deposit feeders, Df; omnivores, Om; carnivores, Ca)	29
Figure 2.3. Biplots of stable carbon and nitrogen isotope compositions ($\delta^{13}\text{C}$ and $\delta^{15}\text{N}$) of deposit feeders by (A) sediment properties (sandy mud and mud) and (B) vegetation type (bare- and vegetated tidal flat) in the Ganghwa tidal flat. The values of the deposit feeders represent the mean of each species sampled at each site during the study period. An asterisk indicates statistical significance	36

Figure 2.4. (A) Group of deposit feeders determined by cluster analysis, based on the measured stable carbon isotope values ($\delta^{13}\text{C}$). The representative phylum of macrofauna (> 25% in relative abundance) is indicated for five habitat types (sandy mud bare; mud bare; sandy mud *Phragmites*; mud *Suaeda*; mud *Phragmites*). The top dominant phylum is shown in red. (A') The proportional distribution of $\delta^{13}\text{C}$ of the deposit feeders; (B) Probability density and mean dietary contribution of potential food sources (SOM and MPB) to deposit feeders in five habitat types40

Figure 3.1. Map showing the study area and information on samples (✓, collected; –, not collected) collected at six sites (Yami, YM; Sinsi, SS; Garyuk1, GR1; Garyuk2, GR2; Woryeon, WY; Anseong, AS) in the Saemangeum tidal flat and lake, Korea. YM is a reference site. In contrast, SS and GR1 are influenced by water discharge (green arrow) from the Sinsi- and Garyuk water gates (black rectangles). The blue arrow indicates the seawater input to the lake47

Figure 3.2. Total monthly exchanged water flow ($10^6 \text{ m}^3/\text{s}$) (inflow, blue; outflow, green) through Sinsi and Garyuk water gates from January 2019 to December 2022 in Saemangeum tidal flat, Korea. Mean water exchanges in period II, highlighted with a red background are different from period I (2019–2020). An asterisk indicates statistical significance ($p < 0.001$) among for years69

Figure 3.3. Monthly water quality parameters (total nitrogen, TN; total phosphorus, TP; silicon dioxide, SiO_2) collected in the water column of both the outer tidal flat (Garyuk1, GR1) and the lake (Garyuk2, GR2) near the Garyuk water gate from 2019 to 2022. 70

Figure 3.4. Carbon and nitrogen stable isotope values ($\delta^{13}\text{C}$ and $\delta^{15}\text{N}$) of particulate organic matter (FPOM and SPOM) collected at three sites in the Saemangeum tidal flat (Yami, YM; Sinsi, SS; Garyuk, GR1), and the two lower reaches of the Mangyeong and Dongjin Rivers (Woryeon, WY; Anseong, AS) from 2019 to 2022 72

Figure 3.5. Spatial distribution of seasonally collected sediment properties (water content, WC; mud content, MC) at the three outer sites (Yami, YM; Sinsi, SS; Garyuk, GR1) in the Saemangeum tidal flat from 2019 to 2022. YM is the reference site, and SS and GR1 are sites influenced by the reservoir discharge water through the Sinsi- and Garyuk water gates. The annual data are described in Table 3.7 75

Figure 3.6. Spatial distribution of seasonally collected sediment porewater nutrient concentrations (total nitrogen, TN; total phosphorus, TP; silicon dioxide, SiO_2) at the three outer sites (Yami, YM; Sinsi, SS; Garyuk, GR1) in the Saemangeum tidal flat from 2019 to 2022. YM is the reference site, and SS and GR1 are sites influenced by the reservoir discharge water through the Sinsi- and Garyuk water gates. The annual data are described in Table 3.8..... 77

Figure 3.7. Spatial distribution of seasonally collected biomass (Chl-*a*), primary production (PP), and primary productivity (P/B) of microphytobenthos at the three outer sites (Yami, YM; Sinsi, SS; Garyuk1, GR1) in the Saemangeum tidal flat from 2019 to 2022. YM is the reference site, and SS and GR1 are sites influenced by the reservoir discharge water through the Sinsi- and Garyuk water gates. The annual data are described in Table 3.9. 79

Figure 3.8. Biplot of stable carbon and nitrogen isotope signatures ($\delta^{13}\text{C}$ and $\delta^{15}\text{N}$) of potential food sources and macrobenthos in the Saemangeum tidal flat. The values of potential food sources (freshwater and seawater particulate organic matter in the Saemangeum, FPOM and seawater POM; sediment organic matter, SOM; microphytobenthos, MPB) represent the total means with standard deviations (black asterisk and line). The values of macrobenthos represent the means of each species collected from 2019 to 2022. A red asterisk represents statistical significance among five functional groups (grazers, Gr; filter feeders, Ff; deposit feeders, Df; omnivores, Om; carnivores, Ca). Full scientific names of organisms described by number are given in Fig. 3.9 and Table 3.10 83

Figure 3.9. Trophic level of 54 benthic consumers in the five phyla [Annelida, (An) ($n=4$); Arthropoda, (Ar) ($n=13$); Brachiopoda, (Br) ($n=1$); Mollusca, (M) ($n=33$); Echinodermata, (E) ($n=3$)] collected in the Saemangeum tidal flat, Korea, from 2019 to 2022. The superscript number indicates the identification of each species described in Fig. 3.8 84

Figure 3.10. Stable carbon and nitrogen isotope signatures ($\delta^{13}\text{C}$ and $\delta^{15}\text{N}$) of filter feeders (Ff) in the Saemangeum tidal flat by site (**A**) and period (**B**). YM, Yami; SS, Sinsi; GR1, Garyuk 1; PI, 2019–2020; PII, 2021–2022. (**C**) Stable isotope niche space of Ff. Red crosses are maximum likelihood estimates. SEA_b , Bayesian standard ellipse area; SEA_c , sample size corrected ellipse area..... 88

Figure 3.11. Stable carbon and nitrogen isotope signatures ($\delta^{13}\text{C}$ and $\delta^{15}\text{N}$) of deposit feeders (Df) in the Saemangeum tidal flat by site (**A**) and period (**B**). YM, Yami; SS, Sinsi; GR1, Garyuk 1; PI, 2019–2020; PII, 2021–2022. (**C**) Stable isotope niche space of Df. Red crosses are maximum likelihood estimates. SEA_b , Bayesian standard ellipse area; SEA_c , sample size corrected ellipse area..... 89

Figure 3.12. Stable carbon and nitrogen isotope values ($\delta^{13}\text{C}$ and $\delta^{15}\text{N}$) of filter feeders (Ff) collected at three sites (Yami, YM; Sinsi, SS; Garyuk1, GR1) in the Saemangeum tidal flat, Korea from 2019 to 2022. Blue and red symbols indicate Ff collected during period I (2019–2020) and period II (2021–2022), respectively 90

Figure 3.13. Stable carbon and nitrogen isotope values ($\delta^{13}\text{C}$ and $\delta^{15}\text{N}$) of deposit feeders (Df) collected at three sites (Yami, YM; Sinsi, SS; Garyuk1, GR1) in the Saemangeum tidal flat, Korea from 2019 to 2022. Blue and red symbols indicate Df collected during period I (2019–2020) and period II (2021–2022), respectively 91

Figure 3.14. Spatio-temporal groups of filter feeder (**A**) and deposit feeder (**B**) determined by cluster analysis based on similarity of their diet utilisation at three sites (Yami, YM; Sinsi, SS; Garyuk1, GR1) in the Saemangeum tidal flat, Korea. The following colours (blue, SPOM; grey, SOM; green, MPB) indicate the contribution (%) of the three diets to the consumers. PI and PII indicate period I (2019-2020) and period II (2021-2022), respectively94

Figure 3.15. Review of stable carbon and nitrogen isotope values ($\delta^{13}\text{C}$ and $\delta^{15}\text{N}$) of benthic consumers (grazers, Gr; filter feeders, Ff; deposit feeders, Df; omnivores, Om; carnivores, Ca) and their potential diets (freshwater and seawater particulate organic matter, F/SPOM; sediment organic matter, SOM; microphytobenthos, MPB) in previous food web studies ($n=21$) on the west and south coasts of Korea. The values investigated in the present study are included for comparison97

Figure 4.1. Map of the study area (Qi'ao Island in the Pearl River Estuary, PRE) with human population and sampling information. n indicates the number of samples analysed including three and four replicates for each diet and organism 102

Figure 4.2. A total of 34 species from three phyla (Chordata, Arthropoda, and Mollusca) collected over three sampling periods (Dry I, February; Wet, July; Dry II, November) in 2019. The full scientific names of the organisms are given in Table 4.7. 105

Figure 4.3. Stable carbon and nitrogen isotope values of potential diets and aquatic organisms in the western Pearl River Estuary, China. Total means with standard deviations (asterisk with black line) represent the values of five potential diets [particulate organic matter, POM; sediment organic matter, SOM; microphytobenthos, MPB; mangrove (*Sonneratia apetala*); C_4 halophyte (*Cyperus malaccensis*)]. Circle and square indicate benthos and fish, respectively. The number in the symbol (listed on the consumers) represents the species listed in Fig. 4.4., and the full scientific names of the organisms are listed in Table 4.7. An asterisk indicates statistical significance ($p<0.05$) between two consumers..... 125

Figure 4.4. Trophic level (TL) of 34 benthic and pelagic consumers in six feeding groups (herbivores, Hb; deposit feeders, Df; planktivores, Pk; filter feeders, Ff; omnivores, Om; carnivores, Ca). Representative organisms with the highest occurrence are shown on the TL of feeding types 126

Figure 4.5. Seasonal stable isotope distribution of carbon and nitrogen of potential diets (particulate organic matter, POM; sediment organic matter, SOM; microphytobenthos, MPB; mangrove [*Sonneratia apetala*]; halophyte [*Cyperus malaccensis*]) and consumers (square, fish; circle, benthos) in 2019 (Dry I, February; Wet, July; Dry II, November). The number of asterisks indicates the degree of statistical significance (*, $p<0.05$; **, $p<0.01$; ***, $p<0.001$) between fish and benthos 130

Figure 4.6. Box plot showing the credible interval (CI) range of the estimated ellipse area (SEA_b) for the seasonal niche of two consumers. The boxed areas represent the 50% (dark grey), 75% (grey), and 95% (light grey) credible intervals of the estimated ellipse areas. The black dot and red cross represent the mode of SEA_b and the maximum likelihood estimate of the small sample corrected standard ellipse area, SEA_c 133

Figure 4.7. Seasonal (Dry I, February; Wet, July; Dry II, November) standard ellipse area Bayesian estimation (SEA_b) with mode (black dots) and probability of data distribution (50%, dark grey boxes; 75%, intermediate grey boxes; 95%, light grey boxes) for **(A)** two functional groups of fish (planktivores; carnivores), and **(B)** five functional groups of benthos (herbivores; filter feeders; deposit feeders; omnivores; carnivores). The standard ellipse area corrected for small sample size (SEA_c) is shown as a red multiplication marker. Each abbreviation (*n*, *n.a.*, and *n.d.*) indicates the number of samples, not analysed, and no data 135

Figure 4.8. Consumer groups [Group 1 (1-1, 1-2, and 1-3); Group 2] determined by cluster analysis based on similarity of seasonal diet utilisation (Dry I, February; Wet, July; Dry II, November) in the western Pearl River Estuary, China. The contribution (%) of five diets to consumers is represented by different colours (blue, POM; white-grey, SOM; green, MPB; orange-brown, mangrove; yellow, C₄ halophyte). Consumers are represented by black symbols. Benthos (all) represents all invertebrates, including arthropods and mollusc. Primary and secondary sources (POM and halophyte) are highlighted with red and blue backgrounds, respectively 136

Figure 4.9. Cluster analysis based on similarity of diet utilisation by three consumers (Chordata, Arthropoda, and Mollusca) over the three seasons. The contribution (%) of the five diets to the consumers is represented by different colours (blue, POM; white-grey, SOM; green, MPB; orange-brown, mangrove; yellow, halophyte). Consumers are described with black symbols 137

Figure 4.10. Review of the stable isotope values of carbon and nitrogen for the potential diets of benthic and pelagic consumers in previous studies (*n*=18) conducted in the three coastal ecosystems in China: **(A)** mangrove forest, **(B)** salt marshes, and **(C)** seagrass habitat. The values obtained in the present study are included for comparison. Fish and benthos were classified into two and five feeding types, respectively. Potential diets included sediment organic matter (SOM), particulate organic matter (POM), microphytobenthos (MPB), mangrove, halophytes (C₃ and C₄), and seagrass. The raw stable isotope data of diet and consumers used in this figure are described in Tables 4.4. and 4.5 141

Figure 4.11. Review of the stable isotope values of carbon and nitrogen for the potential diets and consumers in previous studies conducted in the pristine (white bar, *n*=6) and polluted (grey bar, *n*=1) mangrove habitats in China. The values obtained in the present study (red bar) are included for comparison. Fish and benthos were classified into two and five feeding types, respectively. Potential diets included sediment organic matter (SOM), particulate organic matter (POM), microphytobenthos (MPB), mangroves, and C₄ halophytes. Black square and triangle indicate minimum and maximum values, respectively 142

Figure 5.1. Map of the study area showing the six intertidal (inner, B1; outer, W1 and B2-B5) and five subtidal sites (MC1-MC5), including three sites reported in a previous study (Choy et al., 2011) with records of past glacier retreat since 1956 in Marian Cove, King George Island, Antarctic Peninsula. Top-down images of five sites show the approximate glacier influence with increasing distance from the glacier margin. The base map was obtained from Google Earth (https://earth.google.com/web)	147
Figure 5.2. Spatial vertical (0–20 m) concentration of Chl- <i>a</i> (MC1-MC5) measured with the Sea point Chlorophyll Fluorometer (SCF) in the SBE19 Plus-V2 CTD at five subtidal sampling sites (green, inner MC1; light blue, outer MC2-MC5; blue, total Chl- <i>a</i> of the outer sites) in Marian Cove, King George Island	148
Figure 5.3. The spatial distribution of seawater salinity, DO, and pH reflects the contrasting environmental conditions between inner and outer intertidal sites in Marian Cove, King George Island, Antarctic Peninsula during the present study period (2018–2019)	149
Figure 5.4. Regional variations in summer sea ice extent variation (2000–2018) in Antarctica. Map showing the location of the carbon and nitrogen stable isotope data collection sites based on the present study with literature reviews	151
Figure 5.5. Antarctic summer sea ice extent variation using satellite-based multi-channel passive microwave from 2000 to 2018 (Parkinson et al., 2019). Representative Antarctic summer sea ice concentration (%) estimated in the NASA earth observatory. Medians of three decadal sea ice concentrations are described by a yellow line	152
Figure 5.6. Stable carbon and nitrogen isotopic signatures ($\delta^{13}\text{C}$ and $\delta^{15}\text{N}$) of potential food sources and consumers in Marian Cove, King George Island, Antarctic Peninsula. Stable isotope ranges of potential food sources (particulate organic matter, POM; microphytobenthos, MPB; red and brown macroalgae) are represented by empty blue, green, red, and brown boxes. Consumers represented as grey symbols indicate five taxonomic groups (Mollusca, Arthropoda, Chordata, Cnidaria, and Echinodermata) with total means and standard deviations. Consumers with an asterisk and bold letters with yellow highlighting indicate species collected from both the inner and outer sites in MC. Ranges of trophic level to eight consumers are presented next to the biplot	165
Figure 5.7. Spatial carbon stable isotope distributions ($\delta^{13}\text{C}$) of three potential food sources (particulate organic matter, POM; microphytobenthos, MPB; red and brown macroalgae) and dominant consumers (<i>Nacella concinna</i> , <i>Gondogeneia antarctica</i> , and <i>Tigriopus kingsejongensis</i>) collected from inner (B1) and outer sites (B2, B3, B5, and W1) in Marian Cove, King George Island. Diets and consumers showing significant differences in stable isotope values between inner and outer sites are described with red mean and standard deviation	168

Figure 5.8. Spatial carbon stable isotope distributions ($\delta^{15}\text{N}$) of three potential food sources (particulate organic matter, POM; microphytobenthos, MPB; red and brown macroalgae) and dominant consumers (*Nacella concinna*, *Gondogeneia antarctica*, and *Tigriopus kingsejongensis*) collected from inner (B1) and outer sites (B2, B3, B5, and W1) in Marian Cove, King George Island. Diets and consumers showing significant differences in stable isotope values between inner and outer sites are described with red mean and standard deviation 169

Figure 5.9. Decadal comparison (2009 vs. 2018–2019) of the spatial distribution and function of the Antarctic limpet, *Nacella concinna* population in Marian Cove, King George Island. White rectangles and grey ellipses indicate limpet samples collected in 2009 (Choy et al., 2011) and 2018–2019, respectively. **(A)** small and large limpet groups (groups 1 and 2) determined by cluster analysis based on similarity to shell length (mm). Limpet samples in each group are arranged by distance from the glacier. **(B)** spatial distribution of the stable carbon isotope signature ($\delta^{13}\text{C}$) of eight limpet samples with contributions (%) of three potential diets (particulate organic matter, POM; microalgae; macroalgae) 172

Figure 5.10. Multi-decadal changes in carbon and nitrogen stable isotopes ($\Delta\delta^{13}\text{C}$, and $\Delta\delta^{15}\text{N}$) of classified taxonomic groups with five feeding strategies (grazers, Gr; filter feeders, Ff; deposit feeders, Df; omnivores, Om; scavengers, Sc; carnivores, Ca) between west (downward red triangle) and east (upward blue triangle) showing contrasting sea ice retreat and advance. Mean multi-decadal stable isotope changes of consumers are presented with red and blue backgrounds with arrows 177

Figure 5.11. Multi-decadal changes in the contribution (%) of three diet types (P, pelagic; S, sympagic; B, benthic) to the consumers in **(A)** West Antarctica with substantial sea ice retreat and in **(B)** East Antarctica with substantial sea ice advance. The feeding strategies of the consumers are described by abbreviation in blue letters (grazer, Gr; filter feeder, Ff; deposit feeder, Df; omnivore, Om; scavenger, Sc; carnivore, Ca). Squares with red and blue gradients indicate an increase or decrease in the dietary contribution (%) of three producers to consumers, from 0 to 100%, respectively 181

Figure 6.1. A comprehensive summary of the key findings in the present food web study in Korean salt marsh and tidal flat (temperate zone), Chinese mangrove forest (torrid zone) and Antarctic coast (frigid zone) 186

Figure 6.2. The carbon and nitrogen stable isotope signatures of diets and benthic consumers from **(A)** temperate (Korean salt marsh and tidal flat), **(B)** torrid (Chinese mangrove forest), and **(C)** frigid (Antarctic) coastal ecosystems. A comprehensive comparison of food web structure, providing specific information on food web characteristics in coastal regions: the degree of strength and diversity of the diet and anthropogenic impact **(D)**. Green and blue colours indicate potential diets and benthos, respectively 189

Figure 6.3. The carbon and nitrogen stable isotope signatures of five functional groups (grazers, Gr; filter feeders, Ff; deposit feeders, Df; omnivores, Om; carnivores, Ca) of benthic consumers collected in **(A)** temperate (Korean salt marsh and tidal flat), **(B)** torrid (Chinese mangrove forest), and **(C)** frigid (Antarctica) coastal ecosystems. Colours indicate each functional group of consumers (red, Ca; yellow, Om; grey, Df; blue, Ff; green, Gr). The grey background indicates the overlapping carbon stable isotope range of benthic consumers 190

Figure 6.4. Limitations of the present study and directions for future food web research. Three limitations and corresponding research directions are described in the dark grey and light grey boxes, respectively 192

CHAPTER 1.

INTRODUCTION

1.1. Backgrounds

The coastal zones connecting terrestrial and marine environments are the most productive and biologically diverse ecosystems on the earth (Crossland et al., 2005). Coastal ecosystems support 80% of marine organisms, and the coastal primary production provides energy that supports secondary production in the adjacent ocean (Hyndes et al., 2014) (Fig. 1.1.). Therefore, understanding the structure and function of the coastal ecosystem that supports high marine biodiversity is a priority for effective management and conservation of marine ecosystems.

Most people worldwide live in coastal regions (Jackson et al., 2001; Nicholls et al., 2007; Katsanevakis et al., 2020). Thus, up to 60% of coastal habitats have been degraded or destroyed by various threats (e.g., reclamation, pollution, agriculture, invasion, habitat alteration, overfishing, and global warming) as human activities have increased. Over 40% of salt marsh and mangrove forests in tropical and temperate coastal regions have been severely degraded (Valiela et al., 2001, UNEP 2006, FAO 2007, Silliman et al., 2009; Waycott et al. 2009) (Fig. 1.1). The devastation of salt marshes and mangrove forests has led to a decline in feeding, breeding, and nursery habitats for marine species, and has substantially reduced the populations of marine organisms living in the coastal habitats (Worm et al., 2006; Barbier, 2011). These changes in the coastal ecosystem have also caused a cascade of effects, including the widespread changes in the structure and function of food webs (Ray, 1991).

In contrast, Arctic and Antarctic coastal ecosystems have been severely impacted by a range of climate-related environmental changes (Brierley and Kingsford, 2009), including a shrinking cryosphere, disrupted regional weather patterns, sea-level rise, ocean acidification, altered nutrient loads and ocean circulation. Changes in Antarctic coastal primary production under climate change have affected the regional species composition, spatial distribution, and abundance of many coastal organisms (Shade et al., 2015; Michel et al., 2019; Alurralde et al., 2020). However, the impact of these changes on the functioning of Antarctic coastal food webs remains poorly understood.

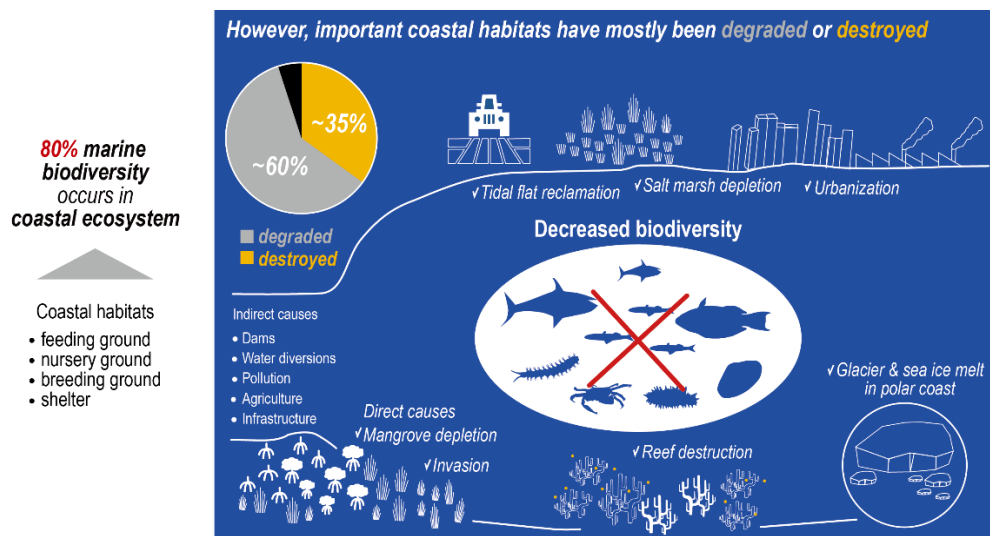


Figure 1.1.

Degraded and destroyed ecologically important coastal habitats (salt marshes, tidal flat, mangrove forests, polar coasts, etc.) which supports 80% of marine biodiversity.

Most of the uncertainty in predicting the effects of such threats on the coastal ecosystem is related to understanding how they will affect the nature of energy interactions among organisms in the coastal ecosystem (Winder and Schindler, 2004). Various effects of emerging threats on the ecosystem can be mediated through the distribution of trophic levels, trophic relationships, and diet production in the food web. Therefore, understanding the food web is essential for effective conservation and management of coastal ecosystems (Nagelkerken et al., 2020).

Stable isotopes of C and N ($\delta^{13}\text{C}$ and $\delta^{15}\text{N}$) have been used to study the food web structure and function in various coastal ecosystems (Layman et al., 2012) (Fig. 1.2.). The $\delta^{13}\text{C}$ signature is useful for identifying the diet of consumers in estuarine- and coastal ecosystems due to the distinct $\delta^{13}\text{C}$ ranges of diets (Lee et al., 2021). In comparison, the $\delta^{15}\text{N}$ value of an organism indicates the trophic level of a community which is calculated from the relative enrichment of the diet (Post, 2002). N stable isotope values of organic matter and primary producers provide information on the degree of anthropogenic influence in the surrounding environment (Lee, 2000).

The benthos comprises major taxonomic groups that contribute significantly to various ecological processes (e.g., nutrient cycling, carbon uptake and energy transfer in the food web) (Gray 1997; Glud 2008). Because benthic invertebrates are relatively sedentary and perennial, their stable isotopic characteristics can be used to estimate the direction and intensity of environmental change (Boesch et al., 1976; Simbouna et al., 1995), and comparisons between target consumers and potential food sources can reflect close and/or long-term associations (Riera et al., 1999; Bae et al., 2018). In addition, their different feeding strategies (e.g., deposit and filter feeding) provide information on sensitivity to environmental changes. Thus, benthic $\delta^{13}\text{C}$ and $\delta^{15}\text{N}$ are efficient indicators of environmental change in coastal ecosystems. Stable isotope values of pelagic consumers provide additional information for a comprehensive understanding of the structure of coastal food webs.

In recent decades, studies of coastal food webs have increased in response to growing concern about the health and services of coastal ecosystems (Fig. 1.3.). However, studies of food web structure and function in temperate coastal habitats such as salt marshes, mudflats and kelp forests are still limited. Although more studies have been conducted on coastal habitats in torrid and frigid zones, studies on

mangrove forests and the Antarctic coast are still limited in each climatic zone. In particular, there are many unanswered questions about the structure of the coastal food web and its response to 1) sediment and halophyte distribution in the salt marsh; 2) discharge of eutrophic water into the tidal flat; 3) seasonal flood dynamics in the mangrove forest; 4) glacier and sea ice dynamics in the Antarctic coastal regions. Therefore, a better understanding of the limitations of previous food web studies in such coastal habitats would be needed for future sustainable management.

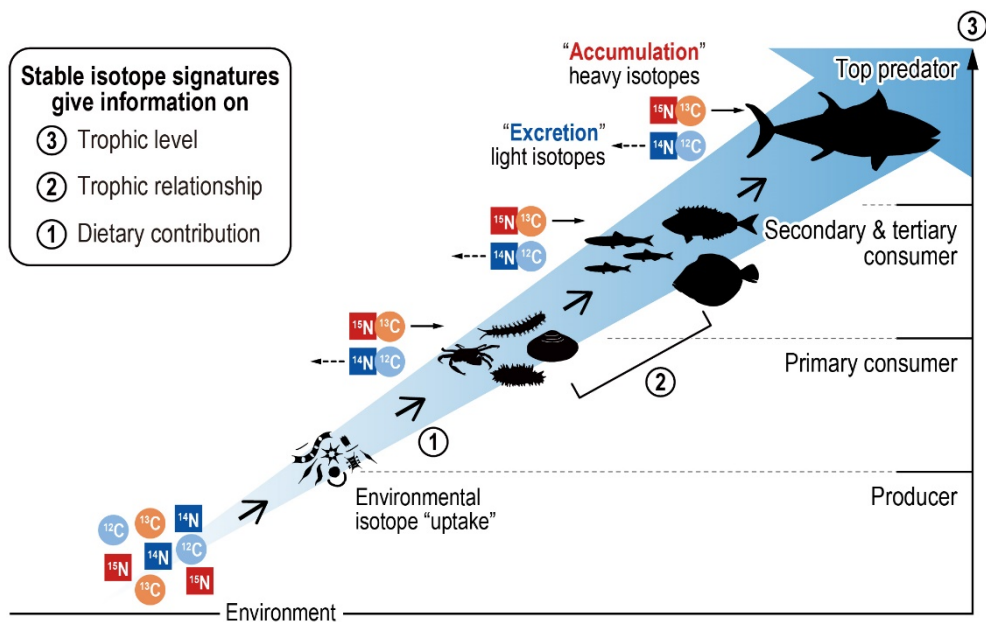


Figure 1.2.

Stable carbon and nitrogen isotopes ($\delta^{13}\text{C}$ and $\delta^{15}\text{N}$) are used in coastal ecosystems to investigate the food web structure and function (1, dietary contribution; 2, trophic relationship; 3, trophic level).

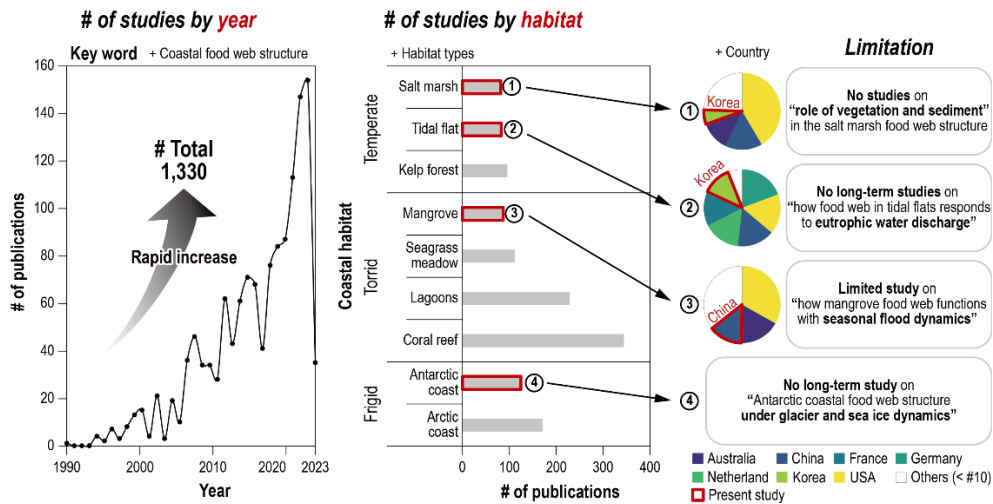


Figure 1.3.

The number of publications for coastal food web structure from 1990 to 2023 (left), the studies conducted in specific habitats (middle), and the study limitations for Korean salt marshes and tidal flats; Chinese mangrove forest; Antarctic coast based on the Scopus review (right).

1.2. Objectives

The present study investigated the food web structure and function in the ecologically important coastal habitats (Korean salt marsh and tidal flat, Chinese mangrove forest, and Antarctic coast). This study based on C and N stable isotope analysis, was designed to provide quantitative scientific information on the overall food web structure, the spatiotemporal changes in the food web structure and function, and the primary diet of consumers in each habitat (Fig. 1.4.). Thus, this dissertation aimed to address the limitations of existing studies and provide a basis for contributing to ecosystem assessment and predictions for future ecosystem-based management in coastal habitats across climatic zones.

The specific objectives of the present study were as follows: 1) to understand the food web structure and its function, especially on the spatial diet utilisation of deposit feeders in different habitat conditions in terms of sediment and halophyte distribution in Ganghwa salt marsh, Korea; 2) to reveal the influence and degree of eutrophic water discharge on the organic matter distribution and diet consumption of filter feeders and deposit feeders in the Saemangeum tidal flat, Korea; 3) to investigate the influence of seasonal flood dynamics on the organic matter distribution and diet utilisation of consumers in the mangrove forest in the Pearl River Estuary surrounded by megacities, China; 4) to investigate the influence of glacier retreat on the spatial distribution of stable isotopes and decadal changes in diet utilisation of limpets in Marian Cove, Antarctica. Literature reviews on stable isotope values of diet and benthic consumers will be conducted to compare the degree of baseline variation and anthropogenic influences in four habitats (Korean salt marsh and tidal flat; Chinese mangrove forest; Antarctic coastal regions) across three climate zones (temperate; torrid; frigid).

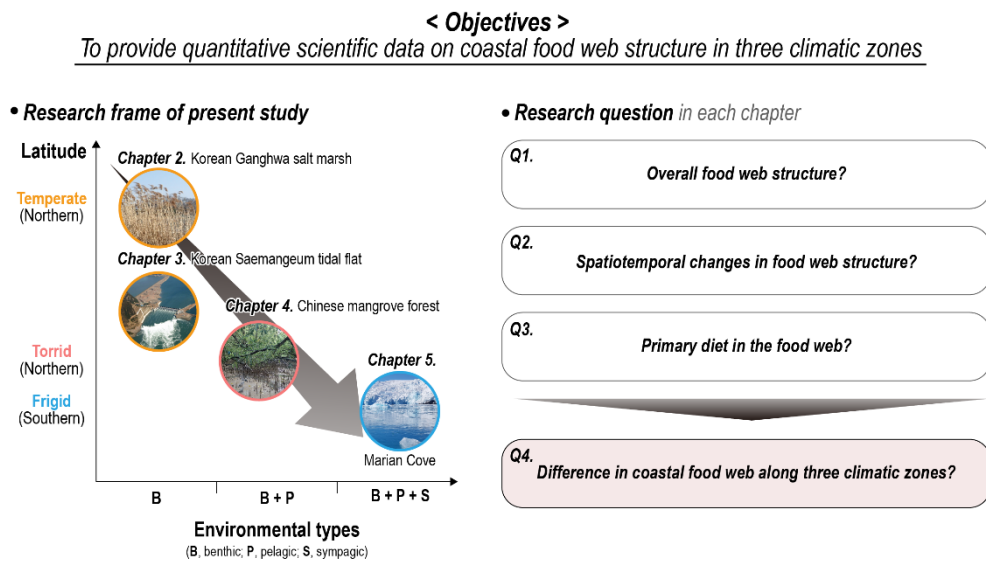
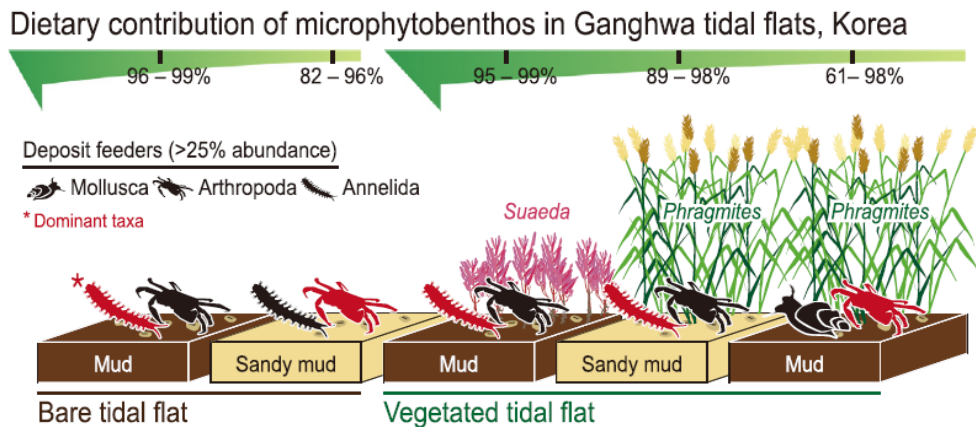


Figure 1.4.

Objectives, research framework, and general research questions of the present study (Chapters 2 to 5). Using case studies, this dissertation addresses the characteristics of the food web structure and its function in four coastal habitats (Korean salt marsh and tidal flat; Chinese mangrove forest; Antarctic coast) in three climate zones (temperate; torrid; frigid).

CHAPTER 2.

Food web structure of Ganghwa salt marsh in Korea with sediment and halophyte distribution



This chapter has been published to Science of Total Environment.

Lee, I. O., Noh, J., Lee, J., Kim, B., Hwang, K., Kwon, B-O, Lee, M. J., Ryu, J., Nam, J., Khim, J.S. Stable isotope signatures reveal the significant contributions of microphytobenthos and salt marsh-driven nutrition in the intertidal benthic food webs. Sci. Total Environ. 2021, 756, 144068

<https://doi.org/10.1016/j.scitotenv.2020.144068>

2.1. Introduction

Coastal ecosystems such as mudflat, salt marsh, and mangrove are highly productive areas globally, particularly representing marine biodiversity hotspots in macro-tidal environment (Armonies, 1986; Ashton and Macintosh, 2002; Koh and Khim, 2014). The high productivity in the macro-tidal areas is fundamentally associated with complex environmental dynamics and interactions between abiotic and biotic components (Koh and Khim, 2014). In addition, macro-tidal environment generally receives plenty of terrestrial sediments and organic matter, which supports diverse habitats with high trophic complexity. Thus, it is important to understand the intertidal trophic dynamics to assess coastal ecosystem health in a functional perspective (Bang et al., 2019).

The Yellow Sea is a large marine ecosystem within a shallow semi-enclosed area possessing the largest tidal flat ($>18,000 \text{ km}^2$) in the world (Koh and de Jonge, 2014). It is well known for the world's top marine biodiversity hot spots (Costello et al., 2010) together with high primary productivity (Kwon et al., 2020). The extensively developed Yellow Sea intertidal flats support diverse soft-bottom invertebrates and their trophic dynamics (Choi et al., 2014; Park et al., 2014). However, their trophic contributions by various feeding type are poorly known, particularly in the large marine ecosystem of the Yellow Sea.

The key biotic components supporting the intertidal trophic system encompass from micro-to macro-flora such as microphytobenthos (MPB) and some halophytes. In the Yellow Sea tidal flat, high biomass, and productivities of MPB were highlighted to enhance the growth and reproduction of some benthic invertebrates (Noh et al., 2019). MPB is fundamentally significant in tidal flat system as they provide primary food sources to upper trophic level organisms and further support the pelagic productivity through tidal resuspension (Macintyre et al. 1996; Underwood and Kromkamp, 1999; Koh et al., 2006). Meantime, salt marsh vegetations would be another class of important food source for various macrofauna by providing significant amounts of plant-derived matters and/or detritus in the given system (Teal, 1962; Shang et al., 2008).

Stable isotopic signatures of carbon and nitrogen ($\delta^{13}\text{C}$ and $\delta^{15}\text{N}$) are widely used to explore the food web structure and its function of marine ecosystems (Layman et al., 2012; Noh et al., 2019). The isotopic analysis can be also used to identify potential food sources for consumers in a complex intertidal trophic system. Our previous study conducted in the Geum River Estuary, Yellow Sea indicated that varying food sources exhibit distinct isotopic ranges, including phytoplankton, zooplankton, MPB, plant detritus, etc. (Noh et al., 2019). As salt marsh benthic invertebrates are relatively sedentary and perennial, the stable isotopic characteristics between target organisms and potential food sources would reflect their close and/or long-term association (Riera et al., 1999; Bae et al., 2018).

In this study, we investigated the intertidal benthic food web structure and its function at the Ganghwa salt marsh in Korea. The specific objectives were to: 1) describe the benthic trophic structure from baseline to consumers with trophic levels in the salt marsh food web; 2) determine the relationship between isotopic signatures of deposit feeders and surrounding environments; 3) examine the spatial dietary contribution to deposit feeders.

2.2. Materials and methods

2.2.1. Study area and data collection

Ganghwa is an Island (241 km²) located on the far north-western coast of South Korea showing the macro-tidal regime; spring tide, 8 m; neap tide, 4 m (Woo and Je, 2002). Gwangha Island encompasses the most extensively developed tidal flat in South Korea, which occur in the southern part of the Han River Estuary (Koh and Khim, 2014). Of note, several intertidal places including Yeongjong Island (100 km²) and Lake Sihwa (180 km²) nearby the Han River Estuary have been reclaimed during the past half century. Such large-scale reclamations have been permitted by the Public Waters Management and Reclamation Act of the Korean government in 1961, accordingly over 500 km² of intertidal areas including Estuary, salt marshes, and mudflats disappeared in the Han River Estuary and adjacent Gyeonggi Bay, South Korea (Koh and Khim, 2014).

The tidal flat is brackish, with a distinct salinity gradient that is influenced by freshwater inflow from the Han River to the main waterways (Koh and Khim, 2014). Hydraulic, chemical, and sedimentary factors in the Ganghwa tidal flat collectively cause a variety of sediments to be distributed across the area; primarily sand in the west and mud in the east (Choi and Jo, 2015). The salt marsh is well developed in the upper intertidal zone of Ganghwa tidal flat, where halophytes absorb hydrodynamic energy, trap organic matter and stimulate sedimentation process (Ha et al., 2018). The diversity of sediment on the Ganghwa tidal flat provides a large amount of potential food sources for intertidal macrofauna, including terrestrial organic matter, settled phytoplankton, and MPB.

The study area is situated in the southern part of Ganghwa Island, where three typical tidal flats are well developed. These tidal flats include Yeocha (YC; YC 1-2), Dongmak (DM; DM 1-2), and Donggeom (DG; DG 1-3) (Fig. 2.1.). YC is dominated by sandy mud sediment, while DM and DG are dominated by muddy bottom sediments. All three tidal flats had relatively well-developed salt marsh vegetation in the upper intertidal zone: *Phragmites australis* in YC, *Suaeda japonica* in DM, *P. australis* and *S. japonica* in DG. Environmental parameters were obtained from the national monitoring station near Ganghwa (MEIS, 2019) (Table 2.1.).

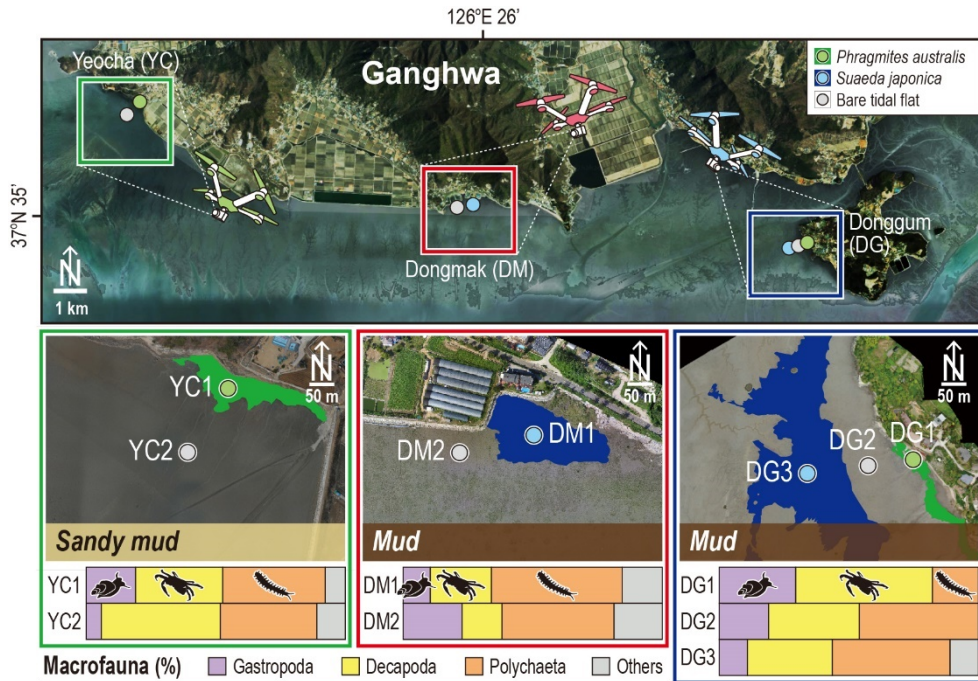


Figure 2.1.

Map of the study area showing the three sites (Yeocha, YC; Dongmak, DM; Donggeom, DG) with seven sampling sites (YC 1-2, DM 1-2, and DG 1-3) around Ganghwa Island, Korea. Habitat characteristics are shown in enlarged maps, with the spatial distribution of vegetated areas and the proportion of dominant macrofauna species in the corresponding sites.

Table 2.1.

Seasonal environmental parameters of seawater obtained from the national monitoring station near to Ganghwa Island.

Parameter	Spring		Summer		Fall		Winter	
	mean	s.d.	mean	s.d.	mean	s.d.	mean	s.d.
pH	7.9	0.0	8.0	0.0	7.8	0.0	8.0	0.0
Temperature (°C)	17.1	0.3	29.2	0.1	13.9	0.0	2.0	0.0
Salinity (psu)	11.5	3.0	28.6	0.2	27.1	0.2	26.2	0.1
Dissolved oxygen (mg L ⁻¹)	7.8	0.7	6.8	0.0	7.9	0.0	11.2	0.0
Suspended solids (mg L ⁻¹)	134	50.6	46.7	17.3	42.6	8.7	220	13.1
Chl- <i>a</i> (µg L ⁻¹)	3.2	1.7	1.5	0.0	1.1	0.1	3.0	0.3

2.2.2. Sample collection and preparation

A year-round seasonal sampling was conducted from 7 locations at three tidal flats of YC, DM, and DG in Ganghwa Island from March 2018 to February 2019. The surface sediment (~0.5 cm) was collected with a stainless-steel spatula and stored in plastic bottles. The sample was subsequently transferred to the laboratory to analyze the general sediment parameters. Rapid partial analysis was used to estimate mud content (MC) (Buchanan, 1984). Textural types of sediment were simply classified as sandy mud (50–75% MC) or mud (>75% MC), based on the classification method of a previous study (Flemming, 2000). Loss on ignition (LOI) was estimated after burning the sediments to ashes (550 °C, 4 h) (Heiri et al., 2001). To analyze total organic carbon (TOC) and total nitrogen (TN), sediments were freeze-dried and powdered using a mortar and pestle. In addition, samples were decalcified with 10% hydrochloric acid before TOC analysis (HCl, Sigma Aldrich, St. Louis, MO).

Surface sediment (0.5 cm) was collected using a syringe corer (inside diameter=3.0 cm) to measure benthic chlorophyll-*a* (Chl-*a*), as a proxy for MPB biomass. Samples were immediately frozen in situ with dry ice and transported to the laboratory. The samples were extracted with 100% acetone (10 mL) for 24 h in a refrigerator maintained at 4 °C and subsequently centrifuged at 3000 rpm (5 min). The absorbance of the extracted solution was measured using a spectrophotometer by placing 3 mL of the solution in a quartz cuvette. We use the Lorenzen (1967) equations to calculate the concentration of Chl-*a* (mg m⁻²) in the sediment.

Potential food sources and benthos were seasonally sampled to analyze $\delta^{13}\text{C}$ and $\delta^{15}\text{N}$. During the high tide, particulate organic matter (POM) was collected at the three sites of YC, DM, and DG. To remove zooplankton and large particles, ~50 L seawater samples were pre-filtered through a 100 μm mesh net and re-filtered with a pre-combusted (450 °C, 4 h) Whatman GF/F glass fiber filter. During the low tide, MPB mats were collected from the sediment surface (0.5 cm) at all sites and extracted following the method of Couch (1989). We also collected sediment organic matter (SOM) samples from the sediment surface (0.5 cm). The leaves of halophytes were collected from all halophytes-beds and scraped with a razor blade to remove epibionts and rinsed with distilled water. Meiofauna that were collected from surface

sediment (1.0 cm) were filtered with a 63 μ m mesh net. All seasonal samples of meiofauna (copepoda and nematoda) were sorted by hands over 3,000 individuals under a binocular microscope and subsequently combined to generate enough samples 0.3 mg and 1.5 mg for carbon and nitrogen stable isotope analysis, respectively.

Macrobenthos were collected by hands in seven locations of Ganghwa tidal flat. In total, we collected >800 individuals of 16 macrobenthos species. Phylum Annelida and Arthropoda were the most dominant taxa accounting for over 50% abundance in five Phylum (Annelida, 37.9%; Arthropoda, 36.6%; Mollusca, 18.2%; Chordata, 7.0%; and Brachiopoda, 0.4%) (Fig. 2.1.). The feeding types of macrobenthos was classified based on the previously documented reports (Table 2.2.). The muscle tissues of organisms were dissected, lyophilised, and homogenised before stable isotope analysis.

Table 2.2.

The list of macrobenthos with corresponding feeding types found on Ganghwa Island, Korea.

Species	Feeding type	Reference
Polychaeta		
<i>Perinereis aibuhitensis</i>	Deposit feeder	Zhang et al., 2008
<i>Paraleonnates uschakovi</i>	Deposit feeder	Metcalf and Glasby, 2008
<i>Glycera</i> sp.	Carnivore	Park et al., 2017
Bivalvia		
<i>Glauconome chinensis</i>	Filter feeder	Wang et al., 2015
<i>Cyclina sinensis</i>	Filter feeder	Noh et al., 2019
<i>Magallana gigas</i>	Filter feeder	Park et al., 2017
<i>Laternula gracilis</i>	Filter feeder	Ahn, 1994
Lingulata		
<i>Lingula anatine</i>	Filter feeder	Darmarini et al., 2017
Gastropoda		
<i>Cerithidea balteata</i>	Deposit feeder	Park et al., 2017
<i>Lunatia fortune</i>	Carnivore	Park et al., 2015
Malacostraca		
<i>Alpheus</i> sp.	Deposit feeder	Palomar et al., 2005
<i>Cleistostoma dilatatum</i>	Deposit feeder	Park et al., 2017
<i>Macrophthalmus japonicus</i>	Deposit feeder	Park et al., 2017
<i>Helice tridens</i>	Omnivore	Park et al., 2015
Actinopterygii		
<i>Periophthalmus modestus</i>	Carnivore	Baeck et al., 2013
<i>Synechogobius hasta</i>	Carnivore	Noh et al., 2019

2.2.3. Stable isotope analysis

A fine powder of POM, SOM, MPB, and halophytes was decalcified by HCl (24 h) and freeze-dried to determine stable carbon isotope values. All lyophilised samples of organisms were ground to a fine powder with a mortar and a pestle, and lipid was subsequently removed with 10 mL dichloromethane/methanol (2:1, v/v). The mixture was sonicated for 10 min. and centrifuged at 2,000 rpm for 15 min. Then, the organic solvent was discarded. We repeated the lipid-removal process for three to five times, depending on the lipid content of the sample. Lipid-free organism samples were placed under a stream of nitrogen gas until fully dried. The samples were weighed in a tin capsule and packed for further stable isotopic analysis. An isotope ratio mass spectrometer connected to an elemental analyzer (Elementar, GmbH, Hanau, Germany) was used to determine the $\delta^{13}\text{C}$ and $\delta^{15}\text{N}$ of samples. High purity CO_2 and N_2 (99.999%) gases were used as reference gases, while He and O_2 were used as carrier and combustion gases, respectively. Stable isotopic values were expressed as ‰ delta notation with the following formula:

$$\delta X (\text{‰}) = [(R_{\text{sample}} / R_{\text{reference}}) - 1] \times 1000$$

where, R_{sample} and $R_{\text{reference}}$ are the ratios ($^{13}\text{C}/^{12}\text{C}$ or $^{15}\text{N}/^{14}\text{N}$) of the sample and reference. The stable isotope values were estimated relative to conventional reference material; Vienna Peedee Belemnite for carbon and atmospheric N_2 for nitrogen. International isotope standards (IAEA-N-2, ammonium sulfate; IAEA-CH-3, cellulose) were used as reference materials to correct any analytical error of C and N. Measurement precision was ca. 0.04‰ for $\delta^{13}\text{C}$ and 0.2‰ for $\delta^{15}\text{N}$.

2.2.4. Trophic level

The most utilised trophic enrichment factor (TEF) of $\delta^{15}\text{N}$ (2.2‰) for primary benthic consumers in Korean tidal flat was used to estimate the trophic level (TL) of benthos collected in Ganghwa Island (McCutchan Jr et al., 2003). We used the average $\delta^{15}\text{N}$ of filter feeders that were collected as the baseline stable nitrogen value of the food web, because their tissue assimilates and reflects seasonal variation in primary producers and organic matter (Riccialdelli et al., 2017). TL of benthic consumers was estimated using a formula published by Vander Zanden and Rasmussen (1999):

$$\text{TL}_i = (\delta^{15}\text{N}_i - \delta^{15}\text{N}_{\text{base}}) / \text{TEF} + \text{TL}_{\text{base}}$$

where, TL_i is the TL of each species considered, $\delta^{15}\text{N}_i$ is the $\delta^{15}\text{N}$ of the species i , and $\delta^{15}\text{N}_{\text{base}}$ and TL_{base} are the mean $\delta^{15}\text{N}$ and the TL of all filter feeders (TL=2), respectively.

2.2.5. Statistical analysis

Statistical analyses were performed with SPSS 26.0 (SPSS INC., Chicago, IL) to reveal site-specific differences of sediment properties among sites. First, one-way analysis of variance (ANOVA) with a Tukey post-hoc test was conducted on spatial differences of sediment mud content and Chl-*a* among the three sites. Second, a Mann-Whitney U test was carried out on all physicochemical parameters of sediment between the bare- and vegetated sampling locations of the three sites. To estimate site-specific variation in the stable isotopes of macrofauna, we performed ANOVA with a Tukey post-hoc test to determine the mean difference of $\delta^{13}\text{C}$ and $\delta^{15}\text{N}$ among the four feeding types (Filter feeder, Ff; Deposit feeder, Df; Omnivore, Om; Carnivore, Ca). The same statistical method was used to investigate the mean difference in stable isotopic values ($\delta^{13}\text{C}$ and $\delta^{15}\text{N}$) of Df at the site with two different aspects: sediment type (sandy mud vs. mud), and vegetation (salt marsh vs. bare tidal flat). Seasonal differences in mean stable isotopic values of the feeding types were also tested. Kruskal-Wallis test was used to estimate the mean difference of stable isotope values in potential food sources, and seasonally investigated functional groups and taxonomic groups of the Df. To evaluate homogeneity of variance, Levene's test was implemented before the statistical analyses. A cluster analysis based on the Euclidean distance was generated from the stable carbon isotope ratio of Df, to identify how habitat characteristics influenced on it. The relative dietary contribution of two food sources (viz., SOM and MPB) to Df, were quantified, using the Bayesian stable isotope mixing model in R (SIMMR) package (Parnell and Inger, 2016). The most utilised TEF in Korean tidal flat ($\delta^{13}\text{C}$, $1.3 \pm 0.3\text{‰}$; $\delta^{15}\text{N}$, $2.2 \pm 0.3\text{‰}$) was utilised for the stable isotope signatures of deposit-feeding consumers in SIMMR (McCutchan Jr et al., 2003).

2.3. Results and discussion

2.3.1. Spatial distribution of sedimentary organic matter

The spatial distribution of the physicochemical parameters of sediments (i.e., mud content, Chl-*a*, LOI, TOC, TN, carbon to nitrogen ratio [C/N], $\delta^{13}\text{C}$, and $\delta^{15}\text{N}$) were measured in the Ganghwa tidal flat (Table 2.3.). ANOVA with the Tukey post-hoc test revealed statistically significant differences in MC ($F=24.2$, $p<0.001$) and Chl-*a* ($F=3.4$, $p<0.05$) among the three sites (Table 2.4.). The lower MC ($57.6\pm23.4\%$) and Chl-*a* values ($25.7\pm10.5\text{ mg m}^{-2}$) in YC were distinctively characteristic compared to the other two sites, which contained relatively higher MC (DM, $91.5\pm7.4\%$; DG, $97.0\pm4.5\%$) and Chl-*a* (DM, $49.4\pm26.1\text{ mg m}^{-2}$; DG, $47.4\pm21.9\text{ mg m}^{-2}$) (Tables 2.3. and 2.5.).

There was no significant difference in any of the physicochemical parameters in the bare versus vegetated areas of the sandy mud site, YC. In contrast, spatial differences in C/N and $\delta^{13}\text{C}$ were detected in association with the distribution of halophytes in the mud site (C/N, $U=80.0$, $p<0.05$; $\delta^{13}\text{C}$, $U=10.0$, $p<0.05$) (Table 2.3.). Lower and higher mean C/N values were recorded in bare- and *P. australis*-sites ($8.8\pm0.6\%$ and $9.6\pm0.3\%$), respectively. Moderate C/N ($9.2\pm0.7\%$) in the *S. japonica*-bed was recorded. In contrast, the mean $\delta^{13}\text{C}$ ($-23.3\pm0.6\%$) was significantly lower at the *P. australis* site compared to bare areas ($-21.6\pm1.1\%$) and the *S. japonica* site ($-21.8\pm1.2\%$) in mud site. Even though there was no significant difference in the C/N and $\delta^{13}\text{C}$ of sediment between the bare and vegetated sites in YC, a similar trend was also detected between bare (C/N, $9.0\pm0.3\%$; $\delta^{13}\text{C}$, $-22.0\pm0.2\%$) and *P. australis*-beds (C/N, $10.2\pm1.8\%$; $\delta^{13}\text{C}$, $-22.6\pm0.9\%$).

The spatial distribution of Chl-*a* was primarily related to sediment property, namely MC, and influenced site-specific variations of benthic primary production in the Ganghwa tidal flat (Tables 2.3. and 2.5.) (Cahoon et al., 1999). Chl-*a*, degraded completely within 1 to 2 months in sediment, representing a useful indicator of fresh microalgae, such as MPB, and live-settled phytoplankton (Sun et al., 1993; Bianchi et al., 2000; Grippo et al., 2010; Grippo et al., 2011). It is possible to distinguish microalgae in sediment with enriched $\delta^{13}\text{C}$ and lower C/N values from

phytoplankton and terrestrial organic matter (France, 1995; Perdue and Koprivnjak, 2007). In the present study, higher Chl-*a* was detected in mud sites (DM and DG) compared to those in the sandy mud site (YC). However, we found no statistical differences to C/N ratio and $\delta^{13}\text{C}$ between sandy mud and mud sites (Table 2.3.). These results imply that a certain portion (~10%) of settled planktons (*Cyclotella* sp. and *Astronella* sp. in microscopic observation) in the given sites would potentially contribute as dietary sources for macrobenthos (Grippo et al., 2010).

The physical presence of vegetation contributes to absorbing hydrodynamic energy and trapping suspended organic matter (Mudd et al., 2010; Ha et al., 2018). High sediment C/N and depleted $\delta^{13}\text{C}$ observed in the vegetated flat, especially in the *P. australis*-bed, supported that more suspended-organic matter (such as phytoplankton and terrestrial materials) are deposited through the trapping effect (Li and Yang, 2009; Kon et al., 2012). The relatively short height and lower density of *S. japonica* compared to *P. australis* might have reduced the effectiveness of trapping, resulting in C/N and $\delta^{13}\text{C}$ values being similar to those of bare sediment at the mud site (DG) (Li and Yang, 2009). To improve our understanding on the relative contribution of MPB and live-settled phytoplankton to sediment, supplementary analysis of microalgal pigments would be useful. The taxa-dependent benthic productivity and/or their trophic contributions as potential food sources for the upper trophic organisms should be addressed by multiple examination.

Table 2.3.

Physicochemical parameters of sediments collected from Yeocha (YC), Dongmak (DM), and Donggeom (DG) on Ganghwa Island. All parameters are expressed as means values with standard deviations (mean±s.d.).

Location	Habitat type	Physicochemical parameter of sediment							
		MC ^a (%)	OC ^b (%)	TOC ^c (%)	TN ^d (%)	C/N ^e (%)	$\delta^{13}\text{C}$ ^f (‰)	$\delta^{15}\text{N}$ ^g (‰)	Chl- <i>a</i> ^h (mg m ⁻²)
YC-1	Sandy mud <i>Phragmites</i>	42.6±23.4	4.5±2.1	0.5±0.2	0.06±0.03	10.2±1.8	-22.6±0.9	9.0±1.7	31.8±12.0
YC-2	Sandy mud bare	72.6±5.5	6.0±3.0	0.7±0.2	0.08±0.02	9.0±0.3	-22.0±0.2	7.7±1.0	19.5±4.0
	Total	57.6±23.4	5.3±2.5	0.6±0.2	0.07±0.03	9.6±1.4	-22.3±0.7	8.3±1.4	25.7±10.5
DM-1	Mud <i>Suaeda</i>	90.7±8.9	7.0±2.8	0.9±0.2	0.10±0.02	9.2±1.0	-22.0±0.5	7.3±0.6	48.1±18.2
DM-2	Mud bare	92.3±6.9	7.9±3.6	1.2±0.2	0.14±0.03	8.3±0.1	-20.9±1.2	7.9±0.5	50.1±32.0
	Total	91.5±7.4	7.5±3.0	1.0±0.3	0.12±0.03	8.7±0.8	-21.5±1.0	7.6±0.6	49.4±26.1
DG-1	Mud <i>Phragmites</i>	93.4±6.9	7.5±2.4	1.2±0.2	0.13±0.02	9.6±0.3	-23.3±0.6	7.9±0.3	44.0±25.1
DG-2	Mud bare	98.6±0.6	7.2±2.4	0.9±0.2	0.09±0.03	9.3±0.5	-22.2±0.6	8.2±0.7	41.7±13.2
DG-3	Mud <i>Suaeda</i>	99.1±0.4	7.5±2.0	1.1±0.4	0.12±0.05	9.2±0.6	-21.6±1.6	8.7±1.3	56.6±27.9
	Total	97.0±4.5	7.4±2.1	1.1±0.3	0.11±0.04	9.3±0.5	-22.4±1.3	8.3±1.4	47.4±21.9

^a mud contents; ^b organic contents; ^c total organic carbon; ^d total nitrogen; ^e carbon to nitrogen ratio; ^f carbon stable isotope ratio; ^g nitrogen stable isotope ratio;

^h Chlorophyll-*a*.

Table 2.4.

Result of one-way analysis of variance (ANOVA) with Tukey post-hoc honest significant difference (HSD) test on the sediment characteristics and microalgal biomass measured at three sites (Yeocha, YC; Dongmak, DM; Donggeom, DG) on Ganghwa Island. Bold values indicate the significance at $p < 0.05$.

Sediment property	<i>df</i>	<i>F</i>	<i>p</i>	Tukey HSD*
Chl- <i>a</i> (mg m ⁻²)	2	3.42	<0.05	YC ^a , DM ^b , DG ^b
Mud content (%)	2	24.21	<0.001	YC ^a , DM ^b , DG ^b
Loss on ignition (%)	2	2.17	>0.05	–
Total organic carbon (%)	2	6.46	<0.01	YC ^a , DM ^b , DG ^b
Total nitrogen (%)	2	4.98	<0.05	YC ^a , DM ^{a,b} , DG ^b
Carbon to nitrogen ratio (%)	2	1.97	>0.05	–
$\delta^{13}\text{C}$ (‰)	2	1.45	>0.05	–
$\delta^{15}\text{N}$ (‰)	2	1.01	>0.05	–

*Sites grouped (a & b) by Tukey HSD test

Table 2.5.

Data on the seasonal sediment properties measured at three sites (Yeocha, YC; Dongmak, DM; Donggeom, DG) on Ganghwa Island from March 2018 to February 2019. All parameters are reported as mean with range (min.–max.).

Sediment property	Season	YC mean (min.–max.)	DM mean (min.–max.)	DG mean (min.–max.)
MC (%)	Spring	77.8 (76.9–78.8)	80.2 (78.3–82.0)	93.3 (83.2–98.7)
	Summer	46.8 (24.4–69.3)	97.3 (95.9–98.7)	97.6 (95.4–99.2)
	Fall	56.0 (36.4–75.6)	96.0 (95.4–96.6)	99.1 (98.6–99.5)
	Winter	49.8 (32.7–66.9)	92.6 (90.4–94.7)	98.1 (96.4–99.0)
	Total	57.6 (24.4–78.8)	91.5 (78.3–98.7)	97.0 (83.2–99.5)
LOI (%)	Spring	4.6 (4.3–5.0)	5.5 (4.8–6.2)	6.8 (6.1–7.8)
	Summer	9.1 (7.6–10.5)	12.0 (11.0–13.1)	10.5 (10.0–11.0)
	Fall	3.4 (2.8–4.1)	5.3 (5.1–5.5)	5.2 (5.0–5.0)
	Winter	3.9 (3.4–4.5)	7.1 (6.8–7.4)	7.1 (7.0–7.2)
	Total	5.3 (2.8–10.5)	7.5 (4.8–13.1)	7.4 (5.0–11.0)
TOC (%)	Spring	0.9 (0.9–0.9)	1.1 (0.9–1.4)	1.3 (0.9–1.6)
	Summer	0.4 (0.3–0.5)	1.1 (1.0–1.1)	0.9 (0.8–1.0)
	Fall	0.6 (0.5–0.7)	0.7 (0.6–0.9)	0.8 (0.5–1.2)
	Winter	0.6 (0.5–0.8)	1.2 (1.1–1.3)	1.3 (1.1–1.4)
	Total	0.6 (0.3–0.9)	1.0 (0.6–1.4)	1.1 (0.5–1.6)
TN (%)	Spring	0.10 (0.10–0.10)	0.13 (0.10–0.17)	0.14 (0.10–0.19)
	Summer	0.04 (0.04–0.05)	0.12 (0.12–0.13)	0.09 (0.08–0.11)
	Fall	0.06 (0.05–0.08)	0.09 (0.07–0.11)	0.09 (0.06–0.12)
	Winter	0.07 (0.05–0.09)	0.14 (0.12–0.16)	0.14 (0.13–0.15)
	Total	0.07 (0.04–0.10)	0.12 (0.07–0.17)	0.11 (0.06–0.19)
C/N (%)	Spring	8.6 (8.6–8.7)	8.6 (8.3–8.8)	9.0 (8.7–9.3)
	Summer	9.2 (8.9–9.4)	8.4 (8.3–8.6)	9.8 (9.4–10.1)
	Fall	10.0 (9.1–10.9)	9.5 (8.4–10.6)	9.4 (9.0–9.8)
	Winter	10.6 (8.7–12.4)	8.5 (8.2–8.7)	9.2 (8.6–9.8)
	Total	9.6 (8.6–12.4)	8.7 (8.2–10.6)	9.3 (8.6–10.1)

Table 2.5. (continued).

Sediment property	Season	YC mean (min.–max.)	DM mean (min.–max.)	DG mean (min.–max.)
$\delta^{13}\text{C}$ (‰)	Spring	–22.3 (–22.3 to –22.3)	–20.8 (–22.1 to –19.6)	–21.2 (–22.9 to –19.5)
	Summer	–21.9 (–22.0 to –21.9)	–20.2 (–22.3 to –22.0)	–22.8 (–23.0 to –22.7)
	Fall	–22.7 (–23.7 to –21.8)	–21.4 (–21.7 to –21.1)	–23.0 (–24.1 to –22.4)
	Winter	–22.2 (–22.7 to –21.7)	–21.0 (–22.0 to –20.0)	–20.6 (–22.9 to –18.3)
	Total	–22.3 (–23.7 to –21.7)	–21.4 (–22.3 to –19.6)	–22.2 (–24.1 to –18.3)
$\delta^{15}\text{N}$ (‰)	Spring	8.8 (8.8–8.9)	7.7 (7.4–7.9)	7.7 (7.5–7.8)
	Summer	9.1 (7.6–10.7)	7.0 (6.6–7.4)	9.1 (8.2–10.3)
	Fall	7.1 (6.8–7.3)	8.2 (8.0–8.4)	8.0 (7.8–8.4)
	Winter	7.3 (7.0–7.3)	7.7 (5.9–9.5)	8.4 (7.2–9.6)
	Total	8.2 (6.8–10.7)	7.6 (6.6–9.5)	8.3 (7.2–10.3)
Chl- <i>a</i> (mg m ^{–2})	Spring	26.2 (19.7–32.8)	84.0 (57.8–108.3)	70.9 (57.7–88.5)
	Summer	18.0 (14.6–21.3)	22.4 (20.6–27.0)	27.7 (23.0–30.1)
	Fall	24.6 (24.4–24.8)	29.2 (23.2–35.2)	30.0 (21.6–36.6)
	Winter	33.8 (19.4–48.2)	65.8 (61.0–70.6)	61.1 (47.3–71.2)
	Total	25.7 (14.6–48.2)	49.4 (22.4–84.0)	47.4 (21.6–88.5)
TN (%)	Spring	0.10 (0.10–0.10)	0.13 (0.10–0.17)	0.14 (0.10–0.19)
	Summer	0.04 (0.04–0.05)	0.12 (0.12–0.13)	0.09 (0.08–0.11)
	Fall	0.06 (0.05–0.08)	0.09 (0.07–0.11)	0.09 (0.06–0.12)
	Winter	0.07 (0.05–0.09)	0.14 (0.12–0.16)	0.14 (0.13–0.15)
	Total	0.07 (0.04–0.10)	0.12 (0.07–0.17)	0.11 (0.06–0.19)
C/N (%)	Spring	8.6 (8.6–8.7)	8.6 (8.3–8.8)	9.0 (8.7–9.3)
	Summer	9.2 (8.9–9.4)	8.4 (8.3–8.6)	9.8 (9.4–10.1)
	Fall	10.0 (9.1–10.9)	9.5 (8.4–10.6)	9.4 (9.0–9.8)
	Winter	10.6 (8.7–12.4)	8.5 (8.2–8.7)	9.2 (8.6–9.8)
	Total	9.6 (8.6–12.4)	8.7 (8.2–10.6)	9.3 (8.6–10.1)

*MC, mud content; OC, organic content; TOC, total organic carbon; TN, total nitrogen; C/N, carbon to nitrogen ratio; $\delta^{13}\text{C}$ and $\delta^{15}\text{N}$, carbon and nitrogen stable isotope ratios; Chl-*a*; Chlorophyll-*a*

2.3.2. Benthic food web structure

Two stable isotope values were significantly different between all the potential food sources investigated ($\delta^{13}\text{C}$, $H=44.3$, $p<0.001$; $\delta^{15}\text{N}$, $H=27.1$, $p<0.001$) (Fig. 2.2., Table 2.6.). The $\delta^{13}\text{C}$ of the food sources greatly varied from halophytes (*P. australis*, $-26.3\pm0.7\text{‰}$; *S. japonica*, $-25.8\pm1.7\text{‰}$) to meiofauna ($-15.3\pm0.5\text{‰}$). Other food sources exhibited moderate values of $\delta^{13}\text{C}$ being distributed between these two extremes (SOM, $-22.1\pm1.1\text{‰}$; POM, $-21.3\pm1.9\text{‰}$; MPB, $-18.9\pm1.2\text{‰}$). Similarly, $\delta^{15}\text{N}$ values of the food sources also revealed significantly varied distribution showing either depleted- or enriched $\delta^{15}\text{N}$ signature for POM ($7.7\pm1.0\text{‰}$) and meiofauna ($12.5\pm0.6\text{‰}$), respectively. The $\delta^{15}\text{N}$ of other potential food sources fell between these extremes (SOM, $8.1\pm1.0\text{‰}$; MPB, $8.7\pm2.0\text{‰}$; *P. australis*, $11.3\pm2.5\text{‰}$; *S. japonica*, $11.5\pm1.9\text{‰}$).

The potential food sources including POM, SOM, *P. australis*, and *S. japonica* identified in the Ganghwa tidal flat were within the reported values of $\delta^{13}\text{C}$ and $\delta^{15}\text{N}$ from the West and South coasts of Korea, supporting the representativeness of the study area as a typical Korean tidal flat (Table 2.7.).

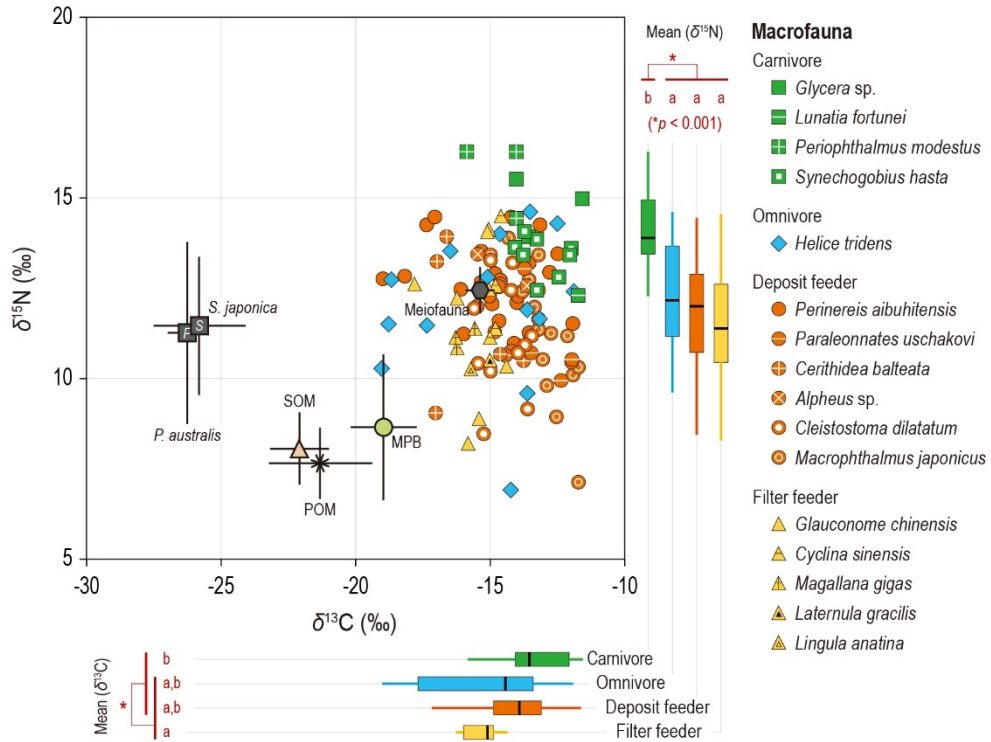


Table 2.6.

Stable carbon and nitrogen isotope values ($\delta^{13}\text{C}$ and $\delta^{15}\text{N}$) of food sources (sediment organic matter, SOM; particulate organic matter, POM; microphytobenthos, MPB; halophytes; meiofauna) and macrofauna collected from Yeocha (YC), Dongmak (DM), and Donggeom (DG) on Ganghwa Island from March 2018 to February 2019, with corresponding trophic level (TL). The feeding types of macrofauna are indicated (deposit feeders, Df; filter feeders, Ff; omnivores, Om; carnivores, Ca). Isotopic values are given as means with range (min.–max.).

Sample	$\delta^{13}\text{C}$ (‰)			$\delta^{15}\text{N}$ (‰)					
	YC	DM	DG	YC	TL	DM	TL	DG	TL
	mean (min. to max.)	mean (min. to max.)	mean (min. to max.)	mean (min.–max.)		mean (min.–max.)		mean (min.–max.)	
POM	–21.4 (–22.5 to –19.7)	–21.5 (–23.2 to –19.1)	–20.9 (–24.4 to –17.6)	7.9 (6.3–9.6)		7.2 (6.1–8.1)		7.9 (6.1–8.1)	
SOM	–22.3 (–23.7 to –21.8)	–21.5 (–22.3 to –19.6)	–22.4 (–24.1 to –19.5)	8.3 (6.8–10.7)		7.6 (6.6–8.4)		8.3 (7.5–10.3)	
MPB	–19.7 (–21.1 to –18.3)	–19.0 (–19.2 to –18.5)	–18.1 (–20.2 to –16.6)	8.7 (5.1–10.8)		8.0 (5.5–10.4)		9.4 (8.1–11.8)	
Halophyte									
<i>Pragmites australis</i>	–26.0 (–26.9 to –24.6)	–	–26.5 (–26.7 to –26.3)	11.7 (7.2–14.1)		–		11.0 (8.9–13.1)	
<i>Suaeda japonica</i>	–	–25.7 (–27.4 to –24.1)	–25.9 (–28.5 to –24.4)	–		11.2 (8.7–13.3)		11.8 (9.4–14.2)	
Meiofauna	–15.8 (–16.2 to –15.4)	–14.7 (–14.9 to –14.5)	–14.7 (–15.7 to –15.4)	12.3 (11.3–13.2)	2.5	12.0 (11.2–12.8)	2.3	13.2 (13.1–13.3)	2.9
Macrofauna									
Polychaeta									
(Df) <i>Perinereis aibuhitensis</i>	–13.7 (–17.2 to –11.8)	–14.6 (–15.8 to –13.4)	–15.3 (–18.8 to –13.4)	12.9 (11.5–14.2)	2.8	11.6 (10.7–12.5)	2.2	12.9 (11.0–14.4)	2.8
(Df) <i>Paraleonnates uschakovi</i>	–12.8 (–13.3 to –12.3)	–11.9 (–12.0 to –11.8)	–13.6 (–13.6 to –13.6)	10.4 (10.0–10.7)	1.6	10.6 (10.5–10.7)	1.7	13.1 (13.1–13.2)	2.8
(Ca) <i>Glycera</i> sp.	–11.6 (–11.6 to –11.5)	–13.6 (–13.8 to –13.3)	–14.0 (–14.2 to –13.9)	15.0 (15.0–15.0)	3.7	13.9 (13.8–14.1)	3.2	15.5 (15.2–15.9)	3.9
Bivalvia									
(Ff) <i>Glaucanome chinensis</i>	–14.8 (–15.1 to –14.4)	–15.4 (–15.5 to –15.4)	–16.0 (–17.8 to –15.1)	12.2 (10.4–14.1)	2.4	8.9 (8.9–8.9)	0.9	12.0 (8.3–14.2)	2.3
(Ff) <i>Cyclina sinensis</i>	–	–14.9 (–15.0 to –14.8)	–14.7 (–14.8 to –14.6)	–		11.3 (11.2–11.4)	2.0	13.6 (12.6–14.5)	3.1
(Ff) <i>Magallana gigas</i>	–16.0 (–16.3 to –15.6)	–	–	11.2 (10.9–11.4)	2.0	–	–	–	
(Ff) <i>Laternula gracilis</i>	–	–15.0 (–15.0 to –15.0)	–	–		10.5 (11.2–11.4)	1.7	–	
Lingulata									
(Ff) <i>Lingula anatine</i>	–	–15.7 (–15.8 to –15.6)	–	–		10.3 (10.0–10.6)	1.6	–	
Gastropoda									
(Df) <i>Cerithidea balteata</i>	–	–14.2 (–14.5 to –13.6)	–16.4 (–16.9 to –15.2)	–		10.6 (10.5–10.7)	1.7	12.2 (9.1–13.9)	2.4
(Ca) <i>Lunatia fortune</i>	–11.7 (–11.7 to –11.7)	–	–	12.3 (12.2–12.4)	2.5	–	–	–	
Malacostraca									
(Df) <i>Alpheus</i> sp.	–13.6 (–13.6 to –13.5)	–	–15.4 (–15.4 to –15.4)	12.6 (12.5–12.7)	2.6	–		13.5 (13.4–13.5)	3.0
(Df) <i>Cleistostoma dilatatum</i>	–14.0 (–15.3 to –13.3)	–14.8 (–14.8 to –14.7)	–14.3 (–15.5 to –13.1)	10.4 (9.2–11.2)	1.6	10.8 (10.2–11.3)	1.8	11.8 (8.5–13.3)	2.3
(Df) <i>Macrophthalmus japonicus</i>	–12.4 (–14.2 to –11.6)	–13.3 (–14.9 to –12.6)	–13.0 (–13.5 to –12.4)	10.8 (7.1–13.9)	1.8	11.4 (9.8–13.5)	2.1	11.7 (9.0–13.4)	2.2
(Om) <i>Helice tridens</i>	–14.5 (–17.4 to –11.9)	–14.1 (–16.5 to –12.5)	–16.1 (–19.0 to –13.5)	11.2 (6.9–14.0)	2.0	13.2 (11.7–14.3)	2.9	11.9 (9.6–14.6)	2.3
Actinopterygii									
(Ca) <i>Periophthalmus modestus</i>	–14.9 (–15.8 to –14.0)	–	–14.0 (–14.1 to –14.0)	15.4 (14.4–16.3)	3.9	–		16.3 (16.0–16.5)	4.3
(Ca) <i>Synechogobius hasta</i>	–12.7 (–14.1 to –12.0)	–13.3 (–13.8 to –12.4)	–13.3 (–13.3 to –13.2)	13.6 (13.4–13.7)	3.1	13.2 (12.5–14.1)	2.9	13.9 (13.8–13.9)	3.2

Table 2.7.

Seasonal stable carbon and nitrogen isotopic values ($\delta^{13}\text{C}$ and $\delta^{15}\text{N}$) of potential food sources (particulate organic matter, POM; sediment organic matter, SOM; microphytobenthos, MPB). Isotopic values are reported as mean with range (min.–max.).

Sample	Season	$\delta^{13}\text{C}$ (‰)			$\delta^{15}\text{N}$ (‰)		
		YC mean (min. to max.)	DM mean (min. to max.)	DG mean (min. to max.)	YC mean (min.–max.)	DM mean (min.–max.)	DG mean (min.–max.)
POM	Spring	–22.5 (–22.9 to –22.1)	–21.4 (–21.5 to –21.2)	–17.6 (–17.9 to –17.4)	6.3 (6.2–6.4)	6.7 (6.3–7.0)	7.8 (7.6–8.0)
	Summer	–22.1 (–22.5 to –21.7)	–23.2 (–23.3 to –23.1)	–24.4 (–25.2 to –23.6)	7.4 (6.9–7.8)	6.1 (5.9–6.2)	7.7 (7.4–8.0)
	Fall	–21.3 (–21.5 to –21.1)	–22.1 (–22.8 to –21.5)	–22.0 (–22.5 to –21.4)	8.4 (7.8–9.1)	8.1 (7.7–8.4)	8.2 (7.2–9.3)
	Winter	–19.7 (–20.1 to –19.3)	–19.1 (–19.3 to –19.0)	–19.8 (–20.6 to –19.0)	9.6 (9.0–10.3)	8.1 (6.3–9.8)	7.8 (6.8–8.9)
	Total	–21.4 (–22.9 to –19.3)	–21.5 (–23.3 to –19.0)	–20.9 (–25.2 to –19.0)	7.9 (6.2–10.3)	7.2 (6.3–9.8)	7.9 (6.8–9.3)
SOM	Spring	–22.3 (–22.4 to –22.2)	–20.6 (–21.8 to –19.5)	–21.2 (–22.7 to –19.8)	8.9 (7.7–10.0)	7.8 (7.3–8.2)	7.7 (7.5–7.8)
	Summer	–21.9 (–22.1 to –21.8)	–22.1 (–22.4 to –21.9)	–22.8 (–23.0 to –22.6)	9.1 (7.4–10.8)	7.2 (6.7–7.6)	9.1 (8.1–10.2)
	Fall	–22.7 (–23.8 to –21.6)	–21.3 (–21.9 to –20.7)	–23.0 (–23.9 to –22.2)	7.1 (6.7–7.4)	8.3 (8.0–8.7)	8.0 (7.7–8.4)
	Winter	–22.4 (–22.7 to –21.7)	–21.0 (–22.0 to –20.0)	–20.0 (–22.9 to –18.3)	7.3 (7.0–7.6)	7.7 (5.9–9.5)	8.4 (7.2–9.7)
	Total	–22.3 (–23.8 to –21.6)	–21.3 (–22.4 to –19.5)	–21.9 (–23.9 to –18.3)	8.1 (6.7–10.8)	7.7 (5.9–9.5)	8.3 (7.2–10.2)
MPB	Spring	–18.3 (–18.7 to –17.8)	–18.5 (–18.5 to –18.5)	–16.6 (–17.6 to –15.5)	5.1 (4.8–5.4)	5.5 (5.5–5.5)	8.6 (5.4–11.9)
	Summer	–21.1 (–21.2 to –21.0)	–19.1 (–19.4 to –18.8)	–18.2 (–18.4 to –17.9)	8.7 (7.5–10.0)	8.8 (7.4–10.1)	8.9 (7.3–10.5)
	Fall	–20.4 (–21.4 to –19.3)	–19.2 (–19.2 to –19.2)	–20.2 (–21.5 to –18.9)	10.2 (8.2–12.2)	10.4 (10.4–10.4)	11.8 (10.3–13.4)
	Winter	–19.0 (–19.9 to –18.0)	–19.1 (–19.8 to –18.5)	–17.7 (–17.8 to –17.5)	10.8 (9.5–12.1)	7.3 (3.6–11.0)	8.1 (7.3–8.9)
	Total	–19.7 (–21.4 to –17.8)	–19.1 (–19.8 to –18.5)	–18.1 (–21.5 to –15.5)	8.7 (4.8–12.2)	8.0 (3.6–11.0)	9.4 (5.4–13.4)
Halophyte <i>Phragmites</i>	Spring	–26.2 (–26.3 to –26.1)	–	–26.3 (–26.7 to –25.9)	11.6 (11.4–11.9)	–	13.1 (12.5–13.6)
	Summer	–26.3 (–26.6 to –26.0)	–	–26.6 (–27.0 to –26.2)	13.8 (13.8–13.8)	–	8.9 (8.8–8.9)
	Fall	–26.9 (–26.9 to –26.9)	–	–26.6 (–26.8 to –26.5)	14.1 (14.1–14.1)	–	12.4 (12.0–12.7)
	Winter	–24.6 (–24.9 to –24.3)	–	–26.7 (–27.3 to –26.0)	7.2 (7.1–7.2)	–	9.5 (8.9–10.1)
	Total	–24.6 (–24.9 to –24.3)	–	–26.5 (–27.3 to –25.9)	11.7 (7.1–14.1)	–	11.0 (8.8–13.6)
<i>Suaeda</i>	Spring	–	–27.4 (–27.7 to –27.2)	–25.5 (–25.8 to –25.3)	–	12.1 (11.3–13.0)	9.4 (9.4–9.4)
	Summer	–	–27.4 (–27.5 to –27.3)	–28.5 (–28.6 to –28.3)	–	10.7 (10.5–11.0)	12.7 (12.5–12.9)
	Fall	–	–27.1 (–24.3 to –23.8)	–24.4 (–24.5 to –24.3)	–	13.3 (13.1–13.4)	14.2 (13.7–14.8)
	Winter	–	–24.1 (–24.1 to –24.1)	–25.2 (–26.0 to –24.4)	–	8.7 (8.0–9.3)	10.9 (10.1–11.6)
	Total	–	–24.1 (–27.7 to –23.8)	–25.9 (–28.6 to –24.3)	–	11.2 (8.0–13.4)	11.8 (9.4–14.8)

The trophic role of salt marsh plants in coastal food web is still subject to debate. A previous study reported that the high content of indigestible fiber and low content of nitrogen in halophytes indicated that only grazers could utilize them as food sources (Mann, 1988). In parallel, Park et al. (2017) reported the low contribution of organic matter derived from marsh plants, such as *P. australis*- and *S. japonica*-bed, was indicative of the nutrition of consumers in the Suncheon tidal flat, Korea. However, the significant role of halophyte detritus as a primary food source to marine organisms was reported long before in coastal habitats (Teal, 1962). Therefore, we considered the very depleted $\delta^{13}\text{C}$ of the two halophytes in the present study are might have entered the benthic food web as deposited organic matter in the sediment of the Ganghwa tidal flat in a historical manner. Meiofauna with $\delta^{15}\text{N}$ and TL as a primary consumer did not represent a potential food source for other primary consumers (Table 2.6.). The stable isotope values of SOM were comparable to those of POM, and clearly reflected the well-coupled benthic and pelagic environments (Kon et al., 2012). Finally, it should be noteworthy that two potential food sources, namely SOM as environmental organic source pool and MPB as primary producer, for primary consumers were distinguished in the Ganghwa tidal flat.

A total of 16 species of benthic consumers was assigned to corresponding feeding types, including Ff, Df, Om, and Ca then their relationships were scrutinised. ANOVA with the Tukey post-hoc test revealed significant differences in the $\delta^{15}\text{N}$ of the consumers across four feeding types ($F=9.0$, $p<0.001$) (Fig. 2.2.). The significantly enriched mean $\delta^{15}\text{N}$ of Ca ($14.0\pm1.5\text{‰}$) was distinct to other feeding groups (Ff, $11.2\pm0.9\text{‰}$; Df, $11.8\pm0.8\text{‰}$; Om, $12.0\pm2.1\text{‰}$). The stepwise increase in the TL of macrobenthos, from Ff (2.0 ± 0.6) to Ca (3.4 ± 0.6), suggested the presence of approximately two TL in the Ganghwa benthic food web (Fig. 2.2., Table 2.6.). In specific, the most depleted- and enriched mean $\delta^{15}\text{N}$ values were detected for Ff, *Glauconome chinensis* ($8.9\pm0.0\text{‰}$), and carnivorous fish, *Periophthalmus modestus* ($16.3\pm0.2\text{‰}$), respectively (Table 2.6.). The largest $\delta^{15}\text{N}$ range was estimated for Om, *H. tridens* (Table 2.6.).

The $\delta^{13}\text{C}$ variation of macrobenthos was observed among four feeding groups (Fig. 2.2., Table 2.6.). ANOVA with the Tukey post-hoc test discriminated three

groups: Ff with the lowest mean $\delta^{13}\text{C}$ ($-15.4 \pm 0.5\text{‰}$), Ca with the highest value ($-13.1 \pm 1.2\text{‰}$), and all other feeders with moderate values (Df, $-14.1 \pm 1.1\text{‰}$; Om, $-15.2 \pm 2.4\text{‰}$) ($F=7.1$, $p<0.001$) (Fig. 2.2.). The largest and narrowest interspecific variation in mean $\delta^{13}\text{C}$ values were obtained for Df (7.2‰) and Ff (3.4‰), respectively. Om varied largely (7.1‰) and was comparable to that investigated in Df. Meantime, at the species level, the most depleted- and enriched $\delta^{13}\text{C}$ were recorded for Ff, *Magallana gigas* ($-16.0 \pm 0.4\text{‰}$) and Ca, *Glycera* sp. ($-11.6 \pm 0.1\text{‰}$), respectively (Table 2.6.).

Comparable mean $\delta^{15}\text{N}$ and TL of the three feeding groups (Ff, Df, and Om) showed that they were likely to utilize similar food sources, despite using different feeding strategies, around Ganghwa Island (Noh et al., 2019). For example, the $\delta^{15}\text{N}$ of Ff showed their lower trophic niche, with this group mainly preying on autotrophs (viz., MPB and phytoplankton) more than other primary consumers (McCutchan Jr et al., 2003; Noh et al., 2019). In contrast, the greatest $\delta^{15}\text{N}$ signature of fish revealed their trophic niche as top predators in the Ganghwa benthic food web. The largest intra-specific $\delta^{15}\text{N}$ variation of Om (*H. tridens*) supported its various trophic roles (herbivore, Df, and Ca) in the marsh ecosystem (Bang et al., 2019). However, the significantly distinguished $\delta^{15}\text{N}$ and TL of Om to Ca suggested that *H. tridens* had a functional role as a primary consumer, not Ca, in the Ganghwa tidal flat.

In the present study, we demonstrated the significantly lower $\delta^{13}\text{C}$ signature of Ff, indicating that they assimilated relatively more ^{13}C -depleted organic matter in their tissue compared to other functional feeding groups. However, the enriched $\delta^{13}\text{C}$ of Ff to organic matter (POM and SOM) reflected the significant contribution of resuspended MPB in the high benthic-pelagic coupling zone of the Ganghwa tidal flat (Griffiths et al., 2017). The four species (*Glycera* sp., *Lunatia fortunei*, *Periophthalmus modestus*, and *Synechogobius hasta*) had significantly high $\delta^{13}\text{C}$, reflecting their carnivorous feeding habit of consuming ^{13}C -enriched benthic invertebrates (Polychaeta, Bivalvia, Amphipoda, and Decapoda) in the study area (Choi et al., 1996; Chiba and Sato, 2012; Baeck et al., 2013; Fauchald, 1979). In general, Ff is exposed to variable and unpredictable food supplies compared to Df, which experience a more constant food supply (Levinton, 1972). However, variation

in $\delta^{13}\text{C}$ was lower in Ff compared to that in Df, demonstrating a constant food supply around Ganghwa Island, in which the massive production and resuspension of MPB both contributing sediment and water column productivity were characteristic (Lee et al., 2019). In contrast, greater variation in the $\delta^{13}\text{C}$ of Df and Om reflected their flexibility in feeding strategies, utilizing the most abundant food resource, irrespective of dietary quality (Lange et al., 2019).

2.3.3. Spatial variation in the stable isotopes of deposit feeders

The $\delta^{13}\text{C}$ of Df varied spatially, ranging from -18.8‰ to -11.6‰ , primarily depending on habitat characteristics, such as sediment mud content (sandy mud or mud) and halophyte distribution (bare, *P. australis* or *S. japonica*) around Ganghwa Island (Fig. 2.3.). In the sandy mud site, Df had significantly enriched mean $\delta^{13}\text{C}$ compared to those in the mud site (sandy mud, $-13.3\pm 1.4\text{‰}$; mud, $-14.5\pm 1.4\text{‰}$) ($F=11.2$, $p<0.001$) (Fig. 2.3.A). In contrast, the $\delta^{15}\text{N}$ of Df did not significantly differ between sandy mud and mud sites, ranging from 7.1‰ to 14.4‰ ($F=1.1$, $p>0.05$) (Fig. 2.3.A).

The mean $\delta^{13}\text{C}$ of Df was significantly enriched in bare sites ($-13.3\pm 1.0\text{‰}$) compared to vegetated ones ($-14.7\pm 1.6\text{‰}$) ($F=14.7$, $p<0.001$) (Fig. 2.3.B.). In addition, Df from the *S. japonica*-bed had relatively enriched mean $\delta^{13}\text{C}$ ($-14.5\pm 1.2\text{‰}$) compared to those in the *P. australis*-bed ($-14.8\pm 1.8\text{‰}$). However, there was no significant difference in the mean $\delta^{15}\text{N}$ of Df between bare sites ($11.8\pm 1.4\text{‰}$) and vegetated sites ($11.8\pm 1.6\text{‰}$) ($F=0.02$, $p>0.05$).

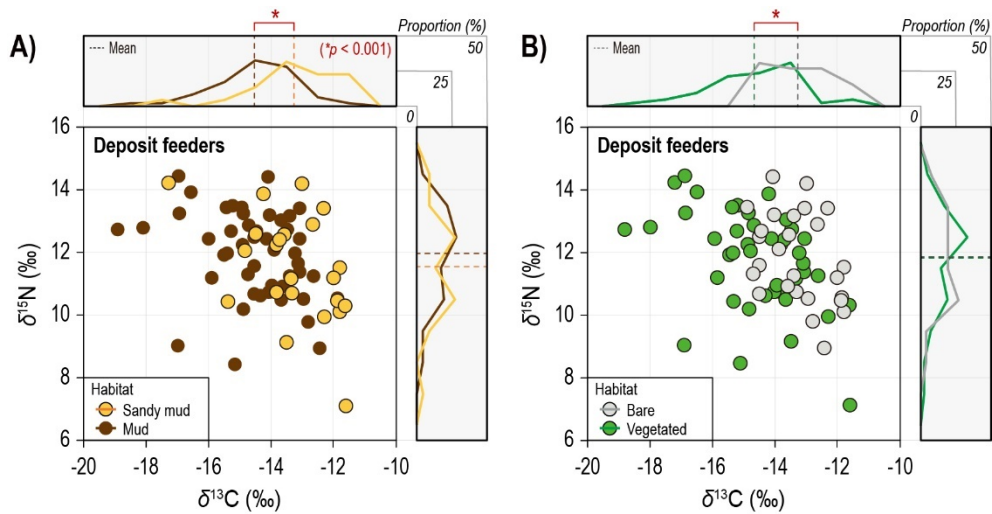


Figure 2.3.

Biplots of stable carbon and nitrogen isotope compositions ($\delta^{13}\text{C}$ and $\delta^{15}\text{N}$) of deposit feeders by (A) sediment properties (sandy mud and mud) and (B) vegetation type (bare- and vegetated tidal flat) in the Ganghwa tidal flat. The values of the deposit feeders represent the mean of each species sampled at each site during the study period. An asterisk indicates statistical significance.

Next, cluster analysis was performed to identify (dis)similarity of Df that had similar stable carbon isotope values and the results indicated three representative groups being delineated (Group 1, 2, and 3) from the five habitat types around Ganghwa Island (Fig. 2.4.A.). First, the most enriched $\delta^{13}\text{C}$ deposit feeders in the sandy mud bare site (YC; $-12.5 \pm 0.7\text{‰}$) were grouped with a relatively narrow range of $\delta^{13}\text{C}$ (-13.6‰ to -11.8‰ ; Group 1). Group 2 encompassed three sites (mud bare, sandy mud *P. australis*, and mud *S. japonica*). In general, Group 2 assemblage had moderate $\delta^{13}\text{C}$ values (mean: $-14.0 \pm 1.2\text{‰}$; range: -18.0 to -11.6‰). Finally, Group 3 was represented by the mud *P. australis* site, with the most depleted $\delta^{13}\text{C}$ signature (mean: $-15.9 \pm 1.5\text{‰}$; range: -18.3 to -13.1‰), which was distinct to the other groups (Fig. 2.4.A').

Overall, the mean dietary contribution of MPB (range: 79.5–97.4%) to Df exceeded that of SOM (range: 2.6–20.5%) in Ganghwa tidal flat. The MPB contribution is higher than the values previously reported in the salt marshes of China (Yellow Sea, 28.1 %; South China Sea, 32.7%) (Feng et al., 2015; Arbi et al., 2018; Chen et al., 2018; Qu et al., 2019). The result broadly reflects the higher significance of MPB as a diet source for the upper trophic organisms in the typical Korean tidal flat compared to that in China.

The five habitat groups of Df (delineated by cluster analysis) clearly indicated the habitat-specific dietary contribution (SOM and MPB) in Ganghwa tidal flat (Fig. 2.4.B.). Overall, the mean dietary contribution of MPB (range: 79.5–97.4%) to Df exceeded that of SOM (range: 2.6–20.5%) in Ganghwa tidal flat. The highest and lowest MPB contributions were obtained in Group 2 (mean: $95.8 \pm 2.1\%$) and Group 3 (mean: $79.5 \pm 18.4\%$), respectively. The MPB contribution to Group 1 (mean: $88.9 \pm 6.8\%$) was higher than Group 3 but lower than Group 2. In particular, the mixing model revealed the relatively more complex diet utilisation of Df in both the *P. australis*-bed of Group 2 and 3 based on a wider range of credibility intervals between dietary contributions. However, lower complexity in dietary sources of Df was detected in the *S. japonica*-bed comparable to the bare mud site in Group 2.

In general, our results demonstrated the habitat-specific $\delta^{13}\text{C}$ dynamics of deposit-feeding macrobenthos in the Ganghwa tidal flat. Differences to the $\delta^{13}\text{C}$ of

Df might have been influenced by variation in the sediment mud content of different habitats. First, the spatial distribution of sediment grain size altered the relative abundance of MPB, phytoplankton, and plant detritus in the sediments of Ganghwa tidal flat. Mud sediment has higher organic cohesion compared to sandy sediment, accordingly the relative ratio of plant detritus and/or microalgae would have reflected spatial differences to the $\delta^{13}\text{C}$ of Df (Grippo et al., 2011). Second, the various sediment-organic matter binding capacity might have influenced on the $\delta^{13}\text{C}$ dynamics of Df in the study area. A previous study reported that the ^{13}C -depleted organic matter is generally widely distributed in sediment with high mud content (Burdige, 2007; Lee et al., 2019). Thus, the depleted $\delta^{13}\text{C}$ values of Df in the mud sites (DM and DG) might reflect that they consumed more ^{13}C -depleted organic matter compared to those inhabiting the sandy mud site (YC). Third, the different degree of motility between epipellic and epipsamic MPB might also influence MPB intake rates of Df. The epipellic MPB in muddy sediments have greater motility compared to epipsamic MPB that attach to sandy sediment (Consalvey et al., 2004; Cartaxana et al., 2011). Therefore, more active epipellic diatoms in mud site (DM and DG) might have disturbed predation rates of Df, and further influenced on the $\delta^{13}\text{C}$ signature.

The significantly depleted $\delta^{13}\text{C}$ of Df inhabiting marsh-plant habitat supported several previous findings (Park et al., 2017), and generally reflected a change in the contribution of specific primary producers to consumer nutrients (Olsen et al., 2011; Park et al., 2016). This phenomenon was ascribed to deposited ^{13}C -depleted potential food sources, such as phytoplankton and terrestrial materials trapped in marsh-plant habitats (*P. australis*, and *S. japonica*) (Li and Yang, 2009; Kon et al., 2012). The slightly depleted $\delta^{13}\text{C}$ of Df in the *P. australis*-bed compared to that in the *S. japonica*-bed revealed the increased contribution of ^{13}C -depleted food sources on it. The trapping effect was significantly enhanced by the high density and the greater height of *P. australis* (Li and Yang, 2009).

Of note, the three delineated Df groups by cluster analysis indicated that three key variables determine the $\delta^{13}\text{C}$ dynamics of deposit feeders. In order of relative significance, these were: 1) presence of vegetation, 2) sediment particle size (i.e.,

mud content), and 3) species of vegetation. In particular, the wide range of $\delta^{13}\text{C}$ in vegetated sites showed that the presence of vegetation induced additional food sources for deposit feeders, including both trapped sediment organic matter and halophyte detritus. Overall, the benthic communities were largely and collectively influenced by the differences in the availability of foods across habitats, site-specific differences in mud content, and the composition of salt marsh vegetation.

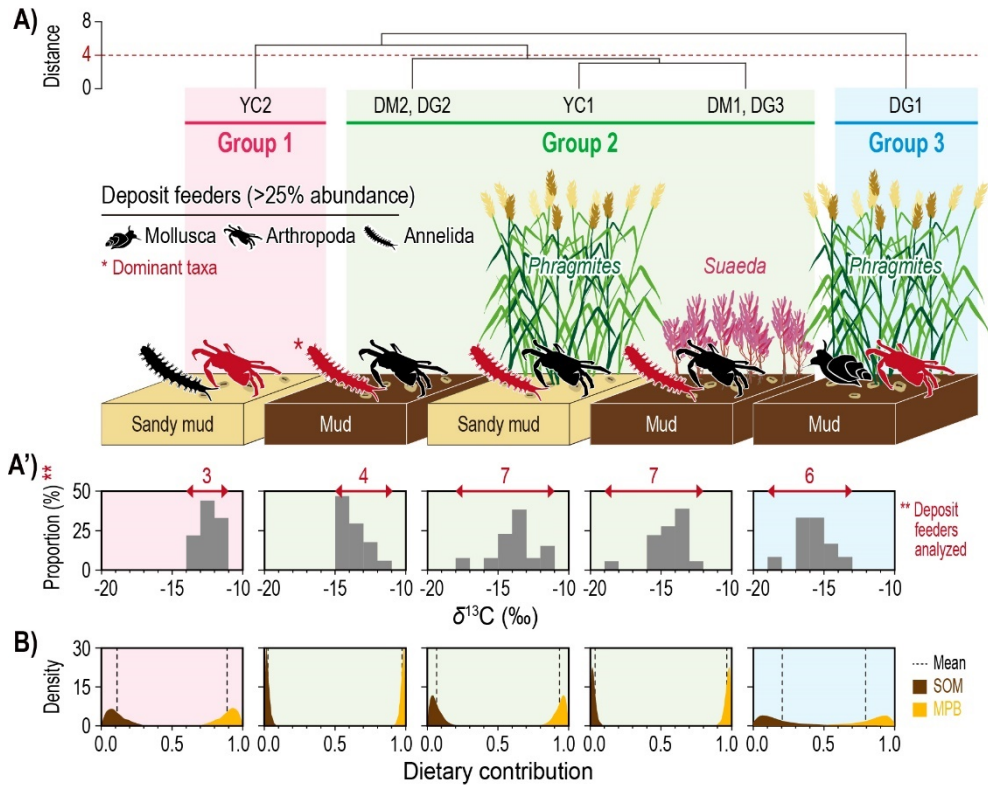
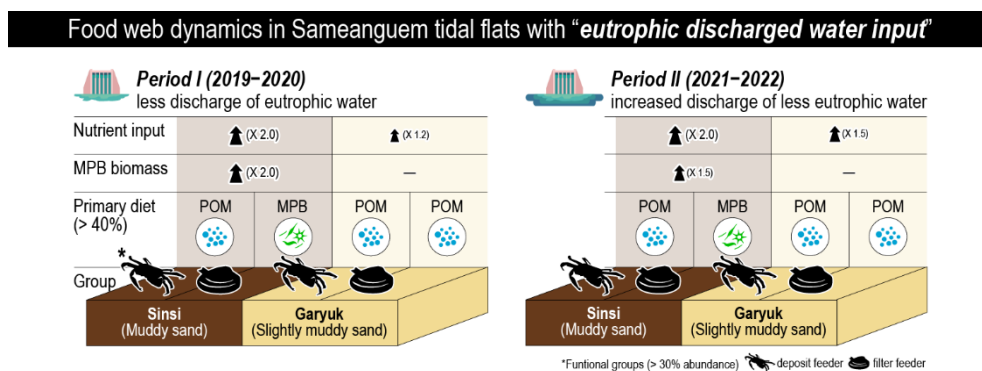


Figure 2.4.

(A) Group of deposit feeders determined by cluster analysis, based on the measured stable carbon isotope values ($\delta^{13}\text{C}$). The representative phylum of macrofauna (> 25% in relative abundance) is indicated for five habitat types (sandy mud bare; mud bare; sandy mud *Phragmites*; mud *Suaeda*; mud *Phragmites*). The top dominant phylum is shown in red. (A') The proportional distribution of $\delta^{13}\text{C}$ of the deposit feeders; (B) Probability density and mean dietary contribution of potential food sources (SOM and MPB) to deposit feeders in five habitat types.

CHAPTER 3.

Food web structure of Saemangeum tidal flat in Korea with water discharge from a dike



This chapter is in preparation.

3.1. Introduction

The Yellow Sea possesses the largest ($>18,000 \text{ km}^2$) tidal flat in the world (Koh and de Jonge, 2014). It is well known as the world's top marine biodiversity hotspot, with high primary productivity (Costello et al., 2010; Kwon et al., 2020). However, this ecologically important tidal flat has been affected by various anthropogenic activities, such as sewage input, port development, dredging and reclamation (Gray, 1997; Feebarani et al., 2016). Many reclamation projects have been conducted in Korea in the last century for national expansion and to secure industrial land, and the Saemangeum projects have been recognised as among the worst (Koh and Khim, 2014), with a 400 km^2 tidal flat area converted to dry land after the completion of the Saemangeum dike (length, 33.9 km) in 2006.

After dike completion, the water quality of the Saemangeum Lake deteriorated due to poor circulation and consistent sewage input from the Mangyeong and Dongjin Rivers (Choi et al., 2013). The water quality and environmental conditions of the lake have relied greatly on exchange through the Sinsi and Garyuk water gates (Kim et al., 2007; MOMAF, 2007; MOMAF, 2009). Thus, eutrophic discharge during this exchange has raised increasing concern, with many questions about its influence on the tidal-flat ecosystem structure and function remaining unanswered.

Studies of the Saemangeum tidal flat have increased since the initiation of dike construction. The succession of benthic and pelagic communities, accompanied by substantial environmental changes (e.g., eutrophication and desalination), in the inner lake has been reported (Table 3.1.) (Park et al., 2009; Ryu et al., 2011a and b; Ryu et al., 2014; Oda et al., 2018; Kim et al., 2020a and b). Fewer studies have focused on the sediment conditions (heavy metal and organic contaminants, suspended sediment distribution, and topography) and macrobenthic community structure of the outer tidal flat (An et al., 2006; Hong et al., 2006; Yoon et al., 2017). A limited number of studies has examined the influence of discharged water on the benthic community structure in the outer tidal flat (Table 3.1.) (Lee et al., 2021; Kim et al., 2022). Lee et al. (2021) revealed that the benthic community structure near the dike's water gates was unstable due to water discharge disturbance. Kim et al. (2022)

reported that mud deposition due to dredging activity in the lake had resulted in the proliferation of opportunistic species in the outer tidal flat. An understanding of the food web structure and function in the Saemangeum tidal flat under water discharge disturbance is important for the future application of appropriate conservation and management efforts, but no study has examined this topic.

Carbon (C) and nitrogen (N) stable isotope values are used widely to investigate food web structure and function reflecting coastal ecosystem health (Layman et al., 2012). C stable isotope ranges for producers are photosynthetic pathway dependent, and thus reflect the diets of consumers in complex coastal ecosystems (Yu et al., 2010). The N stable isotope signatures of coastal organisms indicate trophic positions via relative diet/consumer tissue fractionations (Post, 2002). Bayesian community-wide metrics based on C and N isotope values effectively identify general patterns and enable comparison among periods in these ecosystems (Abrantes et al., 2014). As benthic invertebrates are relatively sedentary and perennial, their stable isotopic characteristics can be used to estimate the direction and intensity of environmental change (Boesch et al., 1976; Simboursa et al., 1995), and comparison between target consumers and potential food sources could reflect close and/or long-term associations (Riera et al., 1999; Bae et al., 2018). In addition, the various feeding strategies (e.g., deposit and filter feeding) of these organisms provide information about sensitivity to environmental changes. Thus, the C and N stable isotope signatures of benthic invertebrates are efficient indicators of environmental changes in coastal ecosystems.

We estimated the spatiotemporal food-web structure and function in the Saemangeum tidal flat under the influence of lake water discharge to understand implications and guide future appropriate ecosystem conservation and management actions. The study objectives were to 1) characterise the food web structure in the Saemangeum tidal flat, 2) determine the spatial and temporal stable isotope distributions for benthic consumers and their diet utilisation under water discharge input, and 3) compare the results with the food web structure and isotopic signature distributions in tidal flats on the western and southern Korean coasts by literature review.

Table 3.1.

Previous studies which conducted in the Saemangeum tidal flat, Korea. The black box indicates the previous study of food web structure in the Saemangeum tidal flat.

Research fields in previous studies			Lake	Tidal flat	References
Category 1	Category 2	Category 3	(n)	(n)	
Biota	Megafauna	Community structure	2	1	9; 12; 37
	Macrofauna	Community structure	7	5	1; 10; 11; 13; 20; 26; 27; 28; 29; 30; 36
		Taxonomy	0	1	32
	Meiofauna	Community structure	3	2	18; 21; 34
	Microfauna	Community structure	3	1	2; 5; 28
		Primary production	1	0	15
		Taxonomy	1	0	23
	Food web	Food web structure	0	0	
	Total		17	10	
Environment	Sediment	Heavy metal	1	1	25
		Organic contaminant	1	2	4; 36
		Physiochemical parameter	2	0	24; 33
		Suspended sediment distribution	0	1	19
	Water	Topography	1	1	17
		Hydrodynamics	1	0	16
		Sedimentation and sediment flux	0	2	10; 11
		Water quality parameter	8	0	3; 6; 7; 8; 14; 22; 31; 35
		Total		14	7

1, An et al., 2006; 2, Choi and Noh, 2008; 3, Choi et al., 2013; 4, Hong et al., 2006; 5, Jang et al., 2009; 6, Jeong and Kwak, 2021; 7, Kim and Park, 2015; 8, Kim et al., 2009; 9; Kim et al., 2020a; 10, Kim et al., 2020b; 11, Kim et al., 2022; 12, Ko et al., 2017; 13, Koo et al., 2008; 14, Kwak, 2019; 15, Kwon et al., 2016; 16, Lee and Park, 2013; 17, Lee et al., 2006; 18, Lee et al., 2009; 19, Lee et al., 2015; 20, Lee et al., 2021; 21, Oda et al., 2018; 22, Oh et al., 2016; 23, Park and Koh, 2012; 24, Park et al., 2009; 25, Ra et al., 2013; 26, Ryu et al., 2011a; 27, Ryu et al., 2011b; 28, Ryu et al., 2014; 29, Sato et al., 2019; 30, Sato, 2006; 31, Song et al., 2022; 32, Torii et al., 2010; 33, Woo et al., 2006; 34, Yoo et al., 2006; 35, Yoo et al., 2021; 36, Yoon et al., 2017; 37, Yoon et al., 2018

3.2. Materials and methods

3.2.1. Sample collection and preparation

A four-year-round seasonal sampling was conducted at six sites (Yami, YM; Sinsi, SS; Garyuk1, GR1; Garyuk2, GR2; Woryeon, WY; Anseong, AS) in the Saemangeum tidal flat from February 2019 to October 2022 (Fig. 3.1.). Among these, WY and AS are in the two lower reaches of the Mangyeong and Dongjin Rivers, respectively. Nutrient concentrations in the water column were collected in both sides (GR1 and GR2) of the Garyuk water gate to examine the influence of discharged water input on the outer tidal flat. Surface sediment (~0.5 cm) was collected in the tidal flat and stored in plastic bottles and transferred to the laboratory to analyze the general sediment parameters (water content, WC; mud content, MC). MC was estimated by the rapid partial analysis (Buchanan, 1984). Textural types of sediment were simply classified with the method in Flemming (2000). Homogenised fine sediment was used to analyze the total organic carbon (TOC) and total nitrogen (TN). The sediment sample was decalcified with 10% hydrochloric acid (HCl, Sigma Aldrich, St. Louis, MO) for TOC analysis. To measure benthic Chlorophyll-*a* (Chl-*a*), a proxy of microphytobenthos (MPB) biomass, surface sediment (~0.5 cm) was collected using a syringe corer ($\varnothing=3.0$ cm). The Chl-*a* samples were immediately frozen on dry ice and transported to the laboratory. The eluted Chl-*a* using 100% acetone (10 mL) (24 h, 4 °C) was extracted in the supernatant after centrifugation (3000 rpm, 5 min.). The absorbance of the extracted 3 mL solution in a quartz cuvette was measured using a spectrophotometer. The concentration of benthic Chl-*a* (mg m^{-2}) was calculated using equations in Lorenzen (1967). The photosynthetic activity of MPB was measured with a diving-PAM II fluorometer (Walz, Effeltrich, Germany). We converted the photosystem II electron transport rate (ETR) measured with a PAM fluorometer to primary production (PP) using the following formula (Blanchard et al., 2000):

$$\text{PP} (\text{mg C m}^{-2} \text{ h}^{-1}) = \text{Chl-}a (\text{mg m}^{-2}) \times 0.043 \times \text{ETR}$$

Potential diets (particulate organic matter in seawater, SPOM; sediment organic matter, SOM; microphytobenthos, MPB) and benthic consumers were seasonally sampled at the three tidal flats (YM, SS, and GR1) to estimate C and N stable isotope signatures. Particulate organic matter in the freshwater (FPOM) was only collected in WY and AS. SPOM and FPOM were pre-filtered in situ to remove zooplankton and large particles using a 200 μm mesh net. POM samples were re-filtered with a pre-combusted Whatman GF/F glass fiber filter ($\text{Ø}=0.7\ \mu\text{m}$). MPB mats were collected from the sediment surface ($\sim 0.5\ \text{cm}$) during low tide, and then it was extracted following the method in Couch (1989). All potential diets were freeze-dried and then homogenised for the next stable isotope analysis. Data for monthly water exchanges (i.e., freshwater outflow and seawater inflow) were offered by the ministry of environment (Fig. 3.2.).

Benthic consumers were collected by hands, and 54 species from five phyla (4 Annelida, 1 Brachiopoda, 33 Mollusca, 13 Arthropoda, and 3 Echinodermata) were classified by expert judgment. To identify the structure and function of the Saemangeum tidal-flat food web, they were also assigned to five functional feeding groups, such as grazer (Gr), filter feeder (Ff), deposit feeder (Df), omnivore (Om), and carnivore (Ca) (Table 3.2.). The muscle tissue of consumers was dissected, lyophilised, and homogenised for the next stable isotope analysis.

In addition, to estimate food web characteristics in the Saemangeum tidal flat, the C and N stable isotope data from potential diets to consumers (6 phyla, 11 classes, 218 species) reported in Southern and Western Korean tidal flats were collected from the previous publications ($n=21$) (Tables 3.3. and 3.4.).

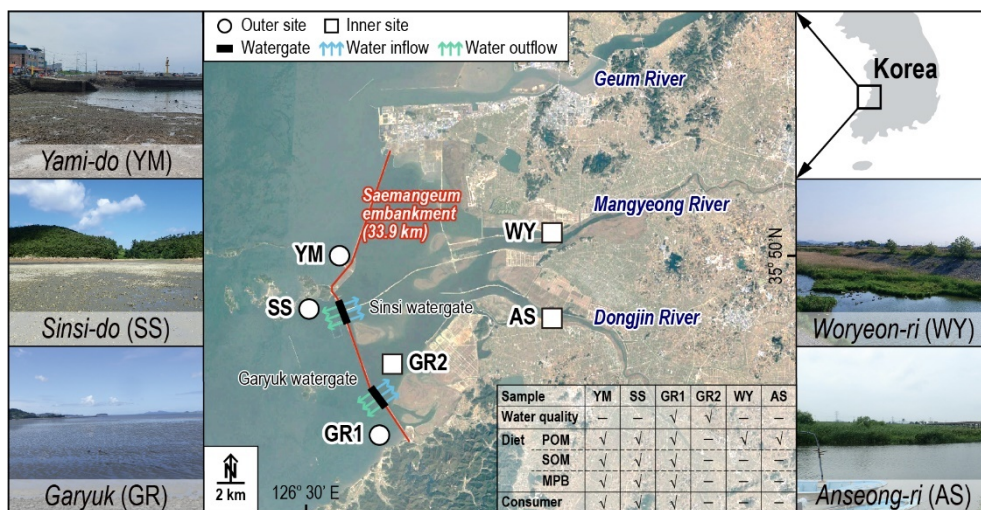


Figure 3.1.

Map showing the study area and information on samples (✓, collected; —, not collected) collected at six sites (Yami, YM; Sinsi, SS; Garyuk1, GR1; Garyuk2, GR2; Woryeon, WY; Anseong, AS) in the Saemangeum tidal flat and lake, Korea. YM is a reference site. In contrast, SS and GR1 are influenced by water discharge (green arrow) from the Sinsi- and Garyuk water gates (black rectangles). The blue arrow indicates the seawater input to the lake.

3.2.2. Stable isotope analysis

The fine powder of organic matter and MPB were decalcified for 24 h in HCl to estimate carbon stable isotope value. Lipid was extracted from the homogenised tissue using a dichloromethane/methanol (2:1, v/v) solvent (10 mL). The lipid-removal process was repeated 3 to 5 times, depending on the lipid content of the sample. Lipid-free samples were placed under a stream of nitrogen gas until they were fully dried. Consumers with exoskeletons (e.g., phylum Echinodermata) were decalcified with 1 N HCl to eliminate inorganic carbon for further carbon stable isotope analysis. Samples were weighed and wrapped in a tin capsule. An isotope ratio mass spectrometer connected to an elemental analyzer, EA-IRMS (Elementar, Hanau, Germany) was used to reveal carbon and nitrogen stable isotope signatures of samples. High-purity CO₂ and N₂ (99.999%) gas were used as reference gas, while He and O₂ were used as carrier and combustion gases, respectively. The percentage carbon and nitrogen composition of samples was directly determined after combustion in EA. The instrument calibrated the value based on standard sulphanilamide (C, 41.8%; N, 16.3%). Resultant gases (CO₂ and N₂) were transferred to the IRMS. Stable isotope abundance was expressed in delta (δ) notation relative to the conventional standard (C, Vienna Pee Dee Belemnite; N, atmospheric N₂), with the following formula:

$$\delta X (\text{‰}) = [(R_{\text{sample}} / R_{\text{reference}}) - 1] \times 1000$$

X: ¹³C or ¹⁵N

R: the ratios (¹³C/¹²C or ¹⁵N/¹⁴N)

IAEA-CH-3 (cellulose) and IAEA-N-2 (ammonium sulfate) was used for the internal calibration of ¹³C and ¹⁵N. Measurement precision of replication for $\delta^{13}\text{C}$ and $\delta^{15}\text{N}$ analyses was ca. 0.04‰ and 0.2‰.

3.2.3. Trophic level

The most utilised trophic enrichment factor (TEF) in Korean tidal flat, 2.2‰ was applied for $\delta^{15}\text{N}$ to examine the trophic level (TL) of the consumers (McCutchan Jr et al., 2003). The average $\delta^{15}\text{N}$ of all diets was utilised as a baseline value of the food web to accurate TL (Ramirez et al., 2021). The TL of benthic consumers was estimated using a formula published by Vander Zanden and Rasmussen (1999):

$$\text{TL}_i = (\delta^{15}\text{N}_i - \delta^{15}\text{N}_{\text{base}}) / \text{TEF} + \text{TL}_{\text{base}}$$

TL_i : TL of each species

$\delta^{15}\text{N}_i$: the $\delta^{15}\text{N}$ of species i

$\delta^{15}\text{N}_{\text{base}}$: the mean $\delta^{15}\text{N}$ of diets

TL_{base} : the TL of diets (TL=1)

3.2.4. Statistical analysis

The homogeneity of variance test was first performed before all parametric and non-parametric tests. One-way analysis of variance (ANOVA) with a Tukey post-hoc test was carried out to estimate the spatial and/or temporal mean differences in the pelagic- and benthic environments: 1) water exchange (inflow and outflow); 2) water quality parameters; 3) sediment physicochemical characteristics; 4) porewater nutrient concentration, 5) Chl-*a*, PP, and P/B of MPB. Pearson correlation analysis was additionally performed on the three nutrient concentrations in the water column between GR1 and GR2. ANOVA test was also conducted to examine the mean stable isotope differences among 1) four diets (FPOM, SPOM, SOM, and MPB); 2) five functional groups of consumers (Gr, Ff, Df, Om, and Ca); 3) spatially distributed diets and consumers in the Saemangeum tidal flat. An independent two-sample *t*-test was conducted on stable isotope values of diets and consumers at three sites (YM, SS, and GR1) located in outer tidal flat between period I (2019–2020) and period II (2021–2022). In addition, to evaluate the influence of the degree of water exchange on the food web in the outer tidal flat, we compared the $\delta^{13}\text{C}$ and $\delta^{15}\text{N}$ distributions of dominant functional groups of consumers (Ff and Df) between periods I and II.

Bayesian standard ellipse area (SEA_b) and niche space of consumers was calculated in the R (SIBER) package (Jackson et al., 2011). The small sample size corrected standard ellipse area (SEA_c) was calculated to compare niche space between two groups of benthos (Df and Ff) with a different number of components (Jackson et al., 2011). The Bayesian stable isotope mixing model in the R (SIMMR) package was used to examine spatiotemporal variation in the diet utilisation of two consumers. The most used TEF ($\delta^{13}\text{C}$, $1.3 \pm 0.3\text{‰}$; $\delta^{15}\text{N}$, $2.2 \pm 0.3\text{‰}$) in Korean tidal flat was applied to analyse the diet contribution to consumers in SIMMR (McCutchan Jr et al., 2003). Cluster analysis (CA) was performed to identify the spatiotemporal patterns in the diet utilisation of two consumer groups. Euclidean distance for cluster analysis was calculated based on the contribution of diets (SPOM, SOM, and MPB) to consumers at three sites (YM, SS, and GR1) between two periods. Statistical analyses were conducted in SPSS 26.0 (SPSS INC., Chicago, IL), PRIMER 6.1.16, and R 4.2.1.

Table 3.2.

List of benthic consumers with corresponding five functional groups (grazers; filter feeders; deposit feeders; omnivores; carnivores) collected in the Saemangeum tidal flat, Korea from 2019 to 2022.

Phylum	Species	Type	Reference
Annelida	Cirratulidae sp.	Deposit feeder	Ryckholdt, 1851
	<i>Glycera</i> sp.	Carnivore	Lee et al., 2021
	<i>Lumbrineris</i> sp.	Carnivore	Carrasco and Oyarzun, 1988
	Nereididae sp.	Deposit feeder	Lee et al., 2021
Brachiopoda	<i>Lingula unguis</i>	Filter feeder	Lee et al., 2021
Mollusca	<i>Anadara kagoshimensis</i>	Filter feeder	Hong, 2006
	<i>Batillaria cumingii</i>	Omnivore	*Sea life base
	<i>Batillaria multiformis</i>	Omnivore	*Sea life base
	<i>Bullacta caurina</i>	Grazer	Hong, 2006
	<i>Cyclina sinensis</i>	Filter feeder	Lee et al., 2021
	<i>Dosinia japonica</i>	Filter feeder	Hong, 2006
	<i>Glaucanome chinensis</i>	Filter feeder	Lee et al., 2021
	<i>Gomphina veneriformis</i>	Filter feeder	Shin et al., 2009
	<i>Laternula gracilis</i>	Filter feeder	Hong, 2006
	<i>Liolophura japonica</i>	Grazer	Hong, 2006
	<i>Lunatia fortunei</i>	Carnivore	Lee et al., 2021
	<i>Lunella coronata</i>	Grazer	Hong, 2006
	<i>Macoma</i> sp.	Deposit feeder	Hylleberg and Gallucci, 1975
	<i>Mactra quadrangularis</i>	Filter feeder	Noh et al., 2020
	<i>Magallana gigas</i>	Filter feeder	Lee et al., 2021
	<i>Megangulus</i> sp.	Deposit feeder	Hong, 2006
	<i>Meretrix lusoria</i>	Filter feeder	Yam et al., 2020
	<i>Monodonta labio</i>	Grazer	Takada, 1999
	Muricidae sp.	Carnivore	*Sea life base
	<i>Mya arenaria</i>	Filter feeder	Riisgard et al., 2003
	<i>Mytilus edulis</i>	Filter feeder	Riisgard et al., 2003
	<i>Mytilus galloprovincialis</i>	Filter feeder	Riisgard et al., 2003
	<i>Nerita japonica</i>	Grazer	Takada, 1999
	<i>Neverita didyma</i>	Carnivore	Chandler et al., 2008
	<i>Nuttallia japonica</i>	Deposit feeder	Tsuchiya and Kurihara, 1980
	<i>Rapana venosa</i>	Carnivore	Hong, 2006
	<i>Reishia clavigera</i>	Carnivore	*Sea life base
	<i>Reishia luteostoma</i>	Carnivore	Taylor and Morton, 1996
	<i>Ruditapes philippinarum</i>	Filter feeder	Wang et al., 2017
	<i>Saccostrea kegaki</i>	Filter feeder	Lee et al., 2021
	<i>Solen strictus</i>	Filter feeder	Hong, 2006
	<i>Tegula kusairo</i>	Grazer	Hong, 2006
	<i>Umbonium thomasi</i>	Filter feeder	Fretter, 1975
Arthropoda	<i>Alpheus</i> sp.	Deposit feeder	Lee et al., 2021
	<i>Charybdis japonica</i>	Carnivore	Oikawa et al., 2004
	<i>Diogenes nitidimanus</i>	Omnivore	Schembri, 1982
	<i>Gaice depressus</i>	Omnivore	Depledge, 1989
	<i>Helice tridens</i>	Omnivore	Lee et al., 2021
	<i>Hemigrapsus penicillatus</i>	Omnivore	Brousseau and Baglivo, 2005
	<i>Hemigrapsus sanguineus</i>	Omnivore	Brousseau and Baglivo, 2005
	<i>Macrophthalmus abbreviatus</i>	Deposit feeder	Lee et al., 2021
	<i>Macrophthalmus japonicus</i>	Deposit feeder	Lee et al., 2021
	<i>Neotrypaea japonica</i>	Filter feeder	*Sea life base

*Sea life base (<https://www.sealifebase.ca/>)

Table 3.2. (Continued.)

Phylum	Species	Type	Reference
Arthropoda	<i>Pyrhila pisum</i>	Deposit feeder	Hong, 2006
	<i>Upogebia major</i>	Filter feeder	*Sea life base
	Varunidae sp.	Omnivore	Brousseau and Baglivo, 2005
Echinodermata	<i>Ophioplocus</i> sp.	Carnivore	*Sea life base
	<i>Patiria pectinifera</i>	Carnivore	*Sea life base
	<i>Protankyra bidentata</i>	Deposit feeder	*Sea life base

*Sea life base (<https://www.sealifebase.ca/>)

Table 3.3.

Review of carbon and nitrogen stable isotope values ($\delta^{13}\text{C}$ and $\delta^{15}\text{N}$) of potential food sources (MPB, microphytobenthos; POM, particulate organic matter; SOM, sediment organic matter) in previous food web studies, western and southern tidal flats, Korea.

Coast	Site	Diet	$\delta^{13}\text{C}$ (‰)	$\delta^{15}\text{N}$ (‰)	References
South	–	MPB	–15.0	11.0	Kang et al., 2003
		POM (Marine)	–15.9	11.1	
		SOM	–13.3	10.5	
	Deukyang Bay	MPB	–14.0	11.0	Kang et al., 2003
		POM (Marine)	–21.0	10.8	
		SOM	–19.3	10.6	
	Dongdae Bay	MPB	–21.2	5.7	Ha et al., 2014
		POM (Marine)	–25.6	3.7	
		SOM	–19.1	5.5	
		MPB	–14.5	8.5	Park et al., 2013
		POM (Marine)	–20.8	5.3	
	Gangjin	MPB	–14.6	8.5	Park et al., 2017
		POM (Freshwater)	–25.1	10.3	
		POM (Marine)	–19.6	9.6	
		SOM	–21.9	8.9	
	Jinju Bay	MPB	–14.5	8.9	Kang et al., 2007
		POM (Freshwater)	–28.5	9.3	
		POM (Marine)	–21.1	5.5	
	Kwangyang Bay	MPB	–13.7	10.8	Kang et al., 2003
		POM (Freshwater)	–23.7	8.6	
		POM (Marine)	–20.2	11.0	
		SOM	–19.6	10.4	
	Nakdong River	MPB	–16.5	8.7	Choy et al., 2008
		POM (Marine)	–23.0	5.7	
	Namhae	POM (Marine)	–18.6	7.4	Park et al., 2021
		SOM	–18.6	6.5	
	Seomjin River Estuary	MPB	–19.8	10.7	Choi et al., 2017
		POM (Marine)	–20.8	7.6	
		SOM	–22.1	7.4	

Table 3.3. (Continued.)

Coast	Site	Diet	$\delta^{13}\text{C}$ (‰)	$\delta^{15}\text{N}$ (‰)	References
South	Seomjin River Estuary	POM (Freshwater)	-26.2	8.7	Park et al., 2020
		POM (Marine)	-19.2	7.7	
		SOM	-21.5	5.6	
	Suncheon	MPB	-14.1	9.0	Park et al., 2015
		POM (Freshwater)	-26.0	9.2	
		POM (Marine)	-20.0	9.0	
		SOM	-14.2	8.5	
		MPB	-14.2	8.8	Park et al., 2017
		POM (Freshwater)	-25.3	9.0	
		POM (Marine)	-19.5	9.0	
		SOM	-21.0	8.7	
	Yoja Bay	MPB	-15.3	8.7	Kang et al., 2015
		POM (Marine)	-19.7	8.5	
		SOM	-20.8	6.8	
		MPB	-14.5	10.8	Kang et al., 2003
		POM (Marine)	-20.2	11.0	
West	Ganghwa Island	SOM	-19.5	10.4	Lee et al., 2021
		MPB	-18.9	8.7	
		POM (Marine)	-21.3	7.7	
	Guem River Estuary	SOM	-22.1	8.1	Noh et al., 2019
		MPB	-17.6	4.7	
		POM (Freshwater)	-25.4	11.9	
		POM (Marine)	-21.9	6.7	
	Gyeonggi Bay	SOM	-20.8	5.9	Bang et al., 2019
		MPB	-14.7	4.2	
		SOM	-24.5	4.0	
	Hampyeong Bay	MPB	-14.8	8.9	Park et al., 2016
		POM (Marine)	-19.8	8.5	
		SOM	-17.7	7.1	
	Paldang Lake	POM (Freshwater)	-23.8	6.4	Gal et al., 2016
	Taean	MPB	-15.7	6.3	Han et al., 2015
		POM (Marine)	-20.7	6.0	

Table 3.3. (Continued.)

Coast	Site	Diet	$\delta^{13}\text{C}$ (‰)	$\delta^{15}\text{N}$ (‰)	References
West	Taean	MPB	−15.0	6.6	Han et al., 2015
		POM (Marine)	−20.5	6.6	
	Yeongsan River Estuary	POM (Marine)	−18.7	9.2	Park et al., 2020
		SOM	−21.3	7.0	

Table 3.4.

Review of stable carbon and nitrogen isotope values ($\delta^{13}\text{C}$ and $\delta^{15}\text{N}$) of potential diets in previous food web studies, western and southern tidal flats, Korea. Five functional groups of consumers are described by abbreviations (grazers, Gr; deposit feeders, Df; filter feeders, Ff; omnivores, Om; carnivores, Ca).

Coast	Site	Phylum	Class	Species	Type	$\delta^{13}\text{C}$ (‰)	$\delta^{15}\text{N}$ (‰)	References
South	Deukyang Bay	Mollusca	Bivalvia	<i>Ruditapes philippinarum</i>	Ff	-16.4	13.3	Kang et al., 2003
	Dongdae Bay	Annelida	Polychaeta	<i>Glycera</i> sp.	Ca	-14.0	14.8	Ha et al., 2014
				<i>Lumbrineris</i> sp.	Ca	-14.1	13.4	
		Arthropoda	Malacostraca	Benthic shrimp	Df	-12.3	10.3	
		Mollusca	Bivalvia	<i>Crassostrea gigas</i>	Ff	-19.5	9.9	
	Gangjin	Annelida	Polychaeta	<i>Glycera</i> sp.	Ca	-18.2	14.3	Park et al., 2017
				<i>Hediste japonica</i>	Om	-19.1	13.2	
				<i>Heteromastus filiformis</i>	Df	-20.7	12.1	
				<i>Phyllodoce koreana</i>	Ca	-15.9	12.6	
				<i>Tharyx</i> sp.	Df	-20.6	12.5	
		Arthropoda	Malacostraca	<i>Chiromantes haematocheir</i>	Df	-21.1	13.0	
				<i>Macrophthalmus japonicus</i>	Df	-14.6	10.6	
		Mollusca	Gastropoda	<i>Assiminea japonica</i>	Df	-18.4	11.5	
				<i>Batillaria cumingii</i>	Df	-17.3	12.2	
		Mollusca	Bivalvia	<i>Crassostrea gigas</i>	Ff	-20.1	11.4	
				<i>Jitlada culter</i>	Ff	-18.3	10.5	
				<i>Mytilus</i> sp.	Ff	-19.7	11.3	
	Jinju Bay	Mollusca	Bivalvia	<i>Ruditapes philippinarum</i>	Ff	-17.4	10.8	Kang et al., 2007
	Kwangyang Bay	Annelida	Polychaeta	<i>Aglaophamus gippslandicus</i>	Ca	-16.1	11.5	Kim et al., 2020
				<i>Aglaophamus sinensis</i>	Ca	-15.5	13.2	
				<i>Anaitides koreana</i>	Ca	-15.8	11.9	
				<i>Armandia lanceolata</i>	Df	-16.7	12.1	
				<i>Capitella capitata</i>	Df	-17.6	11.3	
				<i>Chaetozone setosa</i>	Om	-19.1	12.6	
				<i>Glycera alba</i>	Ca	-15.7	15.7	
				<i>Glycera chirori</i>	Ca	-16.6	13.1	
				<i>Hemipodus yenourensis</i>	Ca	-16.5	13.0	
				<i>Isolda pulchella</i>	Df	-18.7	11.5	
				<i>Lumbrineris</i> sp.	Ca	-16.6	12.7	

Table 3.4. (Continued.)

Coast	Site	Phylum	Class	Species	Type	$\delta^{13}\text{C}$ (‰)	$\delta^{15}\text{N}$ (‰)	References
South	Kwangyang Bay	Annelida	Polychaeta	<i>Magelona japonica</i>	Df	-17.0	9.9	Kim et al., 2020
				<i>Paraprionospio pinnata</i>	Df	-17.2	10.2	
				<i>Praxillella affinis</i>	Df	-19.3	14.1	
				<i>Prionospio japonicus</i>	Df	-17.5	7.8	
				<i>Scoletoma longifolia</i>	Ca	-16.9	11.3	
				<i>Sigambra tentaculata</i>	Ca	-16.1	13.2	
				<i>Sternaspis scutata</i>	Df	-17.8	9.7	
				<i>Terebellides stroemii</i>	Df	-18.9	11.7	
				<i>Tharyx monilaris</i>	Df	-18.6	13.0	
		Arthropoda	Malacostraca	<i>Gammaropsis japonica</i>	Ff	-20.4	9.0	
				<i>Melita</i> sp.	Df	-16.0	9.7	
				<i>Monocorophium acherusicum</i>	Ff	-17.9	9.0	
				<i>Photis</i> sp.	Ff	-15.6	10.4	
				<i>Sinocorophium japonicum</i>	Ff	-16.5	6.4	
				<i>Xenophthalmus pinnotheroides</i>	Df	-17.7	10.9	
		Mollusca	Gastropoda	<i>Philine orientalis</i>	Ca	-15.3	11.5	
			Bivalvia	<i>Arcuatula senhousia</i>	Ff	-18.7	14.1	
				<i>Nitidotellina minuta</i>	Df	-16.5	8.0	
				<i>Raetellops pulchella</i>	Df	-17.9	8.2	
				<i>Raphidopus ciliatus</i>	Df	-17.6	6.5	
				<i>Ruditapes variegatus</i>	Ff	-18.6	8.3	
				<i>Theora fragilis</i>	Df	-17.7	8.6	
Masan Bay		Mollusca	Bivalvia	<i>Ruditapes philippinarum</i>	Ff	-16.5	13.6	Kang et al., 2003
		Annelida	Polychaeta	<i>Perinereis aibuhitensis</i>	Df	-12.7	10.3	Kim et al., 2012
		Arthropoda	Malacostraca	<i>Oratosquilla oratoria</i>	Ca	-13.8	12.9	
		Mollusca	Bivalvia	<i>Atrina pinna</i>	Ff	-13.6	11.0	
				<i>Fulvia mutica</i>	Ff	-13.1	11.3	
				<i>Mytilus edulis</i>	Ff	-13.2	10.6	
				<i>Saxidomus purpurata</i>	Ff	-13.2	12.4	
Nakdong River		Annelida	Polychaeta	<i>Goniada japonica</i>	Ca	-14.0	18.5	Choy et al., 2008
				<i>Hediste japonica</i>	Om	-17.6	12.6	
				<i>Heteromastus filiformis</i>	Df	-19.7	13.6	

Table 3.4. (Continued.)

Coast	Site	Phylum	Class	Species	Type	$\delta^{13}\text{C}$ (‰)	$\delta^{15}\text{N}$ (‰)	References
South	Nakdong River	Annelida	Polychaeta	<i>Lumbrineris</i> sp.	Ca	-14.5	16.5	Choy et al., 2008
				<i>Tylorrhynchus heterochaetus</i>	Df	-17.9	15.1	
		Arthropoda	Malacostraca	<i>Helice tridens</i>	Om	-18.7	14.4	
				<i>Ilyoplax pusilla</i>	Df	-15.5	12.1	
				<i>Neotrypaea japonica</i>	Df	-15.2	12.2	
				<i>Paranthura</i> sp.	Df	-16.5	12.6	
				<i>Sesarma dehaani</i>	Df	-23.1	13.4	
		Mollusca	Gastropoda	<i>Angustassiminea castanea</i>	Df	-16.8	12.6	
				<i>Batillaria cumingii</i>	Df	-9.1	14.9	
				<i>Bullacta caurina</i>	Df	-7.9	13.7	
		Mollusca	Bivalvia	<i>Arcuatula senhousia</i>	Ff	-20.4	8.6	
				<i>Corbicula</i> sp.	Ff	-23.5	9.7	
				<i>Laternula gracilis</i>	Ff	-21.2	10.2	
	Namhae	Annelida	Polychaeta	<i>Aricidea assimilis</i>	Df	-15.8	9.7	Park et al., 2021
				<i>Chaetozone</i> sp.	Om	-15.6	12.7	
				<i>Diopatra bilobata</i>	Ca	-13.3	13.3	
				<i>Eteone longa</i>	Ca	-14.1	13.2	
				<i>Glycera chirori</i>	Ca	-12.8	14.6	
				<i>Heteromastus filiformis</i>	Df	-15.7	9.1	
				<i>Lumbrineris longifolia</i>	Ca	-13.5	13.6	
				<i>Magelona japonica</i>	Df	-16.6	11.4	
				<i>Marphysa sanguinea</i>	Ca	-12.1	14.9	
				<i>Nephtys polybranchia</i>	Ca	-15.2	12.5	
				<i>Prionospio pulchra</i>	Df	-15.6	9.3	
				<i>Spio martinensis</i>	Df	-16.0	9.4	
				<i>Travisia japonica</i>	Om	-14.9	11.5	
				<i>Urechis unicinctus</i>	Df	-15.3	9.0	
		Arthropoda	Malacostraca	Gammaridian amphipod	Df	-15.6	9.1	
				Isopoda unid.	Df	-16.6	9.1	
				<i>Pagurus</i> sp.	Om	-14.0	11.8	
				<i>Palaemon macrodactylus</i>	Ca	-12.9	13.3	
				<i>Upogebia major</i>	Ff	-17.2	9.9	

Table 3.4. (Continued.)

Coast	Site	Phylum	Class	Species	Type	$\delta^{13}\text{C}$ (‰)	$\delta^{15}\text{N}$ (‰)	References
South	Namhae	Echinodermata	Ophiuroidea	<i>Amphiura aestuarii</i>	Om	-14.4	13.4	Park et al., 2021
		Mollusca	Bivalvia	<i>Arcuatula senhousia</i>	Ff	-17.9	9.5	
				<i>Nitidotellina nitidula</i>	Df	-16.1	8.6	
				<i>Nucula paulula</i>	Df	-15.2	8.8	
				<i>Pillucina pisidium</i>	Ff	-18.1	9.4	
		Gastropoda		<i>Ceratostoma burnetti</i>	Ca	-12.6	13.8	
				<i>Crepidula onyx</i>	Ff	-17.9	8.9	
				<i>Sydaphera spengleriana</i>	Ca	-13.7	13.2	
	Seomjin River Estuary	Annelida	Polychaeta	<i>Ampharete arctica</i>	Df	-17.8	14.4	Park et al., 2020
				<i>Amphicteis gunneri</i>	Df	-16.6	11.0	
				<i>Amphitrite oculata</i>	Df	-18.8	10.6	
				<i>Anaitides maculata</i>	Ca	-14.9	12.5	
				<i>Capitella capitata</i>	Df	-18.6	11.8	
				<i>Glycera chirori</i>	Ca	-15.4	14.8	
				<i>Goniada japonica</i>	Ca	-18.2	14.6	
				<i>Goniada maculata</i>	Ca	-16.4	14.8	
				<i>Magelona japonica</i>	Df	-16.5	12.4	
				<i>Nephtys oligobranchia</i>	Ca	-17.1	10.9	
				<i>Nereis multignatha</i>	Ca	-15.0	13.9	
				<i>Nereis paxtonae</i>	Ca	-16.2	11.9	
				<i>Nereis surugaense</i>	Ca	-15.9	13.7	
				<i>Praxillella affinis</i>	Df	-19.2	10.3	
				<i>Praxillella pacifica</i>	Df	-18.5	11.6	
				<i>Prionospio</i> sp.	Df	-18.9	11.8	
				<i>Scoletoma longifolia</i>	Ca	-16.5	11.9	
				<i>Scoloplos armiger</i>	Ca	-17.9	10.6	
				<i>Sternaspis scutata</i>	Df	-17.3	12.3	
				<i>Terebella ehrenbergi</i>	Df	-18.6	12.0	
		Arthropoda	Malacostraca	<i>Alpheus digitalis</i>	DF	-16.3	11.7	
				<i>Alpheus japonicus</i>	DF	-16.4	12.9	
				<i>Crangon hakodatei</i>	Ca	-16.3	12.2	
				Gammaridian amphipod	Df	-20.9	8.4	

Table 3.4. (Continued.)

Coast	Site	Phylum	Class	Species	Type	$\delta^{13}\text{C}$ (‰)	$\delta^{15}\text{N}$ (‰)	References
South	Seomjin River Estuary	Arthropoda	Malacostraca	<i>Neotrypaea japonica</i>	Df	-15.6	10.0	Park et al., 2020
				<i>Oratosquilla oratoria</i>	Ca	-15.0	16.2	
		Echinodermata	Holothuroidea	<i>Protankyra bidentata</i>	Df	-14.8	11.0	
			Ophiuroidea	<i>Amphiopius tricoides</i>	Om	-15.2	12.3	
				<i>Amphioplus ancistrotus</i>	Om	-15.3	12.6	
				<i>Ophiura kinbergi</i>	Om	-15.8	12.4	
				<i>Ophiura sarsii</i>	Om	-17.3	10.6	
		Mollusca	Gastropoda	<i>Philine orientalis</i>	Ca	-16.7	12.0	
			Bivalvia	<i>Arcuatula senhousia</i>	Ff	-21.6	10.7	
				<i>Limaria hakodatensis</i>	Ff	-16.0	9.3	
				<i>Mactra crossei</i>	Ff	-16.6	9.2	
				<i>Nitidotellina nitidula</i>	Df	-16.9	9.5	
				<i>Periploma japonicum</i>	Ff	-17.8	8.7	
				<i>Raetellops pulchella</i>	Df	-17.7	10.0	
				<i>Ruditapes variegatus</i>	Ff	-19.8	10.5	
				<i>Scintilla violescens</i>	Ff	-17.6	9.1	
				<i>Sinocorophium japonicum</i>	Ff	-22.9	10.9	
				<i>Theora fragilis</i>	Ff	-18.1	9.6	
		Annelida	Polychaeta	<i>Glyceridae</i> sp.	Ca	-10.8	15.2	Choi et al., 2017
		Arthropoda	Malacostraca	<i>Macrophthalmus abbreviatus</i>	Df	-11.1	11.2	
				<i>Macrophthalmus japonicus</i>	Df	-11.3	9.3	
		Mollusca	Bivalvia	<i>Crassostrea gigas</i>	Ff	-17.1	8.9	
				<i>Cyclina sinensis</i>	Ff	-16.8	10.2	
Suncheon		Annelida	Polychaeta	<i>Glycera</i> sp.	Ca	-14.5	14.7	Park et al., 2015
				<i>Hediste japonica</i>	Om	-16.5	13.4	
		Arthropoda	Malacostraca	<i>Cleistostoma dilatatum</i>	Df	-17.4	12.2	
				<i>Hemigrapsus penicillatus</i>	Om	-16.8	13.0	
				<i>Ilyoplax pusilla</i>	Df	-13.4	11.9	
				<i>Macrophthalmus japonicus</i>	Df	-13.3	12.2	
				<i>Neotrypaea japonica</i>	Df	-16.5	11.7	
				<i>Philyra pisum</i>	Df	-17.8	11.8	
				<i>Sesarma dehaani</i>	Df	-20.0	13.0	

Table 3.4. (Continued.)

Coast	Site	Phylum	Class	Species	Type	$\delta^{13}\text{C}$ (‰)	$\delta^{15}\text{N}$ (‰)	References
South	Suncheon	Mollusca	Gastropoda	<i>Batillaria cumingii</i>	Df	-13.4	11.7	Park et al., 2015
				<i>Cerithidea balteata</i>	Df	-13.9	11.9	
				<i>Lunatia fortunei</i>	Ca	-14.1	14.3	
				<i>Nassarius livescens</i>	Ca	-14.3	14.2	
				<i>Pirenella cingulata</i>	Df	-13.9	11.9	
			Bivalvia	<i>Crassostrea gigas</i>	Ff	-17.2	11.5	
				<i>Scapharca subcrenata</i>	Ff	-18.0	11.1	
		Annelida	Polychaeta	<i>Glycera</i> sp.	Ca	-14.7	15.1	
				<i>Hediste japonica</i>	Om	-16.7	13.5	
				<i>Perinereis nuntia</i>	Om	-15.1	12.5	
		Arthropoda	Malacostraca	<i>Cleistostoma dilatatum</i>	Df	-17.3	12.8	
				<i>Hemigrapsus penicillatus</i>	Om	-16.3	13.1	
				<i>Macrophthalmus japonicus</i>	Df	-13.4	12.3	
				<i>Philyra pismus</i>	Df	-15.1	12.0	
				<i>Sesarma dehaani</i>	Df	-19.1	13.3	
				<i>Sesarma haematocheir</i>	Df	-18.7	12.7	
		Mollusca	Gastropoda	<i>Batillaria multiformis</i>	Df	-13.4	12.6	
				<i>Bullacta caurina</i>	Df	-12.6	12.3	
				<i>Cerithidea balteata</i>	Df	-13.6	12.3	
				<i>Lunatia fortunei</i>	Ca	-14.1	13.5	
				<i>Nassarius livescens</i>	Ca	-14.4	13.6	
			Bivalvia	<i>Crassostrea gigas</i>	Ff	-17.9	11.2	
	Yoja bay	Mollusca	Bivalvia	<i>Ruditapes philippinarum</i>	Ff	-17.4	15.4	Kang et al., 2003
West	Ganghwa Island	Annelida	Polychaeta	<i>Glycera</i> sp.	Ca	-13.1	14.8	Lee et al., 2021
				<i>Perinereis aibuhitensis</i>	Df	-14.7	12.4	
				<i>Paraleonnates uschakovi</i>	Df	-12.8	11.4	
		Arthropoda	Malacostraca	<i>Alpheus</i> sp.	Df	-14.5	13.1	
				<i>Cleistostoma dilatatum</i>	Df	-14.4	11.0	
				<i>Helice tridens</i>	Om	-14.9	12.1	
				<i>Macrophthalmus japonicus</i>	Df	-12.9	11.3	
		Brachiopoda	Lingulata	<i>Lingula anatina</i>	Ff	-15.7	10.3	
		Chordata	Actinopterygii	<i>Periophthalmus modestus</i>	Ca	-14.5	15.9	

Table 3.4. (Continued.)

Coast	Site	Phylum	Class	Species	Type	$\delta^{13}\text{C}$ (‰)	$\delta^{15}\text{N}$ (‰)	References
West	Ganghwa Island	Mollusca	Gastropoda	<i>Cerithidea balteata</i>	Df	-15.3	11.4	Lee et al., 2021
				<i>Lunatia fortunei</i>	Ca	-11.7	12.3	
			Bivalvia	<i>Cyclina sinensis</i>	Ff	-14.8	12.5	
				<i>Glaucanome chinensis</i>	Ff	-15.4	11.0	
				<i>Laternula gracilis</i>	Ff	-15.0	10.5	
				<i>Magallana gigas</i>	Ff	-16.0	11.2	
	Guem River Estuary	Arthropoda	Malacostraca	<i>Hemigrapsus penicillatus</i>	Om	-16.8	13.4	Noh et al., 2019
				<i>Macrophthalmus japonicus</i>	Df	-13.4	11.9	
				<i>Neotrypaea japonica</i>	Df	-16.8	13.2	
				<i>Squilla oratoria</i>	Ca	-16.7	14.6	
				<i>Upogebia major</i>	Ff	-18.2	12.1	
		Chordata	Actinopterygii	<i>Synechogobius hasta</i>	Ca	-16.0	15.9	
				<i>Tridentiger trigonocephalus</i>	Ca	-18.1	15.3	
		Echinodermata	Holothuroidea	<i>Apostichopus japonicus</i>	Df	-16.7	11.7	
		Mollusca	Bivalvia	<i>Anadara broughtonii</i>	Ff	-17.7	12.0	
				<i>Crassostrea gigas</i>	Ff	-19.2	10.2	
				<i>Cyclina sinensis</i>	Ff	-18.5	12.0	
				<i>Dosinia</i> sp.	Ff	-17.8	13.0	
				<i>Macra quadrangularis</i>	Ff	-17.9	11.3	
				<i>Solen strictus</i>	Ff	-18.7	11.8	
			Gastropoda	<i>Nassarius</i> sp.	Ca	-15.5	13.7	
				<i>Neverita didyma</i>	Ca	-16.0	13.7	
				<i>Rapana venosa</i>	Ca	-17.0	13.3	
	Gyeonggi Bay	Arthropoda	Malacostraca	<i>Helice tridens</i>	Om	-14.7	5.3	Bang et al., 2019
	Hampyeong Bay	Annelida	Polychaeta	<i>Glycera chirori</i>	Ca	-13.5	14.4	Park et al., 2016
				<i>Perinereis aibuhitensis</i>	Df	-13.4	13.6	
				<i>Scoletoma longifolia</i>	Ca	-13.1	14.2	
				<i>Tharyx</i> sp.	Df	-14.4	11.5	
		Arthropoda	Malacostraca	Gammaridian amphipod	Df	-13.0	11.2	
				<i>Hemigrapsus penicillatus</i>	Om	-15.1	12.3	
				<i>Macrophthalmus japonicus</i>	Df	-14.0	11.4	
				<i>Scopimera globosa</i>	Df	-14.1	11.1	

Table 3.4. (Continued.)

Coast	Site	Phylum	Class	Species	Type	$\delta^{13}\text{C}$ (‰)	$\delta^{15}\text{N}$ (‰)	References
West	Hampyeong Bay	Mollusca	Bivalvia	<i>Cyclina sinensis</i>	Ff	-18.6	10.2	Park et al., 2016
			Gastropoda	<i>Batillaria cumingii</i>	Df	-12.9	11.6	
				<i>Batillaria multiformis</i>	Df	-12.9	11.7	
	Seonjae Island	Mollusca	Bivalvia	<i>Ruditapes philippinarum</i>	Ff	-16.0	10.5	Suh and Shin, 2013
	Taean	Annelida	Polychaeta	Ampharetidae unid	Df	-17.5	10.3	Han et al., 2015
				<i>Capitella</i> sp.	Df	-14.9	11.5	
				<i>Cirratulus cirratus</i>	Df	-14.2	8.3	
				<i>Cirriformia tentaculata</i>	Df	-18.1	10.6	
				<i>Diopatra sugokai</i>	Om	-16.8	11.6	
				<i>Glycera</i> sp.	Ca	-16.2	10.5	
				<i>Halosydna</i> sp.	Ca	-16.9	12.9	
				<i>Lagis bocki</i>	Df	-16.6	7.4	
				<i>Lumbrineris</i> sp.	Ca	-16.2	10.1	
				<i>Nereis pelagica</i>	Om	-15.9	8.1	
				<i>Perinereis nuntia</i>	Om	-15.1	10.7	
				<i>Thelepus setosus</i>	Df	-15.8	8.2	
		Arthropoda	Malacostraca	<i>Crangon affinis</i>	Ca	-13.0	10.7	
				<i>Diogenens</i> sp.	Ff	-18.0	7.5	
				<i>Hemigrapsus penicillatus</i>	Om	-15.4	10.7	
				<i>Macrophthalmus abbreviatus</i>	Gr	-12.9	8.4	
				<i>Philyra pisum</i>	Df	-15.2	10.0	
				<i>Portunus trituberculatus</i>	Ca	-16.2	9.4	
			Thecostraca	<i>Balanidae</i> unid.	Ff	-17.2	10.8	
		Echinodermata	Asteroidea	<i>Asterias amurensis</i>	Ca	-16.4	10.3	
				<i>Patiria pectinifera</i>	Om	-16.8	11.5	
			Holothuroidea	<i>Protankyra bidentata</i>	Df	-15.8	9.6	
		Mollusca	Bivalvia	<i>Arcuatula senhousia</i>	Ff	-19.5	8.7	
				<i>Crassostrea gigas</i>	Ff	-18.9	7.2	
				<i>Dosinia japonica</i>	Ff	-16.8	7.6	
				<i>Macoma</i> sp.	Df	-16.0	7.7	
				<i>Mactra quadrangularis</i>	Ff	-19.6	8.2	
				<i>Mytilus galloprovincialis</i>	Ff	-19.1	6.4	

Table 3.4. (Continued.)

Coast	Site	Phylum	Class	Species	Type	$\delta^{13}\text{C}$ (‰)	$\delta^{15}\text{N}$ (‰)	References
West	Taeon	Mollusca	Bivalvia	<i>Ruditapes philippinarum</i>	Ff	-18.4	7.2	Han et al., 2015
				<i>Solen strictus</i>	Ff	-17.3	8.0	
				<i>Theora fragilis</i>	Ff	-17.9	7.4	
			Gastropoda	<i>Batillaria exarata</i>	Df	-15.5	10.6	
				<i>Columbellidae</i> unid.	Ff	-18.1	9.8	
				<i>Glossaulax didyma</i>	Ca	-17.5	11.0	
		Mollusca	Gastropoda	<i>Littorina brevicula</i>	Gr	-15.3	7.3	
				<i>Lunella coronata</i>	Gr	-14.7	11.0	
				<i>Monodonta labio</i>	Gr	-17.3	6.5	
				<i>Nassarius</i> sp.	Ca	-14.8	13.7	
				<i>Nipponacmaea schrenckii</i>	Gr	-15.0	9.6	
				<i>Rapana venosa</i>	Ca	-15.5	11.7	
				<i>Reishia clavigera</i>	Ca	-16.7	10.4	
				<i>Seraphsidae</i>	Df	-18.1	10.1	
				<i>Umbonium costatum</i>	Ff	-16.6	7.7	
		Annelida	Polychaeta	<i>Ditrupea arietina</i>	Ff	-19.1	7.1	Park et al., 2022
				<i>Hydroides ezoensis</i>	Ff	-18.0	6.4	
				<i>Naineris laevigata</i>	Df	-15.8	7.9	
		Arthropoda	Malacostraca	<i>Gammarian amphipod</i>	Df	-17.0	7.0	
				<i>Hemigrapsus penicillatus</i>	Om	-16.9	10.4	
				<i>Pagurus</i> sp.	Om	-15.0	10.4	
				<i>Parhyale</i> sp.	Df	-15.4	9.1	
			Thecostraca	<i>Chthamalus challengerii</i>	Ff	-18.3	5.6	
				<i>Fistulobalanus albicostatus</i>	Ff	-18.4	5.4	
		Echinodermata	Asteroidea	<i>Patiria pectinifera</i>	Om	-13.6	10.4	
		Mollusca	Bivalvia	<i>Lasaea undulata</i>	Ff	-18.5	6.1	
				<i>Magallana gigas</i>	Ff	-17.9	6.5	
				<i>Mytilus galloprovincialis</i>	Ff	-18.8	6.2	
			Gastropoda	<i>Ansola angustata</i>	Df	-16.1	7.4	
				<i>Ceratostoma rorifluum</i>	Ca	-16.7	11.4	
				<i>Chlorostoma lischkei</i>	Gr	-16.2	8.7	
				<i>Echinolittorina radiata</i>	Gr	-15.9	8.6	

Table 3.4. (Continued.)

Coast	Site	Phylum	Class	Species	Type	$\delta^{13}\text{C}$ (‰)	$\delta^{15}\text{N}$ (‰)	References
West	Taean	Mollusca	Gastropoda	<i>Littorina brevicula</i>	Gr	-13.9	8.6	Park et al., 2022
				<i>Lottia dorsuosa</i>	Gr	-13.9	8.2	
				<i>Lottia kogamogai</i>	Gr	-14.1	9.7	
				<i>Lottia tenuisculpta</i>	Gr	-13.3	8.7	
				<i>Lunella correensis</i>	Gr	-13.8	9.7	
				<i>Monodonta neritoides</i>	Gr	-15.0	8.9	
				<i>Nassarius fraterculus</i>	Ca	-15.1	11.8	
			Gastropoda	<i>Nerita japonica</i>	Gr	-16.4	7.9	
				<i>Nipponacmea schrenckii</i>	Gr	-15.7	9.0	
				<i>Ocenebrellus inornatus</i>	Ca	-15.7	11.5	
				<i>Patelliida conulus</i>	Gr	-13.2	9.6	
				<i>Patelloida pygmaea</i>	Gr	-15.8	9.0	
				<i>Reishia clavigera</i>	Ca	-16.9	11.6	
				<i>Tegula rustica</i>	Gr	-15.3	8.0	
				<i>Tegula turbinata</i>	Gr	-16.9	8.8	
			Polyplacophora	<i>Acanthoschitona achates</i>	Gr	-14.1	7.3	
Yeongsan River Estuary		Annelida	Polychaeta	<i>Diopatra sugokai</i>	Ca	-16.2	13.1	Park et al., 2020
				<i>Glycera chirori</i>	Ca	-16.3	15.3	
				<i>Goniada japonica</i>	Ca	-15.1	14.7	
				<i>Heteromastus filiformis</i>	Df	-17.8	11.8	
				<i>Lumbrineris longifolia</i>	Ca	-16.6	14.0	
				<i>Marphysa sanguinea</i>	Ca	-15.4	14.8	
				<i>Nephtys oligobranchia</i>	Ca	-16.8	13.1	
				<i>Nephtys</i> sp.	Ca	-15.8	12.1	
				<i>Scoloplos amiger</i>	Ca	-16.5	11.8	
				<i>Sternopsis scutata</i>	Df	-17.7	11.1	
				<i>Tharyx</i> sp.	Df	-17.5	11.6	
			Arthropoda	<i>Leptochela gracilis</i>	Om	-16.9	13.8	
			Echinodermata	<i>Protankyra bidentata</i>	Df	-17.1	13.0	
		Mollusca	Bivalvia	<i>Arcuatula senhousia</i>	Ff	-16.6	10.4	
				<i>Fulvia mutica</i>	Ff	-17.6	10.6	
				<i>Laternula</i> sp.	Ff	-16.6	9.9	

Table 3.4. (Continued.)

Coast	Site	Phylum	Class	Species	Type	$\delta^{13}\text{C}$ (‰)	$\delta^{15}\text{N}$ (‰)	References
West	Yeongsan River Estuary	Mollusca	Bivalvia	<i>Moerella</i> sp.	Df	−17.0	9.6	Park et al., 2020
				<i>Sinonovacula constricta</i>	Ff	−16.8	9.8	
				<i>Theora fragilis</i>	Ff	−17.7	10.9	
			Gastropoda	<i>Bullacta caurina</i>	Df	−15.8	11.0	
				<i>Crepidula onyx</i>	Ff	−18.2	10.7	

3.3. Results and discussion

3.3.1. Water environmental conditions

The total annual water exchange between Saemangeum Lake and its tidal flat showed significant mean differences from 2019 to 2022 (inflow, $F=25.5$, $p<0.001$; outflow, $F=25.0$, $p<0.001$; Fig. 3.2.). Two periods (I, 2019–2020; II, 2021–2022) were distinguished, and water inflow and outflow were more than 3.5 times greater in period II ($3,470,458\pm1,363,917$ and $3,351,990\pm1,574,749$ 10^6 m^3/s , respectively) than in period I ($982,363\pm679,097$ and $540,796\pm455,605$ 10^6 m^3/s , respectively).

The mean TN, TP, and SiO_2 concentrations in the water column were significantly higher at GR2 than at GR1 (TN, $F=40.0$; TP, $F=45.7$; SiO_2 , $F=16.5$; all $p<0.001$; Fig. 3.3.), indicating that the Saemangeum dike markedly separated the inner and outer environments. However, Pearson correlations between the GR1 and GR2 nutrient concentrations were moderate (TN: $r=0.8$, $p<0.001$; TP: $r=0.4$, $p<0.01$; SiO_2 : $r=0.5$, $p<0.01$), implying the influence of the discharged water on the outer tidal flat (Fig. 3.3.). The TN concentration was significantly higher at GR2 in 2020 (0.8 ± 0.1 mM; $F=21.7$, $p<0.001$) than other periods, reflecting more anthropogenic sewage input to the lake. In general, TN concentrations from 2019 to 2021 exceeded 0.04 mM, reflecting lake eutrophication (Forsberg and Ryding, 1980). However, this concentration decreased between 2021 and 2022 with the increased water exchange.

ANOVA revealed spatial significant differences in salinity ($F=133.2$, $p<0.001$; Table 3.5.). The salinity at WY and AS was characteristic of freshwater, whereas that at the reference site YM and others (SS and GR1) was characteristic of seawater and estuarine environments, respectively. These results imply that discharged water reduced the salinity near the water gates (at SS and GR1). DO concentration was significantly higher at WY and AS than at the outer sites ($F=3.7$, $p<0.05$; Table 3.5.). The high DO concentrations at SS and GR1 relative to that at YM also support the influence of discharged freshwater on the tidal flat near the water gates.

ANOVA revealed significant spatial differences in mean $\delta^{15}N$ values for POM among the five sites in period I (2019: $F=3.4$, $p<0.05$; 2020: $F=3.5$, $p<0.05$), but not period II (Fig. 3.4., Table 3.6.). The enriched N stable isotope value for FPOM

(>10‰) in period I reflected lake eutrophication with agricultural sewage input, which recovered gradually in period II with increased seawater input (Voss et al., 2000). The variation in sewage input from the upstream agricultural area to the Rivers may be another reason for the changes in water quality between periods. The slight $\delta^{15}\text{N}$ enrichment for SPOM collected at the outer sites in period II additionally implies that FPOM influenced the outer tidal flat with increased water outflow. In contrast, the $\delta^{15}\text{C}$ values for POM showed significant spatial differences in both periods, indicating that FPOM did not significantly enter the Saemangeum tidal-flat food web (2019: $F=4.5$, $p<0.05$; 2020: $F=11.3$, $p<0.001$; 2021: $F=13.6$, $p<0.001$; 2022: $F=18.6$, $p<0.001$; Fig. 3.4., Table 3.6.) (Noh et al., 2019). Overall, the discharged FPOM seemed to slightly influence the trophic conditions of the water columns, but not the trophic pathways in the food web of the outer tidal flat.

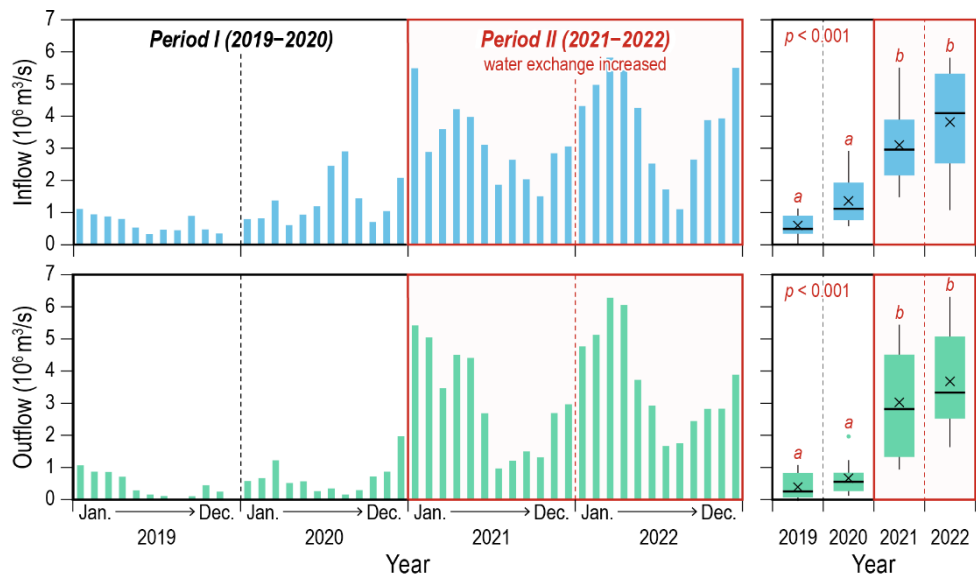


Figure 3.2.

Total monthly exchanged water flow ($10^6 \text{ m}^3/\text{s}$) (inflow, blue; outflow, green) through Sinsi and Garyuk water gates from January 2019 to December 2022 in Saemangeum tidal flat, Korea. Mean water exchanges in period II, highlighted with a red background are different from period I (2019–2020). An asterisk indicates statistical significance ($p < 0.001$) among for years.

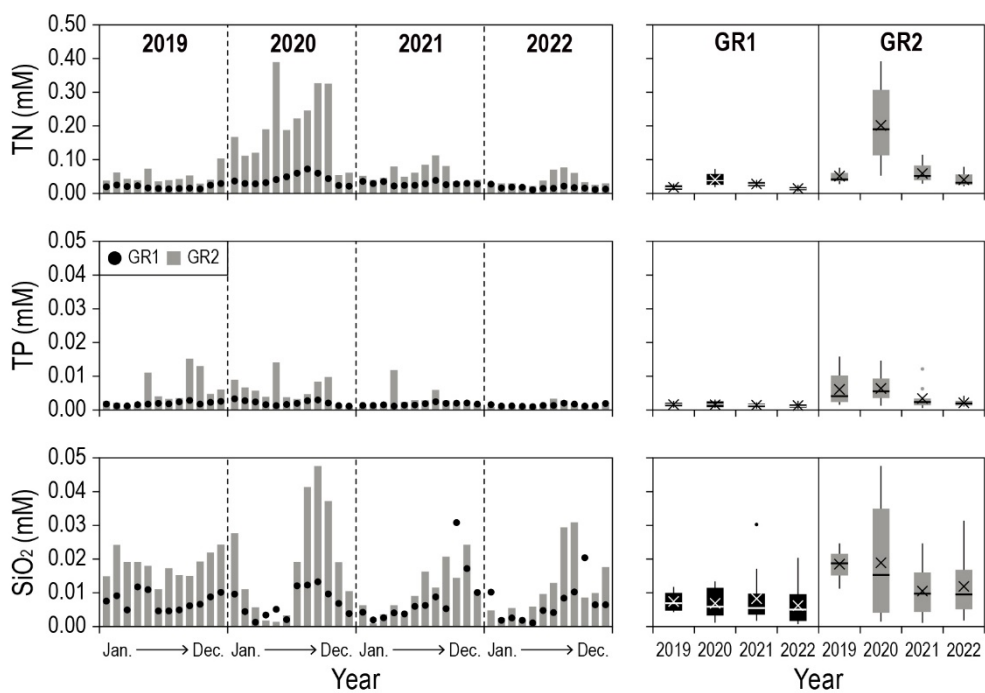


Figure 3.3.

Monthly water quality parameters (total nitrogen, TN; total phosphorus, TP; silicon dioxide, SiO₂) collected in the water column of both the outer tidal flat (Garyuk1, GR1) and the lake (Garyuk2, GR2) near the Garyuk water gate from 2019 to 2022.

Table 3.5.

Water environmental parameters (temperature; salinity; dissolved oxygen, DO; pH) collected in the Saemangeum tidal flat (Yami, YM; Sinsi, SS; Garyuk1, GR1) and two sites located in the tributaries (Woryeon, WY; Anseong, AS) of the Mangyeong and Dongjin Rivers. Values are expressed as annual mean with standard deviation (mean±s.d.). PI and PII indicate period I (2019–2020) and period II (2021–2022), respectively.

Parameters	Period	Year	Site				
			YM	SS	GR1	WY	AS
Temperature (°C)	PI	2019	15.3±8.5	14.8±15.1	16.4±10.3	17.3±9.5	15.5±7.6
		2020	16.1±6.6	18.2±7.8	21.9±6.8	19.7±11.9	16.9±8.8
	2022	16.7±10.3	17.3±9.3	18.9±9.7	17.5±10.1	11.2±10.2	
		Total	16.0±0.6	17.5±2.1	18.2±2.8	17.0±2.6	14.4±2.5
	Salinity (psu)	PI	2019	32.1±5.1	34.1±2.7	34.0±2.6	5.0±6.2
2020			32.6±4.0	31.4±5.7	28.1±11.1	2.5±1.6	2.1±2.2
2022		30.6±1.1	30.8±0.8	30.5±2.6	0.2±0.1	1.5±2.7	
		Total	31.6±0.9	29.8±4.9	30.6±2.5	2.4±2.0	2.6±1.0
DO (mg L ⁻¹)		PI	2019	9.0±3.4	9.0±3.3	9.7±3.1	11.7±2.1
	2020		7.6±2.6	7.3±2.8	6.2±2.1	12.9±4.1	9.1±4.3
	2022	7.7±2.4	8.4±3.7	8.1±3.0	10.4±1.8	10.4±4.4	
		Total	8.1±0.7	8.2±0.7	9.5±3.4	12.4±1.9	10.3±1.1
	pH	PI	2019	7.9±0.6	8.2±0.4	8.0±0.4	6.8±3.4
2020			7.6±0.6	7.4±1.0	7.5±0.7	8.5±0.8	8.1±1.1
2022		7.8±0.4	8.0±0.5	7.9±0.6	7.9±0.7	7.8±1.0	
		Total	7.8±0.1	7.9±0.3	7.8±0.3	7.8±0.7	8.2±0.4

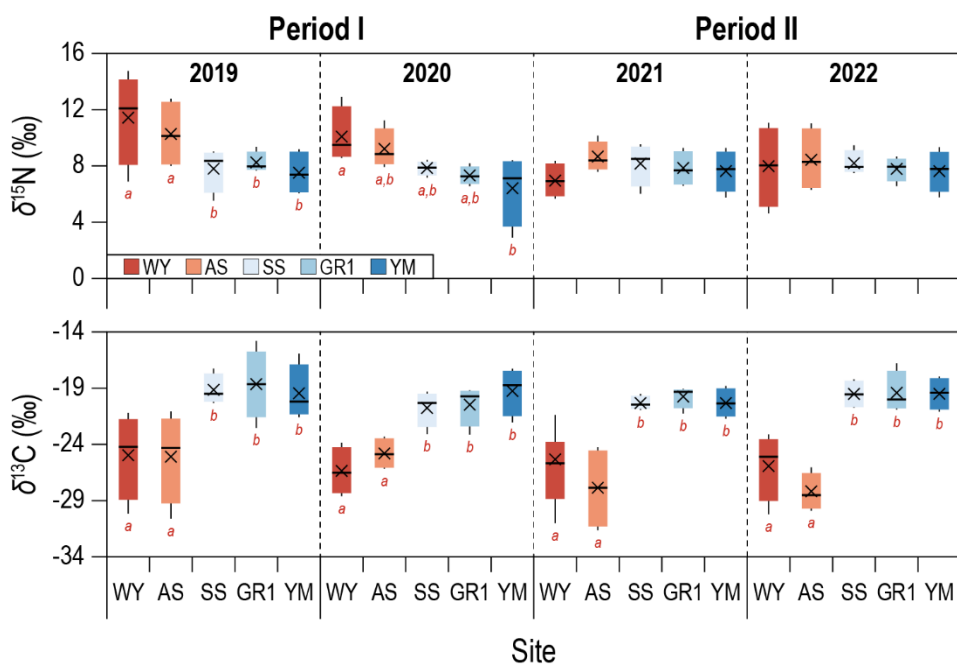


Figure 3.4.

Carbon and nitrogen stable isotope values ($\delta^{13}\text{C}$ and $\delta^{15}\text{N}$) of particulate organic matter (FPOM and SPOM) collected at three sites in the Saemangeum tidal flat (Yami, YM; Sinsi, SS; Garyuk, GR1), and the two lower reaches of the Mangyeong and Dongjin Rivers (Woryeon, WY; Anseong, AS) from 2019 to 2022.

Table 3.6.

Carbon and nitrogen stable isotope values ($\delta^{13}\text{C}$ and $\delta^{15}\text{N}$) of particulate organic matter (FPOM and SPOM) collected from the Saemangeum tidal flat (Yami, YM; Sinsi, SS; Garyuk, GR1), and the two lower reaches of the Mangyeong and Dongjin Rivers (Woryeon, WY; Anseong, AS) from 2019 to 2022. Values are expressed as means with standard deviations (stdev.). PI and PII indicate period I (2019–2020) and period II (2021–2022), respectively.

Parameter	Period	Year	Site				
			WY	AS	SS	GR1	YM
$\delta^{13}\text{C}$ (‰)	PI	2019	-25.0±3.8	-25.1±4.0	-19.2±1.3	-18.7±3.1	-19.5±2.4
		2020	-26.4±2.1	-24.8±1.4	-20.8±1.6	-20.5±1.8	-19.3±2.1
	PII	2021	-25.7±2.2	-27.9±3.6	-20.4±0.6	-19.8±1.0	-20.4±1.2
		2022	-26.0±3.0	-28.3±1.7	-19.6±1.3	-19.5±1.8	-19.5±1.5
		Total	-25.8±2.6	-26.5±3.1	-20.0±1.3	-19.6±1.8	-19.7±1.7
$\delta^{15}\text{N}$ (‰)	PI	2019	11.4±3.3	10.2±2.4	7.8±1.6	8.2±0.7	7.5±1.6
		2020	10.1±1.9	9.2±1.4	7.8±0.5	7.3±0.6	2.5±6.4
	PII	2021	7.0±1.2	8.6±1.1	8.1±1.5	7.8±1.2	8.0±2.4
		2022	7.9±2.9	8.4±2.2	8.2±0.8	7.8±0.8	7.6±1.5
		Total	9.1±2.8	9.1±1.8	8.0±1.1	7.8±0.9	7.4±1.9

3.3.2. Sediment environmental conditions

ANOVA with the post-hoc Tukey test revealed significant differences in the physicochemical characteristics of sediment at three sites in the outer tidal flat (WC: $F=4.0$, $p<0.05$; MC: $F=73.9$, $p<0.001$; TOC: $F=12.2$, $p<0.001$; TN: $F=15.9$, $p<0.001$; C/N ratio, $F=7.6$, $p<0.01$; $\delta^{13}\text{C}$: $F=12.8$, $p<0.001$). Sediment at YM and SS was characterised more by muddy sand than was that at GR1 (Table 3.7.). The sediment $\delta^{13}\text{C}$ value was higher and the C/N ratio was lower at SS ($-19.6\pm1.6\text{‰}$ and $5.8\%\pm1.9\%$, respectively) and GR1 ($-20.1\pm1.8\text{‰}$ and $5.5\%\pm2.5\%$, respectively) than at YM ($-22.2\pm0.9\text{‰}$ and $8.6\pm3.0\%$, respectively). In contrast, no annual mean difference in the physicochemical characteristics of the sediment was detected.

There was no spatial mean difference in the TN, TP, or SiO_2 concentration in porewater (Fig. 3.6., Table 3.8.). However, the concentrations of growth-limiting nutrients of microalgae (e.g., TN and TP) were higher near the water gates than at reference site YM, implying slight influences of the discharged water on the tidal flat (Morris and Lewis, 1988). The mean MPB biomass was significantly greater at SS than at YM and GR1 ($F=5.1$, $p<0.05$). However, no mean difference in PP or P/B was detected among sites (Fig. 3.7., Table 3.9.). The PP differed significantly over time ($F=4.6$, $p<0.05$); it was high at SS and GR1 in 2020 and 2022 and at YM in 2022. These results imply that spatially variable environmental differences affected the PP of MPB in the Saemangeum tidal flat. The enriched $\delta^{13}\text{C}$ and low C/N values for SOM at SS and GR1 reflected relative MPB abundance near the water gates (France, 1995; Perdue and Koprivnjak, 2007). The sediment grain size has been reported to be an important factor influencing the spatial benthic Chl-*a* distribution (Cahoon et al., 1999; Lee et al., 2021). However, despite the similar muddy sand characteristics of sediment at SS and YM, the $\delta^{13}\text{C}$ signature and C/N ratio for SOM at SS were more comparable to those at GR1, which had only slightly muddy sand. This physiochemical difference between SS and YM could be explained by the high MPB biomass induced by nutrient (e.g., TN and TP) input at the sites near the water gates that were regularly influenced by eutrophic water from Saemangeum Lake. The difference in porewater nutrients between SS and GR1 could also be explained by the sediment MC (Erftemeijer and Middelburg, 1993).

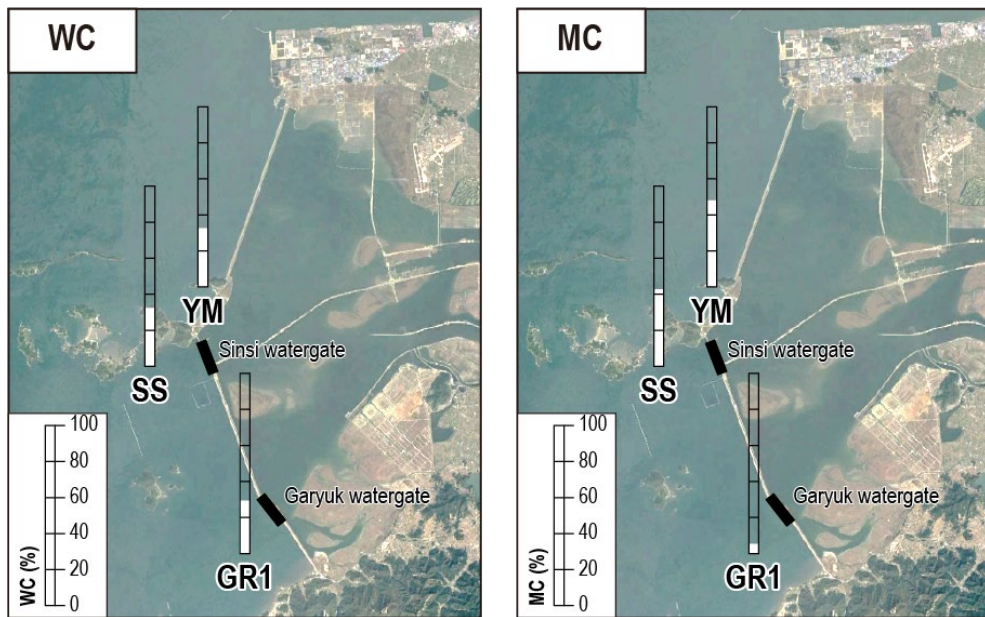


Figure 3.5.

Spatial distribution of seasonally collected sediment properties (water content, WC; mud content, MC) at the three outer sites (Yami, YM; Sinsi, SS; Garyuk, GR1) in the Saemangeum tidal flat from 2019 to 2022. YM is the reference site, and SS and GR1 are sites influenced by the reservoir discharge water through the Sinsi- and Garyuk watergates. The annual data are described in Table 3.7.

Table 3.7.

Sediment physicochemical parameters (water content, WC; mud content, MC; total organic carbon, TOC; total nitrogen, TN; carbon to nitrogen ratio, C/N; carbon and nitrogen stable isotope ratios, $\delta^{13}\text{C}$ and $\delta^{15}\text{N}$) collected seasonally at three sites (Yami, YM; Sinsi, SS; Garyuk, GR1) in the Saemangeum tidal flat, Korea from 2019 to 2022. Values are expressed as annual means with standard deviations (mean \pm s.d.). PI and PII indicate period I (2019–2020) and period II (2021–2022), respectively.

Parameter	Period	Year	Site		
			YM	SS	GR1
WC (%)	PI	2019	34.0 \pm 2.9	31.9 \pm 7.3	28.5 \pm 2.3
		2020	31.7 \pm 1.7	31.8 \pm 3.3	30.7 \pm 4.8
	PII	2021	33.8 \pm 2.0	32.0 \pm 2.1	29.8 \pm 3.9
		2022	33.7 \pm 5.8	34.3 \pm 5.5	29.6 \pm 4.1
		Total	33.3\pm3.3	32.5\pm4.6	29.6\pm3.6
MC (%)	PI	2019	59.6 \pm 22.9	34.3 \pm 8.5	10.3 \pm 11.1
		2020	45.6 \pm 6.2	47.7 \pm 6.4	2.6 \pm 0.3
	PII	2021	43.3 \pm 8.7	49.7 \pm 2.5	4.2 \pm 1.1
		2022	44.8 \pm 14.7	40.5 \pm 10.6	6.9 \pm 6.4
		Total	48.3\pm14.7	43.0\pm9.3	6.0\pm6.5
TOC (%)	PI	2019	0.48 \pm 0.11	0.29 \pm 0.14	0.13 \pm 0.03
		2020	0.38 \pm 0.10	0.21 \pm 0.05	0.14 \pm 0.06
	PII	2021	0.43 \pm 0.11	0.22 \pm 0.08	0.10 \pm 0.03
		2022	0.61 \pm 0.19	0.32 \pm 0.15	0.12 \pm 0.02
		Total	0.48\pm0.10	0.26\pm0.11	0.12\pm0.04
TN (%)	PI	2019	0.05 \pm 0.01	0.06 \pm 0.03	0.02 \pm 0.01
		2020	0.04 \pm 0.00	0.03 \pm 0.01	0.02 \pm 0.00
	PII	2021	0.08 \pm 0.03	0.05 \pm 0.02	0.03 \pm 0.01
		2022	0.07 \pm 0.02	0.05 \pm 0.02	0.02 \pm 0.01
		Total	0.06\pm0.02	0.05\pm0.02	0.02\pm0.01
C/N (%)	PI	2019	10.73 \pm 3.98	5.34 \pm 1.58	5.45 \pm 1.45
		2020	9.19 \pm 2.67	6.84 \pm 3.05	7.02 \pm 3.49
	PII	2021	5.76 \pm 1.47	5.07 \pm 1.43	4.33 \pm 2.83
		2022	8.68 \pm 1.13	5.94 \pm 1.18	5.24 \pm 1.75
		Total	8.59\pm2.96	5.80\pm1.88	5.51\pm2.46
$\delta^{13}\text{C}$ (‰)	PI	2019	-22.95 \pm 1.22	-19.74 \pm 1.34	-20.59 \pm 2.10
		2020	-22.06 \pm 0.41	-18.00 \pm 2.34	-18.44 \pm 1.95
	PII	2021	-21.93 \pm 0.28	-20.38 \pm 0.52	-20.07 \pm 0.76
		2022	-21.67 \pm 1.05	-20.39 \pm 0.26	-21.54 \pm 0.99
		Total	-22.16\pm0.90	-19.63\pm1.59	-20.16\pm1.82
$\delta^{15}\text{N}$ (‰)	PI	2019	8.36 \pm 3.39	8.03 \pm 3.48	7.22 \pm 3.44
		2020	7.94 \pm 2.34	8.69 \pm 3.17	6.35 \pm 1.08
	PII	2021	5.46 \pm 0.73	4.75 \pm 0.84	4.17 \pm 1.03
		2022	6.27 \pm 0.84	5.43 \pm 0.99	4.84 \pm 1.11
		Total	7.01\pm2.27	6.73\pm2.78	5.65\pm2.15

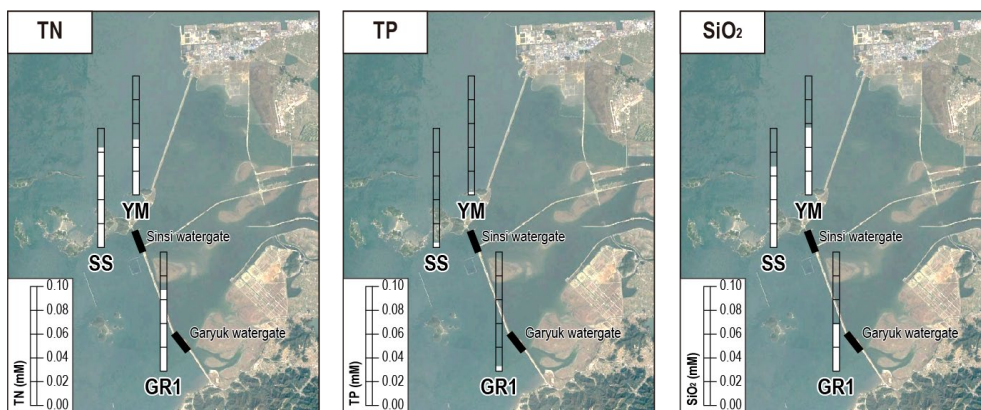


Figure 3.6.

Spatial distribution of seasonally collected sediment porewater nutrient concentrations (total nitrogen, TN; total phosphorus, TP; silicon dioxide, SiO₂) at the three outer sites (Yami, YM; Sinsi, SS; Garyuk, GR1) in the Saemangeum tidal flat from 2019 to 2022. YM is the reference site, and SS and GR1 are sites influenced by the reservoir discharge water through the Sinsi- and Garyuk water gates. The annual data are described in Table 3.8.

Table 3.8.

Seasonally collected nutrient concentrations (total nitrogen, TN; total phosphorus, TP; silicon dioxide, SiO₂) in the sediment porewater at three sites (Yami, YM; Sinsi, SS; Garyuk1, GR1) in the Saemangeum tidal flat, Korea from 2019 to 2022. Values are expressed as annual means with standard deviations (mean±s.d.). PI and PII indicate period I (2019 – 2020) and period II (2021–2022), respectively.

Parameter	Period	Year	Site		
			YM	SS	GR1
TN (mM)	PI	2019	0.05±0.03	0.07±0.02	0.05±0.04
		2020	0.04±0.01	0.10±0.07	0.06±0.03
	PII	2021	0.04±0.03	0.10±0.05	0.06±0.03
		2022	0.05±0.05	0.06±0.04	0.10±0.08
	Total		0.05±0.01	0.08±0.02	0.07±0.02
TP (mM)	PI	2019	0.002±0.002	0.005±0.002	0.004±0.003
		2020	0.002±0.003	0.005±0.005	0.004±0.003
	PII	2021	0.005±0.006	0.005±0.003	0.006±0.008
		2022	0.000±0.000	0.001±0.001	0.002±0.003
	Total		0.002±0.002	0.004±0.002	0.004±0.002
SiO ₂ (mM)	PI	2019	0.04±0.02	0.04±0.02	0.03±0.02
		2020	0.04±0.06	0.08±0.10	0.03±0.02
	PII	2021	0.07±0.05	0.07±0.04	0.03±0.03
		2022	0.07±0.07	0.08±0.05	0.07±0.07
	Total		0.06±0.02	0.07±0.02	0.04±0.02

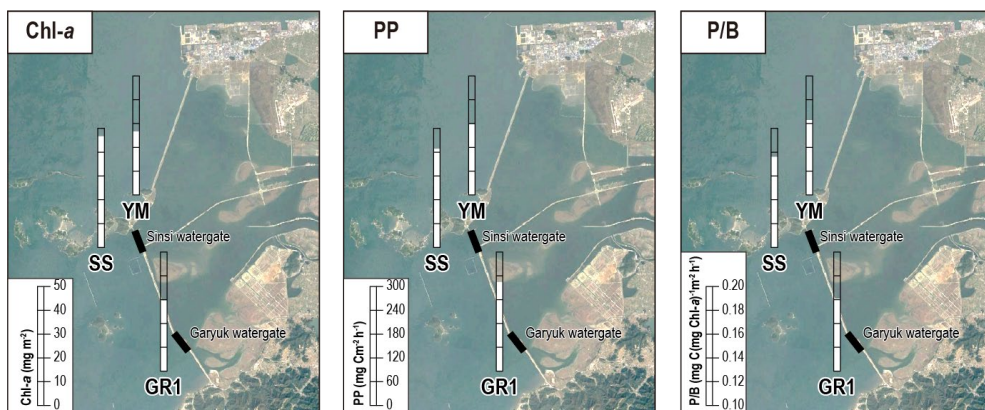


Figure 3.7.

Spatial distribution of seasonally collected biomass (Chl-*a*), primary production (PP), and primary productivity (P/B) of microphytobenthos at the three outer sites (Yami, YM; Sinsi, SS; Garyuk1, GR1) in the Saemangeum tidal flat from 2019 to 2022. YM is the reference site, and SS and GR1 are sites influenced by the reservoir discharge water through the Sinsi- and Garyuk water gates. The annual data are described in Table 3.9.

Table 3.9.

Biomass (Chl-*a*, mg m⁻²), primary production (PP, mg C m⁻²h⁻¹), and primary productivity (P/B, mg C (mg Chl-*a*)⁻¹ h⁻¹) of microphytobenthos collected at three sites (Yami, YM; Sinsi, SS; Garyuk, GR1) in the Saemangeum tidal flat, Korea from 2019 to 2022. Values are expressed as annual means with standard deviations (mean±s.d.). PI and PII indicate period I (2019–2020) and period II (2021–2022), respectively.

Parameter	Period	Year	Site		
			YM	SS	GR1
Chl- <i>a</i>	PI	2019	35.3±21.7	60.0±42.5	29.0±8.2
		2020	16.6±3.9	39.6±9.4	30.6±6.6
	PII	2021	29.3±14.7	33.3±10.0	20.8±16.6
		2022	36.9±21.7	52.6±20.9	37.1±15.7
		Total	29.5±17.4	46.4±24.6	29.4±12.7
PP	PI	2019	145.8±53.6	214.7±58.0	172.6±44.8
		2020	93.3±31.0	256.9±95.7	306.8±246.4
	PII	2021	175.9±57.5	188.8±63.6	90.0±71.9
		2022	339.8±308.7	332.1±56.1	323.6±91.9
		Total	191.6±176.3	250.4±85.2	226.6±163.4
P/B	PI	2019	0.2±0.1	0.2±0.1	0.2±0.1
		2020	0.2±0.0	0.2±0.1	0.1±0.1
	PII	2021	0.2±0.1	0.2±0.1	0.2±0.1
		2022	0.1±0.0	0.2±0.1	0.1±0.0
		Total	0.2±0.1	0.2±0.1	0.2±0.1

3.3.3. Food web structure

There were significant mean differences in $\delta^{13}\text{C}$ and $\delta^{15}\text{N}$ values among four potential diets (FPOM, SPOM, SOM, and MPB; $\delta^{13}\text{C}$: $F=70.9$, $p<0.001$; $\delta^{15}\text{N}$: $F=4.3$, $p<0.05$; Fig. 3.8., Table 3.10.). The significantly depleted $\delta^{13}\text{C}$ and enriched $\delta^{15}\text{N}$ of FPOM ($-26.2\pm1.0\text{‰}$ and $9.1\pm1.4\text{‰}$, respectively) distinguished it from the other three potential diets (SOM, $-20.6\pm1.8\text{‰}$ and $6.5\pm2.4\text{‰}$; SPOM, $-19.8\pm1.7\text{‰}$ and $7.7\pm1.4\text{‰}$; MPB, $-19.7\pm2.0\text{‰}$ and $6.5\pm1.3\text{‰}$). The similarity of values for the latter three diets reflected well-coupled benthic and pelagic environments with high MPB resuspension, typical of western Korean tidal flats (Kon et al., 2012; Griffiths et al., 2017; Lee et al., 2021). The large difference in C stable isotope values between FPOM and consumers indicated that FPOM was not a primary diet (Noh et al., 2019). However, FPOM could have been indirectly consumed by benthos eating SPOM near the water gates. In addition, the enriched $\delta^{15}\text{N}$ signature of FPOM reflected the influence of anthropogenic sewage on the downstream portions of the Mangyeong and Dongjin Rivers (Choi et al., 2013).

Mean differences in the C and N stable isotope signatures were detected among consumer groups ($\delta^{13}\text{C}$: $F=20.2$, $p<0.001$; $\delta^{15}\text{N}$: $F=13.6$, $p<0.001$; Fig. 3.8.). The significantly depleted and enriched C stable isotope signatures of Ff ($-16.7\pm0.9\text{‰}$) and Gr ($-13.2\pm1.2\text{‰}$), respectively, distinguished them from the other feeding groups (Df, $-14.6\pm1.1\text{‰}$; Om, $-14.4\pm1.3\text{‰}$; Ca, $-15.3\pm0.5\text{‰}$). Ca and Df showed the narrowest and broadest $\delta^{13}\text{C}$ distributions, respectively, among consumers.

The depleted C stable isotope value for Ff indicated that this group's tissues had assimilated more ^{13}C -depleted organic matter (i.e., FPOM) than had that of other consumers in the Saemangeum tidal flat (Lee et al., 2021). This difference was related to the Ff feeding strategy, which entailed a strong possibility of encountering FPOM in the water columns relative to the feeding strategies of other consumers. The significantly enriched $\delta^{13}\text{C}$ values for two surface-grazing gastropods (*Bullacta caurina* and *Lunella coronata*) indicated the consumption of a ^{13}C -enriched diet, such as that including cyanobacteria ($\delta^{13}\text{C}$, -16.5 to -5‰) (Calder and Parker, 1973; Page, 1997; Choy et al., 2008). The large $\delta^{13}\text{C}$ range for Df reflected the flexible

feeding strategy of these consumers, which utilise available food resources regardless of their dietary quality (Lange et al., 2019).

The significantly enriched N stable isotope values for Om ($13.2 \pm 1.2\text{‰}$) and Ca ($14.4 \pm 2.0\text{‰}$) distinguished them from other consumers (Ff, $11.0 \pm 1.0\text{‰}$; Df, $11.6 \pm 1.3\text{‰}$; Gr, $11.7 \pm 0.3\text{‰}$). The stepwise increase in the TL of benthos from Ff (range, 1.7–3.3) to Ca (range, 3.0–5.9) suggested the presence of approximately five TLs in the Saemangeum tidal-flat food web (Figs. 3.8 and 3.9., Table 3.10.). At the species level, the most depleted and enriched mean N stable isotope signatures were for the Ff *Mytilus galloprovincialis* ($9.1 \pm 0.0\text{‰}$; TL, 1.7) and the Ca starfish *Patiria pectinifera* ($18.3 \pm 0.0\text{‰}$, TL, 5.9), respectively (Figs. 3.8 and 3.9., Table 3.10.). The larger $\delta^{15}\text{N}$ range for carnivores reflected their niche diversity, based on the inclusion of various taxa (Annelida, Mollusca, Arthropoda, and Echinodermata) in the functional group (Fig. 3.9., Table 3.10.). The comparable mean $\delta^{15}\text{N}$ values and TLs of Gr, Ff and Df indicated that they occupied lower trophic niches as primary consumers and utilised mainly autotrophs, such as MPB and phytoplankton (McCutchan Jr et al., 2003).

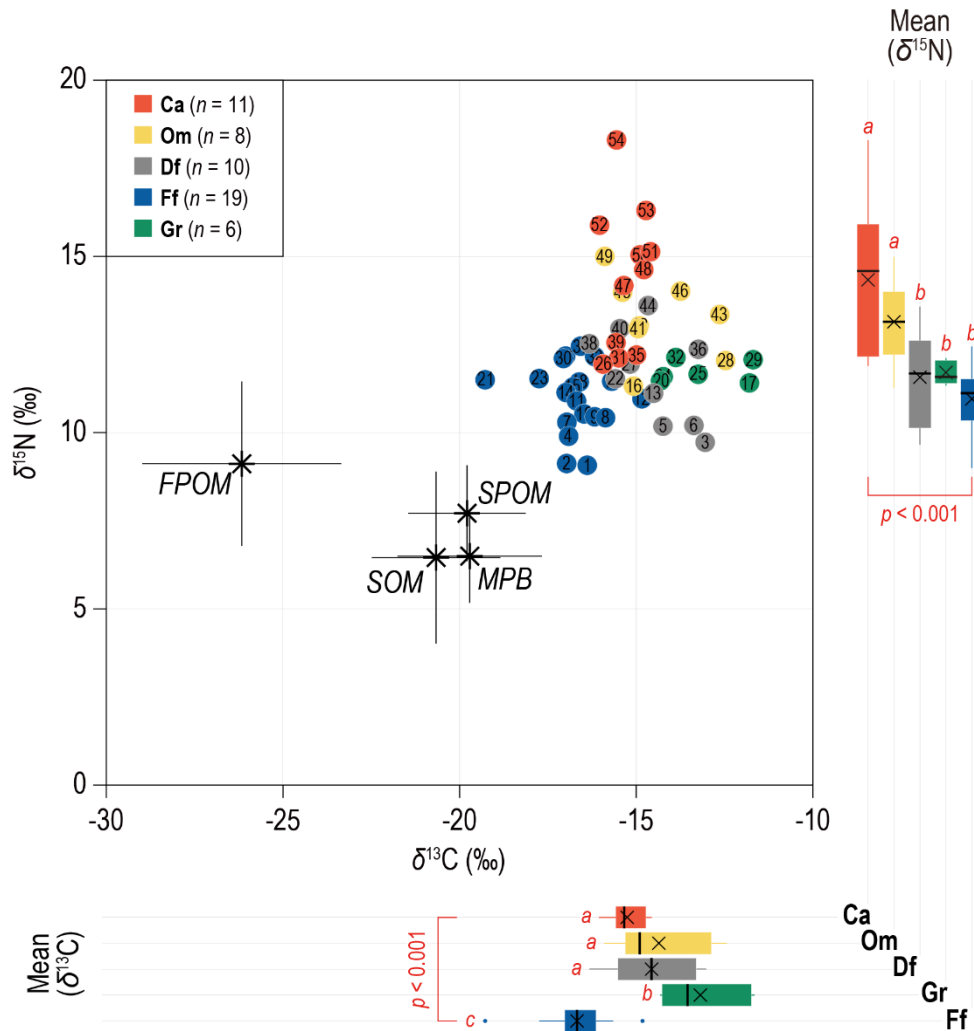


Figure 3.8.

Biplot of stable carbon and nitrogen isotope signatures ($\delta^{13}\text{C}$ and $\delta^{15}\text{N}$) of potential food sources and macrobenthos in the Saemangeum tidal flat. The values of potential food sources (freshwater and seawater particulate organic matter in the Saemangeum, FPOM and seawater POM; sediment organic matter, SOM; microphytobenthos, MPB) represent the total means with standard deviations (black asterisk and line). The values of macrobenthos represent the means of each species collected from 2019 to 2022. A red asterisk represents statistical significance among five functional groups (grazers, Gr; filter feeders, Ff; deposit feeders, Df; omnivores, Om; carnivores, Ca). Full scientific names of organisms described by number are given in Fig. 3.9 and Table 3.10.

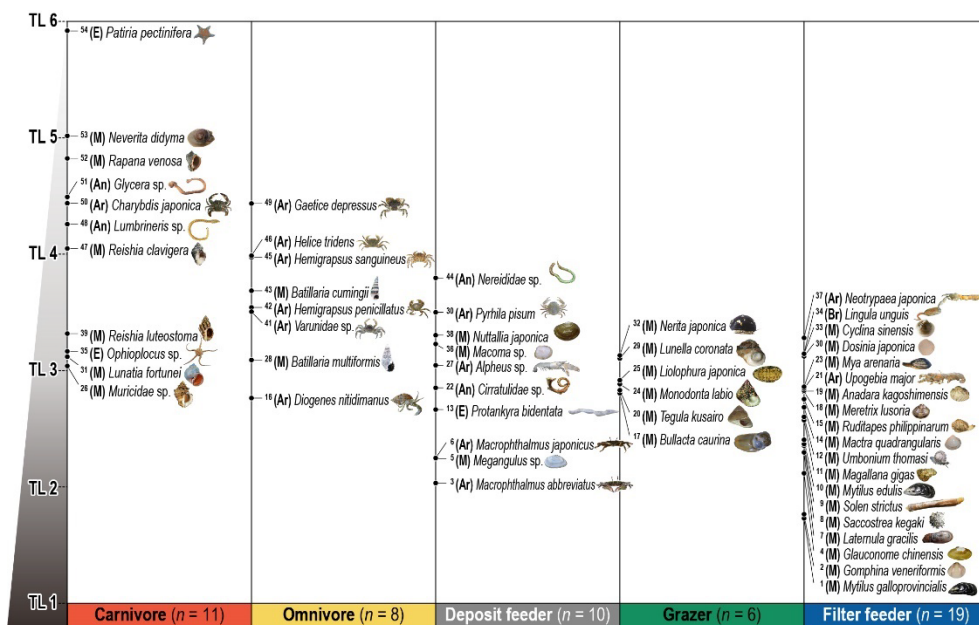


Figure 3.9.

Trophic level of 54 benthic consumers in the five phyla [Annelida, (An) ($n=4$); Arthropoda, (Ar) ($n=13$); Brachiopoda, (Br) ($n=1$); Mollusca, (M) ($n=33$); Echinodermata, (E) ($n=3$)] collected in the Saemangeum tidal flat, Korea, from 2019 to 2022. The superscript number indicates the identification of each species described in Fig. 3.8.

Table 3.10.

Carbon and nitrogen stable isotope values of 54 consumers with six feeding types (grazers, Gr; filter feeders, Ff; deposit feeders, Df; omnivores, Om; carnivores, Ca) and their potential diets [freshwater and seawater particulate organic matter, FPOM and SPOM; sediment organic matter, SOM; microphytobenthos, MPB] collected in the Saemangem tidal flat, Korea from 2019 to 2022. Species are listed with corresponding trophic level (TL) in descending order for each taxon (Annelida; Brachiopoda; Mollusca; Arthropoda; Chordata). Values are expressed as mean with standard deviation (stdev.). The superscript number indicates the identification of each species described in Fig. 3.8.

Sample	$\delta^{13}\text{C}$ (‰)	$\delta^{15}\text{N}$ (‰)	TL
Diet			
FPOM	-26.2±2.8	9.1±2.3	—
SPOM	-19.8±1.7	7.7±1.4	—
SOM	-20.6±1.8	6.5±2.4	—
MPB	-19.7±2.0	6.5±1.3	—
Consumer			
Annelida-Polychaeta			
⁵¹ (Ca) <i>Glycera</i> sp.	-14.6±0.9	15.1±1.5	4.5
⁴⁸ (Ca) <i>Lumbrineris</i> sp.	-14.8±0.7	14.6±1.2	4.3
⁴⁴ (Df) <i>Nereididae</i> sp.	-14.7±0.5	13.6±1.2	3.8
²² (Df) <i>Cirratulidae</i> sp.	-15.6±1.0	11.5±0.6	2.9
Brachiopoda-Lingulata			
³⁴ (Ff) <i>Lingula unguis</i>	-17.0±1.0	12.2±1.6	3.1
Mollusca-Bivalvia			
³⁸ (Df) <i>Nuttallia japonica</i>	-16.3±0.3	12.5±1.9	3.3
³⁶ (Df) <i>Macoma</i> sp.	-13.2±0.8	12.4±0.4	3.2
³³ (Ff) <i>Cyclina sinensis</i>	-16.2±0.5	12.2±0.5	3.1
³⁰ (Ff) <i>Dosinia japonica</i>	-17.1±0.3	12.1±0.1	3.1
²³ (Ff) <i>Mya arenaria</i>	-17.8±0.2	11.5±0.1	2.9
¹⁹ (Ff) <i>Anadara kagoshimensis</i>	-15.7±0.7	11.5±0.2	2.8
¹⁸ (Ff) <i>Meretrix lusoria</i>	-16.6±1.2	11.4±0.2	2.8
¹⁵ (Ff) <i>Ruditapes philippinarum</i>	-16.8±0.6	11.3±0.4	2.8
¹⁴ (Ff) <i>Macra quadrangularis</i>	-17.0±0.8	11.1±1.2	2.7
¹¹ (Ff) <i>Magallana gigas</i>	-16.7±1.3	10.9±0.5	2.6
¹⁰ (Ff) <i>Mytilus edulis</i>	-16.5±0.6	10.5±0.8	2.4
⁹ (Ff) <i>Solen strictus</i>	-16.2±0.2	10.5±0.6	2.4
⁸ (Ff) <i>Saccostrea kegaki</i>	-15.9±0.2	10.4±0.1	2.4
⁷ (Ff) <i>Laternula gracilis</i>	-17.0±0.3	10.3±0.5	2.3
⁵ (Df) <i>Megangulus</i> sp.	-14.3±0.4	10.2±0.7	2.2
⁴ (Ff) <i>Glauconome chinensis</i>	-16.9±0.4	9.9±0.2	2.1
² (Ff) <i>Gomphina veneriformis</i>	-17.0±0.0	9.1±0.1	1.8
¹ (Ff) <i>Mytilus galloprovincialis</i>	-16.4±0.0	9.1±0.0	1.7
Mollusca-Gastropoda			
⁵³ (Ca) <i>Neverita didyma</i>	-14.7±0.0	16.3±0.0	5.0
⁵² (Ca) <i>Rapana venosa</i>	-16.0±0.1	15.9±0.0	4.8
⁴⁷ (Ca) <i>Reishia clavigera</i>	-15.4±0.4	14.2±2.4	4.1
⁴³ (Om) <i>Batillaria cumingii</i>	-12.6±0.4	13.4±1.7	3.7
³⁹ (Ca) <i>Batillaria cumingii</i>	-15.6±1.0	12.6±0.7	3.3
³² (Gr) <i>Nerita japonica</i>	-13.9±0.4	12.1±0.2	3.1
³¹ (Ca) <i>Lunatia fortunei</i>	-15.5±0.7	12.1±1.8	3.1
²⁹ (Gr) <i>Lunella coronata</i>	-11.7±0.8	12.1±0.6	3.1
²⁸ (Om) <i>Batillaria multiformis</i>	-12.5±0.1	12.0±0.1	3.1
²⁶ (Ca) <i>Muricidae</i> sp.	-15.9±1.1	11.9±0.1	3.0
²⁴ (Gr) <i>Monodonta labio</i>	-14.2±0.5	11.6±0.4	2.9
²⁰ (Gr) <i>Tegula kusairo</i>	-14.3±0.2	11.5±0.1	2.8

Table 3.10. (Continued.)

Sample	$\delta^{13}\text{C}$ (‰)	$\delta^{15}\text{N}$ (‰)	TL
Mollusca-Gastropoda			
¹⁷ (Gr) <i>Bullacta caurina</i>	-11.8±0.7	11.4±1.7	2.8
¹² (Ff) <i>Umbonium thomasi</i>	-14.8±0.2	11.0±0.5	2.6
Mollusca-Polyplacophora			
²⁵ (Gr) <i>Liolophura japonica</i>	-13.3±0.2	11.7±0.1	2.9
Arthropoda-Malacostraca			
⁵⁰ (Ca) <i>Charybdis japonica</i>	-14.9±0.6	15.1±1.9	4.5
⁴⁹ (Om) <i>Gaetice depressus</i>	-15.9±0.1	15.0±3.4	4.4
⁴⁶ (Om) <i>Helice tridens</i>	-13.8±0.3	14.0±0.0	4.0
⁴⁵ (Om) <i>Hemigrapsus sanguineus</i>	-15.4±0.0	14.0±0.3	4.0
⁴² (Om) <i>Hemigrapsus penicillatus</i>	-14.9±1.3	13.0±0.7	3.5
⁴¹ (Om) <i>Varunidae</i> sp.	-15.0±1.1	13.0±0.7	3.5
⁴⁰ (Df) <i>Pyrhila pisum</i>	-15.5±0.2	12.9±0.2	3.5
³⁷ (Ff) <i>Neotrypaea japonica</i>	-16.6±0.4	12.5±0.7	3.3
²⁷ (Df) <i>Alpheus</i> sp.	-15.2±1.2	11.9±0.7	3.0
²¹ (Ff) <i>Upogebia major</i>	-19.3±0.3	11.5±0.9	2.8
¹⁶ (Om) <i>Diogenes nitidimanus</i>	-15.1±0.5	11.3±0.2	2.8
⁶ (Df) <i>Macrophthalmus japonicus</i>	-13.4±1.0	10.2±0.6	2.3
³ (Df) <i>Macrophthalmus abbreviatus</i>	-13.1±0.8	9.7±0.6	2.0
Echinodermata-Asteroidea			
⁵⁴ (Ca) <i>Patiria pectinifera</i>	-15.6±0.2	18.3±0.0	5.9
Echinodermata-Ophiuroidea			
³⁵ (Ca) <i>Ophioplocus</i> sp.	-15.0±0.3	12.2±0.1	3.2
Echinodermata-Holothuroidea			
¹³ (Df) <i>Protankyra bidentata</i>	-14.5±1.2	11.1±2.6	2.7

3.3.4. Spatiotemporal stable isotopic dynamics

ANOVA revealed significant spatial mean differences in the $\delta^{13}\text{C}$ values for two functional groups of consumers (Ff: $F=5.2$, $p<0.01$; Df: $F=11.5$, $p<0.001$; Figs. 3.10.A. and 3.11.A.). Ff showed significant $\delta^{13}\text{C}$ enrichment at sites near the water gates relative to YM. Df showed $\delta^{13}\text{C}$ enrichment at SS relative to other sites. The $\delta^{13}\text{C}$ enrichment observed for consumers at SS and GR1 reflected the transfer of the environmental ^{13}C -enriched signature to the baseline (SOM and MPB) and then to consumers through the food chain, and implied high consumption of ^{13}C -enriched diets at sites near the water gates (Lee et al., 2021). Three outlier Ff samples (*Lingula unguis*, *Magallana gigas* and *Macra quadrangularis*) with depleted $\delta^{13}\text{C}$ values were investigated only at sites near the water gates (SS and GR1), and not at YM (Fig. 3.10.A.). The results revealed that some Ff were influenced more by FPOM in the water column near the gates. The larger $\delta^{13}\text{C}$ distribution for Ff at SS and GR1 than at YM additionally revealed the high complexity of the organic matter pool under conditions with high MPB production and FPOM input. The significant spatial mean $\delta^{15}\text{N}$ difference was estimated only for Df ($F=3.5$, $p<0.05$; Fig. 3.11.A.), and revealed a greater trophic role than that of Ff in the Saemangeum tidal flat.

To evaluate the influence of the degree of water exchange on the food web in the outer tidal flat, we compared the consumer $\delta^{13}\text{C}$ and $\delta^{15}\text{N}$ distributions between periods I and II (Figs. 3.10.B. and 3.11.B.). C and N stable isotope values for consumers did not differ between periods at any site (Figs. 3.12. and 3.13.). The SIBER model also revealed temporally consistent small niche spaces, with SEA_c values $<20\text{‰}^2$ for both functional benthos groups at all sites, indicating that the discharged water had no substantial impact on changes in the stable isotope signatures of consumers (Figs. 3.10.C. and 3.11.C.). The small niche spaces reflected the sedentary characteristics of benthos (Lee et al., 2023). The largest and smallest SEA_c values for both consumers were obtained for GR1 (Ff, $2.0\text{--}2.1\text{‰}^2$; Df, $2.5\text{--}7.5\text{‰}^2$) and YM (Ff, $0.6\text{--}0.9\text{‰}^2$; Df, $2.0\text{--}3.7\text{‰}^2$), respectively (Table 3.11.), with moderate values obtained for SS (Ff, $1.2\text{--}2.9\text{‰}^2$; Df, $4.0\text{--}4.0\text{‰}^2$). The larger SEA_c values for Df than for Ff reflect the former's high degree of dietary flexibility and various functional roles in the Saemangeum tidal flat.

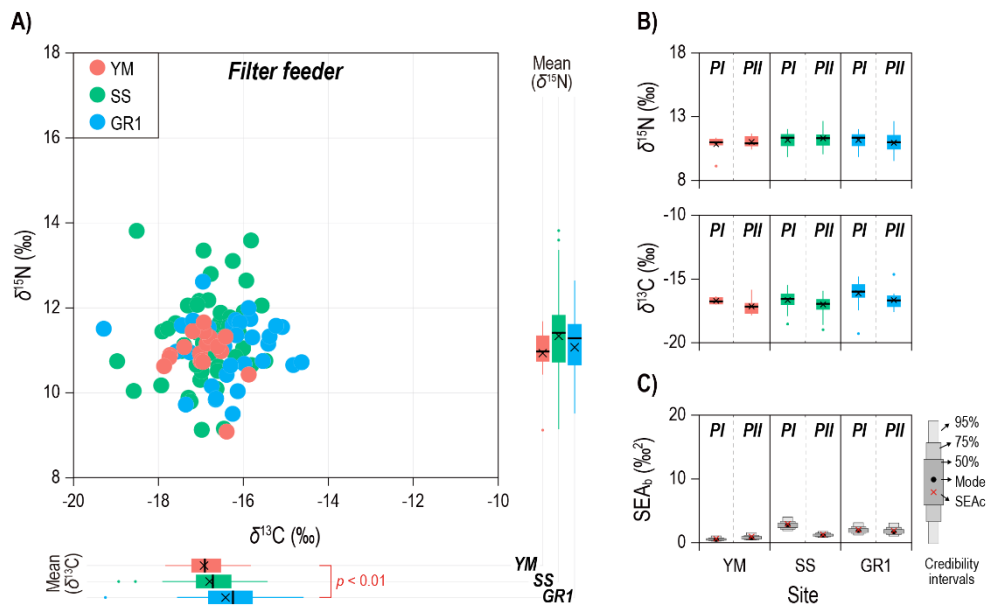


Figure 3.10.

Stable carbon and nitrogen isotope signatures ($\delta^{13}\text{C}$ and $\delta^{15}\text{N}$) of filter feeders (Ff) in the Saemangeum tidal flat by site (A) and period (B). YM, Yami; SS, Sinsi; GR1, Garyuk 1; PI, 2019–2020; PII, 2021–2022. (C) Stable isotope niche space of Ff. Red crosses are maximum likelihood estimates. SEAb , Bayesian standard ellipse area; SEAc , sample size corrected ellipse area.

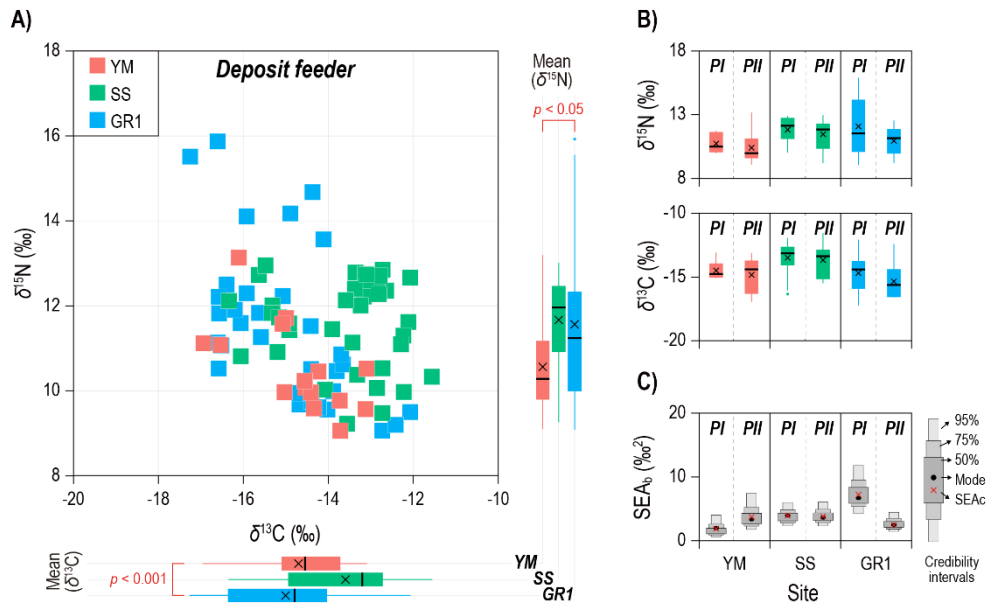


Figure 3.11.

Stable carbon and nitrogen isotope signatures ($\delta^{13}\text{C}$ and $\delta^{15}\text{N}$) of deposit feeders (Df) in the Saemangeum tidal flat by site (A) and period (B). YM, Yami; SS, Sinsi; GR1, Garyuk 1; PI, 2019–2020; PII, 2021–2022. (C) Stable isotope niche space of Df. Red crosses are maximum likelihood estimates. SEAb , Bayesian standard ellipse area; SEAc , sample size corrected ellipse area.

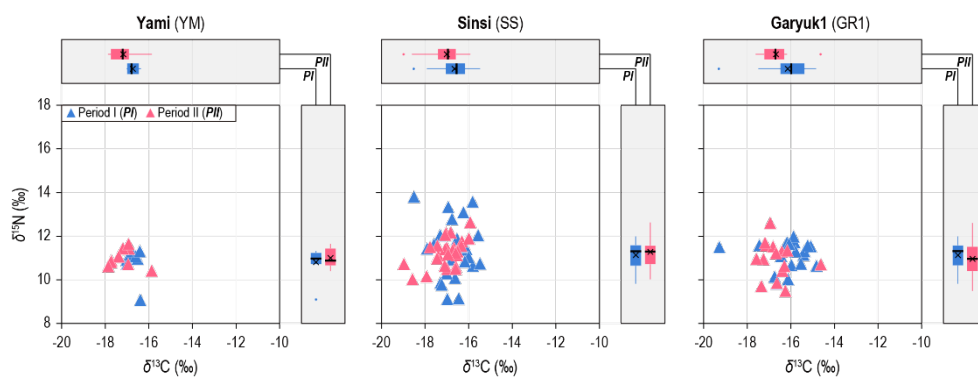


Figure 3.12.

Stable carbon and nitrogen isotope values ($\delta^{13}\text{C}$ and $\delta^{15}\text{N}$) of filter feeders (Ff) collected at three sites (Yami, YM; Sinsi, SS; Garyuk1, GR1) in the Saemangeum tidal flat, Korea from 2019 to 2022. Blue and red symbols indicate Ff collected during period I (2019–2020) and period II (2021–2022), respectively.

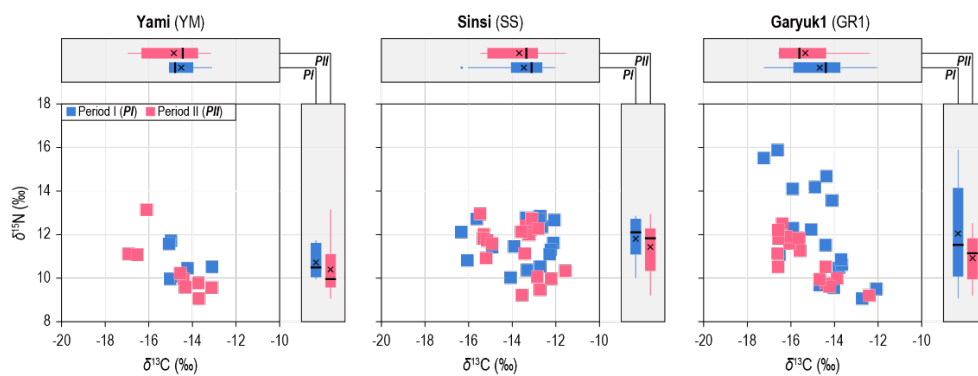


Figure 3.13.

Stable carbon and nitrogen isotope values ($\delta^{13}\text{C}$ and $\delta^{15}\text{N}$) of deposit feeders (Df) collected at three sites (Yami, YM; Sinsi, SS; Garyuk1, GR1) in the Saemangeum tidal flat, Korea from 2019 to 2022. Blue and red symbols indicate Df collected during period I (2019–2020) and period II (2021–2022), respectively.

Table 3.11.

Seasonal niche metrics (Bayesian standard ellipse area, SEA_b ; sample size corrected ellipse area, SEA_c) of deposit- and filter-feeding consumers collected at three sites (Yami, YM; Sinsi, SS; Garyuk1, GR1) in the Saemangeum tidal flat, Korea from 2019 to 2022. PI and PII indicate period I (2019–2020) and period II (2021–2022), respectively.

Sample	Site	Period	SEA_b	SEA_c
Filter feeder	YM	PI	0.5	0.6
		PII	0.8	0.9
	SS	PI	2.7	2.9
		PII	1.2	1.2
	GR1	PI	2.0	2.1
		PII	1.9	2.0
Deposit feeder	YM	PI	1.6	2.0
		PII	3.3	3.7
	SS	PI	3.8	4.0
		PII	3.8	4.0
	GR1	PI	7.0	7.5
		PII	2.3	2.5

In the cluster analysis performed to estimate the spatiotemporal diet consumption of Ff and Df, Ff was divided into two groups with a low degree of similarity based on the Euclidean distance (Fig. 3.14.). Ff group 2 at SS had greater mean MPB consumption ($54.5 \pm 10.3\%$) than did group 1 ($9.2 \pm 2.4\%$). In addition, group 2 utilised more MPB in period I (62%) than in period II (47%). These results reflect the large MPB biomass at SS, especially in period I (Table 3.9.). In contrast, Ff group 2 utilised SPOM intensively ($>75\%$) and other SOM and MPB less ($\sim 10\%$), with no clear difference between periods. Six Df samples collected at YM, SS and GR1 in the two periods showed a high degree of similarity and thus were not separated into groups. Df consumption of the three diets was comparable to that of Ff (Fig. 3.14.B.). The greatest similarity in Df diet utilisation between periods was found for SS. The main and secondary food sources for Df in both periods were SPOM ($63.0 \pm 0.0\%$) and MPB ($23.4 \pm 0.4\%$), respectively. This high MPB utilisation, like that of Ff, reflected the large MPB biomass at SS. The spatiotemporal diet utilisation pattern for Ff reflected variable and unpredictable food supplies relative to that for Df in the Saemangeum tidal flat, particularly near Sinsi watergate (Levinton, 1972). In contrast, the Df food supply was spatiotemporally constant (Lee et al., 2021). Thus, the cluster analysis demonstrated 1) spatiotemporal diet complexity with water discharge disturbance and 2) that functional groups primarily determined the diet utilisation of benthos in the Saemangeum food web. Overall, the mixed-model results show the primary role of SPOM, which provided the greatest dietary contribution (mean, 66.5%; range, 24.2–89.3%) to benthic consumers in the Saemangeum tidal flat. MPB was an important secondary diet (mean, 21.4%; range, 6.3–61.8%), particularly near SS. The MPB contribution was lesser than the $>60\%$ observed in our previous study conducted at Ganghwa tidal flat, reflecting the lesser MPB biomass in the Saemangeum (range, $26.5\text{--}46.4\text{ mg m}^{-2}$) than in the Ganghwa (range, $15.5\text{--}82.1\text{ mg m}^{-2}$) tidal flat (Table 3.9.) (Lee et al., 2021).

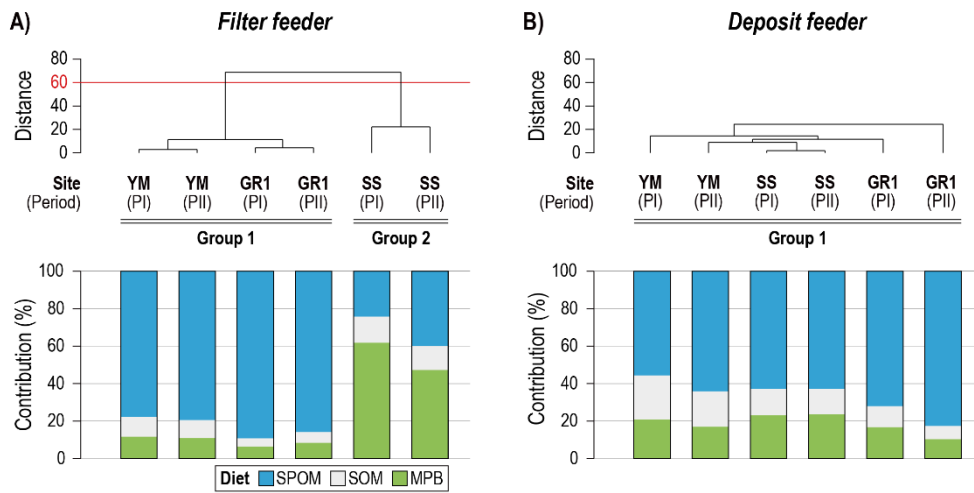


Figure 3.14.

Spatio-temporal groups of filter feeder **(A)** and deposit feeder **(B)** determined by cluster analysis based on similarity of their diet utilisation at three sites (Yami, YM; Sinsi, SS; Garyuk1, GR1) in the Saemangeum tidal flat, Korea. The following colours (blue, SPOM; grey, SOM; green, MPB) indicate the contribution (%) of the three diets to the consumers. PI and PII indicate period I (2019-2020) and period II (2021-2022), respectively.

3.3.5. Comparison of trophic characteristics to other Korean tidal flat

A total of twenty-one previous studies have been conducted to examine food web structure in tidal flats on the western and southern coasts of Korea (Fig. 3.15., Tables 3.3. and 3.4.). The ranges of C and N stable isotope values for SPOM, FPOM and SOM were broader for the Saemangeum tidal-flat food web than reported previously. This was especially true for the FPOM distributions ($\delta^{13}\text{C}$, -31.6 to -21.2‰ ; $\delta^{15}\text{N}$, 4.7 to 14.6‰) relative to those reported previously ($\delta^{13}\text{C}$, -28.5 to -23.7‰ ; $\delta^{15}\text{N}$, 6.4 to 11.9‰), reflecting the highly diverse organic matter distribution in Saemangeum Lake with water exchange with the outer tidal flat. In addition, $\delta^{15}\text{N}$ values for FPOM exceeding 10‰ reflected sewage input from agricultural areas upstream of Saemangeum Lake (Lee, 2000; Duprey et al., 2019). The large range of $\delta^{13}\text{C}$ values for SPOM (-23.2 to -14.9‰) overlapped with the values for FPOM and MPB, implying that organic matter dynamics in the Saemangeum tidal flat were complex due to 1) the dependence of the degree of resuspended MPB input to the water column on spatiotemporal MPB production and 2) the influence of regularly discharged organic matter input from FPOM to SPOM. The relatively ^{13}C -enriched signature for SPOM reflected the large contribution of resuspended MPB in the well-coupled benthic-pelagic environment in the Saemangeum tidal flat (Griffiths et al., 2017; Lee et al., 2021). The $\delta^{15}\text{N}$ values for SPOM and SOM, similar to those for FPOM, reflected the influence of water exchange through the Saemangeum dike between the Lake and tidal flat. The large $\delta^{15}\text{N}$ range in potential diets in the present study indicated a less stable food web baseline with various impacts of natural and anthropogenic sources distributions compared to other Korean tidal flats.

In contrast, consumers in the Saemangeum tidal flat had narrow $\delta^{13}\text{C}$ (-19.3 to -11.7‰) and $\delta^{15}\text{N}$ (9.1 to 18.3‰) ranges relative to those reported for other Korean tidal flats ($\delta^{13}\text{C}$, -23.5 to -7.9‰ ; $\delta^{15}\text{N}$, 5.3 to 18.5‰), indicating no significant transfer of discharged organic matter to consumers through the Saemangeum tidal-flat food web (Fig. 3.15.). The relatively small amount of discharged organic matter in limited time conditions for water exchange might explain the less variation of stable isotope values of consumers compared to potential diets. In addition, the large spatial scales of stable isotope data collection along the

western and southern Korean coasts and the large number ($n=218$) of consumer species may explain the breadth of previously reported C and N stable isotope distributions.

Overall, the comparison of stable isotope values with those from other Korean tidal flats demonstrated the following about the Saemangeum tidal-flat food-web structure and function: 1) the benthic-pelagic environment is well coupled and 2) the organic matter distribution is diverse due to the irregular discharged water input and spatial and seasonal MPB production.

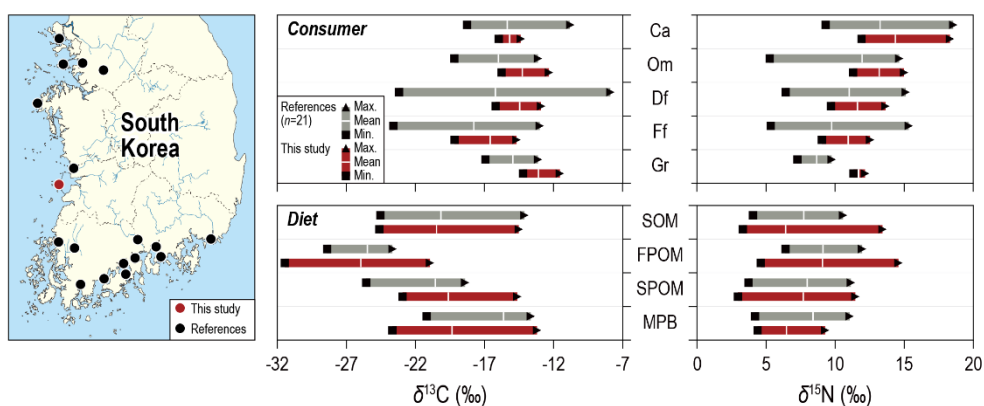
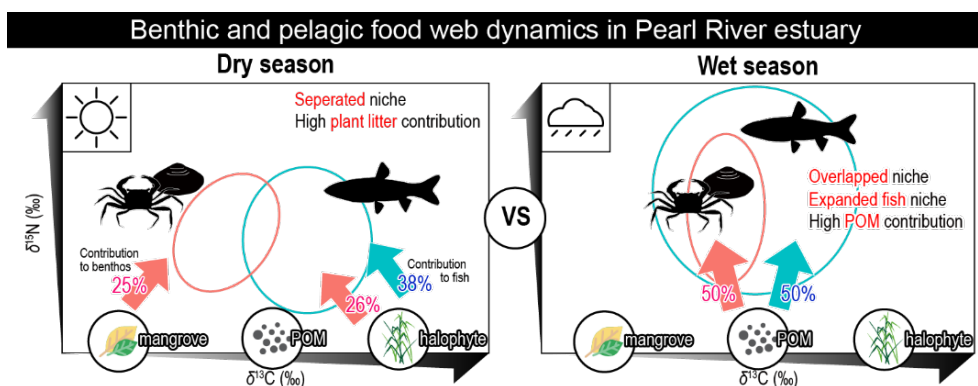


Figure 3.15.

Review of stable carbon and nitrogen isotope values ($\delta^{13}\text{C}$ and $\delta^{15}\text{N}$) of benthic consumers (grazers, Gr; filter feeders, Ff; deposit feeders, Df; omnivores, Om; carnivores, Ca) and their potential diets (freshwater and seawater particulate organic matter, F/SPOM; sediment organic matter, SOM; microphytobenthos, MPB) in previous food web studies ($n=21$) on the west and south coasts of Korea. The values investigated in the present study are included for comparison.

CHAPTER 4.

Food web structure of mangrove forest in Pearl River Estuary in China with seasonal flood dynamics



This chapter has been published to Marine Pollution Bulletin.

Lee, I.O., Noh, J., Kim, B., Kwon, I., Kim, H., Kwon, B-O, Peng, Y., Hu, Z., Khim, J.S.

Food web dynamics in the mangrove ecosystem of the Pearl River Estuary surrounded by megacities. *Mar. Pollut. Bull.* 2023, 189, 114747

<https://doi.org/10.1016/j.marpolbul.2023.114747>

4.1. Introduction

Mangrove ecosystems thrive along coastlines throughout most of the tropics and subtropics (Bouillon et al., 2008a). They provide critical ecosystem services such as nursery, breeding grounds, food production, and shoreline protection for coastal organisms (Lovelock and Reef, 2020; Wang et al., 2020; Chen and Lee, 2022). However, the biodiversity hot spot, the mangrove forests, have suffered degradation and loss due to rapid coastal development in the last two decades (Hamilton and Casey, 2016). The number of mangroves in Southeast Asia have devastated and replaced by aquaculture (mainly shrimp farming) and anthropogenic landscapes (Lee and Khim, 2017). In particular, China has been listed as the country with the greatest relative loss of mangrove forests in the world (Wang et al., 2020). As a result, the Chinese government made an effort to conserve important mangrove ecosystems by establishing a total of 43 mangrove-protected areas (ca. 67% of national mangrove forests) in 2019 (Giri et al., 2011; Wang et al., 2020).

Guangdong province has the largest mangrove forests in China with an area of ~10,331 ha as year of 2018, accounting for 40.22% of the total national mangrove area (Zhang et al., 2021). The Pearl River Estuary (PRE), located in the south of Guangdong province, has long been recognised as ecologically significant region with the spawning, breeding, and feeding habitats for various aquatic organisms and migratory birds (Li and Lee, 1998; Lee, 2000). Unfortunately, the PRE mangroves are being largely exposed to coastal developments and contaminant inputs by urban sewage and agricultural discharges from megacities (Liu et al., 2013; Qiu et al., 2019; Wang et al., 2021). These anthropogenic disturbances are expected to shift the fundamental trophic dynamics in the mangrove ecosystem, resulting alteration of the food web structure and function (Lee, 2016). However, most previous studies conducted in the PRE focused on environmental pollution, and changes in microbiome community structure under anthropogenic influences (Cao et al., 2012; Han and Gu, 2015), and only a few studies were conducted for the impact on trophic structural changes in the eastern PRE (Lee, 2000; Li and Lee, 1988) (Table 4.1.). Li and Lee (1998) highlighted the importance of incorporating anthropogenic

influences into the structure and function of ecosystems in urban settings in PRE. In addition, Lee (2000) reported the importance of anthropogenic POM and microalgae supporting the consumer community in eastern PRE. However, the seasonal understanding of the PRE trophic structure, giving implications for future appropriate conservation and management, is still limited.

Stable isotope analysis is widely used to explore the trophic function of estuarine ecosystems (Layman et al., 2012; Ke et al., 2016; Sabo et al., 2017; Lee et al., 2021). The distinct carbon stable isotope range of primary producers [e.g., phytoplankton, microphytobenthos (MPB), and halophytes] allows us to identify the potential diets of consumers (Gal et al., 2016; Lee et al., 2021). In comparison, the $\delta^{15}\text{N}$ signature of an organism indicates the trophic level of a community, which is calculated from the relative enrichment of the diet (Post, 2002). Bayesian community-wide metrics based on carbon and nitrogen isotope values offer an effective approach for identifying general patterns and making comparisons among sampling periods in complex estuarine ecosystems (Abrantes et al., 2014).

We investigated the seasonal food web structure and its function of the Chinese mangrove ecosystem in Qi'ao Island surrounded by megacities to give implications for future appropriate conservation and management. The objectives were to 1) describe the benthic and pelagic trophic structure from baseline to consumers with trophic levels; 2) determine the seasonal food web structure (trophic niche of benthic and pelagic consumers; and the seasonal dietary contribution to consumers); Finally, 3) characterize the PRE food web structure surrounded by megacities by comparing the C and N stable isotopes distribution of potential diets and consumers in three types of Chinese coastal ecosystem (mangrove forest, salt marsh, and seagrass habitats) using literature reviews.

4.2. Materials and methods

4.2.1. Study area

The study area Qi'ao Island, the provincial mangrove nature reserve, is situated on the western part of the Pearl River Estuary (PRE). The PRE (21°20' to 23°30'N and 112°40' to 114°50'E) is the third largest River in China and is in the subtropical and transitional zone of the East Asian monsoon system. Consequently, there is high seasonal water discharge (Lee et al., 2000; Oiu et al., 2019). The annual mean air temperature ranges from 12.6 to 32.0 °C, and precipitation is ca. 1,700 mm (Wang et al., 2021). Rainfall is intensive particularly during the wet season (April–September), accounting for approximately 80% of annual precipitation. The high seasonality in water discharge generates a diverse natural nutrient source for organisms in the western PRE ecosystem, including terrestrial organic matter, phytoplankton, MPB, and halophyte- and mangrove litter (Lee et al., 2021). In addition, PRE ecosystem connects to many tributaries from megacities in Guangdong Province, with ca. 120 million inhabitants (Peng et al., 2009; Liu et al., 2013; Duprey et al., 2019; Wang et al., 2021) (Fig. 4.1.). Sewage inputs have markedly increased and influenced the PRE environment over the last three decades due to the dense human population, rapid urbanisation, and agricultural development with explosive economic growth (Lee et al., 2000; Duprey et al., 2019).

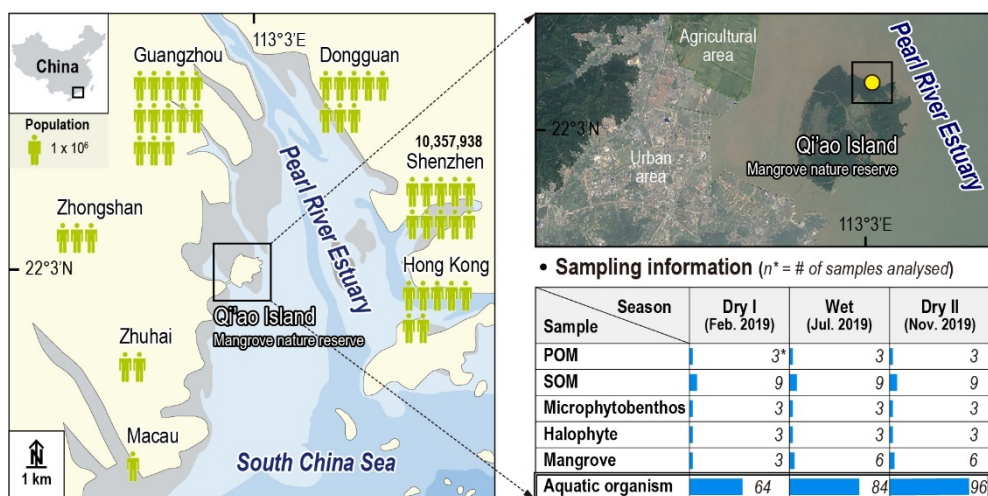


Figure 4.1.

Map of the study area (Qi'ao Island in the Pearl River Estuary, PRE) with human population and sampling information. n indicates the number of samples analysed including three and four replicates for each diet and organism.

4.2.2. Sample collection and preparation

Sampling was seasonally conducted at sites across the mangrove forest and bare tidal flat of Qi'ao Island in 2019. Sampling was separated into three periods: 1) 1st dry season (Dry I, February), 2) wet season (Wet, July), 3) 2nd dry season (Dry II, November) (Fig. 4.1.). Surface sediment (~0.5 cm) was stored in plastic bottles to quantify general sediment parameters in the laboratory. Rapid partial analysis was used to quantify the mud content, MC (Buchanan, 1984). The textural type of sediment was classified following the method of Flemming (2000). Loss on ignition (LOI) was estimated after 4 h of burning sediment to ashes at 550°C (Heiri et al., 2001). Sediment was freeze-dried and powdered using a mortar and pestle to analyse total organic carbon (TOC) and nitrogen (TN). Sediment samples for TOC analysis were decalcified with 10% hydrochloric acid (HCl). Surface sediment (~0.5 cm) was collected using a syringe corer (diameter, 3.0 cm) to estimate benthic chlorophyll-*a* (Chl-*a*). Samples were frozen on dry ice in situ and were transported to the laboratory. Chl-*a* was extracted from samples with 100% acetone (24 h at 4°C), and was subsequently centrifuged (5 min, 3000 rpm). The absorbance of the extracted solution was measured using a spectrophotometer by placing 3 mL solution in a quartz cuvette. The Lorenzen (1967) equation was applied to calculate the Chl-*a* concentration of sediment. We converted the photosystem II electron transport rate (ETR) estimated in a PAM fluorometer to primary production (PP) based on the following formula (Barranguet and Kromkamp, 2000):

$$PP \text{ (mg C m}^{-2} \text{ h}^{-1}\text{)} = \text{Chl-}a \text{ (mg m}^{-2}\text{)} \times 0.043 \times \text{ETR}$$

Particulate organic matter (POM) was pre-filtered using a net (Ø=200 µm) to remove large particles and was then re-filtered with a pre-combusted Whatman GF/F glass fibre filter (Ø=0.7 µm). At low tide, dense MPB mats were collected from the sediment surface (~0.5 cm) and were extracted using a method in Couch (1989). Sediment organic matter (SOM) was also collected from the sediment surface (~0.5 cm). The fresh leaves of a C₄ halophyte, *Cyperus malaccensis*, and mangrove, *Sonneratia apetala* were collected and scraped with a razor blade to remove

epibionts and were rinsed with distilled water. Mangrove detritus was collected in the sediment (~10.0 cm) next to the aerial root of *S. apetala*.

Macrobenthos were collected by hands. Fish were obtained from a fisherman who caught them in the study area. All benthic and pelagic organisms were randomly sampled to produce representativeness of species composition in the PRE. Thirty-four species from three phyla (16 Chordata, 14 Arthropoda, and 4 Mollusca) were classified by expert judgment (Fig. 4.2.). The feeding types of consumers (filter feeder, Ff; herbivore, Hb; deposit feeder, Df; planktivore, Pk; omnivore, Om; carnivore, Ca) were classified based on previous reports (Table 4.2.). After classification, the muscle tissue of organisms was dissected, lyophilised, and homogenised before stable isotope analysis. We also gathered the best available stable isotope data of producers and consumers (8 phyla, 17 classes, 144 species) from 18 previous studies conducted in three types of salt marshes (seagrass, halophyte, and mangrove) in China to elucidate the specific trophic functional characteristics of the PRE mangrove ecosystem.


































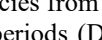
Chordata (16 species)			Arthropoda (14 species)			Mollusca (4 species)		
Family	Species		Family	Species		Family	Species	
Cyprinidae	<i>P. pekinensis</i>		Corophiidae	<i>S. sinensis</i>		Cyrenidae	<i>C. fluminea</i>	
Engraulidae	<i>E. japonicus</i>		Leptocheliidae	<i>C. dubia</i>		Pharidae	<i>Sinonovacula</i> sp.	
Gobiidae	<i>G. giuris</i>		Palaemonidae	<i>P. carinicauda</i>		Ellobiidae	<i>E. aurismidae</i>	
	<i>T. cirratus</i>			<i>P. serrifer</i>		Penaeidae	<i>N. violaceum</i>	
	<i>O. rubicundus</i>		Penaeidae	<i>Metapenaeus</i> sp.				
	<i>P. modestus</i>		Grapsidae	<i>M. quadridentatus</i>				
	<i>M. filifer</i>		Leucosiidae	<i>P. carinata</i>				
	<i>Boleophthalmus</i> sp.		Ocypodidae	<i>O. stimpsoni</i>				
Mugilidae	<i>O. ophuyseni</i>		Portunidae	<i>S. paramamosain</i>				
Pristigasteridae	<i>I. melastoma</i>		Sesarmidae	<i>P. pictum</i>				
Scatophagidae	<i>S. argus</i>			<i>C. haematocheir</i>				
			Varunidae	<i>V. litterata</i>				
Sciaenidae	<i>N. albiglora</i>			<i>M. longipes</i>				
	<i>C. lucidus</i>			<i>E. sinensis</i>				
Sillaginidae	<i>S. sihama</i>							
Tetraodontidae	<i>T. xanthopterus</i>							
	<i>T. ocellatus</i>							

Figure 4.2.

A total of 34 species from three phyla (Chordata, Arthropoda, and Mollusca) collected over three sampling periods (Dry I, February; Wet, July; Dry II, November) in 2019. The full scientific names of the organisms are given in Table 4.7.

Table 4.1.

Previous studies which conducted in the Pearl River Estuary, China. The black box indicates the previous study of food web structure in the Pearl River Estuary.

Research fields in previous studies			<i>n</i>	References
Category 1	Category 2	Category 3		
Biota	Microbiome	Community structure	12	3; 4; 8; 16; 21; 22; 26; 29; 32; 36; 38; 42
	Phytoplankton	Community structure	2	13; 23
	Microphytobenthos	Primary production	1	31
	Mangrove	Population dynamics	1	34
	Food web	Food web structure	2	27; 30
Total			18	
Environment	Physics	Modelling for mangrove storm protection	1	19
	Chemical properties	Organic carbon in the sediment	4	12; 18; 20; 41
		Nutrient concentration	1	39
		Dissolved inorganic carbon in the water	1	2
	Pollution	Antibiotics	1	17
		Heavy metals	4	1; 11; 24; 25
		Microplastics	7	9; 10; 28; 33; 38; 43; 44
		Organophosphate esters (OPEs)	1	37
		Organophosphorus flame retardants (OPFRs)	1	21
		Polybrominated diphenyl ethers (PBDEs)	9	5; 6; 7; 14; 15; 22; 35; 37; 40
		Polychlorinated biphenyls (PCBs)	2	5; 6
	Total			32
1, Bai et al., 2012; 2, Cai et al., 2004; 3, Cao et al., 2011; 4, Cao et al., 2012; 5, Chen et al., 2007; 6, Chen et al., 2011; 7, Chen et al., 2013a; 8, Chen et al., 2013b; 9, Dang et al., 2021; 10, Duan et al., 2021; 11, Feng et al., 2005; 12, Feng et al., 2019; 13, Gao et al., 2018; 14, Guan et al., 2007; 15, Guan et al., 2009; 16, Han and Gu, 2015; 17, He et al., 2012; 18, He et al., 2021; 19, Hespen et al., 2021; 20, Hu et al., 2006; 21, Hu et al., 2017; 22, Hu et al., 2019; 23, Huang et al., 2012; 24, Kulkarni et al., 2018; 25, Lang et al., 2023; 26, Lee et al., 2018; 27, Lee, 2000; 28, Li et al., 2020; 29, Li et al., 2011; 30, Li and Lee, 1988; 31, Liu et al., 2013; 32, Luo et al., 2018; 33, Meera et al., 2022; 34, Peng et al., 2016; 35, Shi et al., 2020; 36, Wang et al., 2012; 37, Xie et al., 2022; 38, Yan et al., 2022; 39, Zhang et al., 2014; 40, Zhang et al., 2015; 41, Zhang et al., 2022; 42, Zhou et al., 2018; 43, Zhou et al., 2020; 44, Zuo et al., 2020				

Table 4.2.

List of benthic and pelagic consumers with corresponding functional groups (herbivores, Hb; deposit feeders, Df; filter feeders, Ff; planktivores, Pk; omnivores, Om; carnivores, Ca) collected in the Pearl River Estuary, China.

Type	Phylum	Species	Feeding type	Reference
Fish	Chordata	<i>Scatophagus argus</i>	Om	Gupta, 2016
		<i>Engraulis japonicus</i>	Pk	Tanaka et al., 2006
		<i>Ilisha melastoma</i>	Ca	Blaber et al., 1998
		<i>Parabramis pekinensis</i>	Om	Gu et al., 2021
		<i>Sillago sihama</i>	Ca	Gunn and Milward, 1985
		<i>Nibea albiflora</i>	Ca	Qin et al., 2020
		<i>Collichthys lucidus</i>	Ca	Zhang et al., 2021
		<i>Glossogobius giuris</i>	Ca	Hossain et al., 2016
		<i>Taenioides cirratus</i>	Ca	Kader et al., 1988
		<i>Odontamblyopus rubicundus</i>	Ca	Tian et al., 2010
		<i>Periophthalmus modestus</i>	Ca	Lee et al., 2021; Beck, 2013
		<i>Myersina filifer</i>	Ca	Pogoreutz and Ahnelt, 2014
		<i>Boleophthalmus</i> sp.	Ca	Ravi, 2013
		<i>Osteomugil ophuyseni</i>	Pk	Larson and Shanks, 1996
Benthos	Mollusca	<i>Takifugu xanthopterus</i>	Ca	Kang et al., 2011
		<i>Takifugu ocellatus</i>	Ca	Kang et al., 2011
		<i>Sinonovacula</i> sp.	Ff	Ke et al., 2019
		<i>Corbicula fluminea</i>	Ff	Way et al., 1990
		<i>Ellobium aurismidae</i>	Df	Teoh et al., 2018
		<i>Neripteron violaceum</i>	Hb	Unabia, 1996
	Arthropoda	<i>Sinocorophium sinensis</i>	Df	Fenchel et al., 1975
		<i>Metopograpsus quadridentatus</i>	Om	Ei-Sayed et al., 2000
		<i>Pyrhila carinata</i>	Df	Quan et al., 2010
		<i>Ocypode stimpsoni</i>	Df	Wong et al., 2012
		<i>Palaemon carinicauda</i>	Om	Quan et al., 2010
		<i>Palaemon serrifer</i>	Om	Antonio et al., 2010
		<i>Metapenaeus</i> sp.	Om	Chu, 1989
		<i>Scylla paramamosain</i>	Ca	Viswanathan and Raffi, 2015
		<i>Parasesarma pictum</i>	Hb	Wang et al., 2021
		<i>Chironantes haematocheir</i>	Hb	Feng et al., 2017
		<i>Varuna litterata</i>	Om	Aneykutty et al., 2013
		<i>Metaplex longipes</i>	Df	Feng et al., 2017
		<i>Eriocheir sinensis</i>	Om	Crocetta et al., 2020
		<i>Chondrochelia dubia</i>	Ff	Mendoza et al., 1982

Table 4.3.

Results of the Chi-square test performed to investigate the difference in occurrence among feeding guilds in each consumer group [benthos (herbivores; filter feeders; deposit feeders; omnivores; carnivores); fish (planktivores; carnivores)] in three seasons.

Group	Chi-square (χ^2)	Degree of freedom (df)	<i>p</i>
Fish	1.3	2	> 0.05
Benthos	6.7	8	> 0.05

Table 4.4.

Review of the stable isotope values for carbon and nitrogen ($\delta^{13}\text{C}$ and $\delta^{15}\text{N}$) of potential diets in previous studies ($n=18$) for six provinces (Fujian, Guangdong, Guangxi, Hong Kong, Shanghai, and Zhejiang) in China. Values are expressed as mean with range (min.–max.).

Vegetation	Province	Type	Species	$\delta^{13}\text{C}$, mean (min. to max.)	$\delta^{15}\text{N}$, mean (min. to max.)	Reference
Mangrove	Guangdong	SOM		–15.0 (–18.8 to –12.1)	7.9 (6.5–9.8)	Arbi et al., 2018
		POM		–15.9 (–19.6 to –12.5)	9.2 (5.9–13.0)	
		MPB		–13.3 (–14.9 to –11.7)	8.0 (6.4–10.2)	
		Mangrove		–27.5 (–29.6 to –25.0)	8.7 (6.9–9.9)	Chen et al., 2018
		POM		–25.4	12.5	
		MPB		–17.0	15.7	
		Mangrove	<i>Avicennia marina</i>	–29.6	9.5	Chen et al., 2021
	Fujian	POM		–24.3 (–24.7 to –23.9)	5.7 (5.6–5.8)	
		Mangrove	<i>Kandelia obovata</i>	–27.3	4.9	
		POM		–24.2	9.6	Feng et al., 2015
		MPB		–23.9	8.8	
		Mangrove	<i>Aegiceras corniculatum</i>	–30.7	6.7	
		Mangrove	<i>Avicennia marina</i>	–27.0	8.4	Gao et al., 2018
		Mangrove	<i>Kandelia obovata</i>	–27.9	5.2	
		SOM		–23.1 (–25.8 to –18.9)	8.6 (8.0–9.4)	
	Zhejiang	Mangrove	<i>Avicennia marina</i>	–27.8	7.8	Liao et al., 2020
		Mangrove	<i>Kandelia obovata</i>	–27.6	8.2	
		SOM		–22.2 (–22.9 to –21.5)	7.0 (6.9–7.0)	Lee et al., 2000
		Mangrove	<i>Kandelia candel</i>	–28.8 (–29.5 to –28.1)	7.7 (6.8–8.5)	
Salt marsh	Guangdong	MPB		–23.0	4.5	Chen et al., 2021
		Halophyte (C3)	<i>Phragmites australis</i>	–26.9	6.1	
		Halophyte (C4)	<i>Spartina alterniflora</i>	–12.7	6.0	
	Fujian	Halophyte (C4)	<i>Spartina alterniflora</i>	–14.1	6.1	Gao et al., 2018
		Halophyte (C4)	<i>Spartina alterniflora</i>	–13.6	10.1	
	Zhejiang	SOM		–21.5	7.0	Liao et al., 2020
		Halophyte (C4)	<i>Spartina alterniflora</i>	–15.3 (–15.5 to –15.0)	7.8 (7.5–8.1)	
	Shanghai	POM		–22.8	5.8	Quan et al., 2007
		MPB		–20.0	4.0	
		Halophyte (C3)	<i>Phragmites australis</i>	–27.1	6.1	
		Halophyte (C3)	<i>Scirpus mariqueter</i>	–27.7	5.0	

Table 4.4. (Continued.).

Vegetation	Province	Type	Species	$\delta^{13}\text{C}$, mean (min. to max)	$\delta^{15}\text{N}$, mean (min. to max)	Reference
Halophyte	Shanghai	Halophyte (C4)	<i>Spartina alterniflora</i>	-12.6	6.1	Quan et al., 2007
		POM		-21.9	5.7	Quan et al., 2012
		MPB		-18.3	6.5	
		Halophyte (C3)	<i>Phragmites australis</i>	-27.3	6.9	
		Halophyte (C3)	<i>Scirpus mariqueter</i>	-27.7	5.0	
		Halophyte (C4)	<i>Spartina alterniflora</i>	-12.6	5.8	
		POM		-22.8 (-23.2 to -22.4)	2.0 (1.8–2.1)	Shang et al., 2008
		MPB		-17.3 (-19.8 to -13.7)	6.9 (6.3–7.5)	
		Halophyte (C3)	<i>Phragmites australis</i>	-26.6 (-26.8 to -26.4)	4.5 (3.3–5.7)	
		Halophyte (C3)	<i>Scirpus mariqueter</i>	-26.8 (-27.2 to -26.5)	4.8 (2.0–7.1)	
		Halophyte (C4)	<i>Spartina alterniflora</i>	-13.1 (-13.2 to -13.1)	3.8 (2.3–5.0)	
		SOM		-23.8 (-24.2 to -23.3)	2.1 (2.0–2.2)	Wang et al., 2014
		POM		-24.2	3.2	
		Halophyte (C3)	<i>Phragmites australis</i>	-25.7	5.0	
		Halophyte (C4)	<i>Spartina alterniflora</i>	-14.2	5.7	
		SOM		-17.1 (-19.2 to -15.0)	2.9 (2.0–3.8)	Wang et al., 2015
		POM		-24.8 (-25.4 to -24.2)	4.5 (4.2–4.8)	
		Halophyte (C3)	<i>Phragmites australis</i>	-26.0 (-26.5 to -25.5)	4.0 (2.5–5.5)	
		Halophyte (C3)	<i>Scirpus mariqueter</i>	-28.0 (-28.2 to -27.8)	4.7 (4.2–5.2)	
		Halophyte (C4)	<i>Spartina alterniflora</i>	-14.4 (-14.8 to -14.0)	5.4 (4.8–6.0)	
		SOM		-21.9 (-23.6 to -19.6)	6.0 (5.8–6.2)	Wang et al., 2020
		POM		-24.3	4.0	
		MPB		-24.1 (-25.0 to -23.5)	5.2 (4.9–5.7)	
		Halophyte (C3)	<i>Phragmites australis</i>	-27.6	6.3	
		Halophyte (C3)	<i>Scirpus mariqueter</i>	-28.1	7.6	
		Halophyte (C4)	<i>Spartina alterniflora</i>	-12.8	7.5	
Seagrass	Guangxi	SOM		-19.3	3.9	Lin et al., 2021
		POM		-23.3	5.6	
		MPB		-19.9	6.6	
		Seagrass	<i>Halophila ovalis</i>	-17.2 (-19.6 to -14.7)	8.9 (8.4–9.3)	
		SOM		-19.0 (-21.1 to -16.8)	6.2 (5.9–6.4)	Xu et al., 2018

Table 4.4. (Continued.)

Vegetation	Province	Type	Species	$\delta^{13}\text{C}$, mean (min. to max)	$\delta^{15}\text{N}$, mean (min. to max)	Reference
Seagrass	Guangxi	POM		−23.4 (−23.6 to −23.1)	6.1 (5.5–6.6)	Xu et al., 2018
		MPB		−21.9 (−22.3 to −21.6)	6.3 (6.2–6.4)	
		Seagrass	<i>Halophila minor</i>	−9.6 (−10.0 to −9.2)	6.3 (5.8–6.7)	
		POM		−23.6	5.5	Xu et al., 2021
		MPB		−22.3	6.4	
		Seagrass	<i>Halophila minor</i>	−10.0	5.8	

Table 4.5.

Review of the stable isotope values for carbon and nitrogen ($\delta^{13}\text{C}$ and $\delta^{15}\text{N}$) of consumers in previous studies ($n=18$) in six provinces of China (Fujian, Guangdong, Guangxi, Hong Kong, Shanghai, and Zhejiang). Six functional groups of consumers are shown with abbreviations (herbivore, Hb; deposit feeder, Df; filter feeder, Ff; planktivore, Pk; omnivore, Om; carnivore, Ca). Values are expressed as mean with range (min.–max.).

Vegetation	Province	Type	Phylum	Species	Group	$\delta^{13}\text{C}$ (‰)	$\delta^{15}\text{N}$ (‰)	Reference
						mean (min. to max.)	mean (min.–max.)	
Mangrove	Guangdong	Benthos	Annelida	<i>Nephtys oligobranchia</i>	Ca	–14.5 (–15.3 to –13.7)	12.8 (12.5–13.1)	Arbi et al., 2018
				<i>Neanthes glandicincta</i>	Df	–15.2 (–16.9 to –13.5)	13.2 (12.5–13.8)	
			Mollusca	<i>Anomalodiscus squamosus</i>	Ff	–15.3 (–16.6 to –14.0)	13.0 (11.8–14.2)	
				<i>Batillaria cumingii</i>	Df	–12.9 (–13.2 to –12.5)	11.9 (11.4–12.3)	
				<i>Cerithidea rhizophorarum</i>	Hb	–13.4 (–14.2 to –12.6)	11.9 (11.6–12.2)	
			Arthropoda	<i>Pagurus angustus</i>	Om	–19.0 (–19.1 to –18.9)	13.8 (12.7–14.8)	
		Fish	Chordata	<i>Periophthalmus cantonensis</i>	Ca	–16.0	14.0	Chen et al., 2018
		Benthos	Annelida	<i>Phascolosoma arcuatum</i>	Ff	–18.2	12.5	
			Mollusca	<i>Cyclina sinensis</i>	Ff	–19.3	12.2	
				<i>Mactra antiquata</i>	Ff	–19.6	11.3	
				<i>Marcia recens</i>	Ff	–19.3	10.9	
			Arthropoda	<i>Alpheus leviuscus</i>	Om	–20.3	12.0	
				<i>Helice tridens</i>	Om	–19.6	11.0	
				<i>Mictyris longicarpus</i>	Hb	–15.8	11.8	
				<i>Sesarma plicata</i>	Hb	–20.1	11.3	
				<i>Tubuca arcuata</i>	Df	–15.3	10.5	
Fujian		Benthos	Annelida	<i>Polychates</i>	Df	–20.5 (–24.2 to –16.8)	12.5 (11.8–13.2)	Chen et al., 2021
		Fish	Chordata	<i>Acanthopagrus latus</i>	Ca	–14.2	10.7	Feng et al., 2015
				<i>Coilia grayii</i>	Ca	–16.1	13.2	
				<i>Lateolabrax japonicas</i>	Ca	–15.0	15.2	
				<i>Ophichthus apicalis</i>	Ca	–15.2	15.6	
				<i>Parachaeturichthys polynern</i>	Ca	–16.2	13.8	
				<i>Osteomugil ophuyseni</i>	Pk	–13.2	14.5	
		Benthos	Mollusca	<i>Pirenella cingulata</i>	Df	–14.7 (–17.0 to –12.7)	11.9 (11.0–13.2)	Feng et al., 2017
			Arthropoda	<i>Helice latimera</i>	Om	–13.5 (–14.5 to –12.5)	10.4 (9.8–11.0)	
				<i>Metaplex longipes</i>	Df	–13.6 (–15.9 to –11.2)	13.5 (13.2–13.8)	
				<i>Tubuca arcuata</i>	Df	–13.0 (–13.0 to –13.0)	11.0 (10.7–11.2)	
				<i>Orisarma dehaani</i>	Hb	–13.0 (–14.2 to –11.8)	9.6 (9.2–10.0)	

Table 4.5. (Continued)

Vegetation	Province	Type	Phylum	Species	Group	$\delta^{13}\text{C}$ (‰)	$\delta^{15}\text{N}$ (‰)	Reference
						mean (min. to max.)	mean (min.–max.)	
Mangrove	Zhejiang	Fish	Chordata	<i>Periophthalmus modestus</i>	Ca	−13.5	12.6	Liao et al., 2020
		Benthos	Mollusca	<i>Optedicerus breviculum</i>	Df	−20.3	8.3	
				<i>Pirenella cingulata</i>	Df	−19.3	9.2	
			Arthropoda	<i>Tubuca arcuata</i>	Df	−16.2	13.8	
Salt marsh	Guangdong	Benthos	Arthropoda	<i>Helice tientsinensis</i>	Om	−19.6 (−21.6 to −17.5)	8.1 (8.0–8.3)	Lee et al., 2000
				<i>Orisarma dehaani</i>	Hb	−19.4 (−22.7 to −16.1)	7.3 (7.0–7.5)	
	Fujian	Benthos	Mollusca	<i>Pirenella cingulata</i>	Df	−13.4 (−13.8 to −13.0)	12.1 (11.5–12.6)	Feng et al., 2017
			Arthropoda	<i>Helice latimera</i>	Om	−11.8	11.2	
				<i>Metaplex longipes</i>	Df	−12.5	13.0	
				<i>Tubuca arcuata</i>	Df	−12.8	11.2	
				<i>Orisarma dehaani</i>	Hb	−10.8	11.0	
				<i>Sesarma plicata</i>	Hb	−11.2 (−12.0 to −10.5)	11.9 (10.5–13.8)	
	Zhejiang	Fish	Chordata	<i>Periophthalmus modestus</i>	Ca	−17.2	13.6	Liao et al., 2020
		Benthos	Mollusca	<i>Optedicerus breviculum</i>	Df	−14.4	9.7	
				<i>Pirenella cingulata</i>	Df	−15.6	10.6	
			Arthropoda	<i>Tubuca arcuata</i>	Df	−14.4	10.1	
	Shanghai	Fish	Chordata	<i>Lateolabrax japonicus</i>	Ca	−18.3	12.5	Quan et al., 2007
				<i>Planiliza haematocheilus</i>	Ca	−16.2	8.9	
				<i>Synechogobius ommaturus</i>	Ca	−16.2	10.3	
				<i>Palaemon carinicauda</i>	Om	−18.4	11.8	
		Benthos	Arthropoda					Quan et al., 2012
		Fish	Chordata	<i>Coilia mystus</i>	Ca	−19.5	8.5	
				<i>Collichthys lucidus</i>	Ca	−19.1	8.3	
				<i>Cynoglossus gracilis</i>	Ca	−19.9	9.4	
				<i>Eleutheronema rhamdinum</i>	Ca	−18.9	9.0	
				<i>Harpadon nehereus</i>	Ca	−18.1	7.6	
				<i>Johnius distinctus</i>	Ca	−19.2	9.3	
				<i>Luciogobius guttatus</i>	Ca	−19.1	10.1	
				<i>Odontamblyopus lacepedii</i>	Ca	−21.2	13.3	
				<i>Pennahia argentata</i>	Ca	−20.0	9.9	
				<i>Odontamblyopus lacepedii</i>	Ca	−21.2	13.3	
				<i>Pennahia argentata</i>	Ca	−20.0	9.9	

Table 4.5. (Continued)

Vegetation	Province	Type	Phylum	Species	Group	$\delta^{13}\text{C}$ (‰)	$\delta^{15}\text{N}$ (‰)	Reference
						mean (min. to max.)	mean (min.–max.)	
Salt marsh	Shanghai	Fish	Chordata	<i>Tachysurus sinensis</i>	Ca	–20.0	10.7	Quan et al., 2012
				<i>Takifugu bimaculatus</i>	Ca	–18.5 (–20.2 to –16.7)	11.6 (10.7–12.5)	
				<i>Tridentiger barbatus</i>	Ca	–19.1	11.4	
				<i>Trypauchen vagina</i>	Ca	–18.3	10.1	
				<i>Planiliza haematocheilus</i>	Om	–14.6	9.5	
		Benthos	Annelida	<i>Perinereis aibuhitensis</i>	Df	–19.6	10.6	Quan et al., 2012
				<i>Rapana bezoar</i>	Ca	–19.5	9.3	
			Mollusca	<i>Scalptia scalariformis</i>	Ca	–18.9	9.4	
				<i>Magallana ariakensis</i>	Ff	–23.1	7.5	
				<i>Mesocibota bistrigata</i>	Ff	–21.1	5.8	
				<i>Vignadula atrata</i>	Ff	–21.9	5.7	
			Arthropoda	<i>Hemigrapsus penicillatus</i>	Ca	–17.4	5.7	
				<i>Hemigrapsus sinensis</i>	Ca	–16.6	7.8	
				<i>Macrobrachium nipponense</i>	Ca	–20.6	11.7	
				<i>Scylla paramamosain</i>	Ca	–17.3	10.1	
				<i>Alpheus japonicus</i>	Om	–21.0	9.5	
				<i>Charybdis japonica</i>	Om	–17.9	10.1	
				<i>Palaemon annandalei</i>	Om	–20.7	8.7	
				<i>Palaemon carinicauda</i>	Om	–19.0	9.7	
				<i>Palaemon macrodactylus</i>	Om	–18.8	10.5	
				<i>Fistulobalanus albicostatus</i>	Ff	–19.8	8.2	
				<i>Philyra pisum</i>	Df	–17.9	8.3	
				<i>Metopograpsus latifrons</i>	Hb	–17.2	8.7	
		Fish	Chordata	<i>Boleophthalmus pectinirostris</i>	Ca	–17.7	10.7	Shang et al., 2008
				<i>Synechogobius ommaturus</i>	Ca	–20.9 (–22.0 to –19.8)	13.9 (13.6–14.2)	
				<i>Mugil cephalus</i>	Om	–15.6 (–16.0 to –15.2)	11.9 (11.4–12.4)	
		Benthos	Mollusca	<i>Corbicula fluminea</i>	Ff	–21.4 (–23.0 to –19.7)	9.5 (8.7–10.3)	
				<i>Euassiminea violacea</i>	Df	–18.5 (–20.6 to –16.2)	7.3 (6.0–8.2)	
			Arthropoda	<i>Palaemon</i> sp.	Om	–17.0	12.6	
				<i>Ilyoplax deschampsii</i>	Df	–18.6 (–21.5 to –16.2)	9.1 (8.2–10.0)	
		Benthos	Mollusca	<i>Cerithideopsis largillierti</i>	Df	–17.1 (–19.1 to –15.0)	8.2 (8.0–8.5)	Wang et al., 2014

Table 4.5. (Continued)

Vegetation	Province	Type	Phylum	Species	Group	$\delta^{13}\text{C}$ (‰)	$\delta^{15}\text{N}$ (‰)	Reference
						mean (min. to max.)	mean (min.–max.)	
Salt marsh	Shanghai	Benthos	Mollusca	<i>Pseudomphala latericea</i>	Df	–16.1 (–19.6 to –12.6)	7.0 (6.2–7.7)	Wang et al., 2014
		Benthos	Mollusca	<i>Glauconome chinensis</i>	Ff	–21.5 (–22.0 to –21.1)	8.6 (7.4–9.9)	Wang et al., 2015
				<i>Sinonovacula constricta</i>	Ff	–21.3 (–22.1 to –20.4)	9.6 (8.6–10.6)	
		Benthos	Annelida	<i>Tylorrhynchus heterochaetus</i>	Ca	–21.4 (–23.3 to –18.3)	9.9 (9.0–11.4)	Wang et al., 2020
				<i>Heteromastus filiformis</i>	Df	–21.6 (–23.6 to –20.6)	11.0 (10.4–11.5)	
			Mollusca	<i>Glauconome chinensis</i>	Ff	–21.4	8.6	
				<i>Sinonovacula constricta</i>	Ff	–19.3	10.5	
				<i>Cerithidea sinensis</i>	Df	–19.4 (–20.8 to –18.4)	7.6 (7.2–8.3)	
				<i>Cerithideopsis largillierti</i>	Df	–19.6 (–20.2 to –18.9)	8.2 (7.9–8.4)	
			Arthropoda	<i>Euassiminea violacea</i>	Df	–19.2 (–20.8 to –16.1)	6.6 (5.9–7.3)	
				<i>Pseudomphala latericea</i>	Df	–19.5 (–20.9 to –17.6)	7.7 (6.6–8.6)	
				<i>Arachnida</i> sp.	Ca	–20.0	10.0	
				<i>Macrobrachium nipponense</i>	Ca	–22.0	12.1	
				<i>Helice tientsinensis</i>	Om	–19.9 (–23.6 to –16.8)	8.1 (7.8–8.7)	
				<i>Ilyoplax deschampsii</i>	Df	–18.0 (–20.1 to –16.4)	6.8 (5.7–8.5)	
				<i>Sinocorophium sinensis</i>	Df	–20.8	8.3	
				<i>Orisarma dehaani</i>	Hb	–15.1	6.9	
Seagrass	Guangxi	Fish	Chordata	<i>Alepes djedaba</i>	Ca	–17.1	14.2	Lin et al., 2021
				<i>Callionymus curvicornis</i>	Ca	–15.8	15.0	
				<i>Johnius grypotus</i>	Ca	–16.1	16.6	
				<i>Lagocephalus spadiceus</i>	Ca	–16.7	15.7	
				<i>Myersina filifer</i>	Ca	–16.6	16.0	
				<i>Paracentropogon longispinis</i>	Ca	–15.5	15.8	
				<i>Platycephalus indicus</i>	Ca	–16.0	16.1	
				<i>Pterois volitans</i>	Ca	–16.2	15.6	
				<i>Scoliodon laticaudus</i>	Ca	–15.2	16.6	
				<i>Sillago sihama</i>	Ca	–15.1	16.0	
				<i>Solea ovate</i>	Ca	–16.8	13.2	
				<i>Soleidae</i> sp.	Ca	–16.8	15.2	
				<i>Suggrundus meerdervoortii</i>	Ca	–17.1	14.9	
				<i>Takifugu alboplumbeus</i>	Ca	–16.2	15.4	

Table 4.5. (Continued)

Vegetation	Province	Type	Phylum	Species	Group	$\delta^{13}\text{C}$ (‰)	$\delta^{15}\text{N}$ (‰)	Reference
						mean (min. to max)	mean (min. to max)	
Seagrass	Guangxi	Fish	Chordata	<i>Trichiurus lepturus</i>	Ca	-18.0	17.6	Lin et al., 2021
				<i>Uroconger lepturus</i>	Ca	-15.6	15.4	
				<i>Zebrias zebra</i>	Ca	-15.8	15.7	
		Benthos	Chordata	<i>Lepidotrigla microptera</i>	Pk	-18.3	12.6	
				<i>Paragyrops edita</i>	Pk	-18.7	13.4	
			Porifera	<i>Demospongiae</i> sp.	Ff	-21.8	8.8	
				<i>Tethya actinia</i>	Ff	-21.4	8.4	
				<i>Neanthes glandicincta</i>	Df	-14.1	11.7	
			Annelida	<i>Sipunculus nudus</i>	Df	-13.1	12.4	
				<i>Indothais lacerus</i>	Ca	-15.2	14.2	
			Mollusca	<i>Lusepiola birostrata</i>	Ca	-16.7	14.3	
				<i>Nassarius pullus</i>	Ca	-15.4	14.0	
				<i>Anadara kagoshimensis</i>	Ff	-18.4	10.8	
				<i>Arca navicularis</i>	Ff	-18.5	11.3	
				<i>Meretrix lyrata</i>	Ff	-18.7	11.4	
				<i>Meretrix meretrix</i>	Ff	-19.1	11.0	
				<i>Mesocibota bistrigata</i>	Ff	-18.9	10.5	
				<i>Perna viridis</i>	Ff	-17.9	10.9	
				<i>Ruditapes philippinarum</i>	Ff	-19.9	9.2	
				<i>Solen strictus</i>	Ff	-19.2	9.2	
				<i>Tapes blecheri</i>	Ff	-18.3	11.3	
				<i>Bursatella leachii</i>	Hb	-16.7	9.8	
				<i>Homoiodoris japonica</i>	Hb	-16.0	9.6	
				<i>Tegula rustica</i>	Hb	-19.0	11.4	
				<i>Turbo bruneus</i>	Hb	-15.1	12.1	
			Arthropoda	<i>Metapenaeus ensis</i>	Ca	-16.0	14.4	
				<i>Metapenaeus joyneri</i>	Ca	-13.7	13.7	
				<i>Metapenaeus moyebi</i>	Ca	-13.6	12.3	
				<i>Oratosquilla oratoria</i>	Ca	-15.7	14.3	
				<i>Penaeus chinensis</i>	Ca	-16.3	14.5	

Table 4.5. (Continued)

Vegetation	Province	Type	Phylum	Species	Group	$\delta^{13}\text{C}$ (‰) mean (min. to max.)	$\delta^{15}\text{N}$ (‰) mean (min. –max.)	Reference
Seagrass	Guangxi	Benthos	Arthropoda	<i>Penaeus japonicus</i>	Ca	–16.2	14.8	Lin et al., 2021
				<i>Alpheopsis distinguendus</i>	Om	–14.7	14.0	
				<i>Alpheopsis</i> sp.	Om	–16.7	12.7	
				<i>Lysmata vittata</i>	Om	–17.3	14.7	
				<i>Sphaerozium nitidus</i>	Om	–15.6	13.6	
				<i>Thalamita sima</i>	Om	–14.8	14.4	
				<i>Diogenes edwardsii</i>	Hb	–16.2	11.4	
				<i>Macromedaeus distinguendus</i>	Hb	–15.0	12.4	
			Echinodermata	<i>Amphioplus depressus</i>	Df	–11.5	11.4	
				<i>Arachnoides placenta</i>	Df	–14.4	10.1	
				<i>Protankyra bidentata</i>	Df	–12.5	11.4	
	Hong Kong	Benthos	Nematoda	Nematodes	Om	–13.7 (–16.6 to –11.7)	12.4 (9.9–15.8)	Xu et al., 2018
				Nematodes	Df	–15.5 (–19.6 to –11.5)	9.3 (8.7–9.8)	
				Nematodes	Hb	–10.7 (–13.0 to –9.4)	9.7 (8.7–10.2)	
			Annelida	<i>Eunice</i> sp.	Ca	–13.9 (–15.4 to –12.5)	13.0 (10.9–15.2)	
				<i>Neanthes</i> sp.	Om	–15.5 (–16.9 to –14.1)	9.9 (9.7–10.1)	
				<i>Cirratulus</i> sp.	Df	–16.3	9.1	
				<i>Prionospio</i> sp.	Df	–16.9 (–17.8 to –16.1)	9.9 (9.6–10.2)	
				Copepod	Om	–15.9 (–20.9 to –11.0)	9.9 (9.7–10.1)	
		Benthos	Nematoda	Nematodes	Om	–16.6	9.9	
					Df	–19.6	8.7	
					Hb	–9.8	8.7	
			Annelida	<i>Eunice</i> sp.	Ca	–15.4	15.2	
				<i>Neanthes</i> sp.	Om	–16.9	9.7	
			Arthropoda	Copepod	Om	–20.9	9.7	

4.2.3. Stable isotope analysis

We decalcified the fine powder of potential diets (POM, SOM, MPB, C₄ halophyte, and mangrove) for 24 h in HCl to examine $\delta^{13}\text{C}$ signatures. All organism samples were lyophilised and ground to a fine powder with a mortar and a pestle. To remove lipids from the tissue, we used a 10 mL dichloromethane/methanol (2:1, v/v) solvent. Small-sized consumers with exoskeletons were decalcified with 1 N HCl to eliminate inorganic carbon for $\delta^{13}\text{C}$ analysis. All samples were weighed and wrapped in a tin capsule. An isotope ratio mass spectrometer connected to an elemental analyser, EA-IRMS (Elementar, Hanau, Germany) was used to determine stable isotope values. The percentage C and N composition of samples was directly determined after combustion in EA. The instrument calibrated the value based on standard sulphanilamide (C, 41.8%; N, 16.3%). Resultant CO₂ and N₂ gases were introduced to the IRMS. Stable isotopic abundance was expressed in delta (δ) notation relative to the conventional standard (C, Vienna Pee Dee Belemnite; N, atmospheric N₂), with the following formula:

$$\delta X (\text{‰}) = [(R_{\text{sample}} / R_{\text{reference}}) - 1] \times 1000$$

where X is ¹³C or ¹⁵N and R is the ratios, ¹³C/¹²C or ¹⁵N/¹⁴N. IAEA-CH-3 (cellulose) and IAEA-N-2 (ammonium sulfate) was used for the internal calibration of ¹³C and ¹⁵N. Measurement precision of replicated analyses was ca. 0.04‰ and 0.2‰ for $\delta^{13}\text{C}$ and $\delta^{15}\text{N}$, respectively.

4.2.4. Trophic level

To estimate the trophic level (TL) of the collected organisms, a trophic enrichment factor (TEF) of $\delta^{15}\text{N}$ (3.3‰) was used (McCutchan Jr et al., 2003). We used the average $\delta^{15}\text{N}$ of all primary producers for accurate TL (Ramirez et al., 2021). The TL of benthic consumers was estimated using a formula published by Vander Zanden and Rasmussen (1999):

$$\text{TL}_i = (\delta^{15}\text{N}_i - \delta^{15}\text{N}_{\text{base}}) / \text{TEF} + \text{TL}_{\text{base}}$$

where, TL_i is the TL of each species considered, $\delta^{15}\text{N}_i$ is the $\delta^{15}\text{N}$ of species i , and $\delta^{15}\text{N}_{\text{base}}$ and TL_{base} are the mean $\delta^{15}\text{N}$ and TL of all primary producers (TL=1), respectively.

4.2.5. Statistical analysis

After the assessment for homogeneity of variance test, one-way analysis of variance (ANOVA) or Kruskal-Wallis test was carried out to determine the seasonal mean difference in: 1) sediment physiochemical parameters, 2) porewater nutrient concentrations, 3) biomass and primary production of microphytobenthos, and 4) stable isotope values of five potential diets and two types of consumers (benthos and fish). ANOVA was additionally performed to estimate the mean difference in C and N stable isotope values between the previous and present food webs in mangrove ecosystems. Pearson correlation analysis was performed between carbon and nitrogen stable isotope values of two consumers (benthos and fish) to estimate the influence of diets on their TL. The Chi-square test was performed to estimate the difference in the occurrence of feeding guilds for each consumer among seasons (Dry I, Wet, and Dry II). The stable isotope values of consumers were utilised for trophic niche analysis by SIBER, after examining no seasonal difference in the occurrence of feeding guilds (Table 4.3.).

The niche space, Bayesian standard ellipse area (SEA_b) of consumers was calculated in the R (SIBER) package (Jackson et al., 2011). The small sample size corrected standard ellipse area (SEA_c) was calculated with the overlap ($\%^2$) in SEA_c between benthos and fish having a different number of components (Jackson et al., 2011). The Bayesian stable isotope mixing model in the R (SIMMR) package was used to examine seasonal variation in diet utilisation of benthic and aquatic consumers. To estimate the contribution of diet to consumers, we used consumer specific TEF of $\delta^{15}N$ in SIMMR: carnivore ($3.3 \pm 0.26\%$); all primary consumers to omnivore ($2.2 \pm 0.3\%$), considering fractionations between diet and consumer tissue (McCutchan Jr et al., 2003). Since the TEF of $\delta^{13}C$ values between adjacent trophic levels were negligible, we used $0.4 \pm 1.3\%$ to adjust the $\delta^{13}C$ of all types of consumers in SIMMR (Post, 2002; Qu et al., 2019). Cluster analysis was performed to identify the seasonal patterns in diet utilisation of consumers using Euclidean distance. Statistical analyses were conducted in SPSS 26.0, PRIMER 6.1.16, and packages ‘SIBER’ and ‘SIMMR’ in R 4.1.2.

4.3. Results and discussion

4.3.1. Environmental conditions

The mean water temperature in PRE was consistently over 25°C across the three seasons, exhibiting subtropical estuarine water characteristics (Table 4.6.). Salinity was low (<0.5 psu) during the monsoonal summer (July), reflecting the high freshwater input to the PRE (Table 4.6.). MC was high (>95%) across all seasons, reflecting the muddy benthic environment of the study area (Flemming, 2000) (Table 4.6.). ANOVA test revealed significant differences across the three seasons for physicochemical parameters: TOC ($F=11.6$, $p<0.01$), TN ($F=7.5$, $p<0.01$), and $\delta^{15}\text{N}$ ($F=6.0$, $p<0.05$) (Table 4.6.). The higher TOC reflected the high detrital carbonate input to the sediment, and the increment in TN reflected agricultural and urban sewage input to the system during the monsoonal summer (Ni et al., 2008; Yang et al., 2011). Significant $\delta^{15}\text{N}$ enrichment of SOM supported the isotopically heavy nitrate input to the area during and directly after the wet season (July and November) (Wang et al., 2013) (Table 4.6.). The C/N (ca. 10%) and $\delta^{13}\text{C}$ (ca. -25.0‰) of SOM was consistent across the three seasons, indicating high input from terrestrial sources to the benthic environment (Yu et al., 2010; Lee et al., 2019) (Table 4.6.). The Kruskal-Wallis test showed a significant mean difference among seasonal MPB biomass (Dry I, $12.2\pm1.3\text{ mg m}^{-2}$; Wet, $20.0\pm3.4\text{ mg m}^{-2}$; Dry II, $17.7\pm10.3\text{ mg m}^{-2}$) ($H=6.7$, $p<0.05$) (Table 4.6.). However, no seasonal trend was determined for MPB primary production. Previous studies also reported an increase in MPB biomass (Chl-*a*) during summer in the intertidal salt marshes of China under optimal benthic environmental conditions and less grazing impact (Liu et al., 2013). Mean MPB biomass in the PRE mangrove ecosystem was lower than that reported for salt marshes in Asian countries (Korea, China, Japan, and Cambodia) ($42.9\pm37.2\text{ mg m}^{-2}$); thus, MPB likely have a minor role in secondary production in the PRE (Kwon et al., 2020).

Table 4.6.

Environmental physicochemical parameters (temperature; salinity; dissolved oxygen, DO; pH; mud content, MC; loss on ignition, LOI; total organic carbon, TOC; total nitrogen, TN; carbon to nitrogen ratio, C/N; carbon and nitrogen stable isotope ratio, $\delta^{13}\text{C}$ and $\delta^{15}\text{N}$), porewater nutrient concentrations, biomass and primary productivity of benthic microalgae (Chlorophyll-*a*, Chl-*a*; primary productivity, PP) collected in the Pearl River Estuary during three seasons in 2019 (Dry I, February; Wet, July; Dry II, November). Variables are expressed as mean with standard deviations (mean \pm s.d.).

Sample	Variable	Season		
		Dry I	Wet	Dry II
Seawater	Temperature ($^{\circ}\text{C}$)	25.2 \pm 0.0	29.5 \pm 0.0	31.8 \pm 0.0
	Salinity (psu)	9.3 \pm 0.0	0.3 \pm 0.0	16.4 \pm 0.0
	DO (mg L^{-1})	6.0 \pm 0.0	5.7 \pm 0.0	6.4 \pm 0.0
	pH	8.5 \pm 0.0	7.8 \pm 0.0	7.7 \pm 0.0
Sediment	MC (%)	99.4 \pm 0.1	98.2 \pm 0.5	98.6 \pm 0.8
	LOI (%)	9.7 \pm 0.2	9.4 \pm 0.2	9.7 \pm 0.3
	TOC (%)	1.5 \pm 0.0	1.7 \pm 0.2	1.4 \pm 0.1
	TN (%)	0.1 \pm 0.0	0.2 \pm 0.0	0.2 \pm 0.0
	C/N (%)	10.2 \pm 0.2	10.0 \pm 0.5	9.9 \pm 1.0
	$\delta^{13}\text{C}$ (‰)	-24.9 \pm 0.2	-25.5 \pm 0.6	-25.0 \pm 0.2
	$\delta^{15}\text{N}$ (‰)	7.2 \pm 0.1	7.7 \pm 0.8	8.4 \pm 0.6
Porewater	$\text{NH}_4\text{-N}$ (mg L^{-1})	0.3 \pm 0.4	0.2 \pm 0.1	1.3 \pm 0.4
	$\text{NO}_2\text{-N}$ (mg L^{-1})	0.02 \pm 0.00	0.01 \pm 0.00	0.01 \pm 0.00
	$\text{NO}_3\text{-N}$ (mg L^{-1})	0.4 \pm 0.3	0.3 \pm 0.1	0.2 \pm 0.1
	TN (mg L^{-1})	0.7 \pm 0.5	0.5 \pm 0.1	1.5 \pm 0.3
	$\text{PO}_4\text{-P}$ (mg L^{-1})	0.02 \pm 0.01	0.00 \pm 0.00	0.01 \pm 0.01
	SiO_2 (mg L^{-1})	0.7 \pm 0.3	0.8 \pm 0.2	1.2 \pm 0.7
Microphytobenthos	Chl- <i>a</i> (mg m^{-2})	12.2 \pm 1.3	20.0 \pm 3.4	17.7 \pm 10.3
	PP ($\text{mg C m}^{-2} \text{ h}^{-1}$)	67.7 \pm 48.0	81.8 \pm 22.6	90.5 \pm 57.8

4.3.2. Food web structure

The carbon stable isotope value was significantly different among the five potential diets ($H=19.2$, $p<0.001$) (Fig. 4.3.). The $\delta^{13}\text{C}$ of diets were distributed from the mangrove, *S. apetala* ($-32.7\pm0.9\text{‰}$) to the halophyte, *C. malaccensis* ($-13.4\pm0.9\text{‰}$). The other diets exhibited the value between these two extremes (POM, $-26.0\pm0.5\text{‰}$; SOM, $-25.1\pm0.4\text{‰}$; MPB, $-23.6\pm1.0\text{‰}$). The large difference in $\delta^{13}\text{C}$ between the two marsh plants likely reflected the method used to fix carbon from environmental CO_2 during photosynthetic processes (C_3 plant, Calvin-Benson cycle; C_4 plant, Hatch-Slack cycle) (Yu et al., 2010). The functional role of marsh plants, such as mangrove and halophytes, in the coastal food web is still subject to debate. One previous study reported grazers as the only consumers able to utilize marsh plants in their diet because of the high content of refractory compounds (Mann, 1988; Lee, 1995). In contrast, other studies have demonstrated that the detritus of marsh plants contributes to biological production in coastal environments (Chen et al., 2018; Then et al., 2020). Bui and Lee (2014) confirmed the dominant role of mangrove litter in the diet of detritivore Grapsid crab and suggested that mangroves provide high trophic support to coastal communities through the detrital food chain. Therefore, we expected the two marsh plants to enter the food web as deposited- and particulate forms, due to their high production in the PRE (Lee, 1990). The moderate $\delta^{13}\text{C}$ value of SOM among the five diets indicated input of various types of organic matter to the benthic environment. There was no significant mean difference among stable nitrogen isotope values of the five potential diets ($H=8.4$, $p>0.05$) (Fig. 4.3.). The $\delta^{15}\text{N}$ of POM ($>10\text{‰}$) demonstrated significant anthropogenic sewage input in the PRE (Lee, 2000; Duprey et al., 2019). However, POM was sampled only once a season, thus, we should carefully interpret the origin of POM in the study area.

Carbon and nitrogen stable isotope values were significantly different between benthos and fish ($\delta^{13}\text{C}$, $F=4.7$, $p<0.05$; $\delta^{15}\text{N}$, $F=4.9$, $p<0.05$) (Fig. 4.3.). Fish had a significantly enriched mean $\delta^{13}\text{C}$ value, with a larger standard deviation ($-21.9\pm2.8\text{‰}$) than benthos ($-23.4\pm1.0\text{‰}$). Thus, fish likely had a more $\delta^{13}\text{C}$ enriched diet, such as C_4 halophytes, and various diets across the PRE (Heithaus et al., 2011). The more enriched mean $\delta^{15}\text{N}$ value ($14.9\pm2.3\text{‰}$) of fish than benthos

($13.4 \pm 1.7\text{‰}$) strongly reflected the high percentage (>70%) of Ca fish in the PRE community (Table 4.2.). The trophic level from Pk, *Engraulis japonicus* (TL=1.1), to Ca, *Collichthys lucidus* (TL=3.6), indicated that three TL were present in the food web of the western PRE (Fig. 4.4., Table 4.7.). Two omnivorous crabs, *Varuna litterata* and *Metopograpsus quadridentatus*, had the most depleted and enriched $\delta^{15}\text{N}$ values, $10.4 \pm 0.4\text{‰}$ and $15.4 \pm 0.4\text{‰}$, indicating different functional roles as primary consumers and carnivores. In general, omnivorous crabs utilize autotrophs in juvenile stage, and animal-origin diets with growth (Aneykuty et al., 2013; Bang et al., 2019). Thus, the distinct stages of two Om crabs (*V. litterata*, juvenile; *M. quadridentatus*, adult) explained their large $\delta^{15}\text{N}$ difference. The result also reflected their feeding flexibility, useful to survive in the highly complex PRE food web (Fig. 4.4.) (Lee et al., 2021).

In addition, the significant correlation between carbon and nitrogen stable isotope values of fish implied that the different TL in fish may partly be attributed to the diet ($r = -0.24$, $p < 0.05$) (Table 4.8.). The weak negative coefficient revealed that fish with high TL were relatively more influenced by the mangrove-derived organic matter. However, benthos did not show the diet influence on the variation for TL (Table 4.8.).

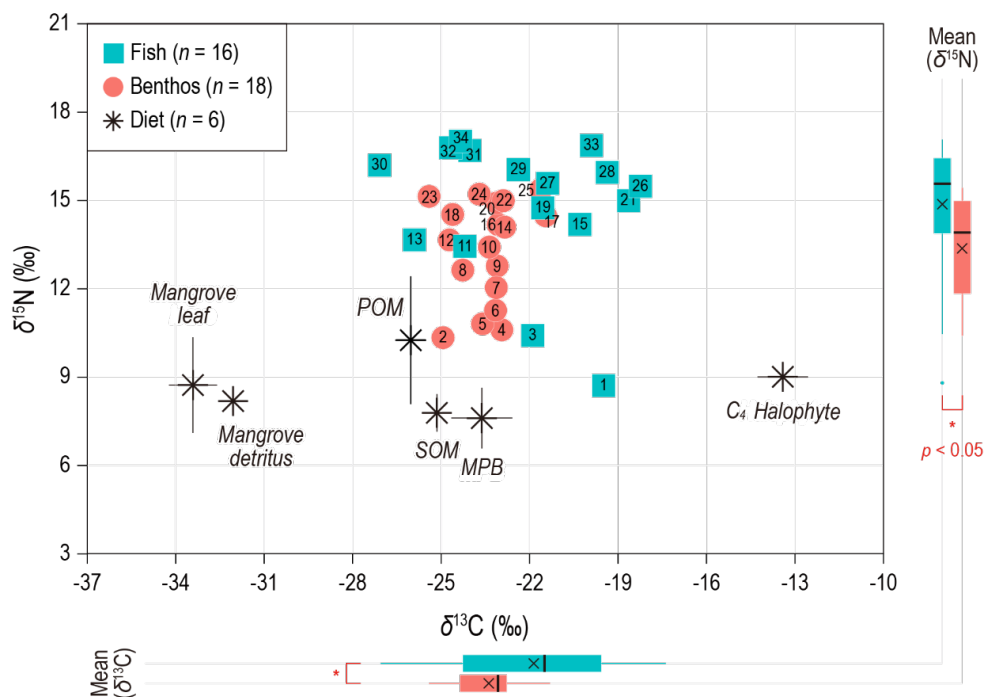


Figure 4.3.

Stable carbon and nitrogen isotope values of potential diets and aquatic organisms in the western Pearl River Estuary, China. Total means with standard deviations (asterisk with black line) represent the values of five potential diets [particulate organic matter, POM; sediment organic matter, SOM; microphytobenthos, MPB; mangrove (*Sonneratia apetala*); C₄ halophyte (*Cyperus malaccensis*)]. Circle and square indicate benthos and fish, respectively. The number in the symbol (listed on the consumers) represents the species listed in Fig. 4.4., and the full scientific names of the organisms are listed in Table 4.7. An asterisk indicates statistical significance ($p < 0.05$) between two consumers.

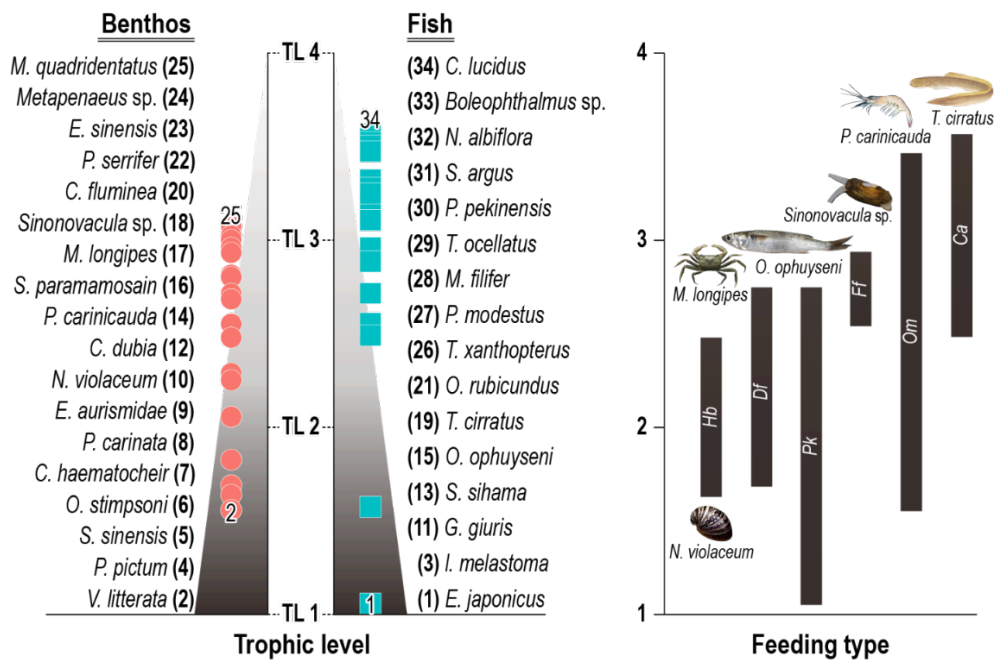


Figure 4.4.

Trophic level (TL) of 34 benthic and pelagic consumers in six feeding groups (herbivores, Hb; deposit feeders, Df; planktivores, Pk; filter feeders, Ff; omnivores, Om; carnivores, Ca). Representative organisms with the highest occurrence are shown on the TL of feeding types.

Table 4.7.

C and N stable isotope values in the diets (particulate organic matter, POM; sediment organic matter, SOM; microphytobenthos, MPB; C₄ halophytes; mangrove) and consumers collected in the Pearl River Estuary, China. Species are listed with the corresponding trophic level (TL) in descending order for each taxon (Mollusca; Arthropoda; Chordata). Values are expressed as mean with range (min.–max.).

Sample	$\delta^{13}\text{C}$ (‰)	$\delta^{15}\text{N}$ (‰)	TL
	mean (min. to max.)	mean (min. – max.)	
Diet			
POM	–26.0 (–26.9 to –25.6)	10.3 (7.2–13.2)	–
SOM	–25.1 (–26.0 to –24.8)	7.8 (7.2–9.0)	–
MPB	–23.6 (–24.9 to –22.5)	7.6 (6.1–8.3)	–
C₄ halophyte			–
<i>Cyperus malaccensis</i>	–13.4 (–14.4 to –12.9)	9.0 (8.7–9.3)	–
Mangrove			–
<i>Sonneratia apetala</i> (leaf)	–33.4 (–34.2 to –32.6)	8.7 (6.9–9.8)	–
<i>Sonneratia apetala</i> (detritus)	–31.6 (–32.2 to –30.6)	9.3 (8.1–11.7)	–
Consumer			
Fish-Chordata			
<i>Collichthys lucidus</i>	–24.3 (–24.4 to –24.3)	17.0 (16.9–17.2)	3.6
<i>Boleophthalmus</i> sp.	–19.9 (–24.7 to –15.1)	16.9 (13.5–20.3)	3.5
<i>Nibea albiflora</i>	–24.7 (–25.2 to –24.4)	16.8 (16.6–17.0)	3.5
<i>Scatophagus argus</i>	–24.0 (–24.2 to –23.8)	16.7 (16.5–16.8)	3.5
<i>Parabramis pekinensis</i>	–27.1 (–27.2 to –27.0)	16.2 (16.0–16.3)	3.3
<i>Takifugu ocellatus</i>	–22.4 (–22.8 to –22.1)	16.1 (15.9–16.2)	3.3
<i>Myersina filifer</i>	–19.4 (–21.3 to –17.5)	16.0 (15.6–16.2)	3.2
<i>Periophthalmus cantonensis</i>	–21.4 (–23.7 to –17.3)	15.6 (12.8–17.6)	3.1
<i>Takifugu xanthopterus</i>	–18.2 (–18.6 to –18.0)	15.5 (14.0–16.4)	3.1
<i>Odontamblyopus rubicundus</i>	–18.6 (–19.0 to –18.4)	15.0 (14.7–15.2)	3.0
<i>Taenioides cirratus</i>	–21.6 (–22.4 to –20.4)	14.8 (10.5–17.3)	2.9
<i>Osteomugil ophuyensis</i>	–20.3 (–25.1 to –15.4)	14.2 (13.6–15.2)	2.7
<i>Sillago sihama</i>	–25.9 (–26.1 to –25.8)	13.7 (13.4–13.8)	2.6
<i>Glossogobius giuris</i>	–24.2 (–25.6 to –21.9)	13.4 (11.6–16.2)	2.5
<i>Ilisha melastoma</i>	–21.9 (–22.0 to –21.7)	10.4 (9.9–10.7)	1.6
<i>Engraulis japonicus</i>	–19.5 (–19.5 to –19.4)	8.7 (8.7–8.7)	1.1
Benthos-Arthropoda			
<i>Metopograpsus quadridentatus</i>	–21.6 (–21.9 to –21.3)	15.4 (15.1–15.6)	3.1
<i>Metapenaeus</i> sp.	–23.7 (–24.4 to –22.9)	15.2 (15.1–15.5)	3.0
<i>Eriocheir sinensis</i>	–25.4 (–25.8 to –25.2)	15.1 (15.0–15.3)	3.0
<i>Palaemon serrifer</i>	–22.9 (–23.5 to –21.8)	15.0 (14.9–15.2)	3.0
<i>Metaplex longipes</i>	–21.5 (–21.8 to –21.2)	14.5 (14.3–14.6)	2.8
<i>Scylla paramamosain</i>	–23.1 (–24.8 to –21.9)	14.2 (11.6–15.6)	2.7
<i>Exopalaemon carinicauda</i>	–22.8 (–24.4 to –21.8)	14.1 (11.4–17.5)	2.7
<i>Chondrochelia dubia</i>	–24.7 (–24.8 to –24.7)	13.7 (13.5–13.9)	2.6
<i>Philyra carinata</i>	–24.3 (–24.3 to –24.2)	12.7 (12.5–12.8)	2.2
<i>Chironantes haematocheir</i>	–23.1 (–25.6 to –20.5)	12.0 (11.7–12.7)	2.1
<i>Ocypoda stimpsoni</i>	–23.2 (–23.3 to –23.0)	11.3 (11.2–11.3)	1.8
<i>Corophium sinensis</i>	–23.6 (–24.2 to –23.2)	10.8 (10.8–10.8)	1.7
<i>Parasarma pictum</i>	–22.9 (–23.8 to –21.5)	10.6 (10.4–10.9)	1.6
<i>Varuna litterata</i>	–24.9 (–25.2 to –24.8)	10.4 (10.1–10.9)	1.6
Benthos-Mollusca			
<i>Corbicula fluminea</i>	–23.1 (–23.1 to –23.1)	14.9 (14.7–15.0)	2.9
<i>Sinonovacula</i> sp.	–24.6 (–24.6 to –24.6)	14.5 (14.5–14.5)	2.8
<i>Neripteron violaceum</i>	–23.4 (–24.6 to –22.3)	13.4 (12.6–13.8)	2.5
<i>Ellobium aurismidae</i>	–23.1 (–23.3 to –22.9)	12.8 (12.7–13.0)	2.3

Table 4.8.

Pearson correlation analysis between carbon and nitrogen stable isotope values in each of the two consumer groups (benthos and fish). Significant correlation coefficient values (r) at $p < 0.05$ are shown in bold italics with an asterisk (*).

Type	Benthos	Fish	All
Coefficient value (r)	0.13	* <i>-0.24</i>	-0.05

4.3.3. Seasonal stable isotopic dynamics

Seasonal mean differences were estimated for the $\delta^{13}\text{C}$ and $\delta^{15}\text{N}$ values of two potential diets, POM ($\delta^{13}\text{C}$, $H=7.8$, $p<0.05$; $\delta^{15}\text{N}$, $F=23.5$, $p<0.01$) and SOM ($\delta^{13}\text{C}$, $H=8.5$, $p<0.05$; $\delta^{15}\text{N}$, $H=10.1$, $p<0.01$) (Fig. 4.5.). These two diets had the significantly depleted $\delta^{13}\text{C}$ during the monsoonal summer, indicating that the food web derives a significant amount of terrestrial organic carbon as a result of floods (Pingram et al., 2012). The $\delta^{15}\text{N}$ enrichment of POM, SOM, and mangrove during the wet season indicated that sewage input to estuarine water and sediment increased, and the further propagation of enriched $\delta^{15}\text{N}$ to primary producers (Bouillon et al., 2008a; Yu et al., 2010; Ke et al., 2016).

The mean difference in $\delta^{13}\text{C}$ between fish and benthos was significant during two seasons (Dry I and Wet) (Fig. 4.5.). The mean difference in $\delta^{13}\text{C}$ between the two consumers decreased from Dry I (3.5‰, $F=23.5$, $p<0.001$) to Wet (1.9‰, $F=23.5$, $p<0.01$), and then became similar in Dry II (0.6‰, $F=1.3$, $p>0.05$). This result revealed the unified energy baseline of benthos and fish during summer. The large mean difference in $\delta^{15}\text{N}$ (1.6‰, $F=11.4$, $p<0.01$) between consumers during the monsoonal summer contrasted to the difference estimated during the dry seasons (Dry I: 0.1‰, $F=0.1$, $p>0.05$; Dry II: 0.9‰, $F=4.6$, $p<0.05$) (Fig. 4.5.). Thus, TL likely increased in fish with expanded feeding areas toward the intertidal zone during the wet season (Heithaus et al., 2011).

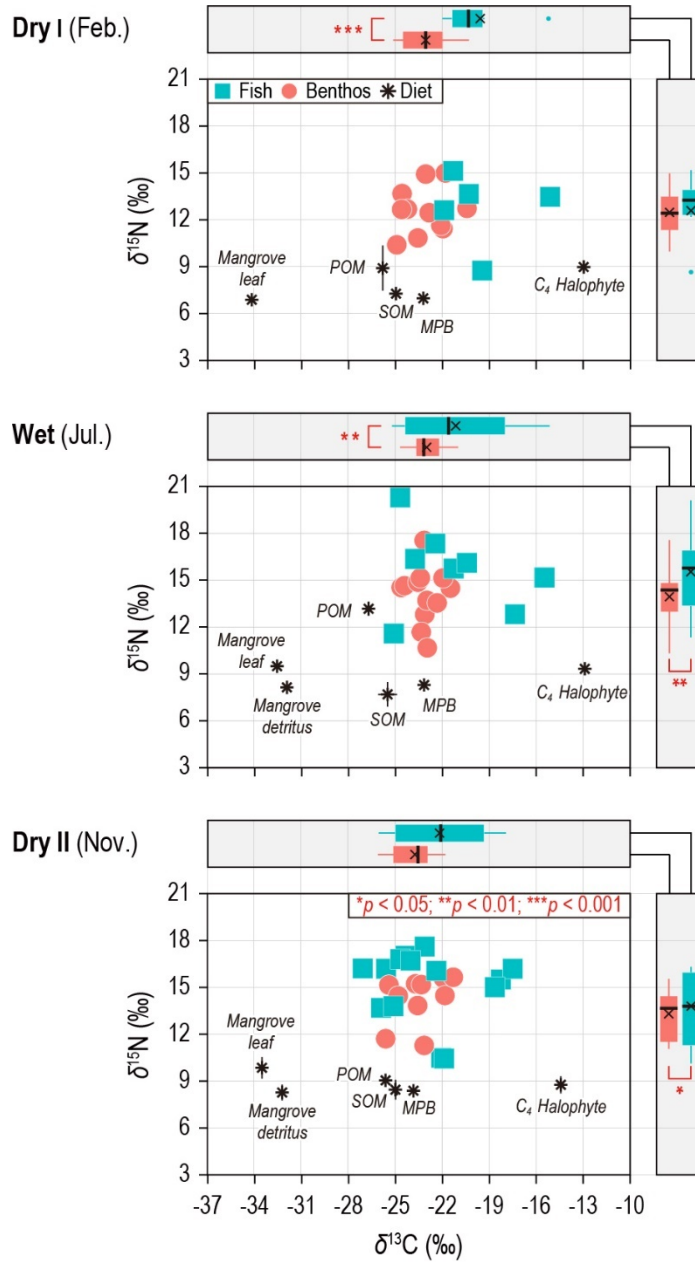


Figure 4.5.

Seasonal stable isotope distribution of carbon and nitrogen of potential diets (particulate organic matter, POM; sediment organic matter, SOM; microphytobenthos, MPB; mangrove [*Sonneratia apetala*]; halophyte [*Cyperus malaccensis*]) and consumers (square, fish; circle, benthos) in 2019 (Dry I, February; Wet, July; Dry II, November). The number of asterisks indicates the degree of statistical significance (*, $p < 0.05$; **, $p < 0.01$; ***, $p < 0.001$) between fish and benthos.

SIBER model revealed seasonal niche space (SEA_c) variation of fish (Fig. 4.6., Table 4.9.). Fish had the largest and smallest SEA_c , which was 26.2‰^2 and 18.1‰^2 in Wet and Dry I, respectively. The higher summer niche space implied opportunistic feeding habits (e.g., shifting feeding locations and that of associated prey) of fish in response to the seasonal changes to the PRE environment (Heithaus et al., 2011). The high frequency (75%) of Ca fish present, which exhibited large variation in seasonal niche space, accounted for seasonal variation in SEA_c in the PRE fish community (Figs. 4.6. and 4.7.). Considering the stable isotopic turnover rate in muscle tissue of adult fish (ca. three months), the estimated higher SEA_c of fish in Dry II also indicated that their stable isotopic signals during the wet season were propagated and were still present after the monsoon (Persson and Hansson, 1999). All functional groups of benthos had small niche space ($<20\text{‰}^2$), with no noticeable seasonal variation (Fig. 4.7.). During Dry I, fish and benthos had the smallest niche overlap, demonstrating the less trophic connectivity between benthic and pelagic ecosystems in PRE (Table 4.9.).

The mixing model revealed the primary role of POM, which had a high contribution (ca. 34.0%) in the PRE, which is in a subtropical region with a long-term monsoon period (Xuan et al., 2020) (Fig. 4.8.). The poor MPB contribution (11.3%) strongly reflected lower MPB biomass in the PRE (Table 4.6.) and indicated the geological variation in energy pathways in the salt marshes of China (MPB contribution: Yellow Sea, 28.1%; South China Sea, 32.7%) (Feng et al., 2015; Chen et al., 2018; Qu et al., 2019; Lee et al., 2021).

The cluster analysis identified the (dis)similarity of consumers based on diet utilisation (%), with two major groups being delineated (Group 1 and 2) (Fig. 4.8.). Group 1 included benthic and pelagic consumers collected in two dry seasons (Dry I, before monsoon; Dry II, after monsoon), and divided into three sub-groups (1-1, fish in Dry I; 1-2, benthos in Dry I; 1-3, benthos and fish in Dry II). Fish (Group 1-1) and benthos (Group 1-2) in the Dry I was distinct to consumers in Dry II with higher plant-derived source consumptions. Especially, fish (Dry I) was distinct from others with the highest halophyte (47.8%) consumption. Group 2 was characterised by consumers collected during monsoonal season, which intensively utilised POM

(fish, 50.0%; benthos, 50.5%) compared to others in two dry seasons (mean, $25.1 \pm 8.1\%$). However, the relatively higher POM contribution to fish (34.8%) and benthos (28.1%) in Dry II (Group 1-3) than that in Dry I, indicates the POM influences in the food web even after the monsoonal period. In addition, the relatively higher similarity between benthos and fish was demonstrated in Group 1-3 and Group 2, supporting the increased niche overlap in Dry II and Wet seasons (Figs. 4.6. and 4.8.). In Dry I, two types of benthos (Arthropoda and Mollusca) were grouped but separated from fish in Dry I (Fig. 4.9.). In contrast, in Wet and Dry II, two taxonomic groups of benthos showed less distance with fish than in Dry I, indicating seasonally strengthened benthic-pelagic coupling in PRE. Overall, the cluster analysis demonstrated that seasonal flooding is a primary factor determining the diet utilisation of consumers in PRE. However, it is challenging to understand the trophic dynamics in a complex estuarine system due to the high biodiversity and dynamic interactions among biotas. Therefore, we suggest that future studies consider all sources of organic matter supporting the PRE food web for a better understanding of the trophic dynamics in it.

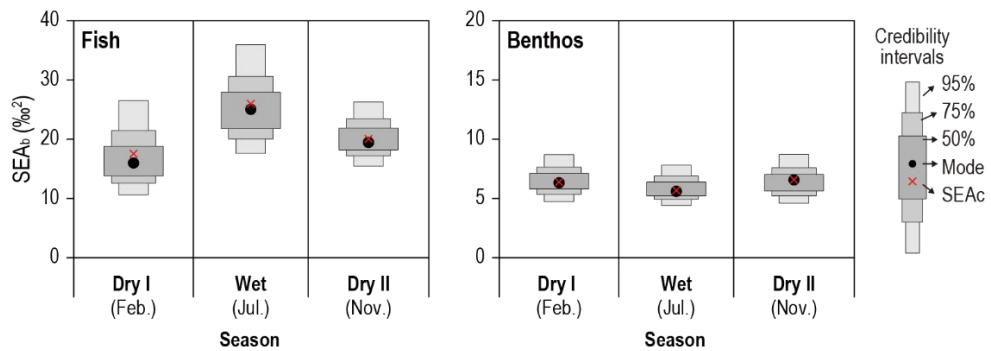


Figure 4.6.

Box plot showing the credible interval (CI) range of the estimated ellipse area (SEA_b) for the seasonal niche of two consumers. The boxed areas represent the 50% (dark grey), 75% (grey), and 95% (light grey) credible intervals of the estimated ellipse areas. The black dot and red cross represent the mode of SEA_b and the maximum likelihood estimate of the small sample corrected standard ellipse area, $SEAc$.

Table 4.9.

Seasonal niche metrics (Bayesian standard ellipse area, SEA_b ; sample size corrected ellipse area, SEA_c ; overlap) of consumers collected in the Pearl River Estuary, China. Isotopic niche overlap between fish and benthos is calculated in each season (Dry I, February; Wet, July; Dry II, November).

Season	Sample	SEA_b	SEA_c	Overlap
Dry I (February)	Fish	17.1	18.1	34.9
	Benthos	6.5	6.6	
Wet (July)	Fish	25.4	26.2	35.4
	Benthos	5.9	6.0	
Dry II (November)	Fish	20.3	20.7	39.4
	Benthos	6.4	6.6	

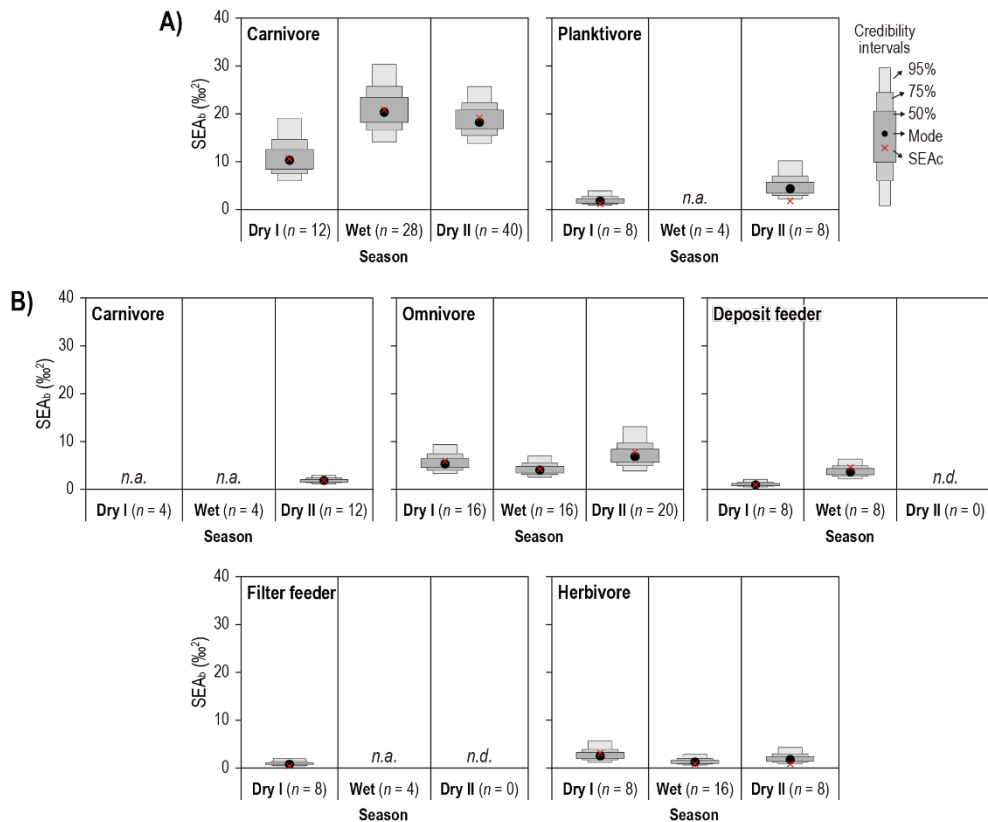


Figure 4.7.

Seasonal (Dry I, February; Wet, July; Dry II, November) standard ellipse area Bayesian estimation (SEA_b) with mode (black dots) and probability of data distribution (50%, dark grey boxes; 75%, intermediate grey boxes; 95%, light grey boxes) for **(A)** two functional groups of fish (planktivores; carnivores), and **(B)** five functional groups of benthos (herbivores; filter feeders; deposit feeders; omnivores; carnivores). The standard ellipse area corrected for small sample size (SEA_c) is shown as a red multiplication marker. Each abbreviation (*n*, *n.a.*, and *n.d.*) indicates the number of samples, not analysed, and no data.

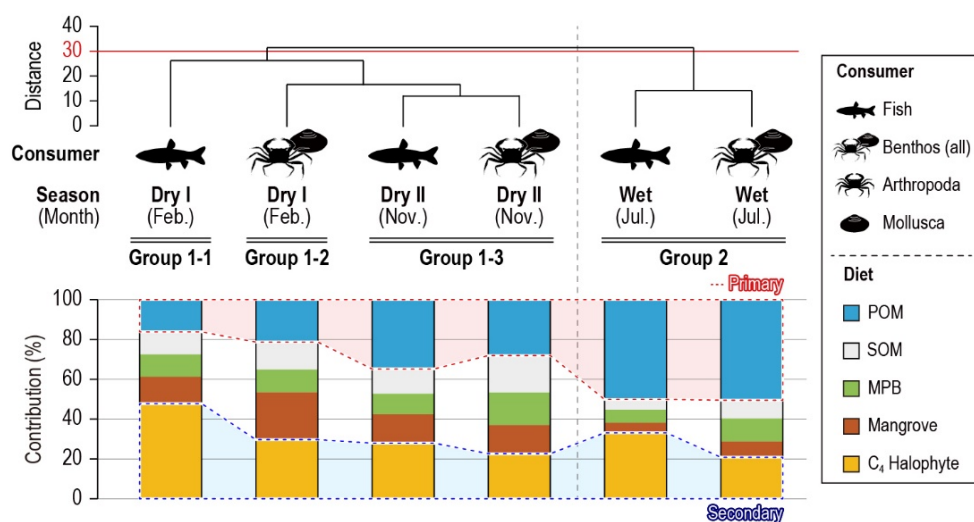


Figure 4.8.

Consumer groups [Group 1 (1-1, 1-2, and 1-3); Group 2] determined by cluster analysis based on similarity of seasonal diet utilisation (Dry I, February; Wet, July; Dry II, November) in the western Pearl River Estuary, China. The contribution (%) of five diets to consumers is represented by different colours (blue, POM; white-grey, SOM; green, MPB; orange-brown, mangrove; yellow, C₄ halophyte). Consumers are represented by black symbols. Benthos (all) represents all invertebrates, including arthropods and mollusc. Primary and secondary sources (POM and halophyte) are highlighted with red and blue backgrounds, respectively.

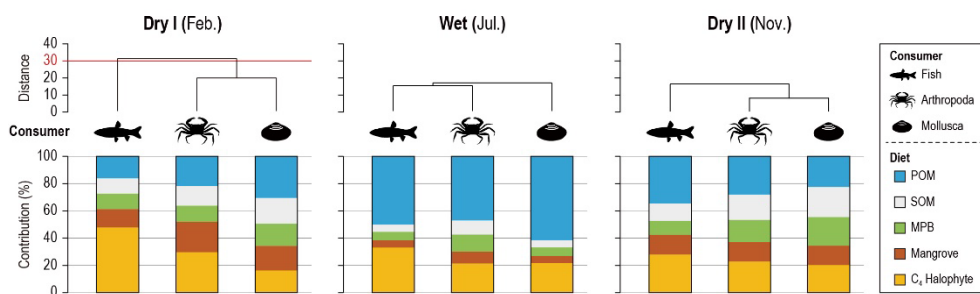


Figure 4.9.

Cluster analysis based on similarity of diet utilisation by three consumers (Chordata, Arthropoda, and Mollusca) over the three seasons. The contribution (%) of the five diets to the consumers is represented by different colours (blue, POM; white-grey, SOM; green, MPB; orange-brown, mangrove; yellow, halophyte). Consumers are described with black symbols.

Table 4.10.

Diet (particulate organic matter, POM; microphytobenthos, MPB; mangrove; C₄ halophyte) contribution to the 34 consumers collected in the Pearl River Estuary, China, during the three seasons (Dry I, February; Wet, July; Dry II, November) in 2019. *n* indicates the number of samples, including replicates. Values are expressed as means with standard deviations (mean±s.d.).

Sample	Season	<i>n</i>	POM	SOM	MPB	Mangrove	Halophyte
<i>C. lucidus</i>	Dry II	4	0.25±0.17	0.23±0.16	0.22±0.16	0.16±0.10	0.15±0.07
<i>Boleophthalmus</i> sp.	Dry I	4	0.07±0.06	0.06±0.05	0.06±0.05	0.05±0.04	0.76±0.10
	Wet	4	0.28±0.18	0.21±0.16	0.21±0.14	0.18±0.11	0.12±0.06
<i>N. albiflora</i>	Dry II	4	0.25±0.17	0.23±0.17	0.22±0.16	0.17±0.10	0.13±0.08
<i>S. argus</i>	Dry II	4	0.24±0.17	0.23±0.16	0.22±0.16	0.15±0.10	0.17±0.08
<i>P. pekinensis</i>	Dry II	4	0.19±0.14	0.17±0.12	0.17±0.12	0.39±0.10	0.09±0.05
<i>T. ocellatus</i>	Dry II	4	0.19±0.13	0.19±0.14	0.19±0.14	0.12±0.08	0.30±0.08
<i>M. filifer</i>	Wet	4	0.22±0.13	0.15±0.10	0.18±0.13	0.12±0.08	0.34±0.07
	Dry II	4	0.09±0.07	0.09±0.07	0.09±0.07	0.06±0.05	0.66±0.12
<i>P. cantonensis</i>	Wet	8	0.30±0.18	0.12±0.10	0.15±0.12	0.11±0.08	0.32±0.13
	Dry II	4	0.21±0.14	0.21±0.15	0.21±0.15	0.13±0.07	0.24±0.08
<i>T. xanthopterus</i>	Dry II	4	0.10±0.08	0.11±0.08	0.10±0.07	0.07±0.05	0.62±0.10
<i>O. rubicundus</i>	Dry II	4	0.11±0.08	0.11±0.08	0.11±0.08	0.08±0.05	0.59±0.09
<i>T. cirratus</i>	Dry I	4	0.20±0.13	0.17±0.12	0.18±0.13	0.13±0.08	0.32±0.08
	Wet	4	0.27±0.15	0.12±0.10	0.16±0.14	0.11±0.08	0.34±0.06
	Dry II	8	0.16±0.12	0.20±0.14	0.22±0.15	0.11±0.08	0.31±0.08
<i>O. ophuyseni</i>	Dry I	4	0.18±0.12	0.15±0.10	0.15±0.11	0.13±0.08	0.41±0.07
	Wet	4	0.09±0.10	0.07±0.05	0.08±0.07	0.06±0.05	0.71±0.15
	Dry II	4	0.27±0.19	0.22±0.16	0.20±0.15	0.20±0.10	0.12±0.07
<i>S. sihama</i>	Dry II	4	0.25±0.18	0.20±0.14	0.18±0.14	0.27±0.11	0.10±0.07
<i>G. giuris</i>	Dry I	4	0.25±0.14	0.15±0.11	0.15±0.11	0.15±0.09	0.30±0.07
	Wet	4	0.11±0.08	0.30±0.17	0.24±0.15	0.24±0.11	0.10±0.06
	Dry II	4	0.24±0.17	0.21±0.15	0.21±0.15	0.24±0.11	0.11±0.07
<i>I. melastoma</i>	Dry II	4	0.16±0.12	0.20±0.14	0.21±0.14	0.11±0.07	0.33±0.07
<i>E. japonicus</i>	Dry I	4	0.13±0.09	0.16±0.11	0.19±0.13	0.09±0.06	0.43±0.08
<i>M. quadridentatus</i>	Wet	4	0.26±0.18	0.16±0.13	0.21±0.17	0.12±0.09	0.25±0.11
	Dry II	4	0.17±0.12	0.17±0.12	0.17±0.12	0.11±0.07	0.38±0.08
<i>Metapenaeus</i> sp.	Dry II	4	0.23±0.16	0.22±0.17	0.22±0.17	0.14±0.09	0.19±0.08
<i>E. sinensis</i>	Dry II	4	0.25±0.18	0.22±0.16	0.21±0.16	0.21±0.11	0.11±0.07
<i>P. serrifer</i>	Dry I	4	0.21±0.13	0.19±0.13	0.19±0.14	0.13±0.08	0.28±0.08
	Wet	4	0.29±0.18	0.17±0.13	0.21±0.16	0.14±0.10	0.18±0.07
	Dry II	4	0.22±0.15	0.21±0.16	0.22±0.16	0.14±0.09	0.22±0.08
<i>M. longipes</i>	Wet	4	0.23±0.14	0.15±0.11	0.19±0.14	0.12±0.08	0.32±0.08
<i>S. paramamosain</i>	Dry I	4	0.21±0.11	0.23±0.13	0.18±0.12	0.12±0.06	0.26±0.06
	Wet	4	0.34±0.18	0.15±0.12	0.19±0.14	0.13±0.09	0.19±0.07
	Dry II	8	0.24±0.18	0.20±0.16	0.20±0.16	0.14±0.10	0.22±0.09
<i>E. carinicauda</i>	Dry I	8	0.29±0.17	0.12±0.09	0.11±0.09	0.19±0.11	0.29±0.07
	Wet	4	0.35±0.18	0.15±0.12	0.19±0.14	0.13±0.10	0.17±0.06
	Dry II	8	0.19±0.13	0.18±0.12	0.18±0.12	0.12±0.07	0.34±0.07
<i>C. dubia</i>	Dry I	4	0.30±0.20	0.22±0.16	0.17±0.12	0.20±0.12	0.11±0.07
<i>P. carinata</i>	Dry I	4	0.31±0.20	0.20±0.16	0.17±0.13	0.19±0.11	0.13±0.07
<i>C. haematocheir</i>	Dry I	4	0.18±0.12	0.15±0.11	0.15±0.12	0.13±0.08	0.39±0.08
	Wt	4	0.23±0.10	0.17±0.11	0.23±0.16	0.17±0.11	0.20±0.08
	Dry II	4	0.29±0.20	0.19±0.15	0.16±0.13	0.25±0.12	0.12±0.07
<i>O. stimpsoni</i>	Dry II	4	0.27±0.19	0.22±0.16	0.20±0.15	0.20±0.10	0.12±0.07
<i>C. sinensis</i>	Dry I	4	0.28±0.15	0.21±0.13	0.18±0.12	0.16±0.09	0.17±0.07
<i>P. pictum</i>	Wt	4	0.08±0.06	0.25±0.16	0.40±0.23	0.12±0.09	0.16±0.08
<i>V. litterata</i>	Dry I	4	0.27±0.16	0.28±0.16	0.18±0.12	0.18±0.09	0.09±0.05

4.3.4. Comparison of trophic characteristics to other Chinese coastal ecosystems

Eighteen studies were previously conducted on the food web structure of tidal flat in China, focusing on three coastal ecosystems (mangroves, salt marshes, and seagrass) (Fig. 4.10., Tables 4.4. and 4.5.). Out of three types of tidal flat, the most enriched and depleted carbon isotope ranges (from baseline to consumers) in the food web were estimated for seagrass habitat (-23.6 to -9.2‰) and mangrove forests (-34.5 to -11.2‰). Salt marshes had a moderate $\delta^{13}\text{C}$ range (-28.2 to -10.5‰) compared to other habitats. The $\delta^{15}\text{N}$ ranges from baseline to consumers in the food web was enriched in order of salt marshes (1.8 – 14.2‰ , 3.6 TL), mangroves (4.9 – 20.3‰ , 4.5 TL) and seagrass habitat (3.9 – 17.6‰ , 4.0 TL). The different carbon stable isotope distributions in the food webs of the three habitats showed that dominant vegetation significantly affected energy transfer in each food chain (Kwak and Zedler, 1997; Bui and Lee, 2014). The largest TL in the food web of the mangrove ecosystem reflected the high biodiversity (Bouillon et al., 2008a; Alongi, 2009; Bui and Lee, 2014).

$\delta^{13}\text{C}$ depletion for POM and SOM in the current study compared to previous studies indicated a large amount of terrestrial source input, and substantial energy potentiality of mangrove-derived organic matter to consumers in the PRE food web (Fig. 4.10.). The highly enriched $\delta^{15}\text{N}$ of POM, which had a large range, closely reflected seasonal fluctuations in sewage input from the megacities to the PRE food web (Qiu et al., 2019) (Fig. 4.10.). The comparable $\delta^{15}\text{N}$ distribution in the present PRE food web (range, 6.1 – 20.3‰) to the value in polluted mangrove habitats (range, 5.2 – 15.7‰) back supported the large anthropogenic impact on the present ecosystem (Fig. 4.11.). Benthic and pelagic consumers from the six feeding types evaluated in the current study exhibited similar depleted carbon and enriched nitrogen stable isotope signatures to that of diets (Fig. 4.10.). Thus, stable isotope signatures of baseline appear to be propagated through the energy pathway from diet to consumers in PRE.

Comparison of the three tidal flats demonstrated the characteristics of food web structure in the studied mangrove ecosystem. First, terrestrial sources significantly influenced the reservoir of particulate and sedimentary organic matter, strongly supporting secondary production in the food web (Bouillon et al., 2008b; Lee et al., 2021). Second, the most depleted carbon pool was derived from the input of large mangrove species (*S. apetala*) to the PRE, rather than other mangrove systems with smaller sized plant species (*Kandelia* sp. and *Avicennia* sp.) (McKee et al., 2002; Bouillon et al., 2008a). Third, the prevalence of organic matter from mangroves in the ecosystem was higher than that from other mangrove systems showing carbon stable isotope enrichment with *Spartina* invasion (Feng et al., 2015; Feng et al., 2017; Chen et al., 2018; Gao et al., 2018; Liao et al., 2020; Chen et al., 2021). *Spartina* has been recorded spreading in parts of the PRE; thus, future trophic shifts are likely to arise in this mangrove ecosystem, impacting primary baseline, primary and secondary production, energy pathways (Zhou et al., 2015).

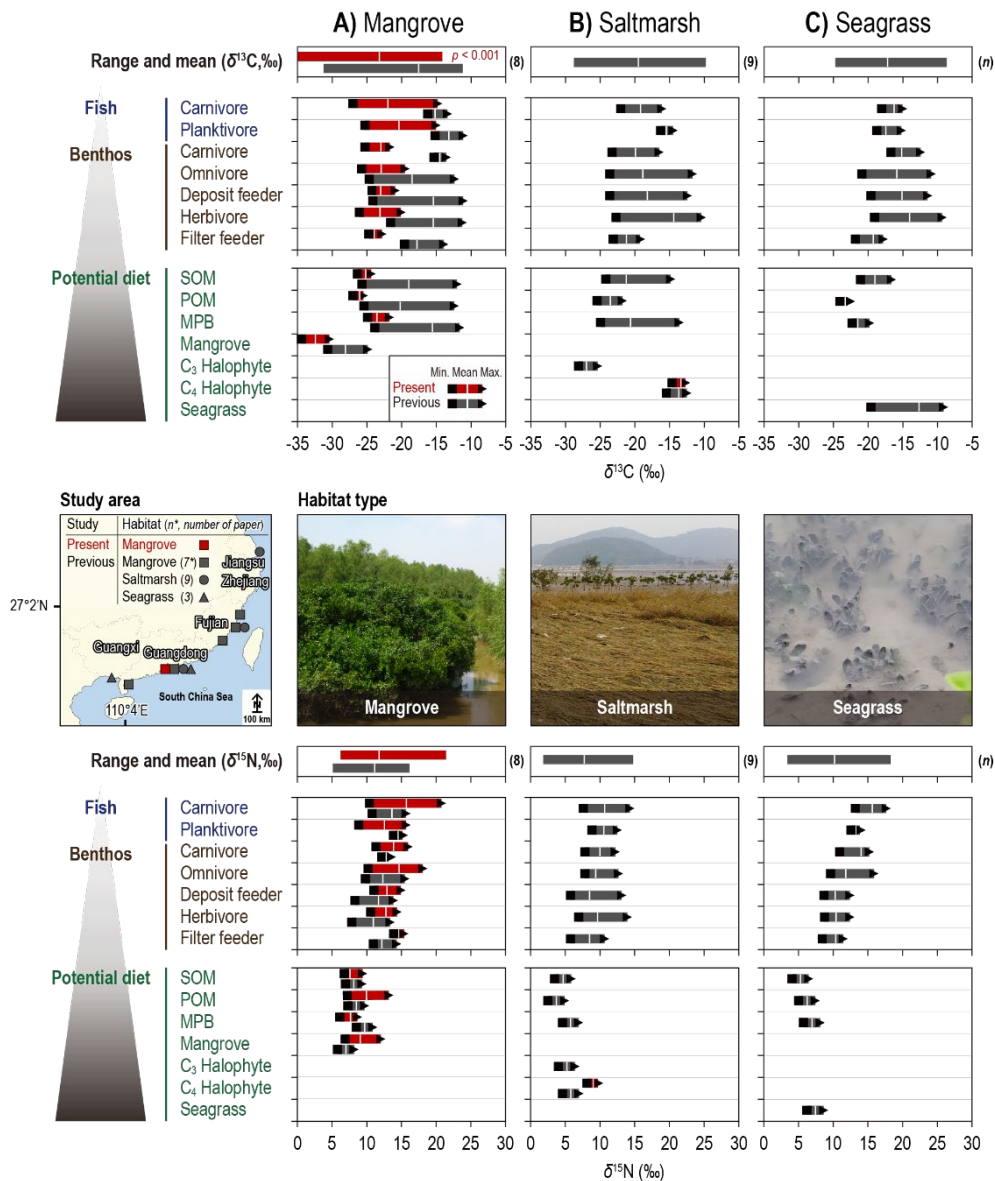


Figure 4.10.

Review of the stable isotope values of carbon and nitrogen for the potential diets of benthic and pelagic consumers in previous studies ($n=18$) conducted in the three coastal ecosystems in China: (A) mangrove forest, (B) salt marsh, and (C) seagrass habitat. The values obtained in the present study are included for comparison. Fish and benthos were classified into two and five feeding types, respectively. Potential diets included sediment organic matter (SOM), particulate organic matter (POM), microphytobenthos (MPB), mangrove, halophytes (C₃ and C₄), and seagrass. The raw stable isotope data of diet and consumers used in this figure are described in Tables 4.4. and 4.5.

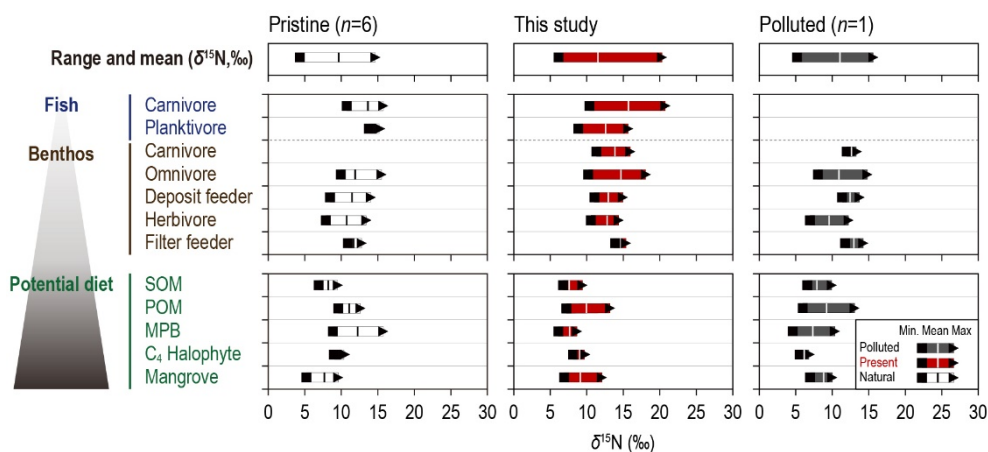
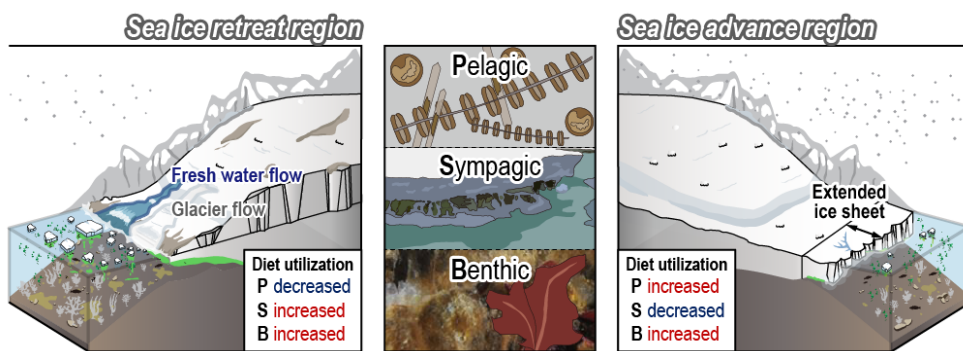


Figure 4.11.

Review of the stable isotope values of carbon and nitrogen for the potential diets and consumers in previous studies conducted in the pristine (white bar, $n=6$) and polluted (grey bar, $n=1$) mangrove habitats in China. The values obtained in the present study (red bar) are included for comparison. Fish and benthos were classified into two and five feeding types, respectively. Potential diets included sediment organic matter (SOM), particulate organic matter (POM), microphytobenthos (MPB), mangroves, and C_4 halophytes. Black square and triangle indicate minimum and maximum values, respectively.

CHAPTER 5.

Food web structure of Marian Cove in Antarctic peninsula with glacier retreat



This chapter is in preparation.

5.1. Introduction

Global warming of the oceans strongly impacts the stability of the polar coastal ecosystem by changing the timing, thickness and extent of seasonal land and sea ice formation (Kedra et al., 2015). Changes to physical and living environments synonymously with polar ice dynamics affect the life history responses of associated marine organisms (Moline et al., 2008), including predator-prey interactions (Fraser et al., 2003; Grebmeier et al., 2006). Changes to food availability with the altered timing, biomass, and species composition of blooms as part of primary production (Moline et al., 2004; Montes-Hugo et al., 2009) under polar ice dynamics impact the growth, reproduction, recruitment, and distribution of primary to apex consumers (Stirling et al., 1993; Hamilton and Haedrich, 1999; Oro et al., 2004). Through various processes, changes to ice cover are expected to alter the whole energy flux of the polar ecosystems.

Antarctic sea ice exhibit complex regional dynamics under the combined effects of atmospheric and oceanic climate, which contrasts with the sharp decrease of sea ice extent in Arctic (Parkinson, 2019). The sea ice extent of the Antarctica noticeably decreased from a maximum to minimum through the 2010s (Parkinson, 2019). Among the Antarctic six regions (West: Bellingshausen, Amundsen, and Ross Sea; East: Western Pacific Ocean, Indian Ocean, and Weddell Sea), rapid warming has driven the large-scale loss of the sea ice shelf and glacier retreat in West Antarctica (Bae et al., 2021). The fastest sea ice loss and glacier retreat have been occurred on West Antarctic Peninsula (WAP) in the Bellingshausen Sea under the most rapid warming on Earth in the last few millennia (Moline et al., 2004). In contrast, sea ice cover has increased in the East Antarctica, possibly in response to changes in atmospheric circulation (Parkinson and Cavalieri, 2012). These contrasting trends of sea ice extent between West and East Antarctica might impact the structure of the coastal ecosystem and its multiple functions (food web structure, stability, and efficiency) with regional complexity.

Previous studies reported that coastal ecosystem structure and function were altered by sediment-laden meltwater intrusion under glacier and sea ice retreat with climate change in the WAP (Shade et al., 2015; Alurralde et al., 2020). The

implications of significant changes to primary production on coastal ecosystem function has been reported under increasing sea ice cover in the East Antarctica (Michel et al., 2019). Although most Antarctic species are benthic, most published studies focused on reporting the responses of pelagic organisms with limited information on a small number of benthic species from specific feeding groups (Alurralde et al., 2020; Michel et al., 2019; Barnes et al., 2011). The impact of glacier retreat and climate warming on the coastal food web structure and its function in the WAP is of increasing concern. However, the response of coastal food web dynamics in the WAP remains poorly understood. The ecological impact of long-term regional sea ice retreats and advances on West and East Antarctic food webs must be elucidated to implement rational management and conservation actions. Most uncertainty in forecasting the effects of climate change on the Antarctic ecosystem is linked to understanding how it will affect the nature of energy interactions among organisms (Winder and Schindler, 2004).

Therefore, here, we investigated food web dynamics over a few decades based on carbon and nitrogen stable isotope analysis in an Antarctic coastal ecosystem exposed to the complex glacier and sea ice dynamics. We first investigated the substantial glacier retreat influence on food web dynamics in Marian Cove (MC) in the WAP, West Antarctica. In MC, we analysed: 1) the spatial distribution of stable isotope values of producers and consumers under meltwater intrusion with glacier retreat; and 2) changes in the spatial distribution and trophic function of the representative intertidal consumer, the Antarctic limpet, *Nacella concinna* over a decadal glacier retreat. Finally, we extended the study area to overall Antarctica and estimated: 3) food web dynamics over multiple decades between West and East Antarctica, exposed to respective sea ice retreats and advances, to provide reference data on how changes to sea ice extent are affecting the functioning of the whole coastal ecosystem of Antarctica based on the literature review.

5.2. Materials and methods

5.2.1. Sample and data collection

From 2018 to 2019, sampling was conducted at five intertidal sites during the austral summer to estimate how glacier retreat affects the food web dynamics of the MC, King George Island (Fig. 5.1.). Three replicated vertical (every 1 m from the surface to 30 m depth) phytoplankton biomass (Chl-*a*) was measured with a Sea point Chlorophyll Fluorometer (SCF) in SBE19 Plus-V2 CTD at five subtidal sites (Fig. 5.2.). Intertidal seawater properties (temperature; salinity; dissolved oxygen, DO; pH) were measured in situ using a multi-parameter water quality probe (YSI-Professional plus, USA) (Fig. 5.3.). Potential producers (particulate organic matter, POM; microalgae; macroalgae) and eight consumers were collected to analyse carbon and nitrogen stable isotope values. POM was collected at high tide and was filtered through a 200 μ m mesh net. Epilithic microalgae were sampled from the rock surface with a toothbrush. POM and microalgae were filtered with a Whatman GF/F glass fibre filter and were then collected. Drifted dominant macroalgae (red, *Iridaea cordata*; brown, *Adenocystis utricularis*) from the subtidal to intertidal zone were collected from tidal pools. Copepods were manually sampled using a 200 μ m net. Among copepods, the common occurring *Tigriopus kingsejongensis* was sorted using forceps under a binocular microscope. The amphipod *Gondogeneia Antarctica*, limpet *N. concinna*, and jellyfish *Halichystus antarcticus* were randomly collected by hands during the ebb tide. Two fish species (*Notothenia coriiceps*, *Trematomus* sp.) were sampled using a fish trap near B3. Others, such as krill (*Euphausiacea* sp.) and starfish (*Odontaster validus*) were collected near the King Sejong base camp.

We performed gut depuration of limpets for 24 h in the laboratory. The shell length of limpets was measured using Vernier Calipers, with an accuracy of 0.01 mm. All consumers were dissected, freeze-dried, and homogenised with a mortar and pestle. To examine decadal structural and functional changes in the MC food web, we compared obtained data (shell length distribution, $\delta^{13}\text{C}$ value, and diet utilisation) of the dominant consumer, the Antarctic limpet in MC (the Antarctic limpet) to previously collected data (Choy et al., 2011).

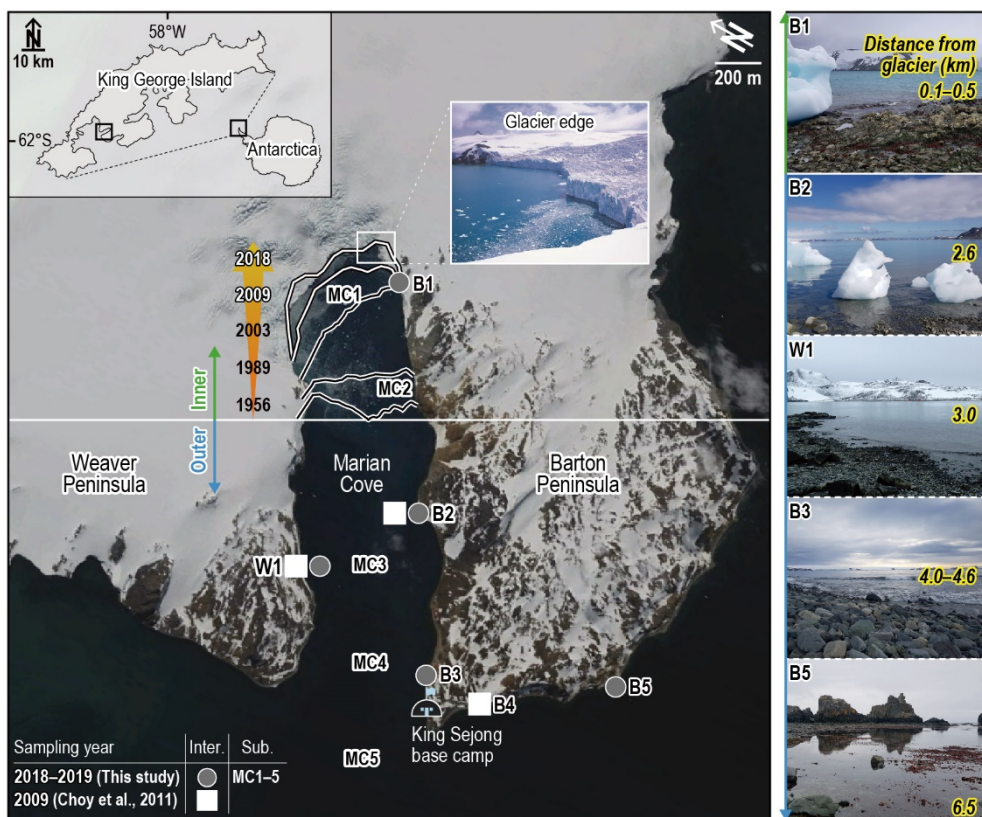


Figure 5.1.

Map of the study area showing the six intertidal (inner, B1; outer, W1 and B2-B5) and five subtidal sites (MC1-MC5), including three sites reported in a previous study (Choy et al., 2011) with records of past glacier retreat since 1956 in Marian Cove, King George Island, Antarctic Peninsula. Top-down images of five sites show the approximate glacier influence with increasing distance from the glacier margin. The base map was obtained from Google Earth (<https://earth.google.com/web>).

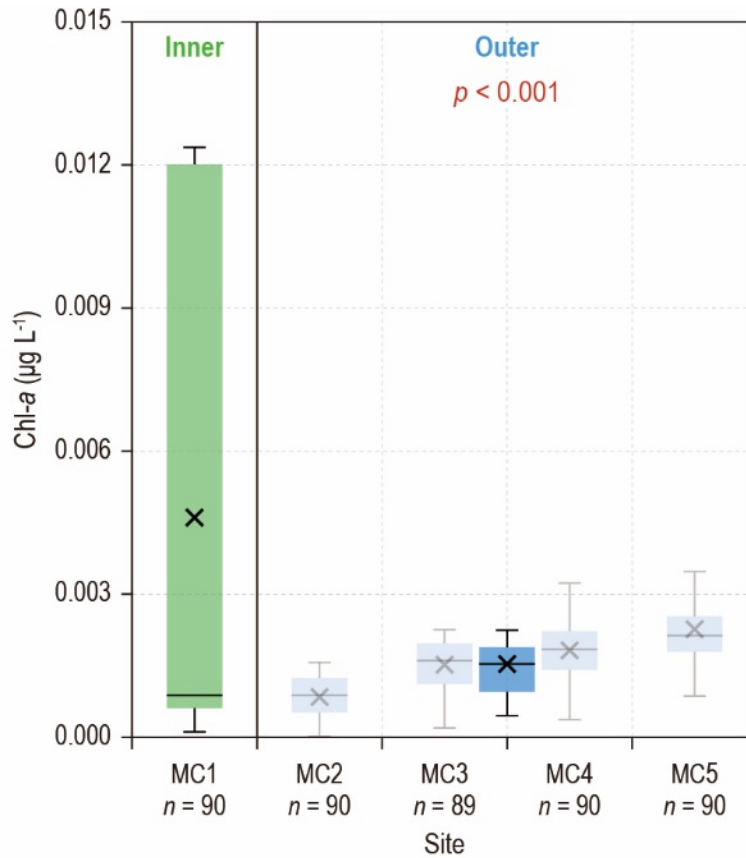


Figure 5.2.

Spatial vertical (0–20 m) concentration of Chl-*a* (MC1-MC5) measured with the Sea point Chlorophyll Fluorometer (SCF) in the SBE19 Plus-V2 CTD at five subtidal sampling sites (green, inner MC1; light blue, outer MC2-MC5; blue, total Chl-*a* of the outer sites) in Marian Cove, King George Island.

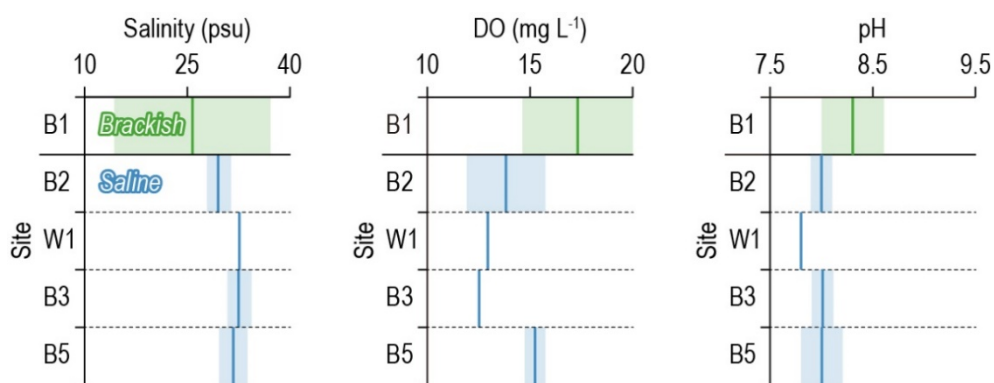


Figure 5.3.

The spatial distribution of seawater salinity, DO, and pH reflects the contrasting environmental conditions between inner and outer intertidal sites in Marian Cove, King George Island, Antarctic Peninsula during the present study period (2018–2019).

To understand trends in sea ice dynamics in Antarctica, we first compiled data on summer sea ice extent annually from 2000 to 2018, based on previously reported data using satellite-based multi-channel passive microwave (Figs. 5.4. and 5.5.) (Parkinson, 2019). Sea ice concentration (%) during summer and the three-decadal median were obtained from the NASA earth observatory (Fig. 5.5.).

To elucidate food web dynamics under changing sea ice extent in Antarctica over multiple decades, we extracted the best available stable isotope data of producers and consumers (9 phyla, 18 class, 133 species) from 30 studies published in two periods; 1990s–2010s and 2010s, representing before and after sea ice conversion in Antarctica, respectively (Table 5.1.). We limited the habitat depth of organisms to ca. 200 m, which was the depth of the continental shelf, to eliminate significant environmental disturbance of habitats on the stable isotope values. The corresponding feeding types of each consumer are presented in Table 5.1. Previous reports ($n=16$) on the benthic, pelagic, and sympagic production in the Antarctic coast and ocean related to glacier and sea ice dynamics were additionally collected to understand its spatial and temporal trends and influence on the diet utilisation of Antarctic consumers (Table 5.2.).

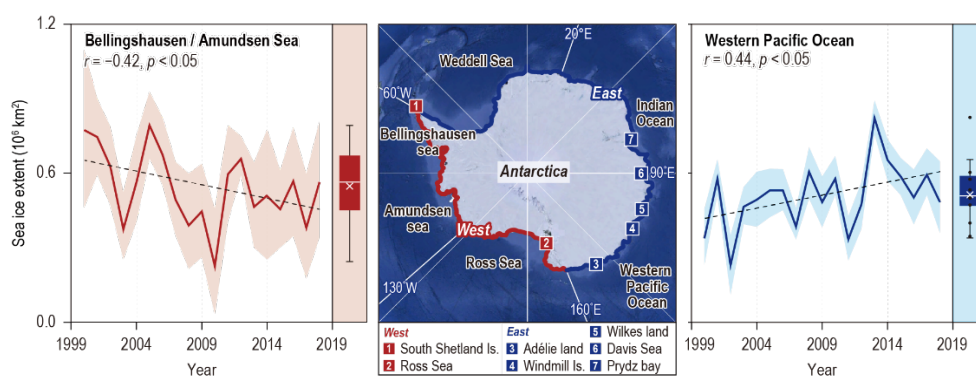


Figure 5.4.

Regional variations in summer sea ice extent variation (2000–2018) in Antarctica. Map showing the location of the carbon and nitrogen stable isotope data collection sites based on the present study with literature reviews.

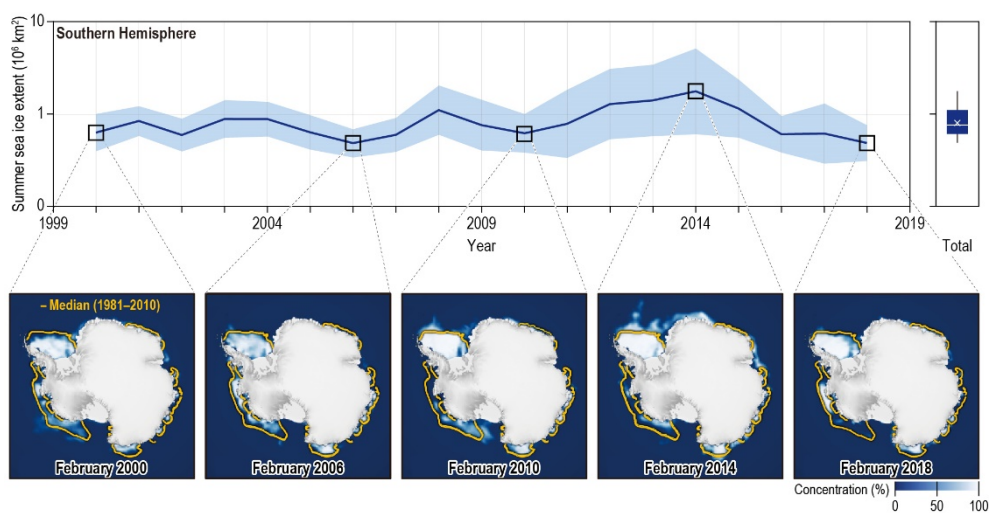


Figure 5.5.

Antarctic summer sea ice extent variation using satellite-based multi-channel passive microwave from 2000 to 2018 (Parkinson et al., 2019). Representative Antarctic summer sea ice concentration (%) estimated in the NASA earth observatory. Medians of three decadal sea ice concentrations are described by a yellow line.

Table 5.1.

List of Antarctic consumers with corresponding feeding types (grazers, Gr; filter feeders, Ff; deposit feeders, Df; omnivores, Om; scavengers, Sc; carnivores, Ca).

Phylum	Order	Family	Species	Ref. *	Feeding types
Chordata	Actinopterygii	Artedidraconidae	<i>Artedidraco orianae</i>	13	Ca
			<i>Artedidraco skottsbergi</i>	13	
		Channichthyidae	<i>Chaenocephalus aceratus</i>	2	
			<i>Chaenodraco wilsoni</i>	9	
			<i>Champscephalus gunnari</i>	2	
			<i>Chionodraco hamatus</i>	5	
			<i>Pagetopsis macropterus</i>	2	
		Harpagiferidae	<i>Harpagifer antarcticus</i>	16	
		Muraenolepididae	<i>Muraenolepis microps</i>	2	
		Myctophidae	<i>Electrona</i> sp.	2	
		Nototheniidae	<i>Dissostichus mawsoni</i>	14	
			<i>Lepidonotothen squamifrons</i>	16	
			<i>Lindbergichthys nudifrons</i>	16	
			<i>Nothotenia coriiceps</i>	16	
			<i>Nothotenia rosii</i>	16	
			<i>Nothotenia coriiceps</i>	4	
			<i>Pagothenia borchgrevinki</i>	7	
			<i>Pleuragramma antarctica</i>	4	
			<i>Trematomus bernacchii</i>	5	
			<i>Trematomus eulepidotus</i>	2	
			<i>Trematomus hansonii</i>	13	
			<i>Trematomus lepidorhinus</i>	2	
			<i>Trematomus loennbergi</i>	2	
			<i>Trematomus newnesi</i>	13	
			<i>Trematomus pennellii</i>	2	
			<i>Trematomus scotti</i>	2	
Annelida	Polychaeta	Sabellidae	<i>Perkinsiana</i> cf. <i>antarctica</i>	4	Ff

*1, Atkinson, 1995; 2, Corsolini and Sara, 2017; 3, Dunton et al., 2001; 4, Gillies et al., 2012; 5, Gillies et al., 2013; 6, Ha et al., 2019; 7, McMullin et al., 2017; 8, Michel et al., 2019; 9, Mincks et al., 2008; 10, Nyssen et al., 2005; 11, Pakhomov et al., 1998; 12, Pasotti et al., 2015; 13, Signa et al., 2019; 14, Steven et al., 2019; 15, Yen et al., 1991; 16, Zenteno, 2019; 17, This study

Table 5.1. (Continued).

Phylum	Order	Family	Species	Ref. *	Feeding types
Annelida	Polychaeta	Capitellidae	Capitellidae sp.	12	Df, Om, Sc, Ca
		Cerratulidae	Cerratulidae sp.	12	
		Flabelligeridae	<i>Flabelligera mundata</i>	8	
		Maldanidae	Maldanidae sp.	12	
		Nephtyidae	<i>Aglaophamus trissophyllus</i>	12	
		Orbiniidae	Orbiniidae sp.	4	
		Polynoidae	Harmothoe sp.	8	
			Polynoidae sp.	6	
			<i>Barrukia cristata</i>	12	
		Priapulidae	Priapulida sp.	4	
		Spionidae	Spionidae sp.	12	
		Terebellidae	<i>Polycirrus</i> sp.	8	
Arthropoda	Amphipoda	Pontogeneiidae	<i>Djerboa furcipes</i>	16	Gr
			<i>Paramoera walkeri</i>	4	
			<i>Prostebbingia gracilis</i>	16	
		Ampeliscidae	<i>Ampelisca richardsoni</i>	10	Df, Om, Sc, Ca
		Epimeriidae	<i>Epimeria georgiana</i>	10	
			<i>Epimeria similis</i>	10	
			<i>Methalimedon nordenskjoldi</i>	4	
		Iphimediidae	<i>Echiniphimedia hodgsoni</i>	10	
			<i>Iphimediella</i> sp.	10	
			<i>Iphimediella cyclogena</i>	10	
		Lysianassidae	<i>Charcotia obesa</i>	8	
			<i>Waldeckia obesa</i>	4	
		Maeridae	<i>Paracerodocus miersii</i>	16	
		Phoxocephalidae	<i>Heterophoxus videns</i>	4	
			<i>Phoxocephalidae</i> sp.	6	
			<i>Themisto gaudichaudii</i>	6	

*1, Atkinson, 1995; 2, Corsolini and Sara, 2017; 3, Dunton et al., 2001; 4, Gillies et al., 2012; 5, Gillies et al., 2013; 6, Ha et al., 2019; 7, McMullin et al., 2017; 8, Michel et al., 2019; 9, Mincks et al., 2008; 10, Nyssen et al., 2005; 11, Pakhomov et al., 1998; 12, Pasotti et al., 2015; 13, Signa et al., 2019; 14, Steven et al., 2019; 15, Yen et al., 1991; 16, Zenteno, 2019; 17, This study

Table 5.1. (Continued).

Phylum	Order	Family	Species	Ref. *	Feeding types
Arthropoda	Amphipoda	Phrosinidae	<i>Primno macropa</i>	16	Df, Om, Sc, Ca
		Pontogeneiidae	<i>Bovallia gigantea</i>	16	
			<i>Gondogeneia antarctica</i>	16	
		Tryphosidae	<i>Cheirimedon femoratus</i>	16	
		Tryphosidae	<i>Orchomenella franklini</i>	4	
			<i>Orchomenella pinguides</i>	10	
			<i>Parschisturella carinata</i>	16	
			<i>Pseudorchomene coatsi</i>	10	
	Copepoda	Calanidae	<i>Calanoides acutus</i>	4	Gr
			<i>Calanus propinquus</i>	4	
		Eucalanidae	<i>Eucalanus longiceps</i>	15	Df, Om, Ca
			<i>Paraeuchaeta antarctica</i>	6	
		Harpacticidae	<i>Harpacticoids</i> sp.	12	
			<i>Tigriopus kingsejongensis</i>	17	
		Metridinidae	<i>Metridia gerlachei</i>	1	
	Pycnogonida	Ammonotheidae	<i>Ammonothea carolinensis</i>	8	Sc, Ca
		Colossendeidae	<i>Decolopoda australis</i>	8	
		Nymphonidae	<i>Nymphon australe</i>	4	
	Euphausiacea	Euphausiidae	<i>Euphausia crystallorophias</i>	3	Gr
			<i>Euphausia superba</i>	3	
			<i>Thysanoessa macrura</i>	11	
	Ostracoda	Cypridinidae	<i>Doloria</i> sp.	4	Df
		Philomedidae	<i>Scleroconcha</i> sp.	4	
Echinodermata	Asteroidea	Asteriidae	<i>Cryptasterias</i> sp.	6	Ca
			<i>Diplasterias brucei</i>	8	
			<i>Saliasterias brachiata</i>	8	
		Astropectinidae	<i>Psilaster charcoti</i>	4	
		Ganeriidae	<i>Cuenotaster involutus</i>	4	

*1, Atkinson, 1995; 2, Corsolini and Sara, 2017; 3, Dunton et al., 2001; 4, Gillies et al., 2012; 5, Gillies et al., 2013; 6, Ha et al., 2019; 7, McMullin et al., 2017; 8, Michel et al., 2019; 9, Mincks et al., 2008; 10, Nyssen et al., 2005; 11, Pakhomov et al., 1998; 12, Pasotti et al., 2015; 13, Signa et al., 2019; 14, Steven et al., 2019; 15, Yen et al., 1991; 16, Zenteno, 2019; 17, This study

Table 5.1. (Continued).

Phylum	Order	Family	Species	Ref. *	Feeding types
Echinodermata		Odontasteridae	<i>Acodontaster cf. hodgsoni</i>	4	Ca
			<i>Acodontaster</i> sp.	8	
			<i>Odontaster validus</i>	13	
	Ophiuroidea	Ophiuridae	<i>Ophionotus victoriae</i>	5	Ca
	Ophiuroidea	Ophiuridae	<i>Ophiosparte gigas</i>	4	Ca
			<i>Ophiura crassa</i>	4	
	Echinoidea	Echinidae	<i>Sterechinus neumayeri</i>	8	Om
		Schizasteridae	<i>Abatus</i> sp.	4	
	Holothuroidea	Cucumariidae	<i>Cucumaria</i> sp.	4	Df
			<i>Staurocucumis</i> sp.	8	
			<i>Heterocucumis</i> sp.	4	
Mollusca	Pteropoda	Clionidae	<i>Clione limacina</i>	13	Ca
			<i>Clione limacina antarctica</i>	13	
	Gastropoda	Buccinidae	<i>Neobuccinum eatoni</i>	6	Sc, Ca
		Calliostomatidae	<i>Margarella antarctica</i>	16	
		Muricidae	<i>Trophonella longstaffi</i>	5	
		Velutinidae	<i>Marseniopsis</i> sp.	8	
		Cingulopsidae	<i>Skenella paludinoides</i>	4	Gr
		Nacellidae	<i>Nacella concinna</i>	3	
	Bivalvia	Cyamiidae	<i>Kidderia bicolor</i>	16	Ff
		Laternulidae	<i>Laternula elliptica</i>	8	
		Pectinidae	<i>Adamussium colbecki</i>	8	
		Sareptidae	<i>Aequiyoldia eightsi</i>	12	
Nemertea	–	Leptosomatidae	<i>Deontostoma</i> sp.	8	Df, Om, Ca
		Lineidae	<i>Parborlasia corrugatus</i>	4	
Cnidaria	Anthozoa	Actiniidae	<i>Actiniidae</i> sp.	6	Ca
			<i>Urticinopsis antarctica</i>	4	
			<i>Isotealia antarctica</i>	8	
		Kophobelemnidae	<i>Malacobelemnion daytoni</i>	12	

*1, Atkinson, 1995; 2, Corsolini and Sara, 2017; 3, Dunton et al., 2001; 4, Gillies et al., 2012; 5, Gillies et al., 2013; 6, Ha et al., 2019; 7, McMullin et al., 2017; 8, Michel et al., 2019; 9, Mincks et al., 2008; 10, Nyssen et al., 2005; 11, Pakhomov et al., 1998; 12, Pasotti et al., 2015; 13, Signa et al., 2019; 14, Steven et al., 2019; 15, Yen et al., 1991; 16, Zenteno, 2019; 17, This study

Table 5.1. (Continued).

Phylum	Order	Family	Species	Ref. *	Feeding types
Porifera	Demospongiae	Axinellidae	<i>Homaxinella balfourensis</i>	8	Ff
		Chalinidae	<i>Haliclona</i> sp.	13	
		Demospongiae	<i>Demospongiae Indet.</i>	8	
		Hymedesmiidae	<i>Kirkpatrickia variolosa</i>	5	
		Isodictyidae	<i>Isodictya setifera</i>	4	Ff
		Mycalidae	<i>Mycale acerata</i>	8	
		Niphatidae	<i>Hemigellius</i> sp.	8	
		Polymastiidae	<i>Sphaerotylus antarcticus</i>	5	

*1, Atkinson, 1995; 2, Corsolini and Sara, 2017; 3, Dunton et al., 2001; 4, Gillies et al., 2012; 5, Gillies et al., 2013; 6, Ha et al., 2019; 7, McMullin et al., 2017; 8, Michel et al., 2019; 9, Mincks et al., 2008; 10, Nyssen et al., 2005; 11, Pakhomov et al., 1998; 12, Pasotti et al., 2015; 13, Signa et al., 2019; 14, Steven et al., 2019; 15, Yen et al., 1991; 16, Zenteno, 2019; 17, This study

Table 5.2. Review ($n=16$) of spatial and temporal changes in sympagic, pelagic, and benthic primary production along the Antarctic coast.

Region	Type	Condition in study area	Trend	References
West Antarctica	Benthic production	Glacier retreat	Increase ▲	Cordone et al., 2018
		Glacier retreat	Increase ▲	Braeckman et al., 2019
		Increased sea ice free duration	Increase ▲	Dayton and Oliver, 1977
	Pelagic production	Increased distance from sea ice	Decrease ▼	Garibotti et al., 2003
		Increased turbulent	Decrease ▼	Scholoss et al., 2002
		Sea ice melt	Increase ▲	Eveleth et al., 2017
		Sea ice melt	Increase ▲	Lee et al., 2022
		Sea ice melt	Increase ▲	Vernet et al., 2008
	Sympagic production	Sea ice covered	Increase ▲	Wing et al., 2012
East Antarctica	Benthic production	Increased sea ice free duration	Increase ▲	Clark et al., 2017
	Pelagic production	Sea ice melt	Increase ▲	Gobin et al., 2005
		Sea ice melt	Increase ▲	Wright et al., 2010
		Absence of sea ice break up	Increase ▲	Michel et al., 2019
		Extended sea ice	Increase ▲	Hirawake et al., 2005
	Sympagic production	Sea ice melt	Increase ▲	Wright et al., 2010
		Absence of sea ice break up	Increase ▲	Michel et al., 2019
Antarctica	Benthic production	Glacier and sea ice retreat	Increase ▲	Huovinen, 2020
	Pelagic production	Sea ice melt	Increase ▲	Behera et al., 2020

5.2.2. Stable isotope analysis

We decalcified the fine powder of POM, microalgae and macroalgae to examine $\delta^{13}\text{C}$ values. To remove lipids from the tissue of consumers, we used 10 mL dichloromethane/methanol (2:1, v/v) solvent. Some consumers were decalcified with 1 N HCl (Sigma Aldrich) to eliminate inorganic carbon, which interferes with $\delta^{13}\text{C}$ signature (Carabel et al., 2006). Decalcified and lipid-free samples were fully lyophilised. We did not perform any pre-treatment for $\delta^{15}\text{N}$ analysis. All samples were weighed and wrapped in a tin container. An isotope ratio mass spectrometer connected to an elemental analyser (EA-IRMS) was used to determine the $\delta^{13}\text{C}$ and $\delta^{15}\text{N}$ of samples. The percentage C and N compositions of samples were directly determined after combustion in EA. The instrument calibrated the value based on standard sulfanilamide (C, 41.8%; N, 16.3%). Resultant CO_2 and N_2 gases were introduced to the IRMS. Stable isotope abundance was expressed in delta (δ) notation relative to the conventional standard (C, Vienna Pee Dee Belemnite; N, atmospheric N_2), with the following formula:

$$\delta X (\text{‰}) = [(R_{\text{sample}} / R_{\text{reference}}) - 1] \times 1000$$

where X is ^{13}C or ^{15}N and R is the ratios, $^{13}\text{C}/^{12}\text{C}$ or $^{15}\text{N}/^{14}\text{N}$. IAEA-CH-3 cellulose and IAEA-N-2 ammonium sulfate were used for the internal calibration of ^{13}C and ^{15}N . Measurement precision of replicated analyses was ca. 0.04‰ for $\delta^{13}\text{C}$ and 0.2‰ for $\delta^{15}\text{N}$.

5.2.3. Trophic level

A trophic enrichment factor of $\delta^{15}\text{N}$, 2.3‰ was used to estimate the trophic level (TL) of Antarctic marine organisms (McCutchan Jr et al., 2003). The average $\delta^{15}\text{N}$ of primary consumers (filter feeder and grazer) was collected as the baseline $\delta^{15}\text{N}$ of the food web because their tissues assimilate primary producers and organic matter (Riccialdelli, 2017). The TL of consumers was estimated using a formula constructed by Vander Zanden and Rasmussen (1999):

$$\text{TL}_i = (\delta^{15}\text{N}_i - \delta^{15}\text{N}_{\text{base}}) / \text{TEF} + \text{TL}_{\text{base}}$$

where, TL_i is the TL of each species considered, $\delta^{15}\text{N}_i$ is the $\delta^{15}\text{N}$ of species i , and $\delta^{15}\text{N}_{\text{base}}$ and TL_{base} are the mean $\delta^{15}\text{N}$ and TL of primary consumers, respectively (TL=2).

5.2.4. Statistical analysis

SPSS 26.0 (SPSS INC., Chicago, IL) was used to carry out a One-sample t-test, Independent two-sample t-test, One-way analysis of variance (ANOVA), Kruskal-Wallis test, Correlation, and Regression analyses. Cluster analysis was performed in PRIMER 6.1.16. The Bayesian stable isotope mixing model in the R (SIMMR) package was used to examine the diet utilisation of marine organisms in Antarctica (Parnell and Inger, 2016). To compare the present trophic function of limpets, we used the TEF ($\delta^{13}\text{C}$, $0.8 \pm 1.0\text{‰}$; $\delta^{15}\text{N}$, $2.2 \pm 1.0\text{‰}$) (Dunton, 2001) from a previous study (Choy et al., 2011) to adjust the stable isotope ratios of Antarctic limpets in SIMMR. As there is no specific TEF, we used widely applicable $\delta^{13}\text{C}$ ($0.4 \pm 1.2\text{‰}$) and $\delta^{15}\text{N}$ ($2.3 \pm 1.6\text{‰}$) utilised in previous study for the reviewed stable isotope signatures of Antarctic organisms (McCutchan Jr et al., 2003; Michel et al., 2019). To reveal baseline changes in Antarctica under changing sea ice extent, pelagic, sympagic and benthic contributions to Antarctic consumers were estimated during two periods (1990s–2000s vs. 2010s). A priori aggregation of benthic primary producers (microalgae and macroalgae) was performed to interpret the mixing model results logically.

5.3. Results and discussion

5.3.1. Environment in Marian Cove (MC), King George Island

Spatial differences in the environment were investigated between the inner and outer sites of MC. Salinity was significantly lower in inner site B1, which had a larger standard deviation (25.7 ± 11.3) than the outer sites (31.7 ± 1.4) ($t=8.7$, $p<0.01$) (Fig. 5.3.). DO and pH were higher in the inner site (DO: 17.4 ± 2.8 mg L⁻¹; pH: 8.3 ± 0.3) compared to the outer sites (DO: 13.6 ± 1.2 mg L⁻¹; pH: 8.0 ± 0.1) (DO: $t=-7.3$, $p<0.01$; pH: $t=-7.8$, $p<0.01$) (Fig. 5.3.). Subtidal phytoplankton biomass (Chl-*a*) was significantly higher in the inner site (0.004 ± 0.005 µg⁻¹) than the outer sites (0.002 ± 0.001 µg⁻¹) ($F=27.8$, $p<0.001$) (Fig. 5.2.).

The lower salinity (with a large standard deviation), and higher DO and pH, in B1 reflected meltwater intrusion near glacier edge. Higher phytoplankton production in B1 might be related to iron (Fe) input from glaciers (Alderkamp et al., 2012; Brault et al., 2019; Höfer et al., 2019). Phytoplankton and ice algae were reported as a primary source to consumers on the Antarctic coast (Leu et al., 2011). However, the phytoplanktonic production in MC was generally lower compared to that in other Antarctic coastal areas (Schloss and Ferreyra, 2002). Thus, micro- and macroalgae likely constitute an important food supply for benthic organisms in MC (Hoffmann et al., 2018; Braeckman et al., 2019).

5.3.2. Food web structure in MC

Four potential producers and eight consumers were collected in MC (Fig. 5.6., Table 5.3.). Stable isotope signatures differed significantly among food sources ($\delta^{13}\text{C}$: $F=22.0$, $p<0.001$; $\delta^{15}\text{N}$: $F=25.4$, $p<0.001$). Brown macroalgae ($-11.7\pm0.6\text{‰}$) and POM ($-21.7\pm3.1\text{‰}$) had the most enriched and depleted $\delta^{13}\text{C}$. Microalgae and red macroalgae had the highest and lowest $\delta^{15}\text{N}$, 6.6 ± 1.2 and $2.2\pm1.8\text{‰}$, respectively.

Much of the $\delta^{13}\text{C}$ variability of marine primary producers was attributed to different uptake of CO_2 from the surrounding environment (Choy et al., 2011; Wing et al., 2012). Therefore, the significant uptake of atmospheric CO_2 was likely the reason for the depleted $\delta^{13}\text{C}$ of phytoplankton and intertidal microalgae (Wada et al., 1987; Cooper and McRoy, 1988). In contrast, enriched $\delta^{13}\text{C}$ of macroalgae reflected the effective HCO_3^- utilisation of it in the subtidal environment (Axelesson et al., 2000). The variation in $\delta^{15}\text{N}$ of primary producers reflected the dynamics of inorganic nitrogen (N_2 , NH_4^+ , and NO_3^-) in their inter- and subtidal habitats (Bae et al., 2021; Altabet, 1988).

Significant differences in stable isotope values were estimated for eight consumer species ($\delta^{13}\text{C}$: $H=56.7$, $p<0.001$; $\delta^{15}\text{N}$: $H=60.1$, $p<0.001$) (Fig. 5.6.). The Antarctic krill, *Euphausiacea* sp. ($-23.4\pm0.3\text{‰}$), and limpet, *Nacella concinna* ($-14.6\pm1.5\text{‰}$), had the most depleted and enriched $\delta^{13}\text{C}$. The highest and lowest $\delta^{15}\text{N}$ were recorded for Antarctic cod *Notothenia coriiceps* ($10.4\pm0.1\text{‰}$) and limpet ($5.6\pm0.8\text{‰}$). The stepwise $\delta^{15}\text{N}$ increase in consumers from grazer limpet to carnivorous fish indicates the presence of approximately four TL in the MC food web (Fig. 5.6.).

Antarctic krill mainly consume ice algae with enriched $\delta^{13}\text{C}$ signature (Carscallen et al., 2012). However, krill had the most depleted $\delta^{13}\text{C}$ value, indicating that it utilised alternative sources such as particulate organic matter and phytoplankton to reduce the nutritional stress when ice algae availability was low due to the absence of the ice foot, even during winter in MC (Alurralde et al., 2020; Michel et al., 2019; Choy et al., 2011). The two herbivores (limpets and krill) had contrasting $\delta^{13}\text{C}$ values, indicating they utilize different baseline sources in benthic and pelagic systems. The depleted $\delta^{15}\text{N}$ and low TL of the omnivore, *Gondogeneia*

Antarctica, and carnivore, *Haliclystus antarcticus*, revealed the altered functional role of consumers, which was associated with adaptive traits and trophic plasticity under glacier retreat (Michel et al., 2019; Calizza et al., 2018).

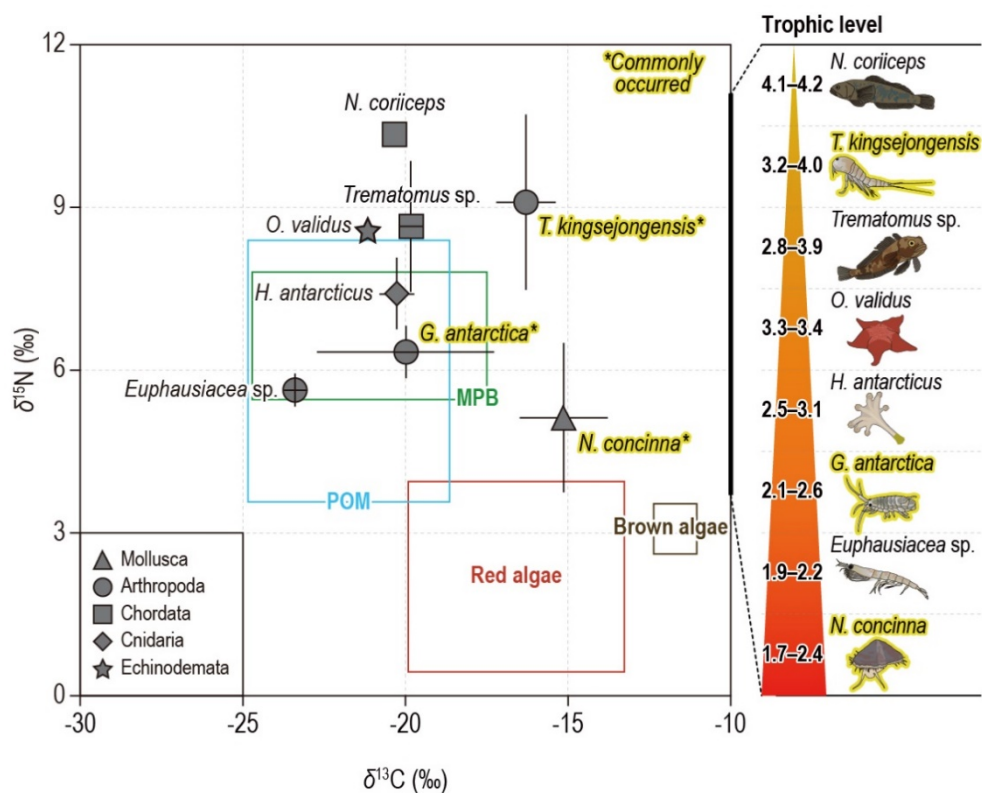


Figure 5.6.

Stable carbon and nitrogen isotopic signatures ($\delta^{13}\text{C}$ and $\delta^{15}\text{N}$) of potential food sources and consumers in Marian Cove, King George Island, Antarctic Peninsula. Stable isotope ranges of potential food sources (particulate organic matter, POM; microphytobenthos, MPB; red and brown macroalgae) are represented by empty blue, green, red, and brown boxes. Consumers represented as grey symbols indicate five taxonomic groups (Mollusca, Arthropoda, Chordata, Cnidaria, and Echinodermata) with total means and standard deviations. Consumers with an asterisk and bold letters with yellow highlighting indicate species collected from both the inner and outer sites in MC. Ranges of trophic level to eight consumers are presented next to the biplot.

Table 5.3.

Stable carbon and nitrogen isotope ratios ($\delta^{13}\text{C}$ and $\delta^{15}\text{N}$) of food sources (POM, particulate organic matter; microalgae; macroalgae) and eight consumers collected from the five intertidal sites along the Marian Cove, King George Island during the summer of 2018 to 2019 with corresponding trophic level (TL). Isotopic values are reported as means with standard deviations (s.d.). *n* indicates the number of samples.

Species	Site*	<i>n</i>	$\delta^{13}\text{C}$ (‰)		$\delta^{15}\text{N}$ (‰)		TL	
			mean	s.d.	mean	s.d.		
POM	Inner	B1	1	-18.1	0.1	6.1	1.7	-
	Outer	B2	1	-18.4	0.0	10.7	0.9	-
		B3	1	-24.1	0.4	4.3	0.9	-
		B5	1	-24.5	0.5	5.1	0.3	-
	Total			-21.3	3.5	6.5	2.8	-
Microalgae	Inner	B1	1	-16.4	0.6	6.3	1.3	-
	Outer	B2	1	-20.0	1.8	6.3	0.8	-
		B3	1	-25.0	1.7	6.5	1.5	-
		B5	1	-23.2	0.2	7.5	0.9	-
	Total			-21.2	3.8	6.6	0.6	-
Macroalgae	Inner	B1	2	-13.0	0.4	0.3	1.3	-
	Outer	B2	2	-19.7	2.2	3.7	0.9	-
		B5	2	-17.0	2.3	2.6	0.7	-
	Total			-16.6	3.4	2.2	1.8	-
<i>Nacella concinna</i>	Inner	B1	54	-13.4	0.5	5.7	0.4	2.1
	Outer	B2	96	-13.8	0.7	4.8	0.9	1.7
		W1	11	-14.5	0.4	3.9	1.1	1.3
		B3	21	-16.7	0.8	4.3	0.3	1.5
		B5	30	-16.4	0.6	6.6	0.7	2.5
	Total			-14.6	1.5	5.5	0.7	2.0
<i>Tigriopus kingsejongensis</i>	Inner	B1	-	-15.2	0.4	10.4	0.2	4.1
	Outer	B2	-	-14.4	0.3	9.1	0.6	3.6
		B3	-	-18.0	0.5	8.6	0.5	3.4
		B5	-	-17.6	0.3	8.3	0.1	3.2
	Total			-16.3	1.8	9.1	0.9	3.6
<i>Gondogeneia antarctica</i>	Inner	B1	-	-16.0	0.7	6.4	0.7	2.4
	Outer	B2	-	-19.7	1.2	6.6	0.2	2.5
		B3	-	-21.4	0.7	5.9	0.2	2.2
		B5	-	-22.8	0.6	6.4	0.4	2.4
	Total			-20.0	2.9	6.3	0.3	2.4
<i>Euphausiacea</i> sp.	Outer	B3	5	-23.4	0.3	5.6	0.3	2.1
<i>Halichystus antarcticus</i>	Outer	B3	6	-20.3	0.5	7.4	0.7	2.8
<i>Odontaster validus</i>	Outer	B3	1	-21.2	0.1	8.6	0.2	3.3
<i>Trematomus</i> sp.	Outer	B3	1	-19.8	0.2	8.7	1.2	3.4
<i>Notothenia coriiceps</i>	Outer	B3	1	-20.3	0.0	10.4	0.1	4.1

*B, Barton peninsula; W, Weaver peninsula described in Fig. 5.1.

*B, Barton peninsula; W, Weaver peninsula described in Fig. 5.1.

5.3.3. Spatial stable isotopic distribution of producers and consumers in MC

All potential diets exhibited significant ^{13}C enrichment in B1 (POM: $t=7.1, p<0.001$; microalgae: $t=9.1, p<0.001$; macroalgae: $t=5.2, p<0.01$) (Fig. 5.7., Table 5.3.). This change to baseline $\delta^{13}\text{C}$ in the inner site (B1) led to the significant $\delta^{13}\text{C}$ enrichment of three commonly occurred consumers (*N. concinna*: $t=2.7, p<0.05$; *G. antarctica*: $t=11.3, p<0.001$; *Tigriopus kingsejongensis*: $t=2.4, p<0.05$) (Fig. 5.7., Table 5.3.) (Lee et al., 2021). The $\delta^{13}\text{C}$ enrichment of producers and consumers in the inner site was similar to the phenomenon reported in the previous studies (Bae et al., 2021; Alurralde et al., 2020).

The $\delta^{13}\text{C}$ enrichment of producers might be related to increased HCO_3^- utilisation and production of organic materials in the enclosed environment beneath glaciers (Bae et al., 2021). We expected that the enriched $\delta^{13}\text{C}$ was propagated from producers to consumers through the energy pathway in B1 (Raven et al., 1982). There was no spatial difference in $\delta^{15}\text{N}$ in all food sources (Fig. 5.8., Table 5.3.). The copepod *T. kingsejongensis* only exhibited significant spatial differences in $\delta^{15}\text{N}$ ($t=8.9, p<0.01$), implying that it has various functional roles in the MC.

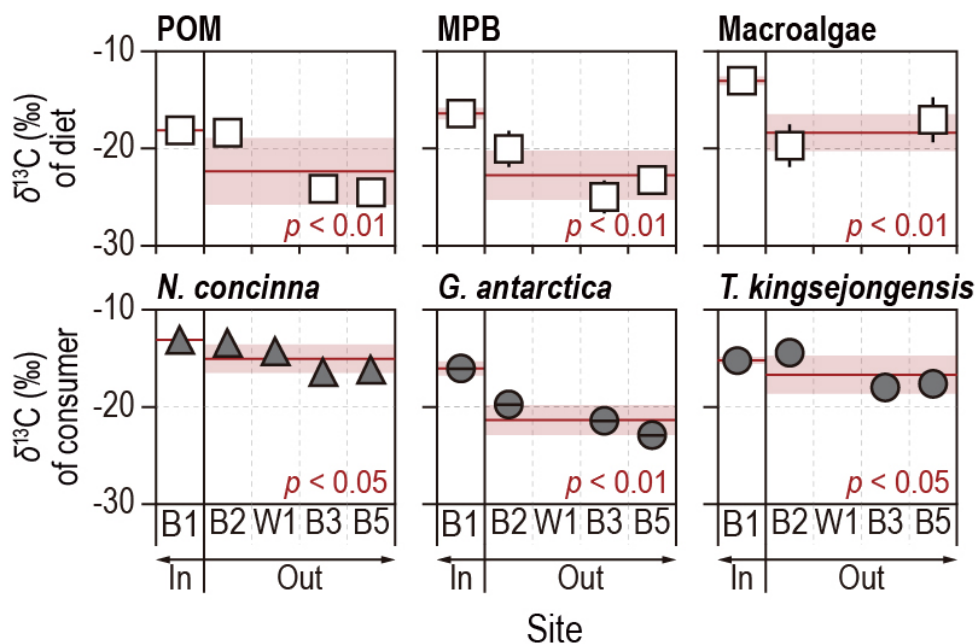


Figure 5.7.

Spatial carbon stable isotope distributions ($\delta^{13}\text{C}$) of three potential food sources (particulate organic matter, POM; microphytobenthos, MPB; red and brown macroalgae) and dominant consumers (*Nacella concinna*, *Gondogeneia antarctica*, and *Tigriopus kingsejongensis*) collected from inner (B1) and outer sites (B2, B3, B5, and W1) in Marian Cove, King George Island. Diets and consumers showing significant differences in stable isotope values between inner and outer sites are described with red mean and standard deviation.

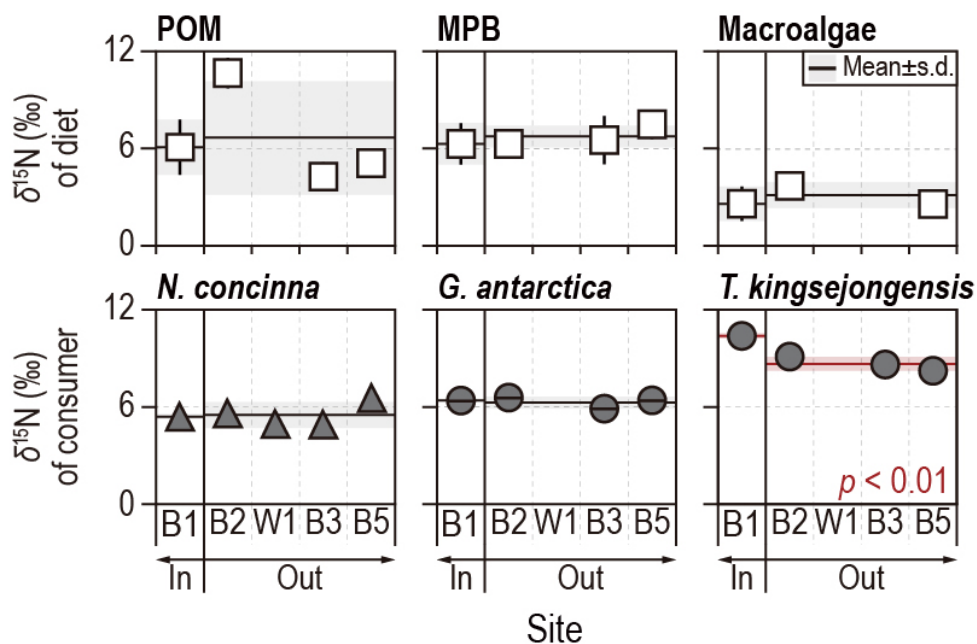


Figure 5.8.

Spatial carbon stable isotope distributions ($\delta^{15}\text{N}$) of three potential food sources (particulate organic matter, POM; microphytobenthos, MPB; red and brown macroalgae) and dominant consumers (*Nacella concinna*, *Gondogeneia antarctica*, and *Tigriopus kingsejongensis*) collected from inner (B1) and outer sites (B2, B3, B5, and W1) in Marian Cove, King George Island. Diets and consumers showing significant differences in stable isotope values between inner and outer sites are described with red mean and standard deviation.

5.3.4. Decadal changes in the structure and function of the Antarctic limpet in MC

Cluster analysis was performed to estimate decadal changes to the spatial distribution of the limpet population in MC. This analysis identified the (dis)similarity of *N. concinna* samples based on shell length, delineating two major groups (Group 1 and 2) (Fig. 5.9.A.). Group 1 included large limpets (36.4 ± 4.1 mm) that inhabited B2 and W1 in 2009, and B1 in 2018–2019. In contrast, Group 2 encompassed small limpets (27.7 ± 2.3 mm) that were mostly collected from outer sites in each of the two periods (Fig. 5.9.A.). Large limpets more actively immigrated to recently created ice-free habitat compared to the smaller limpets, indicating size-dependent adaptability and intraspecific competition to expand a species niche in source-limited intertidal rocky shore (Underwood, 1978; Connell, 1983; Boaventura et al., 2003). Both limpet groups exhibited significant $\delta^{13}\text{C}$ enrichment over a narrower range in 2018–2019 compared to that estimated in 2009 (Group 1, $t = -21.1$, $p < 0.01$; Group 2, $t = 6.3$, $p < 0.01$) (Fig. 5.9.B., Table 5.4.). Thus, limpets in 2018–2019 intensively consumed a more $\delta^{13}\text{C}$ enriched diet (including macroalgae) compared to limpets collected in 2009. The decadal increase in macroalgal contribution and decrease in microalgal contribution to limpets supported this result (Fig. 5.9.B.).

Previous studies reported that many benthic organisms living in the coastal area in King George Island depend on benthic micro- and macroalgae in environments with low phytoplankton biomass (Schloss and Ferreyra, 2002; Ahn, 1993). We estimated that the benthic contribution for limpets was high under low subtidal pelagic production, supporting previous reports in MC (Figs. 5.2. and 5.9.B.). Decadal changes to diet were more noticeable in the large-sized group inhabiting the area near the glacier edge compared to the small-sized group inhabiting the outer sites (Fig. 5.9.B., Table 5.4.). The decadal increase in macroalgae dependence of the large limpets at B1 to the similar dependence levels of small limpets in outer sites reflected the simplified trophic function in the coastal ecosystem of MC. This phenomenon was related to the substantial increase in macroalgal biomass in MC, which was induced by the combined effect of increased light availability and nutrient input from the glacier (Braeckman et al., 2019).

Because macroalgae had a significant fundamental role in the late 2010s, they might have (in)directly affected the function and stability of the food web structure in MC (Cordone et al., 2018). Under the future climatic crisis, the loss of macroalgae under conditions over critical temperature ranges could propagate a cascade of secondary extinctions through the oversimplified MC food web.

Rocky shore species has been reported as cost-effective sentinel responding to global climatic change in the long-term previous studies (Hawkins et al., 2009; Burrows et al., 2020). In particular, space-occupying key organisms, gastropod grazer, is well known as useful study taxa for predictive modelling to ecological processes that generate spatial and temporal changes in abundance (Hawkins et al., 2009). In this study, we first suggested the carbon and nitrogen stable isotope values of the limpet can also be utilised as an effective indicator of climatic changes in the nearshore ecosystem.

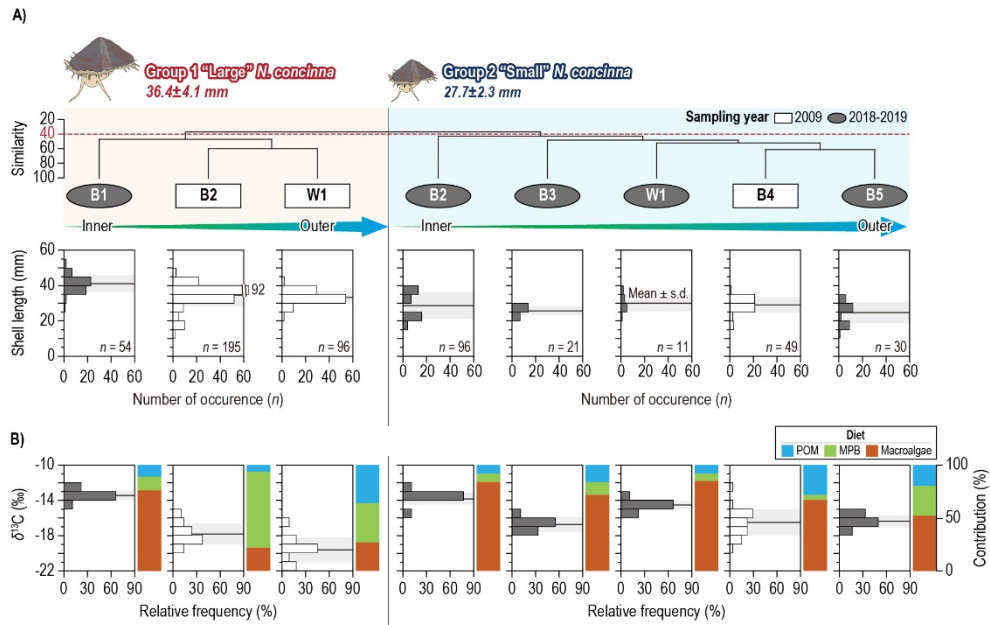


Figure 5.9.

Decadal comparison (2009 vs. 2018–2019) of the spatial distribution and function of the Antarctic limpet, *Nacella concinna* population in Marian Cove, King George Island. White rectangles and grey ellipses indicate limpet samples collected in 2009 (Choy et al., 2011) and 2018–2019, respectively. **(A)** small and large limpet groups (groups 1 and 2) determined by cluster analysis based on similarity to shell length (mm). Limpet samples in each group are arranged by distance from the glacier. **(B)** spatial distribution of the stable carbon isotope signature ($\delta^{13}\text{C}$) of eight limpet samples with contributions (%) of three potential diets (particulate organic matter, POM; microalgae; macroalgae).

Table 5.4.

Decadal comparison of spatial stable isotope variability ($\delta^{13}\text{C}$ and $\delta^{15}\text{N}$) and dietary utilisation of *Nacella concinna* in Marian Cove, King George Island during summer. Isotopic values and contributions are reported as means with standard deviations (s.d.) and means with range (min.–max.), respectively.

Type	Species	Site*		Period	
				2018 to 2019 (This study)	2009 (Choy et al., 2011)
$\delta^{13}\text{C}$, ‰ (mean±s.d.)	<i>N. concinna</i>	Inner	B1	−13.4±0.5	–
			B2	−13.8±0.7	−17.8±1.2
		Outer	W1	−14.5±0.4	−19.6±1.4
			B3	−16.7±0.8	–
			B4	–	−16.5±1.5
			B5	−16.4±0.6	–
$\delta^{15}\text{N}$, ‰ (mean±s.d.)	<i>N. concinna</i>	Inner	B1	5.7±0.4	–
			B2	4.8±0.9	6.0±0.7
		Outer	W1	3.9±1.1	4.9±0.6
			B3	4.3±0.3	–
			B4	–	5.0±0.6
			B5	6.6±0.7	–
Diet contribution, % [mean (min.–max.)]	POM	Inner	B1	10.9(5.1–16.7)	–
			B2	8.2(3.1–13.3)	6.0
		Outer	W1	8.1(2.9–3.3)	36.0
			B3	16.0(5.1–26.9)	–
			B4	–	28.0
			B5	19.7(12.2–27.2)	–
	MPB	Inner	B1	12.9(6.6–19.2)	–
			B2	7.7(3.0–12.4)	72.0
		Outer	W1	6.9(2.3–11.5)	37.0
			B3	12.2(3.4–21.0)	–
			B4	–	5.0
	Macroalgae	Inner	B1	76.3(70.1–82.5)	–
			B2	84.1(77.9–90.3)	22.0
		Outer	W1	85.1(78.3–91.9)	27.0
			B3	71.8(57.7–85.9)	–
			B4	–	67.0
			B5	52.1(47.7–56.5)	–
			B3	71.8(57.7–85.9)	–

*B, Barton peninsula; W, Weaver peninsula described in Fig. 5.1.

5.3.5. Influence of multi-decadal changes to sea ice extent on the spatial variation of stable isotopes for producers and consumers in Antarctica

Significantly negative and positive relationships between year and summer sea ice extent were obtained for West (Bellingshausen and Amundsen Sea: $r=-0.42$, $p<0.05$) and East (Western Pacific Ocean: $r=0.44$, $p<0.05$) Antarctica, respectively (Fig. 5.4.). Changes to sea ice extent in the Antarctica are driven by multiple atmospheric and oceanic influences (Parkinson, 2019; Stuecker et al., 2017; Wang et al., 2019). In Antarctic coastal ecosystems, the food web dynamics are inevitably linked to the sea ice conditions affecting the magnitude of primary food sources available to consumers (Norkko et al., 2007). Therefore, we hypothesised that the contrasting changes to sea ice extent between West and East in Antarctica might influence the food web dynamics in both regions via different processes.

In the 2010s, significant changes in $\delta^{13}\text{C}$ were estimated for marine organisms under rapid ice extent conversion in Antarctica (Fig. 5.10., Table 5.5.). In West Antarctica, marine organisms exhibited significant mean $\delta^{13}\text{C}$ enrichment, reaching 2.6‰ in the 2010s ($F=6.7$, $p<0.05$). In contrast, in East Antarctica, marine organisms exhibited a significant mean decrease in $\delta^{13}\text{C}$ signatures ca. 3.2‰ after conversion ($F=4.3$, $p<0.05$). These contrasting horizontal changes to $\delta^{13}\text{C}$ value indicated that distinctive dietary shifts occurred in consumers exposed to different multi-decadal changes to sea ice extent in West and East Antarctica. The change to the mean contribution of the three producers (pelagic phytoplankton, sympagic ice algae, benthic micro- and macroalgae) to West and East Antarctic organisms supported the contrasting changes of $\delta^{13}\text{C}$ in consumers (Fig. 5.11.). In West Antarctica with retreating sea ice, the mean contribution of benthic producer to marine consumers increased by >90% in the 2010s (Fig. 5.11.A.). However, the mean utilisation of pelagic sources by West Antarctic consumers decreased by 40%. In particular, all consumer groups used more benthic sources in the late 2010s.

The increased utilisation of benthic sources by consumers closely reflected the marked increase in benthic production driven by sufficient light availability and nutrient input from meltwater under the loss of sea ice extent in West Antarctica (Braeckman et al., 2019) (Table 5.2.). Although the phytoplankton biomass was also increased in regions where glaciers and sea ice are being lost (Table 5.2.), we found

decreased pelagic contribution to consumers along the West Antarctic coast (Fig. 5.11.). The lower phytoplankton contribution to consumers in the 2010s reflected the lower importance of pelagic diets than benthic diets for consumers mainly collected in the Belleingshaun-Amundsen Sea with low phytoplanktonic biomass (Lu et al., 2020). Benthic (micro- and macroalgae) production was particularly reported as the main support for a large fraction of the secondary production of Antarctic consumers in the habitat where other resources are scarce (Huovinen, 2020). Thus, the observed trend in carbon stable isotope changes back supported the important role of benthic production in the West Antarctic coastal food web with low pelagic production (Braeckman et al., 2019). In West Antarctica with retreating sea ice, the mean contribution of sympagic was increased by 50% (Fig. 5.11.A). The increased sympagic contribution reflected released ice algal transfer to the consumer in the food web under the glacier and sea ice melting conditions (Table 5.2.) (Wright et al., 2010). However, we expect that the trend will be changed from an increasing to decreasing pattern with future substantial glacier and sea ice loss in the Antarctic coastal habitats. Thus, we suggest that future studies perform long-term monitoring of stable isotope distribution in the West Antarctic food web for sustainable Antarctic coastal ecosystem management.

In the 2010s, East Antarctic organisms exhibited a highly increased dependence on pelagic phytoplankton, reflecting the increased importance of phytoplanktonic production in the food web under sea ice advance condition (Fig. 5.11.) (Hirawake et al., 2005; Michel et al., 2019). This result was related to the low abundance of micro- and macrophytes on the seafloor, which are limited by the low light levels beneath the sea ice for most of the year (Dayton and Oliver, 1977). Although the sympagic production is increased with sea ice advance in East Antarctica, sympagic contributions to consumers were generally decreased by increased relative importance of pelagic production (Fig. 5.11.B.). However, the increasing trends of sympagic contribution to Amphipoda, Copepoda, and Euphausiacea including grazers revealed the limited impact of changes in the sympagic production to only specific functional groups of consumers. Overall, it revealed the least importance of sympagic production in the East Antarctic coastal food web (Michel et al., 2019).

Long-term changes to $\delta^{13}\text{C}$ values in coastal organisms might also be related to the contrasting intrusion of atmospheric depleted $\delta^{13}\text{C}$ signatures on the West and East Antarctic coast, originating from fossil fuel combustion (Lorrain et al., 2020). A previous study reported that $\delta^{13}\text{C}$ had declined in globally distributed fish due to fossil fuel-derived and isotopic light carbon incorporation into the marine ecosystem (Lorrain et al., 2020). Therefore, we suggest that the $\delta^{13}\text{C}$ depletion of East Antarctic organisms would be influenced by atmospheric depleted $\delta^{13}\text{C}$ under reduced meltwater intrusion. However, this effect seemed negligible in West Antarctic marine organisms living in an environment with complex impacts by various factors including meltwater interference. Out of the 22 taxonomic and functional groups, multi-functional consumers exhibited the greatest total changes to $\Delta\delta^{13}\text{C}$ in the West and East Antarctic coast (Fig. 5.10.). The carnivorous gastropod exhibited the greatest total $\Delta\delta^{13}\text{C}$ variation in West and East, followed by the deposit-feeding ostracod exposed to various source input in benthic environment (Table 5.5.). The $\delta^{13}\text{C}$ range of consumers reflected their ability to adapt to changes in the availability of producers. Therefore, the large changes to $\delta^{13}\text{C}$ of multi-functional consumers indicated high trophic plasticity, which is an adaptive trait encountered in Antarctic environments that change significantly (Michel et al., 2019). However, the relatively small $\Delta\delta^{13}\text{C}$ of consumers with a single feeding strategy reflected specific dietary preferences, with their continued existence under the rapidly changing Antarctic environment being at risk. There was no noticeable change to $\delta^{15}\text{N}$ of marine organisms in both regions (Fig. 5.10.). This result indicates that the overall change to sea ice extent has significantly influenced the trophic niche rather than the trophic roles of Antarctic coastal organisms.

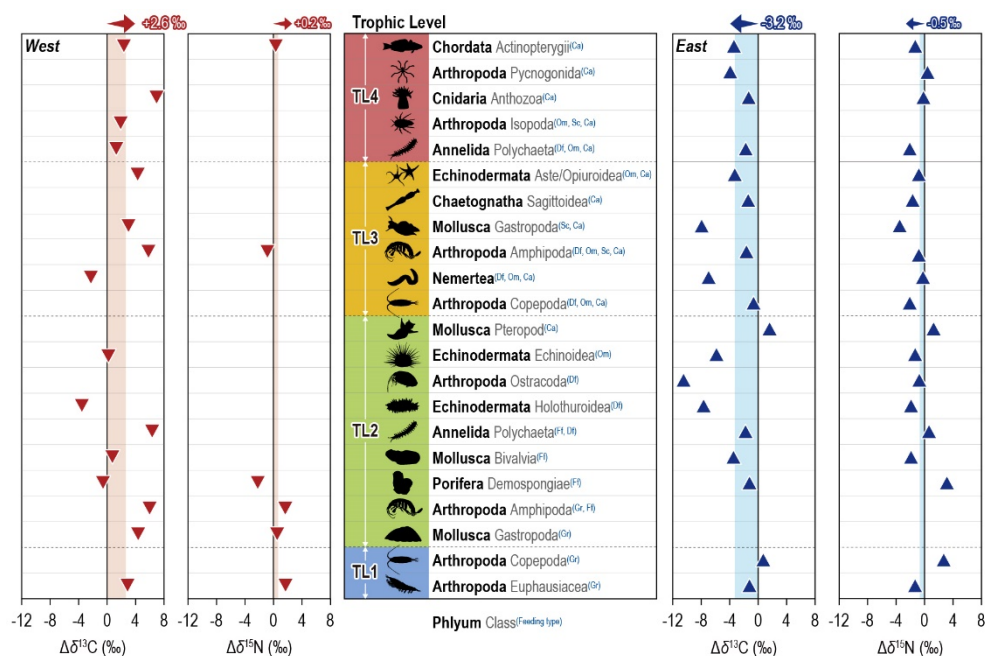


Figure 5.10.

Multi-decadal changes in carbon and nitrogen stable isotopes ($\Delta\delta^{13}\text{C}$, and $\Delta\delta^{15}\text{N}$) of classified taxonomic groups with five feeding strategies (grazers, Gr; filter feeders, Ff; deposit feeders, Df; omnivores, Om; scavengers, Sc; carnivores, Ca) between west (downward red triangle) and east (upward blue triangle) showing contrasting sea ice retreat and advance. Mean multi-decadal stable isotope changes of consumers are presented with red and blue backgrounds with arrows.

Table 5.5.

Stable carbon and nitrogen isotope ratios ($\delta^{13}\text{C}$ and $\delta^{15}\text{N}$) of the consumers with six feeding strategies (grazers, Gr; filter feeders, Ff; deposit feeders, Df; omnivores, Om; scavengers, Sc; carnivores, Ca) in the ice extent decreased in western Antarctica and increased in eastern Antarctica during summer as reported in previous studies. Species isotopic values are reported as means with standard deviations (s.d.).

Region	Samples	$\delta^{13}\text{C}$ (‰)		$\delta^{15}\text{N}$ (‰)		References*
		2000s	2010s	2000s	2010s	
Ice extent decreased	Diet					
	SOM	-16.7	-21.1±1.8	–	4.5±1.1	3, 9, 16, 22, 27, 30, 31
	POM	-27.1±4.0	-23.6±3.2	1.6±0.4	3.8±2.9	1, 3, 6, 21, 23, 25, 26, 29, 31
	Ice algae	–	-14.1±6.1	–	1.8±2.1	26
	Microalgae	-18.9±1.4	-21.0±3.7	4.3±0.8	6.2±1.5	3, 6, 9, 10, 15, 21, 31
	Macroalgae					
	Red algae	-15.4±3.5	-18.9±3.4	4.5±1.2	3.1±1.6	6, 10, 23, 26, 29, 31
	Brown algae	-13.6±1.9	-12.1±1.1	4.1±0.6	3.2±0.5	6, 10, 31
	Green algae	-23.3	-18.5	9.4	3.9	9, 10, 19, 29
	Consumer					
	Porifera					
	(Ff) Demospongiae	-23.0±0.5	-23.5±1.7	7.5±2.3	5.3±1.6	15, 26, 27
	Cnidaria					
	(Ca) Anthozoa	-26.5	-19.4±4.6	–	7.8±0.9	8, 15, 21
	Nemertea					
	(Df, Om, Ca)	-16.7±1.6	-18.8±1.8	–	8.4±1.3	8, 15, 21, 29
	Mollusca					
	(Ff) Bivalvia	-20.9±5.0	-20.0±4.8	–	5.3±2.0	3, 8, 15, 21, 26, 29
	(Gr) Gastropoda	-19.2±3.8	-14.7±1.3	5.2±1.4	5.7±0.8	6, 7, 8, 29, 31
	(Sc, Ca) Gastropoda	-20.7	-17.6±2.7	–	7.7±1.8	8, 15, 29
	(Ca) Ptropods	–	-21.2±1.9	–	6.0±0.5	26
	Annelida					
	(Ff, Df) Polychaeta	-26.6±2.9	-20.3±2.4	–	5.6±0.8	8, 15, 26
	(Df, Om, Ca) Polychaeta	-19.3±0.5	-17.7±2.0	–	10.1±1.9	8, 15, 21, 26
	Arthropoda					
	(Gr) Euphausiacea	-25.9±1.1	-23.0±1.4	4.8±2.0	6.4±1.6	7, 8, 9, 21, 22, 25, 26, 31
	(Gr) Copepoda	–	-23.8±0.6	–	6.7±0.1	21, 26

Table 5.5. (continued).

Region	Samples	$\delta^{13}\text{C}$ (‰)		$\delta^{15}\text{N}$ (‰)		References*
		2000s	2010s	2000s	2010s	
Ice extent decreased	Arthropoda					
	(Df, Om, Ca) Copepoda	–	–16.6±1.9	–	9.2±0.9	21, 31
	(Gr, Ff) Amphipoda	–25.3±5.7	–19.3±2.5	4.5±0.6	8.0±2.9	8, 19, 29, 31
	(Df, Om, Sc, Ca) Amphipoda	–23.3±1.0	–17.4±2.8	8.9±1.7	6.2±0.9	8, 19, 21, 29
	(Om, Sc, Ca) Isopoda	–19.1±1.4	–17.0±0.5	–	11.4±1.0	8, 15, 21
	(Gr) Copepoda	–	–23.8±0.6	–	6.7±0.1	21, 26
	Echinodermata					
	(Om, Ca) Aste/Opiuroidea	–21.7	–17.1±4.3	–	8.2±1.1	8, 15, 26, 29, 31
	(Df) Holothuroidea	–20.3	–23.8±1.9	–	5.7±1.3	8, 26
	(Om) Echinoidea	–19.1	–19.0±3.8	–	5.2±1.3	3, 8, 15, 23, 26
	Chordata					
	(Ca) Actinopterygii	–24.3±2.5	–21.8±2.2	11.2±1.6	11.5±2.1	2, 7, 8, 9, 24, 26, 29, 31
Ice extent increased	Food sources					
	SOM	–18.3±0.2	–	4.1±0.6	–	9, 11, 13
	POM	–25.4±5.0	–28.0±2.7	1.3±4.9	3.7±2.4	9, 11, 13, 14, 17, 18, 19, 28, 30
	Ice algae	–10.2±1.5	–12.5	2.9±0.1	5.3	9, 11, 13, 17, 18
	Microalgae	–11.2	–	5.3	–	11
	Macroalgae					
	Red algae	–17.2±0.8	–	3.7±1.0	–	9, 11, 13
	Brown algae	–21.2±2.5	–22.3±1.1	3.7±0.5	5.5±3.6	9, 11, 13, 18
	Green algae	–17.7±1.6	–	6.1±0.3	–	11, 13
	Consumer					
	Porifera					
	(Ff) Demospongiae	–18.7±0.3	–19.9±0.7	6.2±0.3	9.4±1.3	11, 13, 18
	Cnidaria					
	(Ca) Anthozoa	–14.9±0.2	–16.2	10.8±0.3	10.7	11, 13, 18
	Nemertea (Df, Om, Ca)	–14.8±0.2	–21.8±3.5	9.9±0.6	9.7±0.6	11, 13, 18
	Mollusca					
	(Ff) Bivalvia	–17.4±0.7	–21.0±2.1	6.2±0.3	4.5±0.1	9, 11, 13, 18
	(Sc, Ca) Gastropoda	–13.1±0.3	–21.0±2.0	11.4±0.2	8.0±0.1	11, 13, 18
	(Ca) Ptropods	–25.1±0.5	–23.5±0.6	4.7±1.3	6.0±1.2	14, 17

Table 5.5. (continued).

Region	Samples	$\delta^{13}\text{C}$ (‰)		$\delta^{15}\text{N}$ (‰)		References*
		2000s	2010s	2000s	2010s	
Ice extent increased	Annelida					
	(Ff, Df) Polychaeta	-15.2±2.8	-17.0±1.3	6.7±0.9	7.4±0.3	9, 11, 13, 18
	(Df, Om, Ca) Polychaeta	-15.0±3.5	-16.7	10.9±1.3	8.7	11, 13, 18
	Arthropoda					
	(Df) Ostracoda	-14.8±0.6	-25.2	7.1±0.7	6.5	11, 17
	(Gr) Euphausiacea	-25.6±0.7	-26.8±1.7	—	—	5, 6, 14, 16, 17, 30
	(Gr) Copepoda	-27.6±0.8	-26.9±3.3	—	—	17, 28
	(Df, Om, Ca) Copepoda	-26.3±1.0	-26.9±4.3	7.6±5.8	5.7±1.7	14, 17, 28
	(Gr, Ff) Amphipoda	-13.3±0.2	—	6.9±2.1	—	9, 11, 13
	(Df, Om, Sc, Ca) Amphipoda	-20.5±4.6	-22.2±2.2	9.3±2.3	8.5±0.9	11, 13, 14, 17, 19
	(Ca) Pycnogonida	-16.4±0.2	-20.4±0.6	9.9±0.2	10.4±0.8	11, 13, 18
	Chaetognatha	-25.9±2.1	-27.3	9.9±2.2	8.4	14, 17
	(Ca) Sagittoidea					
	Echinodermata					
	(Om, Ca) Aste/Opiuroidea	-13.2±1.5	-16.5±1.8	9.7±1.2	9.0±1.3	9, 11, 13, 18
	(Df) Holothuroidea	-17.3±3.6	-24.9±0.8	8.1±0.1	6.4±0.1	9, 11, 18
	(Om) Echinoidea	-8.6±1.5	-14.5	8.4±1.2	7.2	9, 11, 13, 18
	Chordata					
	(Ca) Actinopterygii	-21.5±4.1	-24.9	11.6±2.0	10.3	9, 11, 13, 14, 16, 20

*1, Brault et al., 2019; 2, Burns et al., 1998; 3, Calizza et al., 2018; 4, Cherel, 2008; 5, Cherel et al., 2011; 6, Choy et al., 2011; 7, Cipro et al., 2017; 8, Corbisier et al., 2004; 9, Corsolini and Sara, 2017; 10, Dunton et al., 2001; 11, Gillies et al., 2012a; 12, Gillies et al., 2012b; 13, Gillies et al., 2013; 14, Giraldo et al., 2011; 15, Ha et al., 2019; 16, Hodum and Hobson, 2000; 17, Jia et al., 2016; 18, Michel et al., 2019; 19, Nyssen et al., 2000; 20, Park et al., 2015; 21, Pasotti et al., 2015; 22, Polito et al., 2013; 23, Rossi et al., 2019; 24, Rumolo et al., 2020; 25, Seyboth et al., 2018; 26, Signa et al., 2019; 27, Thurber, 2007; 28, Yang et al., 2016; 29, Zenteno et al., 2019; 30, Zhang et al., 2017; 31, This study

A. Sea ice retreat region (West)

B. Sea ice advance region (East)

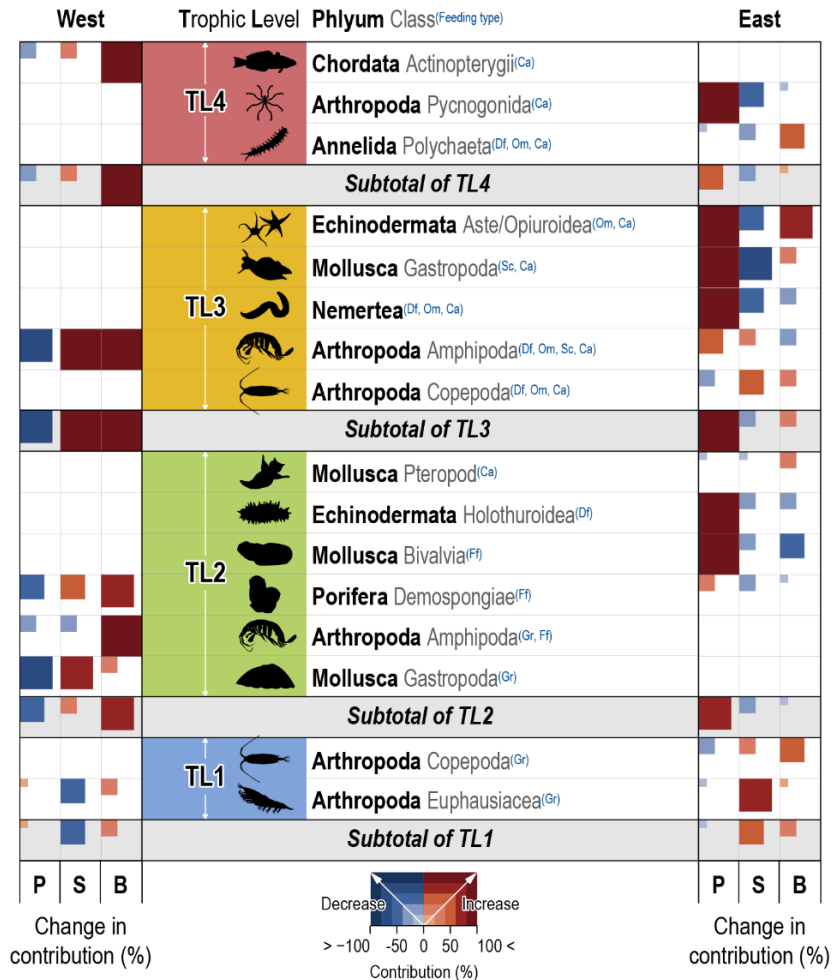
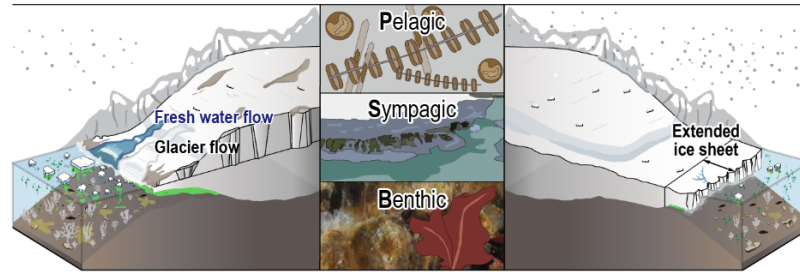


Figure 5.11.

Multi-decadal changes in the contribution (%) of three diet types (P, pelagic; S, sympagic; B, benthic) to the consumers in **(A)** West Antarctica with substantial sea ice retreat and in **(B)** East Antarctica with substantial sea ice advance. The feeding strategies of the consumers are described by abbreviation in blue letters (grazer, Gr; filter feeder, Ff; deposit feeder, Df; omnivore, Om; scavenger, Sc; carnivore, Ca). Squares with red and blue gradients indicate an increase or decrease in the dietary contribution (%) of three producers to consumers, from 0 to 100%, respectively.

CHAPTER 6.

CONCLUSIONS

6.1. Summary

The present study investigated the spatiotemporal structure and function of food webs in four ecologically important coastal habitats experiencing severe habitat degradation in three climate zones (temperate, torrid, and frigid): Korean salt marsh and mudflat, Chinese mangrove forest and Antarctic coasts. This section presents a summary of the main findings of this study (Fig. 6.1.).

Chapter 2 investigated the benthic food web structure of the Korean Ganghwa tidal flat. The key factors influencing the spatial stable isotope dynamics in macrofauna were identified by investigating multiple habitats. The present work successfully demonstrated that benthic macrofauna had an important role as intermediary forms of energy transfer in the salt marsh ecosystem. The results confirmed that the mud content of the sediment and the distribution of halophytes had an important role in the food supply and the $\delta^{13}\text{C}$ dynamics of the deposit feeders in mesoscale spatial differences. The contribution of organic matter of different origins to deposit feeders indicated site-specific dietary shifts of benthic organisms. MPB was an important diet for primary consumers in Ganghwa tidal flat, accounting for a maximum of ~90%, indicating an important role of MPB in Korean salt marsh habitats. Overall, stable isotope analysis served as a powerful tool to investigate how different habitat conditions naturally influence food web structure and pathways.

Chapter 3 demonstrated the influence of dike water discharge on the spatial and temporal dynamics of benthic food web in a Korean tidal flat. Eutrophic water discharge increased TN concentration and MPB biomass at sites near the water gates of the Saemangeum dike. The distinct carbon stable isotope signature of FPOM for the consumers revealed its minor role as a base of the food web. However, it was used by benthos consuming SPOM. The depleted $\delta^{13}\text{C}$ for filter feeders implied the assimilation of FPOM in their tissues and their susceptibility to anthropogenic impacts. Deposit feeders had feeding flexibility and consumed relatively similar amounts of each diet compared to filter feeders. SPOM was the primary diet of consumers in the Saemangeum tidal flat, accounting for a maximum of ~90%. In conclusion, this study provided background information explaining the complexity of the tidal flat food web affected by the discharge of water from the dike and provided implications and guidance for sustainable management of the tidal flats.

Chapter 4 characterised the seasonal trophic dynamics of the benthic and pelagic food web in a mangrove nature reserve, the PRE, surrounded by megacities. The results confirmed that the seasonal variation in River discharge had an essential role in the food distribution and trophic interactions between benthic and pelagic organisms between the dry and wet seasons. During the dry season, plant-derived organic matter was a primary diet for both benthic and pelagic consumers. In contrast, high River discharge during the monsoon summer increased the contribution of particulate organic matter to two consumers and promoted their interactions. Based on the literature review, the trophic function of the PRE mangrove ecosystem was additionally characterised, with significant amounts of both natural mangrove and anthropogenic organic matter in the food web. In conclusion, this study provided background information explaining the seasonal food web complexity of the PRE food web for future sustainable mangrove ecosystem management.

Chapter 5 identified multi-decadal food web dynamics in the Antarctic coast, which experiences complex regional glacier and sea ice dynamics. This study highlighted that the altered baseline production and potential effects of nutrient inputs under long-term changes in sea ice extent, which induced $\delta^{13}\text{C}$ dynamics of producers and consumers along the coast. The enriched $\delta^{13}\text{C}$ values of producers and consumers reflected the influence of meltwater intrusion in response to glacier retreat in the MC. Decadal changes in the spatial distribution of the Antarctic limpet reflected changes in its habitat extent, while its substantial decadal increase in macroalgal consumption reflected large baseline changes in WAP under glacial retreat. The contrasting multi-decadal changes in $\delta^{13}\text{C}$ and the relative contributions of benthic, pelagic, and sympagic diets to consumers between West and East Antarctica, followed regionally contrasting changes in sea ice extent. Overall, these long-term changes to the food web, encompassing structural- and functional components, demonstrate that the trophic baseline in Antarctica has significantly altered under the global climate crisis. Ultimately, these changes are expected to cause ecosystem stability to decline through the propagation of the (in)direct effect of trophic cascades in the Antarctic ecosystem.

Overall, the present study demonstrated the spatiotemporal structure and function of the food web in the severely degraded coastal habitats in three climate

zones (Fig. 6.1.). The set of results on coastal food web structure revealed the spatial and temporal distribution of organic matter in coastal ecosystems. The spatial distribution of organic matter (i.e., baseline) in the coastal food web was related to variables such as habitat conditions (sediment characteristics; presence of vegetation; vegetation species) and distance from eutrophic lakes and glaciers. Among these, glacier retreat had the strongest effect on the spatial $\delta^{13}\text{C}$ distribution and their transfer to consumers. In contrast, habitat conditions and eutrophication had less influence on the spatial variation of the food web structure. These variables only altered the degree of contribution of diet, but not the priority of diet in the coastal food web. The seasonal distribution of organic matter in the coastal food web was related to flood and ice (i.e., glacier and sea ice) dynamics. Both caused changes in the priority of diets in the coastal food web. The impact of the flood dynamics was particularly strong in the mangrove forest. This is due to the strong seasonality in the torrid zone. In conclusion, the degree of spatiotemporal food web dynamics in each coastal habitat varied across three climate zones. In particular, the spatiotemporal change in the food web as a result of climate change was enormous in comparison to those under other variables. Future management of coastal ecosystems therefore needs to be climate change focused. The data provided in this study will serve as baseline information and will contribute to the conservation and management of coastal ecosystems.

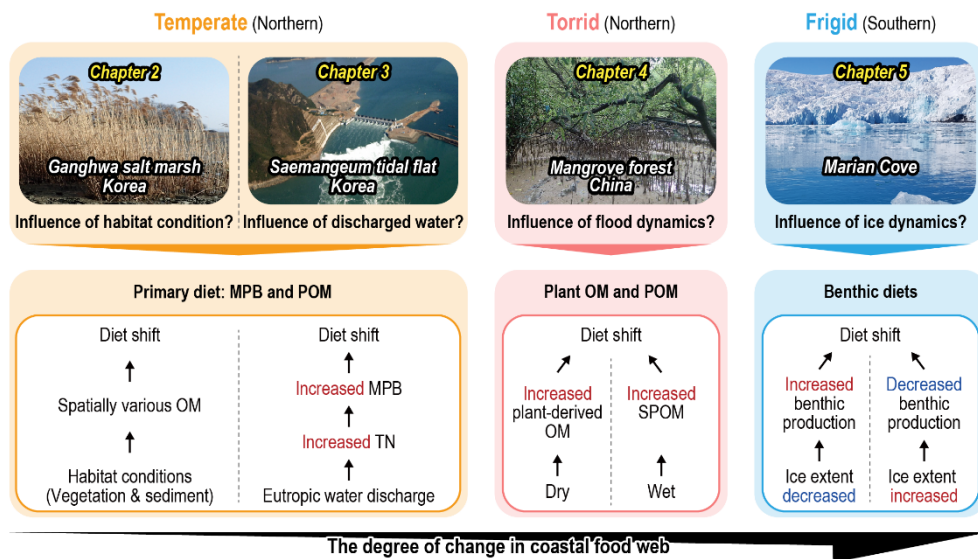


Figure 6.1.

A comprehensive summary of the key findings in the present food web study in Korean salt marsh and tidal flat (temperate zone), Chinese mangrove forest (torrid zone) and Antarctic coast (frigid zone).

6.2. Ecological implications

The present series of studies using carbon and nitrogen stable isotope analysis provides a comprehensive understanding of 1) the characteristics of food web structure in four coastal habitats (salt marsh; tidal flat; mangrove forest; Antarctic coast) undergoing severe degradation; 2) the degree of the changes in coastal food web structure and function under natural, anthropogenic, and climate change-driven impacts.

The general description of the coastal food web using a biplot of the $\delta^{13}\text{C}$ and $\delta^{15}\text{N}$ from potential diets to benthos was different among four coastal habitats (Fig. 6.2.). The narrow range of $\delta^{13}\text{C}$ of potential diets and benthic consumers in the Korean salt marsh and tidal flat in the temperate zone was different from other coastal habitats in two extreme climatic zones (i.e., torrid, and frigid) (Fig. 6.2.A.). It indicated that the salt marsh and tidal flat food webs in temperate regions have less $\delta^{13}\text{C}$ diversity of the baseline (from C_3 halophyte to MPB) than other food webs (Fig. 6.2.D.). In general, the enriched $\delta^{13}\text{C}$ of benthos described the import ecological role of the ^{13}C -enriched diet, MPB, in the food web.

In contrast, the large $\delta^{13}\text{C}$ range of the food web in the mangrove forest reflected the diverse distribution of baseline $\delta^{13}\text{C}$ following the high biodiversity of autotrophs in the tropical coast (Fig. 6.2.B.). The unusual ^{13}C -enriched value of the baseline in the Chinese mangrove forest indicated the significant influence of the *Spartina* invasion in the Chinese coastal mangrove ecosystem (Fig. 6.2.D.). Furthermore, the $\delta^{13}\text{C}$ signatures of the benthos between mangrove and *spartina* indicated that they consumed various diets in the mangrove forest, providing additional implications of *Spartina* utilisation in this coastal ecosystem.

In the Antarctic coast, both diets and benthic consumers showed the widest $\delta^{13}\text{C}$ distribution among coastal habitats in three climate zones (Fig. 6.2.C.). Baseline C stable isotope values were distributed from ^{13}C -depleted phytoplankton to ^{13}C -enriched coastal sea ice POM. The result showed that the primary producers on the Antarctic coast used very diverse $\delta^{13}\text{C}$ of dissolved inorganic carbon under different environmental conditions and significant environmental changes.

The highly depleted $\delta^{13}\text{C}$ signature of phytoplankton reflected their high use of ^{13}C -depleted inorganic carbon in the Antarctic coast. The largest $\delta^{13}\text{C}$ range of

benthos reflected their utilisation of a diverse diet with the substantial environmental changes under glacier and sea ice extent variations (Fig. 6.2.D.). The degree of food web dynamics in the Antarctic coastal ecosystem was more extensive than other coasts in different climatic zones, suggesting urgent management action.

In contrast, the opposite $\delta^{15}\text{N}$ distribution was observed in the coastal food web across the climatic zones (Fig. 6.2.). A wide range of $\delta^{15}\text{N}$ with enriched values ($>10\text{‰}$) was observed in the baseline in the Korean and Chinese coastal food webs (Fig. 6.2.A. and 6.2.B.). The result indicated the substantial anthropogenic sewage input to the coastal salt marsh, tidal flat, and mangrove forest surrounded by highly urbanised- and/or agricultural areas (Fig. 6.2.D.). Although human activities have increased, the low $\delta^{15}\text{N}$ value in the Antarctic coastal food web showed that there is still less anthropogenic disturbance (Fig. 6.2.C.).

The $\delta^{13}\text{C}$ distribution of five functional groups of benthos provides additional information on the coastal food web structure in three climate zones (Fig. 6.3.). In the temperate zone, the Korean salt marshes and tidal flats showed the least overlapping $\delta^{13}\text{C}$ range among functional groups (Fig. 6.3.A.). This result suggested less competition for diets among consumers, allowing sustainable coexistence of species in the Korean coastal habitats. In contrast, in the Chinese mangrove forest and the Antarctic coast, five consumer groups showed larger $\delta^{13}\text{C}$ overlap areas than in the Korean habitats. This indicated the existence of a common important baseline for all types of consumers in the Chinese mangrove forest and Antarctic coastal food webs (Figs. 6.3.B. and 6.3.C.). The high dietary diversity in the mangrove forest in the torrid zone seems to reduce the competition among consumers. However, the relatively large $\delta^{13}\text{C}$ overlap of consumers may induce substantial structural changes in the Antarctic coastal food webs, which are subject to strong baseline simplification.

Overall, the present study has ecological implications by providing quantitative data on the degree of food web dynamics in the ecologically important coastal habitats along the climatic zones. It provides comprehensive insights for predicting food web dynamics under various impacts for future efficient management and conservation actions for the coastal ecosystems under increasing human impacts and climate change.

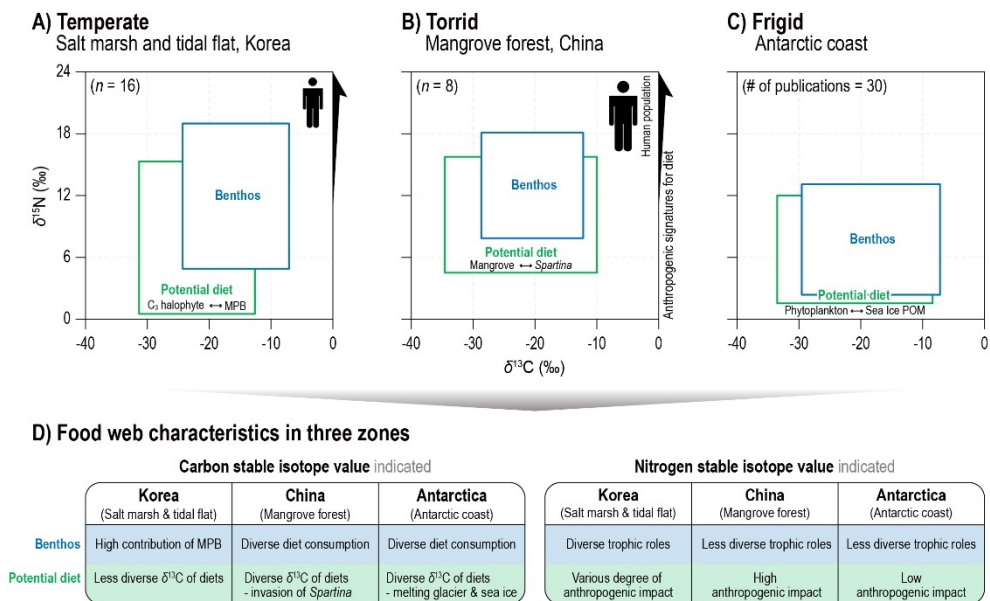


Figure 6.2.

The carbon and nitrogen stable isotope signatures of diets and benthic consumers from **(A)** temperate (Korean salt marsh and tidal flat), **(B)** torrid (Chinese mangrove forest), and **(C)** frigid (Antarctic) coastal ecosystems. A comprehensive comparison of food web structure, providing specific information on food web characteristics in coastal regions: the degree of strength and diversity of the diet and anthropogenic impact **(D)**. Green and blue colours indicate potential diets and benthos, respectively.

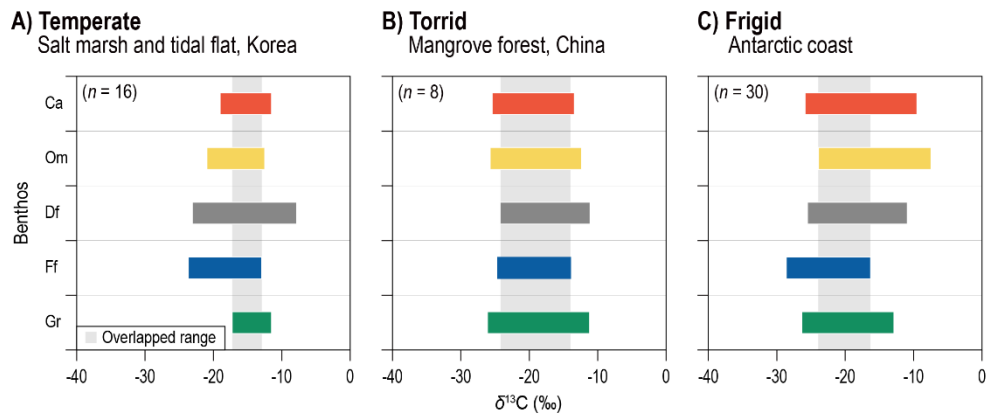


Figure 6.3.

The carbon and nitrogen stable isotope signatures of five functional groups (grazers, Gr; filter feeders, Ff; deposit feeders, Df; omnivores, Om; carnivores, Ca) of benthic consumers collected in **(A)** temperate (Korean salt marsh and tidal flat), **(B)** torrid (Chinese mangrove forest), and **(C)** frigid (Antarctica) coastal ecosystems. Colours indicate each functional group of consumers (red, Ca; yellow, Om; grey, Df; blue, Ff; green, Gr). The grey background indicates the overlapping carbon stable isotope range of benthic consumers.

6.3. Limitations and future research directions

The present study confirmed that the carbon and nitrogen stable isotope signatures of benthic organisms are well suited to describe the trophic structural and functional changes in four coastal ecosystems (salt marsh, tidal flat, mangrove forest, and Antarctic coast) due to their sedentary characteristics with relatively long-life spans. It can be used as an efficient indicator to track the spatial and temporal variations in organic matter distributions in response to altered coastal ecosystems under environmental changes due to various causes (e.g., habitat diversity, human activities, climate change, etc.). However, the use of stable isotope signatures of benthos as an ecological monitoring tool is not sufficiently developed, due to the lack of data on various benthic organisms. Thus, it is therefore necessary to develop an ecological database of different species to find an efficient indicator of food web dynamics that can be applied to different coastal regions.

Understanding coastal food web dynamics in complex coastal ecosystems with varying spatial and temporal inputs of organic matter from Rivers and oceans is challenging. In particular, complex combined natural, anthropogenic and climatic influences on the coastal ecosystem make it difficult for researchers to understand food web structure and function in ecologically important coastal ecosystems in temperate and torrid zones. Therefore, a future study should be carried out together with a mesocosm experiment in a controlled environment to assess the exact impact of each influence on coastal food web dynamics. The mesocosm study will provide specific information on the influence of each variable (e.g., nutrient concentrations, sediment types, vegetation, tides, etc.) on coastal food web dynamics to support conservation and management plans for each environmental variable.

In particular, in terms of food web function, studies are needed to understand in depth the overall direction of energy pathways and storage amount in each trophic level from primary producers to top predators in the coastal food web. Therefore, future study is essentially to investigate the changes in biomass of different organisms in the food web using an additional modeling program (e.g., ecopath). Through this process, we can elucidate the vulnerability of the coastal organisms at each trophic level and prioritise management and conservation actions for them in coastal habitats experiencing different environmental changes (Fig.6.4.).

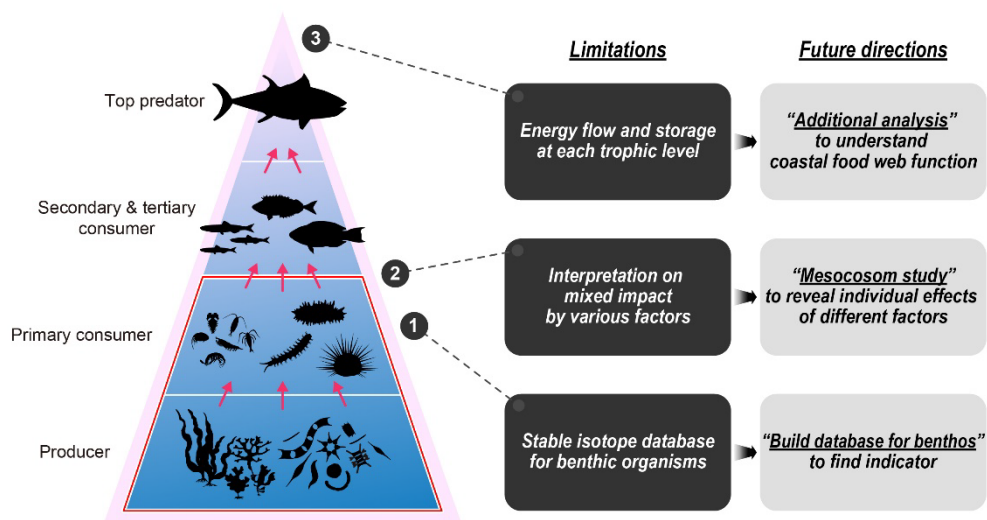


Figure 6.4.

Limitations of the present study and directions for future food web research. Three limitations and corresponding research directions are described in the dark grey and light grey boxes, respectively.

BIBLIOGRAPHY

Abele, D., 2015. Climate change and glacier retreat drive shifts in an Antarctic benthic ecosystem. *Sci. Adv.*, 1(10), e1500050.

Abrantes, K.G., Barnett, A., Bouillon, S., 2014. Stable isotope-based community metrics as a tool to identify patterns in food web structure in east African estuaries. *Funct. Ecol.*, 28(1), 270–282.

Ahn, I.-Y., 1994. Ecology of the Antarctic bivalve *Laternula elliptica* (king and broderip) in collins harbor, King George Island: benthic environment and an adaptive strategy. *Mem. Natl. Inst. Polar Res.*, 50, 1–10.

Alderkamp, A.C., Mills, M.M., van Dijken, G.L., Laan, P., Thuroczy, C.E., Gerringa, L.J., Barr, H.J., Payne, C.D., Visser, R.J., Buma, A.G., Arrigo, K.R., 2012. Iron from melting glaciers fuels phytoplankton blooms in the Amundsen Sea (Southern Ocean): Phytoplankton characteristics and productivity. *Deep Sea Res. Pt. II Top. Stud. Oceanogr.*, 71, 32–48.

Alongi, D.M., 2009. Introduction in the Energetics of Mangrove Forests. Springer Science and Business Media BV, New York.

Altabet, M.A., 1988. Variations in nitrogen isotopic composition between sinking and suspended particles: Implications for nitrogen cycling and particle transformation in the open ocean. *Deep Sea Res. Pt. I Oceanogr. Res. Pap.*, 35(4), 535–554.

Alurralde, G., Fuentes, V.L., Troch, M.D., Tatian, M., 2020. Suspension feeders as natural sentinels of the spatial variability in food sources in an Antarctic fjord: a stable isotope approach. *Ecol. Indic.*, 115, 106378.

An, S.Q., Gu, B.H., Zhou, C.F., Wang, Z.S., Deng, Z.F., Zhi, Y.B., Li, H.L., Chen, L., Yu, D.H., Liu, Y.H., 2007. *Spartina* invasion in China: implications for invasive species management and future research. *Weed Res.*, 47(3), 183–191.

An, S.M., Lee, J.H., Woo, H.J., Koo, B.J., Lee, H.G., Yoo, J.W., Je, J.G., 2006. Benthic environment and macrofaunal community changes during the dike construction in Saemangeum subtidal area, Korea. *Ocean Polar Res.*, 28(4), 369–383.

Aneykutty, J., Deepthi, G.N., Lakshmi Devi, P., 2013. Habitat ecology and food and feeding of the herring bow crab *Varuna litterata* (Fabricius, 1798) of Cochin backwaters, Kerala, India. *Arthropods*, 2(4), 172–188.

Antonio, E.S., Kasai, A., Ueno, M., Won, N.I., Ishihi, Y., Yokoyama, H., Yamashita, Y., 2010. Spatial variation in organic matter utilization by benthic communities from Yura River–Estuary to offshore of Tango Sea, Japan. *Estuar. Coast. Shelf S.*, 86(1), 107–117.

Arbi, I., Liu, S., Zhang, J., Wu, Y., Huang, X., 2018. Detection of terrigenous and marine organic matters flow into a eutrophic semi-enclosed bay by $\delta^{13}\text{C}$ and $\delta^{15}\text{N}$ of intertidal macrobenthos and basal food sources. *Sci. Total Environ.*, 613, 847–860.

Armonies, W., 1986. Plathelminth abundance in North Sea salt marshes: environmental instability causes high diversity. *Helgoländer Meeresuntersuchungen*, 40, 229–240.

Ashton, E.C., Macintosh, D.J., 2002. Preliminary assessment of the plant diversity and community ecology of the Sematan mangrove forest, Sarawak, Malaysia. *Forest. Ecol. Manag.*, 166, 111–129.

Atkinson, A., 1995. Omnivory and feeding selectivity in five copepod species during spring in the Bellingshausen Sea, Antarctica. *ICES J. Mar. Sci.*, 52(3–4), 385–396.

Axelsson, L., Mercado, J., Figueroa, F., 2000. Utilization of HCO_3^{3-} at high pH by the brown macroalga *Laminaria saccharina*. *Eur. J. Phycol.*, 35(1), 53–59.

Bae, H., Lee, J.-H., Song, S.J., Ryu, J., Noh, J., Kwon, B.-O., Choi, K., Khim, J.S., 2018. Spatiotemporal variations in macrofaunal assemblages linked to site-specific environmental factors in two contrasting nearshore habitats. *Environ. Pollut.*, 241, 596–606.

Bae, H., Ahn, I.Y., Park, J., Song, S.J., Noh, J., Kim, H., Khim, J.S., 2021. Shift in polar benthic community structure in a fast-retreating glacial area of Marian Cove, West Antarctica. *Sci. Rep.*, 11(1), 1–10.

Baeck, G.W., Yoon, Y.H., Park, J.M., 2013. Ontogenetic and diel changes in diets of two sympatric mudskippers *Periophthalmus modestus* and *Periophthalmus magnuspinnatus* on the tidal flats of Suncheon Bay, Korea. *Fisheries Sci.*, 79, 629–637.

Bai, J., Xiao, R., Zhang, K., Gao, H., 2012. Arsenic and heavy metal pollution in wetland soils from tidal freshwater and salt marshes before and after the flow–sediment regulation regime in the Yellow River Delta, China. *J. Hydrol.*, 450, 244–253.

Bang, J.H., Joo, S., Lee, E.J., Kim, M.-S., Jeong, S., Park, S., 2019. Diet of the mud-flat crab *Helice tientsinensis* in a Korean salt marsh. *Wetlands*, 40, 311–319.

Barbier, E.B., Hacker, S.D., Kennedy, C., Koch, E.W., Stier, A.C., Silliman, B.R., 2011. The value of estuarine and coastal ecosystem services. *Ecol. Monogr.*, 81(2), 169–193.

Barnes, D.K., Souster, T., 2011. Reduced survival of Antarctic benthos linked to climate-induced iceberg scouring. *Nat. Clim. Change*, 1(7), 365–368.

Barnes, D.K., Fenton, M., Cordingley, A., 2014. Climate-linked iceberg activity massively reduces spatial competition in Antarctic shallow waters. *Curr. Biol.*, 24(12), R553–R554.

Barranguet, C., Kromkamp, J., 2000. Estimating primary production rates from photosynthetic electron transport in estuarine microphytobenthos. *Mar. Ecol. Prog. Series*, 204, 39–52.

Behera, N., Swain, D., Sil, S., 2020. Effect of Antarctic sea ice on chlorophyll concentration in the Southern Ocean. *Deep Sea Res. Part II: Top. Stud. Oceanogr.*, 178, 104853.

Bianchi, T.S., Johansson, B., Elmgren, R., 2000. Breakdown of phytoplankton pigments in Baltic sediments: effects of anoxia and loss of deposit-feeding macrofauna. *J. Exp. Mar. Biol. Ecol.*, 251, 161–183.

Blaber, S.J.M., Staunton-Smith, J., Milton, D.A., Fry, G., Van der Velde, T., Pang, J., Wong, P., Boon-Teck, O., 1998. The Biology and Life-history Strategies of Illisha (Teleostei: Pristigasteridae) in the coastal waters and estuaries of Sarawak. *Estuar. Coast. Shelf S.*, 47(4), 499–511.

- Blanchard, G.F., Paterson, D.M., Stal, L.J., Richard, P., Galois, R., Huet, V., Kelly, J., Honeywill, C., Brouwer, J. de., Dyer, K., Christie, M., Seguignes, M., 2000. The effect of geomorphological structures on potential biostabilisation by microphytobenthos on intertidal mudflats. *Cont. Shelf Res.*, 20(10–11), 1243–1256.
- Boaventura, D., Da Fonseca, L.C., Hawkins, S.J., 2003. Size matters: competition within populations of the limpet *Patella depressa*. *J. Anim. Ecol.*, 72(3), 435–446.
- Boesch, D.F., Wass, M.L., Virnstein, R.W., 1976. The dynamics of estuarine benthic communities. In *Estuarine processes*, 177–196. Academic Press.
- Bouillon, S., Borges, A.V., Castañeda-Moya, E., Diele, K., Dittmar, T., Duke, N.C., Kristensen, E., Lee, S.Y., Marchand, C., Middelburg, J.J., Rivera-Monroy, V.H., Smith, T.J., Twilley, R.R., 2008a. Mangrove production and carbon sinks: a revision of global budget estimates. *Global Biogeochem. Cy.*, 22(2).
- Bouillon, S., Connolly, R.M., Lee, S.Y., 2008b. Organic matter exchange and cycling in mangrove ecosystems: recent insights from stable isotope studies. *J. Sea Res.*, 59(1–2), 44–58.
- Braeckman, U., Pasotti, F., Vázquez, S., Zacher, K., Hoffmann, R., Elvert, M., Marchant, H., Buckner, C., Quartino, M.L., Cormack, W.M., Soetaert, K., Wenzhöfer, F., Vanreusel, A., 2019. Degradation of macroalgal detritus in shallow coastal Antarctic sediments. *Limnol. Oceanogr.*, 64(4), 1423–1441.
- Brault, E.K., Koch, P.L., Costa, D.P., McCarthy, M.D., Hückstädt, L.A., Goetz, K.T., McMahon, K.W., Goebel, M.E., Karlsson, O., Teilmann, J., Harkonen, T., Harding, K.C., 2019. Trophic position and foraging ecology of Ross, Weddell, and crabeater seals revealed by compound-specific isotope analysis. *Mar. Ecol. Prog. Ser.*, 611, 1–18.
- Brierley, A.S., Kingsford, M.J., 2009. Impacts of climate change on marine organisms and ecosystems. *Curr. Biol.*, 19(14), R602–R614.
- Buchanan, J.B., 1984. Sediment analysis. In: Holme, N.A., McIntyre, A.D. (Eds.), *Methods for the study of marine benthos*. Blackwell, Oxford, 41–65.
- Bui, T.H.H., Lee, S.Y., 2014. Does ‘you are what you eat’ apply to mangrove grapsid crabs?. *PloS One*, 9(2), e89074.
- Burdige, D.J., 2007. Preservation of organic matter in marine sediments: controls, mechanisms, and an imbalance in sediment organic carbon budgets? *Chem. Rev.*, 107, 467–485.
- Burns, J.M., Trumble, S.J., Castellini, M.A., Testa, J.W., 1998. The diet of Weddell seals in McMurdo Sound, Antarctica as determined from scat collections and stable isotope analysis. *Polar Biol.*, 19, 272–282.
- Burrows, M.T., Hawkins, S.J., Moore, J.J., Adams, L., Sugden, H., Firth, L., Mieszkowska, N., 2020. Global-scale species distributions predict temperature-related changes in species composition of rocky shore communities in Britain. *Glob. Change Biol.*, 26(4), 2093–2105.

- Cahoon, L.B., Nearhoof, J.E., Tilton, C.L., 1999. Sediment grain size effect on benthic microalgal biomass in shallow aquatic ecosystems. *Estuaries*, 22, 735–741.
- Cai, W.J., Dai, M., Wang, Y., Zhai, W., Huang, T., Chen, S., Zhang, F., Chen, Z., Wang, Z., 2004. The biogeochemistry of inorganic carbon and nutrients in the Pearl River estuary and the adjacent Northern South China Sea. *Cont. Shelf Res.*, 24(12), 1301–1319.
- Calizza, E., Careddu, G., Sporta Caputi, S., Rossi, L., Costantini, M.L., 2018. Time–and depth–wise trophic niche shifts in Antarctic benthos. *PloS One*, 13(3), e0194796.
- Cao, H., Hong, Y., Li, M., Gu, J. D., 2011. Diversity and abundance of ammonia–oxidizing prokaryotes in sediments from the coastal Pearl River estuary to the South China Sea. *A. Van Lee.*, 100(4), 545–556.
- Cao, H., Hong, Y., Li, M., Gu, J.D., 2012. Community shift of ammonia–oxidizing bacteria along an anthropogenic pollution gradient from the Pearl River Delta to the South China Sea. *Appl. Microbiol. Biot.*, 94(1), 247–259.
- Calder, J.A., Parker, P.L., 1973. Geochemical implications of induced changes in C^{13} fractionation by blue–green algae. *Geochim. Cosmochim. Ac.*, 37(1), 133–140.
- Carabel, S., Godínez-Domínguez, E., Verísimo, P., Fernández, L., Freire, J., 2006. An assessment of sample processing methods for stable isotope analyses of marine food webs. *J. Exp. Mar. Biol. Ecol.*, 336(2), 254–261.
- Carl, R., 2000. Seasonal variation in $\delta^{13}C$ and $\delta^{15}N$ of size–fractionated plankton at a coastal station in the northern Baltic proper. *Mar. Ecol. Prog. Ser.*, 203, 47–65.
- Carscallen, W.M.A., Vandenberg, K., Lawson, J.M., Martinez, N.D., Romanuk, T.N., 2012. Estimating trophic position in marine and estuarine food webs. *Ecosphere*, 3(3), 1–20.
- Cartaxana, P., Ruivo, M., Hubas, C., Davidson, I., Serôdio, J., Jesus, B., 2011. Physiological versus behavioral photoprotection in intertidal epipelagic and epipsammic benthic diatom communities. *J. Exp. Mar. Biol. Ecol.*, 405, 120–127.
- Chen, H., Feng, J., Zhang, Y., Wei, S., Chen, Z., Lin, G., 2021. Significant but short time assimilation of organic matter from decomposed exotic *Spartina alterniflora* leaf litter by mangrove polychaetes. *Estuar. Coast. Shelf S.*, 259, 107436.
- Chen, J., Wang, F., Jiang, L., Yin, X., Xiao, X., 2013. Stratified communities of active archaea in shallow sediments of the Pearl River estuary, Southern China. *Curr. Microbiol.*, 67(1), 41–50.
- Chen, M.Y., Yu, M., Luo, X.J., Chen, S.J., Mai, B.X., 2011. The factors controlling the partitioning of polybrominated diphenyl ethers and polychlorinated biphenyls in the water–column of the Pearl River Estuary in South China. *Mar. Pollut. Bull.*, 62(1), 29–35.
- Chen, S.J., Luo, X.J., Lin, Z., Luo, Y., Li, K.C., Peng, X.Z., Mai, B.-X., Ran, Y., Zeng, E.Y., 2007. Time trends of polybrominated diphenyl ethers in sediment cores from the Pearl River Estuary, South China. *Environ. Sci. Technol.*, 41(16), 5595–5600.

- Chen, S.J., Feng, A.H., He, M.J., Chen, M.Y., Luo, X.J., Mai, B.X., 2013. Current levels and composition profiles of PBDEs and alternative flame retardants in surface sediments from the Pearl River Delta, southern China: comparison with historical data. *Sci. Total Environ.*, 444, 205–211.
- Chen, Q., Xu, G., Zhang, S., Ma, K., 2018. Consumption of an exotic plant (*Spartina alterniflora*) by the macrobenthic fauna in a mangrove wetland at Zhanjiang, China. *Wetlands*, 38, 327–335.
- Chen, Z.L., Lee, S.Y., 2022. Tidal flats as a significant carbon reservoir in global coastal ecosystems. *Front. Mar. Sci.*, 9, 900896.
- Cherel, Y., 2008. Isotopic niches of emperor and Adélie penguins in Adélie Land, Antarctica. *Mar. Biol.*, 154, 813–821.
- Cherel, Y., Koubbi, P., Giraldo, C., Penot, F., Tavernier, E., Moteki, M., Ozouf-Costaz, C., Causse, R., Chartier, A., Hosie, G., 2011. Isotopic niches of fishes in coastal, neritic and oceanic waters off Adélie land, Antarctica. *Polar Sci.*, 5(2), 286–297.
- Chiba, T., Sato, S.I., 2012. Size-selective predation and drillhole–site selectivity in *Euspira fortunei* (Gastropoda: Naticidae): implications for ecological and palaeoecological studies. *J. Mollus. Stud.*, 78, 205–212.
- Choi, B., Ha, S.Y., Lee, J.S., Chikaraishi, Y., Ohkouchi, N., Shin, K.H., 2017. Trophic interaction among organisms in a seagrass meadow ecosystem as revealed by bulk $\delta^{13}\text{C}$ and amino acid $\delta^{15}\text{N}$ analyses. *Limnol. Oceanogr.*, 62(4), 1426–1435.
- Choi, C.-Y., Battley, P.F., Potter, M.A., Ma, Z., Liu, W., 2014. Factors affecting the distribution patterns of benthic invertebrates at a major shorebird staging site in the Yellow Sea, China. *Wetlands*, 34, 1085–1096.
- Choi, J.H., Oh, C.S., Cho, Y.K., Ahn, C.H., 2013. Consideration on the operation of water level management and environmental change associated with inner dike constructions in saemangeum reservoir. *J. Korean Soc. Mar. Environ. Energy*, 16(4), 290–298.
- Choi, K., Jo, J.H., 2015. Morphodynamics of tidal channels in the open coast macrotidal flat, southern Ganghwa Island in Gyeonggi Bay, West Coast of Korea. *J. Sediment. Res.*, 85, 582–595.
- Choi, Y., Kim, I.-S., Ryu, B.-S., Park, J.-Y., 1996. Ecology of *Synechogobius hasta* (Pisces: Gobiidae) in the Kum River estuary, Korea. *J. Korean Soc. Fisheries*, 29, 115–123.
- Choy, E.J., An, S., Kang, C.-K., 2008. Pathways of organic matter through food webs of diverse habitats in the regulated Nakdong River estuary (Korea). *Estuar. Coast. Shelf S.*, 78, 215–226.
- Choy, E.J., Park, H., Kim, J.H., Ahn, I.Y., Kang, C.K., 2011. Isotopic shift for defining habitat exploitation by the Antarctic limpet *Nacella concinna* from rocky coastal habitats (Marian Cove, King George Island). *Estuar. Coast. Shelf S.*, 92(3), 339–346.
- Chu, K.H., 1989. *Chaetoceros gracilis* as the exclusive feed for the larvae and postlarvae of the shrimp *Metapenaeus ensis*. *Aquaculture*, 83(3–4), 281–287.

- Cipro, C.V., Montone, R.C., Bustamante, P., 2017. Mercury in the ecosystem of Admiralty Bay, King George Island, Antarctica: occurrence and trophic distribution. *Mar. Pollut. Bull.*, 114(1), 564–570.
- Clark, G.F., Stark, J.S., Palmer, A.S., Riddle, M.J., Johnston, E.L., 2017. The roles of sea-ice, light and sedimentation in structuring shallow Antarctic benthic communities. *PLoS One*, 12(1), e0168391.
- Connell, J.H., 1983. On the prevalence and relative importance of interspecific competition: evidence from field experiments. *Am. Nat.*, 122(5), 661–696.
- Consalvey, M., Paterson, D.M., Underwood, G.J.C., 2004. The ups and downs of life in a benthic biofilm: migration of benthic diatoms. *Diatom Res.*, 19, 181–202.
- Cooper, L.W., McRoy, C.P., 1988. Stable carbon isotope ratio variations in marine macrophytes along intertidal gradients. *Oecologia*, 77, 238–241.
- Corbisier, T.N., Petti, M.A., Skowronski, R.S., Brito, T.A., 2004. Trophic relationships in the nearshore zone of Martel Inlet (King George Island, Antarctica): $\delta^{13}\text{C}$ stable-isotope analysis. *Polar Biol.*, 27, 75–82.
- Cordone, G., Marina, T.I., Salinas, V., Doyle, S.R., Saravia, L.A., Momo, F.R., 2018. Effects of macroalgae loss in an Antarctic marine food web: applying extinction thresholds to food web studies. *PeerJ*, 6, e5531.
- Corsolini, S., Sarà, G., 2017. The trophic transfer of persistent pollutants (HCB, DDTs, PCBs) within polar marine food webs. *Chemosphere*, 177, 189–199.
- Costello, M.J., Coll, M., Danovaro, R., Halpin, P., Ojaveer, H., Miloslavich, P., 2010. A census of marine biodiversity knowledge, resources, and future challenges. *PloS One*, 5, e12110.
- Couch, C.A., 1989. Carbon and nitrogen stable isotopes of meiobenthos and their food resources. *Estuar. Coast. Shelf S.*, 28, 433–441.
- Crocetta, F., Tanduo, V., Osca, D., Turolla, E., 2020. The Chinese mitten crab *Eriocheir sinensis* H. Milne Edwards, 1853 (Crustacea: Decapoda: Varunidae) reappears in the northern Adriatic Sea: Another intrusion attempt or the trace of an overlooked population?. *Mar. Pollut. Bull.*, 156, 111221.
- Crossland, C.J., Kremer, H.H., Lindeboom, H., Crossland, J.I. M., Le Tissier, M.D., 2005. Coastal fluxes in the Anthropocene: the land–ocean interactions in the coastal zone project of the International Geosphere–Biosphere Programme. Springer Science and Business Media.
- Dayton, P.K., Oliver, J.S., 1977. Antarctic soft–bottom benthos in oligotrophic and eutrophic environments. *Science*, 197(4298), 55–58.
- Deng, H., He, J., Feng, D., Zhao, Y., Sun, W., Yu, H., Ge, C., 2021. Microplastics pollution in mangrove ecosystems: a critical review of current knowledge and future directions. *Sci. Total Environ.*, 753, 142041.

- Duan, J., Han, J., Cheung, S.G., Chong, R.K.Y., Lo, C.M., Lee, F.W.F., Xu, S.J.L., Yang, Y., Tam, N.F., Zhou, H.C. 2021. How mangrove plants affect microplastic distribution in sediments of coastal wetlands: Case study in Shenzhen Bay, South China. *Sci. Total Environ.*, 767, 144695.
- Dunton, K.H., 2001. $\delta^{15}\text{N}$ and $\delta^{13}\text{C}$ measurements of Antarctic Peninsula fauna: trophic relationships and assimilation of benthic seaweeds. *Am. Zool.*, 41(1), 99–112.
- Duprey, N.N., Wang, T.X., Kim, T., Cybulski, J.D., Vonhof, H.B., Crutzen, P.J., Haug, G.H., Sigman, D.M., Martínez-García, A., Baker, D.M., 2019. Megacity development and the demise of coastal coral communities: evidence from coral skeleton $\delta^{15}\text{N}$ records in the Pearl River estuary. *Glob. Chang. Biol.*, 26(3), 1338–1353.
- El-Sayed, A., Fouda, F., El-Meaddawy, A., 2000. Food habits and ultrastructure of gastric mill of the grapsid crab, *Metopograpsus Messor* (forskal, 1775) from the red sea, egypt. *Egypt. J. Aquat. Biol. Fish.*, 4(1), 239–264.
- Erftemeijer, P.L., Middelburg, J.J., 1993. Sediment–nutrient interactions in tropical seagrass beds: a comparison between a terrigenous and a carbonate sedimentary environment in South Sulawesi (Indonesia). *Mar. Ecol. Prog. Ser.*, 187–198.
- Eveleth, R., Cassar, N., Sherrell, R.M., Ducklow, H., Meredith, M.P., Venables, H.J., Lin, Y., Li, Z., 2017. Ice melt influence on summertime net community production along the Western Antarctic Peninsula. *Deep Sea Res. Part II: Top. Stud. Oceanogr.*, 139, 89–102.
- Fang, T., Li, X., Zhang, G., 2005. Acid volatile sulfide and simultaneously extracted metals in the sediment cores of the Pearl River Estuary, South China. *Ecotox. Environ. Safe.*, 61(3), 420–431.
- Fauchald, K., 1979. The diet of worms: a study of polychaete feeding guilds. *Oceanogra. Mar. Biol.*, 17, 193–284.
- Feebarani, J., Joydas, T.V., Damodaran, R., Borja, A., 2016. Benthic quality assessment in a naturally–and human–stressed tropical estuary. *Ecol. Indic.*, 67, 380–390.
- Fenchel, T., Kofoed, L.H., Lappalainen, A., 1975. Particle size–selection of two deposit feeders: the amphipod *Corophium volutator* and the prosobranch *Hydrobia ulvae*. *Mar. Biol.*, 30(2), 119–128.
- Feng, J., Huang, Q., Chen, H., Guo, J., Lin, G., 2017. Restoration of native mangrove wetlands can reverse diet shifts of benthic macrofauna caused by invasive cordgrass. *J. Appl. Ecol.*, 55(2), 905–916.
- Feng, J., Huang, Q., Qi, F., Guo, J., Lin, G., 2015. Utilization of exotic *Spartina alterniflora* by fish community in the mangrove ecosystem of Zhangjiang Estuary: evidence from stable isotope analyses. *Biol. Invasions*, 17, 2113–2121.
- Feng, J., Wang, S., Wang, S., Ying, R., Yin, F., Jiang, L., Li, Z., 2019. Effects of invasive *Spartina alterniflora* Loisel. and subsequent ecological replacement by *Sonneratia apetala* Buch.–Ham. on soil organic carbon fractions and stock. *Forests*, 10(2), 171.

- Flemming, B.W., 2000. A revised textural classification of gravel-free muddy sediments on the basis of ternary diagrams. *Cont. Shelf Res.*, 20, 1125–1137.
- Forsberg, C., 1980. Eutrophication parameters and trophic state indices in 30 Swedish-receiving lakes. *Arch. Hydrobiologia*, 89, 189–207.
- France, R.L., 1995. Carbon-13 enrichment in benthic compared to planktonic algae: foodweb implications. *Mar. Ecol. Prog. Ser.*, 124, 307–312.
- Fraser, W.R., Hofmann, E.E., 2003. A predator's perspective on causal links between climate change, physical forcing and ecosystem response. *Mar. Ecol. Prog. Ser.*, 265, 1–15.
- Gal, J.K., Ock, G., Park, H.K., Shin, K.H., 2016. The effect of summer monsoon on pelagic and littoral food webs in a large regulated reservoir (Lake Paldang, Korea): a stable isotope approach. *J. Freshw. Ecol.*, 31 (3), 327–340.
- Gao, X., Wang, M., Wu, H., Wang, W., Tu, Z., 2018. Effects of *Spartina alterniflora* invasion on the diet of mangrove crabs (*Parasesarma plicata*) in the Zhangjiang Estuary, China. *J. Coastal Res.*, 34(1), 106–113.
- Gao, Y., Lin, G., 2018. Algal diversity and their importance in ecological processes in typical mangrove ecosystems. *Biodivers. Sci.*, 26(11), 1223.
- Garibotti, I.A., Vernet, M., Ferrario, M.E., Smith, R.C., Ross, R.M., Quetin, L.B., 2003. Phytoplankton spatial distribution patterns along the western Antarctic Peninsula (Southern Ocean). *Mar. Ecol. Prog. Ser.*, 261, 21–39.
- Gillies, C.L., Stark, J.S., Johnstone, G.J., Smith, S.D., 2012. Carbon flow and trophic structure of an Antarctic coastal benthic community as determined by $\delta^{13}\text{C}$ and $\delta^{15}\text{N}$. *Estuar. Coast. Shelf S.*, 97, 44–57.
- Gillies, C.L., Stark, J.S., Johnstone, G.J., Smith, S.D., 2013. Establishing a food web model for coastal Antarctic benthic communities: a case study from the Vestfold Hills. *Mar. Ecol. Prog. Ser.*, 478, 27–41.
- Giraldo, C., Cherel, Y., Vallet, C., Mayzaud, P., Tavernier, E., Moteki, M., Hosie, G., Koubbi, P., 2011. Ontogenic changes in the feeding ecology of the early life stages of the Antarctic silverfish (*Pleuragramma antarcticum*) documented by stable isotopes and diet analysis in the Dumont d'Urville Sea (East Antarctica). *Polar Sci.*, 5(2), 252–263.
- Giri, C., Ochieng, E., Tieszen, L.L., Zhu, Z., Singh, A., Loveland, T., Masek, J., Duke, N., 2011. Status and distribution of mangrove forests of the world using earth observation satellite data. *Glob. Ecol. Biogeogr.*, 20(1), 154–159.
- Glud, R.N. 2008. Oxygen dynamics of marine sediments. *Mar. Biol. Res.*, 4(4), 243–289
- Riaux-Gobin, C., Tréguer, P., Dieckmann, G., Maria, E., Vétion, G., Poulin, M., 2005. Land-fast ice off Adélie Land (Antarctica): short-term variations in nutrients and chlorophyll just before ice break-up. *J. Mar. Syst.*, 55(3–4), 235–248.
- Goering, J., Alexander, V., Haubenstock, N., 1990. Seasonal variability of stable carbon and nitrogen isotope ratios of organisms in a North Pacific Bay. *Estuar. Coast. Shelf S.*, 30, 239–260.

- Gray, J.S. 1997. Marine biodiversity: patterns, threats and conservation needs. *Biodivers. Conserv.*, 6:153–175
- Grebmeier, J.M., Overland, J.E., Moore, S.E., Farley, E.V., Carmack, E.C., Cooper, L.W., Frey, K.E., Helle, J.H., McLaughlin, F.A., McNutt, S.L., 2006. A major ecosystem shift in the northern Bering Sea. *Science*, 311(5766), 1461–1464.
- Griffiths, J.R., Kadin, M., Nascimento, F.J.A., Tamelander, T., Törnroos, A., Bonaglia, S., Bonsdorff, E., Brüchert, V., Gårdmark, A., Järnström, M., Kotta, J., Lindegren, M., Nordström, M.C., Norkko, A., Olsson, J., Weigel, B., Žydelis, R., Blenckner, T., Niiranen, S., Winder, M., 2017. The importance of benthic–pelagic coupling for marine ecosystem functioning in a changing world. *Glob. Change Biol.*, 23, 2179–2196.
- Grippo, M.A., Fleeger, J.W., Dubois, S.F., Condrey, R., 2011. Spatial variation in basal resources supporting benthic food webs revealed for the inner continental shelf. *Limnol. Oceanogr.*, 56, 841–856.
- Grippo, M.A., Fleeger, J.W., Rabalais, N.N., Condrey, R., Carman, K.R., 2010. Contribution of phytoplankton and benthic microalgae to inner shelf sediments of the north-central Gulf of Mexico. *Cont. Shelf Res.*, 30, 456–466.
- Gu, H., Feng, Y., Zhang, Y., Yin, D., Yang, Z., Tang, W., 2021. Differential study of the *Parabramis pekinensis* intestinal microbiota according to different habitats and different parts of the intestine. *Ann. Microbiol.*, 71(1), 1–11.
- Guan, Y.F., Sojinu, O.S., Li, S.M., Zeng, E.Y., 2009. Fate of polybrominated diphenyl ethers in the environment of the Pearl River Estuary, South China. *Environ. Pollut.*, 157(7), 2166–2172.
- Guan, Y.F., Wang, J.Z., Ni, H.G., Luo, X.J., Mai, B.X., Zeng, E.Y., 2007. Riverine inputs of polybrominated diphenyl ethers from the Pearl River Delta (China) to the coastal ocean. *Environ. Sci. Technol.*, 41(17), 6007–6013.
- Gunn, J.S., Milward, N.E., 1985. The food, feeding habits and feeding structures of the whiting species *Sillago sihama* (Forsskal) and *Sillago analis* Whitley from Townsville, North Queensland, Australia. *J. Fish Biol.*, 26(4), 411–427.
- Gupta, S., 2016. An overview on morphology, biology, and culture of spotted scat *Scatophagus argus* (Linnaeus 1766). *Rev. Fish. Sci. Aquac.*, 24(2), 203–212.
- Ha, H.K., Ha, H.J., Seo, J.Y., Choi, S.M., 2018. Effects of vegetation and fecal pellets on the erodibility of cohesive sediments: Ganghwa tidal flat, West Coast of Korea. *Environ. Pollut.*, 241, 468–474.
- Ha, S.Y., Ahn, I.Y., Moon, H.W., Choi, B., Shin, K.H., 2019. Tight trophic association between benthic diatom blooms and shallow water megabenthic communities in a rapidly deglaciated Antarctic fjord. *Estuar. Coast. Shelf S.*, 218, 258–267.
- Ha, S.-Y., Min, W.-K., Kim, D.-S., Shin, K.-H., 2014. Trophic importance of meiofauna to polychaetes in a seagrass (*Zostera marina*) bed as traced by stable isotopes. *J. Mar. Biol. Assoc. Uk.*, 94(1), 121–127.

Han, E., Park, H., Bergamino, L., Choi, K.-S., Choy, E.J., Yu, O.H., Lee, T.W., Park, H.-S., Shim, W. J., Kang, C.-K., 2015. Stable isotope analysis of a newly established macrofaunal food web 1.5 years after the Hebei Spirit oil spill. *Mar. Pollut. Bull.*, 90, 167–180.

Han, P., Gu, J.D., 2015. Further analysis of anammox bacterial community structures along an anthropogenic nitrogen-input gradient from the riparian sediments of the Pearl River Delta to the deep-ocean sediments of the South China Sea. *Geomicrobiol J.*, 32(9), 789–798.

Hamilton, L.C., Haedrich, R.L., 1999. Ecological and population changes in fishing communities of the North Atlantic Arc. *Polar Res.*, 18(2), 383–388.

Hamilton, S.E., Casey, D., 2016. Creation of a high spatio-temporal resolution global database of continuous mangrove forest cover for the 21st century (CGMFC-21). *Glob. Ecol. Biogeogr.*, 25(6), 729–738.

Hawkins, S.J., Sugden, H.E., Mieszkowska, N., Moore, P.J., Poloczanska, E., Leaper, R., Herbert, R.J.H., Genner, M.J., Moschella, P.S., Thompson, R.C., Jenkins, S.R., Southward, A.J., Burrows, M.T., 2009. Consequences of climate-driven biodiversity changes for ecosystem functioning of North European rocky shores. *Mar. Ecol. Prog. Ser.*, 396, 245–259.

He, X., Wang, Z., Nie, X., Yang, Y., Pan, D., Leung, A.O., Cheng, Z., Yang, Y., Li, K., Chen, K., 2012. Residues of fluoroquinolones in marine aquaculture environment of the Pearl River Delta, South China. *Environ. Geochem. Hlth.*, 34(3), 323–335.

He, Z., Sun, H., Yu, X., Yin, Z., Wu, M., Zhao, L., Hu, Z., Peng, Y., Lee, S.Y., 2021. Monoculture or mixed culture? Relevance of fine root dynamics to carbon sequestration oriented mangrove afforestation and restoration. *Front. Mar. Sci.*, 8, 763922.

Heiri, O., Lotter, A.F., Lemcke, G., 2001. Loss on ignition as a method for estimating organic and carbonate content in sediments: reproducibility and comparability of results. *J. Paleolimnol.*, 25, 101–110.

Heithaus, E.R., Heithaus, P.A., Heithaus, M.R., Burkholder, D., Layman, C.A., 2011. Trophic dynamics in a relatively pristine subtropical fringing mangrove community. *Mar. Ecol. Prog. Series*, 428, 49–61.

Herzka, S.Z., Holt, G.J., 2000. Changes in isotopic composition of red drum (*Sciaenops ocellatus*) larvae in response to dietary shifts: potential applications to settlement studies. *Can. J. Fish Aquat. Sci.*, 57, 137–147.

Hirawake, T., Kudoh, S., Aoki, S., Odate, T., Fukuchi, M., 2005. Inter-annual variability of chlorophyll and sea-ice in the Antarctic Divergence region: an attempt to derive their quantitative relationship. *Int. J. Remote Sens.*, 26(10), 2035–2044.

Hobson, K.A., Clark, R.G., 1992. Assessing avian diets using stable isotope: I. turnover of ^{13}C in tissues. *Condor*, 194, 181–188.

Hodum, P. J., Hobson, K.A., 2000. Trophic relationships among Antarctic fulmarine petrels: insights into dietary overlap and chick provisioning strategies inferred from stable-isotope ($\delta^{15}\text{N}$ and $\delta^{13}\text{C}$) analyses. *Mar. Ecol. Prog. Ser.*, 198, 273–281.

Hoffmann, R., Pasotti, F., Vazquez, S., Lefaible, N., Torstensson, A., MacCormack, W., Wenzhöfer, F., Braeckman, U., 2018. Spatial variability of biogeochemistry in shallow

coastal benthic communities of Potter Cove (Antarctica) and the impact of a melting glacier. *PloS One*, 13(12), e0207917.

Hong, S.H., Shim, W.J., Li, D.H., Yim, U.H., Oh, J.R., Kim, E.S., 2006. Contamination status and characteristics of persistent organochlorine pesticides in the Saemangeum environment. *Ocean Polar Res.*, 28(3), 317–329.

Hossain, M.S., Roy, A., Rahman, M.L., 2016. Food and feeding habit of Bele *Glossogobius giuris* (Hamilton and Buchannan, 1822) collected from Mithamain Haor of Kishoreganj districts, northeastern Bangladesh. *Int. J. Fish. Aquat. Sci.*, 4(5), 84–88.

Höfer, J., Giesecke, R., Hopwood, M.J., Carrera, V., Alarcón, E., González, H.E., 2019. The role of water column stability and wind mixing in the production/export dynamics of two bays in the Western Antarctic Peninsula. *Prog. Oceanogr.*, 174, 105–116.

Hu, J., Jia, G., Mai, B., Zhang, G., 2006. Distribution and sources of organic carbon, nitrogen and their isotopes in sediments of the subtropical Pearl River estuary and adjacent shelf, Southern China. *Mar. Chem.*, 98(2–4), 274–285.

Hu, Y., Pei, N., Sun, Y., Xu, X., Zhang, Z., Li, H., Wang, W., Zuo, L., Xiong, Y., Zeng, Y., He, K., Mai, B., 2019. Halogenated flame retardants in mangrove sediments from the Pearl River Estuary, South China: Comparison with historical data and correlation with microbial community. *Chemosphere*, 227, 315–322.

Hu, Y.X., Sun, Y.X., Li, X., Xu, W.H., Zhang, Y., Luo, X.J., Dai, S.H., Xu, X.R., Mai, B.X., 2017. Organophosphorus flame retardants in mangrove sediments from the Pearl River Estuary, South China. *Chemosphere*, 181, 433–439.

Huang, Q., Liu, Y., Zheng, X., Chen, G., 2012. Phytoplankton community and the purification effect of mangrove in the mangrove plantation–aquaculture coupling systems in the Pearl River Estuary. *Procedia Environ. Sci.*, 15, 12–21.

Hyndes, G.A., Nagelkerken, I., McLeod, R.J., Connolly, R.M., Lavery, P.S., Vanderklift, M.A., 2014. Mechanisms and ecological role of carbon transfer within coastal seascapes. *Biol. Rev.*, 89(1), 232–254.

Jackson, A.L., Inger, R., Parnell, A.C., Bearhop, S., 2011. Comparing isotopic niche widths among and within communities: SIBER-Stable Isotope Bayesian Ellipses in R. *J. Anim. Ecol.*, 80(3), 595–602.

Jackson, J.B., Kirby, M.X., Berger, W.H., Bjorndal, K.A., Botsford, L.W., Bourque, B.J., Bradbury, R.H., Cooke, R., Erlandson, J., Estes, J.A., Hughes, T.P., Kidwell, S., Lange, C.B., Lenihan, H.S., Pandolfi, J.M., Peterson, C.H., Steneck, R.S., Tegner, M.J., Warner, R.R., 2001. Historical overfishing and the recent collapse of coastal ecosystems. *Science*, 293(5530), 629–637.

Jia, Z., Swadling, K.M., Meiners, K.M., Kawaguchi, S., Virtue, P., 2016. The zooplankton food web under East Antarctic pack ice—A stable isotope study. *Deep Sea Res. Pt. II Top. Stud. Oceanogr.*, 131, 189–202.

Kader, M.A., Bhuiyan, A.L., Manzur-I-Khuda, A.R.M.M., 1988. Food and feeding habits of *Gobioides Rubicundus* and some feeding experiments on it. *Indian J. Fish.*, 35(4), 312–316.

Katsanevakis, S., Coll, M., Fraschetti, S., Giakoumi, S., Goldsborough, D., Mačić, V., Mackelworth, P., Rilov, G., Stelzenüller, V., Albano, P.G., Bates, A.E., Bevilacqua, S., Gissi, E., Hermoso, V., Mazaris, A.D., Pita, C., Rossi, V., Teff-Seker, Y., Yates, K. 2020. Twelve recommendations for advancing marine conservation in European and contiguous seas. *Front. Mar. Sci.*, 7, 879.

Kang, C.-K., Kim, J. B., Lee, K.-S., Kim, J. B., Lee, P.-Y., Hong, J.-S., 2003. Trophic importance of benthic microalgae to macrozoobenthos in coastal bay systems in Korea: dual stable C and N isotope analyses. *Mar. Ecol. Prog. Ser.*, 259, 79–92.

Kang, C.K., Kang, Y.S., Choy, E.J., Kim, D.S., Shim, B.T., Lee, P.Y., 2007. Condition, reproductive activity, and gross biochemical composition of the Manila clam, *Tapes philippinarum* in natural and newly created sandy habitats of the southern coast of Korea. *J. Shellfish Res.*, 26(2), 401–412.

Kang, C.-K., Park, H.J., Choy, E.J., Choi, K.-S., Hwang, K., Kim, J.-B. 2015. Linking intertidal and subtidal food webs: consumer-mediated transport of intertidal benthic microalgal carbon. *Plos One*, e0139802.

Kang, D.Y., Kim, H.C., Kang, H.W., 2011. Influence of density and feeding frequency on early life history and cannibalism of river puffer, *Takifugu obscurus*. *Dev. Reprod.*, 15(2), 77–85.

Ke, Y., Wang, W.X., 2019. Dietary metal bioavailability in razor clam *Sinonovacula constricta* under fluctuating seston environments. *Sci. Total Environ.*, 653, 131–139.

Ke, Z., Tan, Y., Huang, L., Zhao, C., Liu, H., 2016. Trophic structure of shrimp-trawl catches in the Pearl River Estuary in winter, using stable isotope analyses. *Aquat. Ecosyst. Health*, 19(4), 468–475.

Kędra, M., Moritz, C., Choy, E.S., David, C., Degen, R., Duerksen, S., Ellingsen, I., Górska, B., Grebmeier, J.M., Kirievskaya, D., Oevelen, D.V., Piwosz, K., Samuelsen, A., Węśławski, J.M., 2015. Status and trends in the structure of Arctic benthic food webs. *Polar Res.*, 34(1), 23775.

Kim, D., Jo, J., Kim, B., Ryu, J., Choi, K., 2020. Influence of dike-induced morphologic and sedimentologic changes on the benthic ecosystem in the sheltered tidal flats, Saemangeum area, west coast of Korea. *Environ. Pollut.*, 257, 113507.

Kim, D., Ko, J., Jo, J., Ryu, J., Choi, K., 2022. Decoupling natural and man-made impacts on the morphologic and sedimentologic changes in the tidal flats, Saemangeum area, west coast of Korea: Implications for benthic ecosystem stability. *Sci. Total Environ.*, 807, 151779.

Kim, E., Kim, H., Shin, K.-H., Kim, M.-S., Kundu, S.R., Lee, B.-G., Han, S., 2012. Biomagnification of mercury through the benthic food webs of a temperate estuary: Masa Bay, Korea. *Environ. Toxicol. Chem.*, 31, 1254–1263.

Kim, H.K., Lee, H.W., Choi, J.H. and Park, S.S., 2007, A modeling study for change of tidal zone and flushing rate by the construction of sea dike. *J. Korean Soc. Environ. Eng.*, 29(10), 1106–1113.

Kim, J.H., Park, S.H., Baek, S.H., Jang, M.H., Yoon, J.D., 2020. Changes in fish assemblages after dike construction in the Saemangeum area. *Ocean Sci. J.*, 55, 129–142.

- Koh, C.-H., Khim, J.S., Araki, H., Yamanishi, H., Mogi, H., Koga, K., 2006. Tidal resuspension of microphytobenthic chlorophyll-*a* in a Nanaura mudflat, Saga, Ariake Sea, Japan: flood-ebb and spring-neap variation. *Mar. Ecol. Prog. Ser.*, 312, 85–100.
- Koh, C.-H., Khim, J.S., 2014. The Korean tidal flat of the Yellow Sea: physical setting, ecosystem and management. *Ocean Coast. Manage.*, 102, 398–414.
- Koh, C.-H., de Jonge, V.N., 2014. Stopping the disastrous embankments of coastal wetlands by implementing effective management principles: Yellow Sea and Korea compared to the European Wadden Sea. *Ocean Coast. Manage.*, 102, 604–621.
- Kon, K., Hoshino, Y., Kanou, K., Okazaki, D., Nakayama, S., Kohno, H., 2012. Importance of allochthonous material in benthic macrofaunal community functioning in estuarine salt marshes. *Estuar. Coast. Shelf S.*, 96, 236–244.
- Kulkarni, R., Deobagkar, D., Zinjarde, S., 2018. Metals in mangrove ecosystems and associated biota: a global perspective. *Ecotoxicol. Environ. Saf.*, 153, 215–228.
- Kwak, T.J., Zedler, J.B., 1997. Food web analysis of southern California coastal wetlands using multiple stable isotopes. *Oecologia*, 110(2), 262–277.
- Kwon, B.-O., Kim, H., Noh, J., Lee, S.Y., Nam, J., Khim, J.S., 2020. Spatiotemporal variability in microphytobenthic primary production across bare intertidal flat, saltmarsh, and mangrove forest of Asia and Australia. *Mar. Pollut. Bull.*, 151, 110707.
- Lang, T., Tam, N.F.Y., Hussain, M., Ke, X., Wei, J., Fu, Y., Li, M., Huang, X., Huang, S., Xiong, Z., Wu, K., Li, F., Chen, Z., Hu, Z., Gao, C., Yang, Q., Zhou, H., 2023. Dynamics of heavy metals during the development and decomposition of leaves of *Avicennia marina* and *Kandelia obovata* in a subtropical mangrove swamp. *Sci. Total Environ.*, 855, 158700.
- Lange, G., Schmitt, J.A., Kröncke, I., Moorthi, S.D., Rohde, S., Scheu, S., Schupp, P.J., 2019. The role of invasive marine plants for macrofauna nutrition in the Wadden Sea. *J. Exp. Mar. Biol. Ecol.*, 512, 1–11.
- Larson, E.T., Shanks, A.L., 1996. Consumption of marine snow by two species of juvenile mullet and its contribution to their growth. *Mar. Ecol. Prog. Ser.*, 130, 19–28.
- Layman, C.A., Araújo, M.S., Boucek, R., Hammerschlag-Peyer, C.M., Elizabeth Harrison, E., Jud, Z.R., Matich, P., Rosenblatt, A.E., Vaudo, J.J., Yeager, L.A., Post, D.M., Bearhop, S., 2012. Applying stable isotopes to examine foodweb structure: an overview of analytical tools. *Biol. Rev.*, 87, 545–562.
- Lee, I.O., Noh, J., Kim, B., Kwon, I., Kim, H., Kwon, B.O., Peng, Y., Hu, Z., Khim, J.S., 2023. Food web dynamics in the mangrove ecosystem of the Pearl River Estuary surrounded by megacities. *Mar. Pollut. Bull.*, 189, 114747.
- Lee, I.O., Noh, J., Lee, J., Kim, B., Hwang, K., Kwon, B.O., Lee, M.J., Ryu, J., Nam, J., Khim, J.S., 2021. Stable isotope signatures reveal the significant contributions of microphytobenthos and saltmarsh-driven nutrition in the intertidal benthic food webs. *Sci. Total Environ.*, 756, 144068.

- Lee, J., Kwon, B.-O., Kim, B., Noh, J., Hwang, K., Ryu, J., Park, J., Hong, S., Khim, J.S., 2019. Natural and anthropogenic signatures on sedimentary organic matters across varying intertidal habitats in the Korean waters. *Environ. Int.*, 133, 105166.
- Lee, K.H., Wang, Y.F., Wang, Y., Gu, J.D., Jiao, J.J., 2018. Abundance and diversity of aerobic/anaerobic ammonia/ammonium-oxidizing microorganisms in an ammonium-rich aquitard in the Pearl River Delta of South China. *Microb. Ecol.*, 76(1), 81–91.
- Lee, S.Y., 1990. Primary productivity and particulate organic matter flow in an estuarine mangrove-wetland in Hong Kong. *Mar. Biol.*, 106(3), 453–463.
- Lee, S.Y., 1995. Mangrove outwelling: a review. *Hydrobiologia*, 295(1), 203–212.
- Lee, S.Y., 2000. Carbon dynamics of Deep Bay, eastern Pearl River estuary, China. II: trophic relationship based on carbon-and nitrogen-stable isotopes. *Mar. Ecol. Prog. Ser.*, 205, 1–10.
- Lee, S.Y., 2016. From blue to black: anthropogenic forcing of carbon and nitrogen influx to mangrove-lined estuaries in the South China Sea. *Mar. Pollut. Bull.*, 109 (2), 682–690.
- Lee, S.Y., Khim, J.S., 2017. Hard science is essential to restoring soft-sediment intertidal habitats in burgeoning East Asia. *Chemosphere*, 168, 765–776.
- Lee, Y., Park, J., Jung, J., Kim, T.W., 2022. Unprecedented differences in phytoplankton community structures in the Amundsen Sea Polynyas, West Antarctica. *Environ. Res. Lett.*, 17(11), 114022.
- Leu, E., Søreide, J.E., Hessen, D.O., Falk-Petersen, S., Berge, J., 2011. Consequences of changing sea-ice cover for primary and secondary producers in the European Arctic shelf seas: timing, quantity, and quality. *Prog. Oceanogr.*, 90(1–4), 18–32.
- Levinton, J., 1972. Stability and trophic structure in deposit-feeding and suspension-feeding communities. *T. Am. Nat.*, 106, 472–486.
- Li, H., Yang, S.L., 2009. Trapping effect of tidal marsh vegetation on suspended sediment, Yangtze delta. *J. Coastal. Res.*, 25, 915–924.
- Li, M., Hong, Y.G., Cao, H.L., Gu, J.D., 2011. Mangrove trees affect the community structure and distribution of anammox bacteria at an anthropogenic-polluted mangrove in the Pearl River Delta reflected by 16S rRNA and hydrazine oxidoreductase (HZO) encoding gene analyses. *Ecotoxicology*, 20(8), 1780–1790.
- Li, M.S., Lee, S.Y., 1998. Carbon dynamics of Deep Bay, eastern Pearl River Estuary, China. I: A mass balance budget and implications for shorebird conservation. *Mar. Ecol. Prog. Series*, 172, 73–87.
- Li, R., Yu, L., Chai, M., Wu, H., Zhu, X., 2020. The distribution, characteristics and ecological risks of microplastics in the mangroves of Southern China. *Sci. Total Environ.*, 708, 135025.
- Liao, Y., Shou, L., Tang, Y., Zeng, J., Chen, Q., Yan, X., 2020. Effects of non-indigenous plants on food sources of intertidal macrobenthos in Yueqing Bay, China: combining stable isotope and fatty acid analyses. *Estuar. Coast. Shelf S.*, 241, 106801.

Lin, J., Liu, X., Lai, T., He, B., Du, J., Zheng, X., 2021. Trophic importance of the seagrass *Halophila ovalis* in the food web of a Hepu seagrass bed and adjacent waters, Beihai, China. *Ecol. Indic.*, 125, 107607.

Liu, W., Zhang, J., Tian, G., Xu, H., Yan, X., 2013. Temporal and vertical distribution of microphytobenthos biomass in mangrove sediments of Zhujiang (Pearl River) Estuary. *Acta Oceanol. Sin.*, 32(4), 82–88.

Lorenzen, C.J., 1967. Determination of chlorophyll and phaeo-pigments: spectrophotometric equations. *Limnol. Oceanogr.*, 12, 343–346.

Lorrain, A., Paulet, Y.-M., Chauvaud, L., Savoye, N., Donval, A., Saout, C., 2002. Differential $\delta^{13}\text{C}$ and $\delta^{15}\text{N}$ signatures among scallop tissues: implications for ecology and physiology. *J. Exp. Mar. Biol. Ecol.*, 275, 47–61.

Lorrain, A., Pethybridge, H., Cassar, N., Receveur, A., Allain, V., Bodin, N., Bopp, L., Choy, C.A., Duffy, L., Fry, B., Goñi, N., Graham, B.S., Hobday, A.J., Logan, J.M., Ménard, F., Menkes, C.E., Olson, R.J., Pagendam, D.E., Point, D., Revill, A.T., Young, J.W., 2020. Trends in tuna carbon isotopes suggest global changes in pelagic phytoplankton communities. *Glob. Change Biol.*, 26(2), 458–470.

Lovelock, C.E., Reef, R., 2020. Variable impacts of climate change on blue carbon. *One Earth*, 3(2), 195–211.

Lu, Z., Liu, D., Liao, J., Wang, J., Li, H., Zhang, J., 2020. Characterizing spatial distribution of chlorophyll-a in the Southern Ocean on a circumpolar cruise in summer. *Sci. Total Environ.*, 708, 134833.

Luo, L., Gu, J.D., 2018. Nutrient limitation status in a subtropical mangrove ecosystem revealed by analysis of enzymatic stoichiometry and microbial abundance for sediment carbon cycling. *Int. Biodeterior. Biodegradation*, 128, 3–10.

Macintyre, H.L., Geider, R.J., Miller, D.C., 1996. Microphytobenthos: the ecological role of the “secret garden” of unvegetated, shallow-water marine habitats. I. distribution, abundance and primary product. *Estuaries*, 19, 186–201.

Mann, K.H., 1988. Production and use of detritus in various freshwater, estuarine, and coastal marine ecosystems. *Limnol. Oceanogr.*, 33, 910–930.

McCutchan Jr, J.H., Lewis Jr, W.M., Kendall, C., McGrath, C.C., 2003. Variation in trophic shift for stable isotope ratios of carbon, nitrogen, and sulfur. *Oikos*, 102, 378–390.

McKee, K.L., Feller, I.C., Popp, M., Wanek, W., 2002. Mangrove isotopic ($\delta^{15}\text{N}$ and $\delta^{13}\text{C}$) fractionation across a nitrogen vs. phosphorus limitation gradient. *Ecology*, 83(4), 1065–1075.

McMullin, R.M., Wing, S.R., Wing, L.C., Shatova, O.A., 2017. Trophic position of Antarctic ice fishes reflects food web structure along a gradient in sea ice persistence. *Mar. Ecol. Prog. Ser.*, 564, 87–98.

Meera, S.P., Bhattacharyya, M., Nizam, A., Kumar, A., 2021. A review on microplastic pollution in the mangrove wetlands and microbial strategies for its remediation. *Environ. Sci. Pollut. Res.*, 1–15.

- Mendoza, J.A., 1982. Some aspects of the autecology of *Leptochelia dubia* (Krøyer, 1842) (Tanaidacea). *Crustaceana*, 43(3), 225–240.
- Michel, L.N., Danis, B., Dubois, P., Eleaume, M., Fournier, J., Gallut, C., Jane, P., Lepoint, G., 2019. Increased sea ice cover alters food web structure in East Antarctica. *Sci. Rep.*, 9, 8062.
- Mincks, S.L., Smith, C.R., Jeffreys, R.M., Sumida, P.Y., 2008. Trophic structure on the West Antarctic Peninsula shelf: detritivory and benthic inertia revealed by $\delta^{13}\text{C}$ and $\delta^{15}\text{N}$ analysis. *Deep Sea Res. Pt. II Top. Stud. Oceanogr.*, 55(22–23), 2502–2514.
- Moline, M.A., Claustre, H., Frazer, T.K., Schofield, O., Vernet, M., 2004. Alteration of the food web along the Antarctic Peninsula in response to a regional warming trend. *Glob. Change Biol.*, 10(12), 1973–1980.
- Moline, M.A., Karnovsky, N.J., Brown, Z., Divoky, G.J., Frazer, T.K., Jacoby, C.A., Torres, J.J., Fraser, W.R., 2008. High latitude changes in ice dynamics and their impact on polar marine ecosystems. *Ann. N. Y. Acad. Sci.*, 1134(1), 267–319.
- Montes-Hugo, M., Doney, S.C., Ducklow, H.W., Fraser, W., Martinson, D., Stammerjohn, S. E., Schofield, O., 2009. Recent changes in phytoplankton communities associated with rapid regional climate change along the western Antarctic Peninsula. *Science*, 323(5920), 1470–1473.
- Morris, D.P., Lewis Jr, W.M., 1988. Phytoplankton nutrient limitation in Colorado mountain lakes. *Freshwater Biol.*, 20(3), 315–327.
- MOMAF, 2007, Intergrated preservation study on the marine environments in the Saemangeum area (1st Year of 2nd Phase, 2006). KORDI Research Report, BSPM 37900–1854–1.
- MOMAF, 2009, Intergrated preservation study on the marine environments in the Saemangeum area (2008). KORDI Research Report, BSPM 51001–2041–2.
- Mudd, S.M., D'Alpaos, A., Morris, J.T., 2010. How does vegetation affect sedimentation on tidal marshes? Investigating particle capture and hydrodynamic controls on biologically mediated sedimentation. *J. Geophys. Res.*, 115, F03029.
- Nagelkerken, I., Goldenberg, S.U., Ferreira, C.M., Ullah, H., Connell, S.D., 2020. Trophic pyramids reorganize when food web architecture fails to adjust to ocean change. *Science*, 369(6505), 829–832.
- Ni, H.G., Lu, F.H., Luo, X.L., Tian, H.Y., Zeng, E.Y., 2008. Riverine inputs of total organic carbon and suspended particulate matter from the Pearl River Delta to the coastal ocean off South China. *Mar. Pollut. Bull.*, 56(6), 1150–1157.
- Noh, J., Kim, H., Lee, C., Yoon, S.J., Chu, S., Kwon, B.-O., Ryu, J., Kim, J.-J., Lee, H., Yim, U.H., Giesy, J.P., Khim, J.S., 2018. Bioaccumulation of polycyclic aromatic hydrocarbons (PAHs) by the marine clam, *Macra veneriformis*, chronically exposed to oil-suspended particulate matter aggregates. *Environ. Sci. Technol.*, 52, 7910–7920.

- Noh, J., Yoon, S.J., Kim, H., Lee, C., Kwon, B.-O., Lee, Y., Hong, S., Kim, J., Ryu, J., Khim, J.S., 2019. Anthropogenic influences on benthic food web dynamics by interrupted freshwater discharge in a closed Geum River estuary, Korea. *Environ. Int.*, 131, 104981.
- Norkko, A., Thrush, S.F., Cummings, V.J., Gibbs, M.M., Andrew, N.L., Norkko, J., Schwarz, A.M., 2007. Trophic structure of coastal Antarctic food webs associated with changes in sea ice and food supply. *Ecology*, 88(11), 2810–2820.
- Nyssen, F., Brey, T., Dauby, P., Graeve, M., 2005. Trophic position of Antarctic amphipods-enhanced analysis by a 2-dimensional biomarker assay. *Mar. Ecol. Prog. Ser.*, 300, 135–145.
- O'Brien, D.M., 2015. Stable isotope ratios as biomarkers of diet for health research. *Annu. Rev. Nutr.*, 35, 565–594.
- Oda, Y., Nakano, S., Suh, J.M., Oh, H.J., Jin, M.Y., Kim, Y.J., Sakamoto, M., Chang, K.H., 2018. Spatiotemporal variability in a copepod community associated with fluctuations in salinity and trophic state in an artificial brackish reservoir at Saemangeum, South Korea. *PloS One*, 13(12), e0209403.
- Olsen, Y.S., Fox, S.E., Teichberg, M., Otter, M., Valiela, I., 2011. $\delta^{15}\text{N}$ and $\delta^{13}\text{C}$ reveal differences in carbon flow through estuarine benthic food webs in response to the relative availability of macroalgae and eelgrass. *Mar. Ecol. Prog. Ser.*, 421, 83–96.
- Oro, D., Cam, E., Pradel, R., Martínez-Abraín, A., 2004. Influence of food availability on demography and local population dynamics in a long-lived seabird. *Proceedings of the Royal Society of London. Ser. B: Biol. Sci.*, 271(1537), 387–396.
- Page, H.M., 1997. Importance of vascular plant and algal production to macro-invertebrate consumers in a southern California salt marsh. *Estuar. Coast. Shelf S.*, 45(6), 823–834.
- Pakhomov, E.A., Perissinotto, R., Froneman, P.W., 1998. Abundance and trophodynamics of *Euphausia crystallorophias* in the shelf region of the Lazarev Sea during austral spring and summer. *J. Mar. Sys.*, 17(1–4), 313–324.
- Park, J., Song, S.J., Ryu, J., Kwon, B.-O., Hong, S., Bae, H., Choi, J.-W., Khim, J.S., 2014. Macrozoobenthos of Korean tidal flats: a review on species assemblages and distribution. *Ocean. Coast. Manage.*, 102, 483–492.
- Park, J.K., Kim, E.S., Kim, K.T., Cho, S.R., Song, T.Y., Yoo, J.K., Park, Y.C., 2009. Characteristics in organic carbon distribution in the Seomangeum area during the construction of artificial sea dike, Korea. *J. Korean Soc. Mar. Environ. Energy*, 12(2), 75–83.
- Park, H.J., Choy, E.J., Lee, K.-S., Kang, C.-K., 2013. Trophic transfer between coastal habitats in a seagrass-dominated macrotidal embayment system as determined by stable isotope and fatty acid signatures. *Mar. Freshwater Res.*, 64, 1169–1183.
- Park, H.J., Han, E., Lee, Y.-J., Kang, C.-K., 2016. Trophic linkage of a temperate intertidal macrobenthic food web under opportunistic macroalgal blooms: a stable isotope approach. *Mar. Pollut. Bull.*, 111, 86–94.
- Park, H.J., Kang, H.Y., Park, T.H., Kang, C.-K., 2017. Comparative trophic structures of macrobenthic food web in two macrotidal wetlands with and without a dike on the temperate coast of Korea as revealed by stable isotopes. *Mar. Environ. Res.*, 131, 134–145.

- Park, H.J., Kim, C., Kang, C.K., 2022. Recovery of macrobenthic food web on rocky shores following the hebei spirit oil spill as revealed by c and n stable isotopes. *Water*, 14(15), 2335.
- Park, H.J., Kwak, J.H., Kang, C.K., 2015. Trophic consistency of benthic invertebrates among diversified vegetational habitats in a temperate coastal wetland of Korea as determined by stable isotopes. *Estuaries Coast.*, 38, 599–611.
- Park, H.J., Kwak, J.H., Lee, Y.J., Kang, H.Y., Choy, E.J., Kang, C.K., 2020. Trophic structures of two contrasting estuarine ecosystems with and without a dike on the temperate coast of Korea as determined by stable isotopes. *Estuaries Coast.*, 43, 560–577.
- Park, H.J., Park, T.H., Kang, H.Y., Lee, K.S., Kim, Y.K., Kang, C.K., 2021. Assessment of restoration success in a transplanted seagrass bed based on isotopic niche metrics. *Ecol. Eng.*, 166, 106239.
- Park, H.J., Yeon, I., Han, E., Lee, Y.J., Hanchet, S.M., Baeck, G.W., Kwon, Y.K., Choi, S.G., Lee, D.W., Kang, C.K., 2015. Diet study of Antarctic toothfish caught in the east Antarctic based on stomach content, fatty acid and stable isotope analyses. *CCAMLR Sci*, 22, 29–44.
- Parkinson, C.L., 2019. A 40-y record reveals gradual Antarctic sea ice increases followed by decreases at rates far exceeding the rates seen in the Arctic. *P. Natl. A. Sci.*, 116(29), 14414–14423.
- Parkinson, C.L., Cavalieri, D.J., 2012. Antarctic sea ice variability and trends, 1979–2010. *The Cryosphere*, 6, 871–880.
- Parnell, A., Inger, R., 2016. Stable isotope mixing models in R with SIMMR. <https://cran.r-project.org/web/packages/simmr/vignettes/simmr.html>
- Pasotti, F., Saravia, L.A., De Troch, M., Tarantelli, M.S., Sahade, R., Vanreusel, A., 2015. Benthic trophic interactions in an Antarctic shallow water ecosystem affected by recent glacier retreat. *PloS One*, 10(11), e0141742.
- Peng, Y., Chen, G., Tian, G., Yang, X., 2009. Niches of plant populations in mangrove reserve of Qi'ao Island, Pearl River Estuary. *Acta Ecol. Sin.*, 29(6), 357–361.
- Peng, Y., Zheng, M., Zheng, Z., Wu, G., Chen, Y., Xu, H., Tian, G., Peng, S., Chen, G., Lee, S.Y., 2016. Virtual increase or latent loss? A reassessment of mangrove populations and their conservation in Guangdong, southern China. *Mar. Pollut. Bull.*, 109(2), 691–699.
- Perdue, E.M., Koprivnjak, J.-F., 2007. Using the C/N ratio to estimate terrigenous inputs of organic matter to aquatic environments. *Estuar. Coast. Shelf S.*, 73, 65–72.
- Persson, A., Hansson, L.A., 1999. Diet shift in fish following competitive release. *Can. J. Fish. Aquat. Sci.*, 56(1), 70–78.
- Pingram, M.A., Collier, K.J., Hamilton, D.P., David, B.O., Hicks, B.J., 2012. Carbon sources supporting large river food webs: a review of ecological theories and evidence from stable isotopes. *Fr. Rev.*, 5(2), 85–103.
- Pogoreutz, C., Ahnelt, H., 2014. Gut morphology and relative gut length do not reliably reflect trophic level in gobiids: a comparison of four species from a tropical Indo-Pacific seagrass bed. *J. Appl. Ichthyol.*, 30(2), 408–410.

- Polito, M.J., Reiss, C.S., Trivelpiece, W.Z., Patterson, W.P., Emslie, S.D., 2013. Stable isotopes identify an ontogenetic niche expansion in Antarctic krill (*Euphausia superba*) from the South Shetland Islands, Antarctica. *Mar. Biol.*, 160, 1311–1323.
- Post, D.M., 2002. Using stable isotopes to estimate trophic position: models, methods, and assumptions. *Ecology*, 83(3), 703–718.
- Qiu, D., Zhong, Y., Chen, Y., Tan, Y., Song, X., Huang, L., 2019. Short-term phytoplankton dynamics during typhoon season in and near the Pearl River Estuary, South China Sea. *J. Geophys. Res. Biogeosci.*, 124(2), 274–292.
- Qin, G., Xu, D., Lou, B., Chen, R., Wang, L., Tan, P., 2020. iTRAQ-based quantitative phosphoproteomics provides insights into the metabolic and physiological responses of a carnivorous marine fish (*Nibea albiflora*) fed a linseed oil-rich diet. *J. proteomics*, 228, 103917.
- Qu, P., Zhang, Z., Pang, M., Li, Z., Zhao, L., Zhou, X., Wang, W., Li, X., 2019. Stable isotope analysis of food sources sustaining the subtidal food web of the Yellow River estuary. *Ecol. Indic.*, 101, 303–312.
- Quan, W., Fu, C., Jin, B., Luo, Y., Li, B., Chen, J., Wu, J., 2007. Tidal marshes as energy sources for commercially important nektonic organisms: stable isotope analysis. *Mar. Ecol. Prog. Ser.*, 352, 89–99.
- Quan, W., Shi, L., Chen, Y., 2010. Stable isotopes in aquatic food web of an artificial lagoon in the Hangzhou Bay, China. *Chin. J. Oceanol. Limn.*, 28(3), 489–497.
- Quan, W.M., Humphries, A.T., Shi, L.Y., Chen, Y.Q., 2012. Determination of trophic transfer at a created intertidal oyster (*Crassostrea ariakensis*) reef in the Yangtze River estuary using stable isotope analyses. *Estuar. Coast.*, 35(1), 109–120.
- Huovinen, P., 2020. Antarctic seaweeds: diversity, adaptation and ecosystem services. I. Gómez, & P. Huovinen (Eds.). Cham: Springer International Publishing.
- Ramirez, M.D., Besser, A.C., Newsome, S.D., McMahon, K.W., 2021. Meta-analysis of primary producer amino acid $\delta^{15}\text{N}$ values and their influence on trophic position estimation. *Methods Ecol. Evol.*, 12(10), 1750–1767.
- Ravi, V., 2013. Food and feeding habits of the mudskipper, *Boleophthalmus boddarti* (Pallas, 1770) from Pichavaram mangroves, southeast coast of India. *Int. J. Mar. Sci.*, 3(12).
- Ray, G.C., 1991. Coastal-zone biodiversity patterns. *Bioscience*, 41(7), 490–498.
- Reven, J., 1982. Inorganic C-source for Lemanea, Cladophora and Ranunculus in a fast-flowing stream: Measurements of gas exchange and of carbon isotope ratio and their ecological implications. *Oecologia*, 53, 66–78.
- Riccialdelli, L., Newsome, S.D., Fogel, M.L., Fernández, D.A., 2017. Trophic interactions and food web structure of a subantarctic marine food web in the Beagle Channel: Bahía Lapataia, Argentina. *Polar Biol.*, 40, 807–821.

Riera, P., Richard, P., Gremare, A., Blanchard, G., 1996. Food source of intertidal nematodes in the bay of Marennes–Oleron (France), as determined by dual stable isotope analysis. *Mar. Ecol. Prog. Ser.*, 142, 303–309.

Riera, P., Stal, L.J., Nieuwenhuize, J., Richard, P., Blanchard, G., Gentil, F., 1999. Determination of food sources for benthic invertebrates in a salt marsh (Aiguillon Bay, France) by carbon and nitrogen stable isotopes: importance of locally produced sources. *Mar. Ecol. Prog. Ser.*, 187, 301–307.

Rossi, L., Sporta Caputi, S., Calizza, E., Careddu, G., Oliverio, M., Schiaparelli, S., Costantini, M.L., 2019. Antarctic food web architecture under varying dynamics of sea ice cover. *Sci. Rep.*, 9(1), 12454.

Rumolo, P., Zappes, I.A., Fabiani, A., Barra, M., Rakaj, A., Palozzi, R., Allegrucci, G., 2020. The diet of Weddell seals (*Leptonychotes weddellii*) in Terra Nova Bay using stable isotope analysis. *Europe. Zool. J.*, 87(1), 94–104.

Ryu, J., Khim, J. S., Choi, J. W., Shin, H. C., An, S., Park, J., Kang, D., Lee, C.-H., Koh, C. H., 2011. Environmentally associated spatial changes of a macrozoobenthic community in the Saemangeum tidal flat, Korea. *J. Sea Res.*, 65(4), 390–400.

Ryu, J., Kim, H.C., Khim, J.S., Kim, Y.H., Park, J., Kang, D., Hwang, J. H., Lee, C.-H., Koh, C.H., 2011. Prediction of macrozoobenthic species distribution in the Korean Saemangeum tidal flat based on a logistic regression model of environmental parameters. *Ecol. Res.*, 26, 659–668.

Ryu, J., Nam, J., Park, J., Kwon, B.O., Lee, J.H., Song, S.J., Hong, S.J., Chang, W.K., Khim, J.S., 2014. The Saemangeum tidal flat: long-term environmental and ecological changes in marine benthic flora and fauna in relation to the embankment. *Ocean Coast. Manage.*, 102, 559–571.

Sabo, J.L., Caron, M., Doucett, R., Dibble, K.L., Ruhi, A., Marks, J.C., Hungate, B.A., Kennedy, T.A., 2017. Pulsed flows, tributary inputs and food-web structure in a highly regulated river. *J. Appl. Ecol.*, 55(4), 1884–1895.

Saout, C., 2000. Contrôle de la reproduction chez *Pecten Maximus* (L.) (études in situ et expérimentales). Université de Bretagne Occidentale, 1, 143–152.

Sahade, R., Lagger, C., Torre, L., Momo, F., Monien, P., Schloss, I., Barnes, D.K., Servetto, N., Tarantelli, S., Tatian, M., Zamboni, N., Abele, D., 2015. Climate change and glacier retreat drive shifts in an Antarctic benthic ecosystem. *Sci. Adv.*, 1(10), e1500050.

Sato, S.I., Hong, J.S., Kim, S.H., 2019. Macrobenthic faunal change after dike construction in Saemangeum Lake, South Korea, with special emphasis on mollusks. *Plankton and Benthos Res.*, 14(4), 251–260.

Schloss, I.R., Ferreyra, G.A., 2002. Primary production, light and vertical mixing in Potter Cove, a shallow bay in the maritime Antarctic. *Polar Biol.*, 25, 41–48.

Seyboth, E., Botta, S., Mendes, C.R.B., Negrete, J., Dalla Rosa, L., Secchi, E.R., 2018. Isotopic evidence of the effect of warming on the northern Antarctic Peninsula ecosystem. *Deep Sea Res. Pt. II Top. Stud. Oceanogr.*, 149, 218–228.

- Shang, X., Zhang, G.S., Zhange, Z., 2008. Relative importance of vascular plants and algal production in the food web of *Spartina*-invaded salt marsh in the Yangtze River estuary. *Mar. Ecol. Prog. Ser.*, 367, 93–107.
- Shi, Y., Zhang, Y., Du, Y., Kong, D., Wu, Q., Hong, Y., Wang, Y., Tam, N.F.Y., Leung, J., 2020. Occurrence, composition and biological risk of organophosphate esters (OPEs) in water of the Pearl River Estuary, South China. *Environ. Sci. Pollut. Res.*, 27(13), 14852–14862.
- Signa, G., Calizza, E., Costantini, M.L., Tramati, C., Caputi, S.S., Mazzola, A., Rossi, L., Vizzini, S., 2019. Horizontal and vertical food web structure drives trace element trophic transfer in Terra Nova Bay, Antarctica. *Environ. Pollut.*, 246, 772–781.
- Silliman, B.R., Grosholz, T., Bertness, M.D., 2009. Salt marshes under global siege. 391–398. University of California Press: Berkeley, CA, USA.
- Simbora, N., A. Zenetus, P. Panayotides, A. Makra., 1995. Changes in benthic community structure along an environmental pollution gradient. *Mar. Pollut. Bull.*, 30, 470–474.
- Stevens, D.W., Dunn, M.R., Pinkerton, M.H., Forman, J.S., 2014. Diet of Antarctic toothfish (*Dissostichus mawsoni*) from the continental slope and oceanic features of the Ross Sea region, Antarctica. *Antarct. Sci.*, 26(5), 502–512.
- Stirling, I., Derocher, A.E., 1993. Possible impacts of climatic warming on polar bears. *Arctic.*, 46, 240–245.
- Stuecker, M.F., Bitz, C.M., Armour, K.C., 2017. Conditions leading to the unprecedented low Antarctic Sea ice extent during the 2016 austral spring season. *Geophys. Res. Lett.*, 44(17), 9008–9019.
- Suh, Y.J., Shin, K.H., 2013. Size-related and seasonal diet of the manila clam (*Ruditapes philippinarum*), as determined using dual stable isotopes. *Estuar., Coast. Shelf Sci.*, 135, 94–105.
- Sun, M.-Y., Lee, C., Aller, R.C., 1993. Anoxic and oxic degradation of ^{14}C -labeled chloropigments and a ^{14}C -labeled diatom in Long Island Sound sediments. *Limnol. Oceanogr.*, 38, 1438–1451.
- Tanaka, H., Aoki, I., Ohshimo, S., 2006. Feeding habits and gill raker morphology of three planktivorous pelagic fish species off the coast of northern and western Kyushu in summer. *J. Fish Biol.*, 68(4), 1041–1061.
- Teal, J.M., 1962. Energy flow in the salt marsh ecosystem of Georgia. *Ecology*, 43, 614–624.
- Teoh, H.W., Sasekumar, A., Ismail, M.H., Chong, V.C., 2018. Trophic discrimination factor and the significance of mangrove litter to benthic detritivorous gastropod, *Ellobium aurisjudae* (Linnaeus). *J. Sea Res.*, 131, 79–84.
- Tian, S., Zhu, L., Liu, M., 2010. Bioaccumulation and distribution of polybrominated diphenyl ethers in marine species from Bohai Bay, China. *Environ. Toxicol. Chem.*, 29(10), 2278–2285.

- Tieszen, L.L., Boutton, T.W., Tesdahl, K.G., Slade, N.A., 1983. Fractionation and turn-over of stable carbon isotopes in animal tissues: implications for $\delta^{13}\text{C}$ analysis of diet. *Oecologia*, 57, 32–37.
- Then, A.Y.H., Adame, M.F., Fry, B., Chong, V.C., Riekenberg, P.M., Mohammad Zakaria, R., Lee, S.Y., 2020. Stable isotopes clearly track mangrove inputs and food web changes along a reforestation gradient. *Ecosystems*, 24(4), 939–954.
- Thompson, D.R., Phillips, R.A., Stewart, F.M., Waldron, S., 2000. Low $\delta^{13}\text{C}$ signatures in pelagic seabirds: lipid ingestion as a potential source of ^{13}C -depleted carbon in the procellariiformes. *Mar. Ecol. Prog. Ser.*, 208, 265–271.
- Thurber, A.R., 2007. Diets of Antarctic sponges: links between the pelagic microbial loop and benthic metazoan food web. *Mar. Ecol. Prog. Ser.*, 351, 77–89.
- Unabia, C.R.C., 1996. Radular structure in the gastropod order Neritopsina: a source of phylogenetic information. University of Hawai'i at Manoa. (Dissertation, Ph.D. Thesis), 274.
- Underwood, A.J., 1978. An experimental evaluation of competition between three species of intertidal prosobranch gastropods. *Oecologia*, 33, 185–202.
- Underwood, G.J.C., Kromkamp, J., 1999. Primary production by phytoplankton and microphytobenthos in estuaries. *Estuaries*, 29, 93–139.
- UNEP [United Nations Environment Programme], 2006. Marine and coastal ecosystems and human wellbeing: a synthesis report based on the findings of the millennium ecosystem assessment. UNEP, Nairobi, Kenya.
- Valiela, I., J.L. Bowen, and J.K. York., 2001. Mangrove forests: one of the world's threatened major tropical environments. *BioScience*, 51:807–815.
- Vander Zanden, M.J., Rasmussen, J.B., 1999. Primary consumer $\delta^{13}\text{C}$ and $\delta^{15}\text{N}$ and the trophic position of aquatic consumers. *Ecology*, 80, 1395–1404.
- Van Hespén, R., Hu, Z., Peng, Y., Borsje, B. W., Kleinhans, M., Ysebaert, T., Bouma, T.J., 2021. Analysis of coastal storm damage resistance in successional mangrove species. *Limnol. Oceanogr.*, 66(8), 3221–3236.
- Vernet, M., Martinson, D., Iannuzzi, R., Stammerjohn, S., Kozłowski, W., Sines, K., Smith, R., Garibotti, I., 2008. Primary production within the sea-ice zone west of the Antarctic Peninsula: I-Sea ice, summer mixed layer, and irradiance. *Deep Sea Res. Pt. II Top. Stud. Oceanogr.*, 55(18–19), 2068–2085.
- Viswanathan, C., Raffi, S.M., 2015. The natural diet of the mud crab *Scylla olivacea* (Herbst, 1896) in Pichavaram mangroves, India. *Saudi J. Biol. Sci.*, 22(6), 698–705.
- Voss, M., Larsen, B., Leivuori, M., Vallius, H., 2000. Stable isotope signals of eutrophication in Baltic Sea sediments. *J. Mar. Syst.*, 25(3–4), 287–298.
- Wada, E., Terazaki, M., Kabaya, Y., Nemoto, T., 1987. ^{15}N and ^{13}C abundances in the Antarctic Ocean with emphasis on the biogeochemical structure of the food web. *Deep Sea Res. Pt. I Oceanogr. Res. Pap.*, 34(5–6), 829–841.

- Wang, D., Yao, L., Yu, J., Chen, P., Hu, R., 2021. Response to Environmental Factors of Spawning Ground in the Pearl River Estuary, China. *J. Mar. Sci. Eng.*, 9(7), 763.
- Wang, G., Hendon, H.H., Arblaster, J.M., Lim, E.P., Abhik, S., Van Rensch, P., 2019. Compounding tropical and stratospheric forcing of the record low Antarctic sea-ice in 2016. *Nat. Commun.*, 10(1), 13.
- Wang, H., Peng, Y., Wang, C., Wen, Q., Xu, J., Hu, Z., Jia, X., Zhao, X., Lian, W., Temmerman, S., Wolf, J., Bouma, T., 2021. Mangrove loss and gain in a densely populated urban estuary: lessons from the Guangdong–Hong Kong–Macao Greater Bay Area. *Front. Mar. Sci.*, 8, 693450.
- Wang, S., Chu, T., Huang, D., Li, B., Wu, J., 2014. Incorporation of exotic *Spartina alterniflora* into diet of deposit-feeding snails in the Yangtze river estuary salt marsh: stable isotope and fatty acid analyses. *Ecosystems*, 17(4), 567–577.
- Wang, S., He, Q., Zhang, Y., Sheng, Q., Li, B., Wu, J., 2021. Habitat-dependent impacts of exotic plant invasions on benthic food webs in a coastal wetland. *Limnol. Oceanogr.*, 66(4), 1256–1267.
- Wang, S., Jin, B., Qin, H., Sheng, Q., Wu, J., 2015. Trophic dynamics of filter feeding bivalves in the Yangtze estuarine intertidal marsh: Stable isotope and fatty acid analyses. *PloS One*, 10(8), e0135604.
- Wang, S., Zhu, G., Peng, Y., Jetten, M. S., Yin, C., 2012. Anammox bacterial abundance, activity, and contribution in riparian sediments of the Pearl River estuary. *Environ. Sci. Technol.*, 46(16), 8834–8842.
- Wang, W., Fu, H., Lee, S.Y., Fan, H., Wang, M., 2020. Can strict protection stop the decline of mangrove ecosystems in China? From rapid destruction to rampant degradation. *Forests*, 11(1), 55.
- Wang, Y., Liu, D., Richard, P., Li, X., 2013. A geochemical record of environmental changes in sediments from Sishili Bay, northern Yellow Sea, China: anthropogenic influence on organic matter sources and composition over the last 100 years. *Mar. Pollut. Bull.*, 77 (1–2), 227–236.
- Wang, Z., Tang, D., Shen, C., Wu, L., 2022. Identification of genes involved in digestion from transcriptome of *parasesarma pictum* and *parasesarma affine* hepatopancreas. *Thalassas: Intl. J. Mar. Sci.*, 38(1), 93–101.
- Way, C.M., Hornbach, D.J., Miller–Way, C.A., Payne, B.S., Miller, A.C., 1990. Dynamics of filter feeding in *Corbicula fluminea* (Bivalvia: Corbiculidae). *Can. J. Zool.*, 68(1), 115–120.
- Waycott, M., Duarte, C.M., Carruthers, T.J., Orth, R.J., Dennison, W.C., Olyarnik, S., Calladine, A., Fourqurean, J.W., Heck, K.L., Hughes, A.R., Kendrick, G.A., Kenworthy, W.J., Short, F.T., Williams, S.L., 2009. Accelerating loss of seagrasses across the globe threatens coastal ecosystems. *Proc. Natl. Acad. Sci.*, 106(30), 12377–12381.
- Winder, M., Schindler, D.E., 2004. Climate change uncouples trophic interactions in an aquatic ecosystem. *Ecology*, 85(8), 2100–2106.

Wing, S.R., McLeod, R.J., Leichter, J.J., Frew, R.D., Lamare, M.D., 2012. Sea ice microbial production supports Ross Sea benthic communities: influence of a small but stable subsidy. *Ecology*, 93(2), 314–323.

Wong, K.J., Shih, H.T., Chan, B.K., 2012. The ghost crab *Ocypode mortoni* George, 1982 (Crustacea: Decapoda: Ocypodidae): redescription, distribution at its type locality, and the phylogeny of East Asian Ocypode species. *Zootaxa*, 3550(1), 71–87.

Woo, H.J., Je, J.-G., 2002. Changes of sedimentary environments in the southern tidal flat of Ganghwa Island. *Ocean Polar Res.*, 24, 331–343.

Worm, B., Barbier, E.B., Beaumont, N., Duffy, J.E., Folke, C., Halpern, B.S., Jackson, J.B., Lotze, H.K., Micheli, F., Palumbi, S.R., Sala, E., Selkoe, K.A., Stachowicz, J.J., Watson, R., 2006. Impacts of biodiversity loss on ocean ecosystem services. *Science*, 314(5800), 787–790.

Wright, S.W., van den Enden, R.L., Pearce, I., Davidson, A.T., Scott, F.J., Westwood, K.J., 2010. Phytoplankton community structure and stocks in the Southern Ocean (30–80 E) determined by CHEMTAX analysis of HPLC pigment signatures. *Deep Sea Res. Pt. II Top. Stud. Oceanogr.*, 57(9–10), 758–778.

Xie, J., Pei, N., Sun, Y., Chen, Z., Cheng, Y., Chen, L., Xie, C., Dai, S., Zhu, C., Luo, X., Zhang, L., Mai, B., 2022. Bioaccumulation and translocation of organophosphate esters in a Mangrove Nature Reserve from the Pearl River Estuary, South China. *J. Hazard. Mater.*, 427, 127909.

Xu, W.Z., Cheung, S.G., Zhang, Z.N., Shin, P.K., 2018. Dual isotope assessment of trophic dynamics of an intertidal infaunal community with seasonal shifts in food sources. *Mar. Biol.*, 165(1), 1–13.

Xu, W., Dang, Y., Cheung, S.G., Zhang, Z., Sun, J., Teng, A., Shin, P.K., 2021. Stable isotope tracer addition reveals trophic status of benthic infauna at an intertidal area adjacent to a seagrass bed. *Front. Mar. Sci.*, 1443.

Xuan, Y., Tang, C., Liu, G., Cao, Y., 2020. Carbon and nitrogen isotopic records of effects of urbanization and hydrology on particulate and sedimentary organic matter in the highly urbanized Pearl River Delta, China. *J. Hydrol.*, 591, 125565.

Yan, M., Chen, X., Chu, W., Li, W., Li, M., Cai, Z., Gong, H., 2022. Microplastic pollution and enrichment of distinct microbiota in sediment of mangrove in Zhujiang River estuary, China. *J. Oceanol. Limnol.*, 1–14.

Yang, G., Li, C., Guilini, K., Peng, Q., Wang, Y., Zhang, Y., Zhang, Y., 2016. Feeding strategies of four dominant copepod species in Prydz Bay, Antarctica: insights from a combined fatty acid biomarker and stable isotopic approach. *Deep Sea Res. Pt. I Oceanogr. Res. Pap.*, 114, 55–63.

Yang, S., Tang, M., Yim, W.W.S., Zong, Y., Huang, G., Switzer, A.D., Saito, Y., 2011. Burial of organic carbon in Holocene sediments of the Zhujiang (Pearl River) and Changjiang (Yangtze River) estuaries. *Mar. Chem.*, 123, 1–10.

Yen, J., 1991. Predatory feeding behavior of an Antarctic marine copepod, *Euchaeta antarctica*. *Polar Res.*, 10, 433–442.

Yoon, S.J., Hong, S., Kwon, B.O., Ryu, J., Lee, C.H., Nam, J., Khim, J.S., 2017. Distributions of persistent organic contaminants in sediments and their potential impact on macrobenthic faunal community of the Geum River Estuary and Saemangeum Coast, Korea. *Chemosphere*, 173, 216–226.

Yu, F., Zong, Y., Lloyd, J.M., Huang, G., Leng, M.J., Kendrick, C., Lamb, A.L., Yim, W.W.S., 2010. Bulk organic $\delta^{13}\text{C}$ and C/N as indicators for sediment sources in the Pearl River delta and estuary, southern China. *Estuar. Coast. Shelf S.*, 87(4), 618–630.

Zenteno, L., Cárdenas, L., Valdivia, N., Gómez, I., Höfer, J., Garrido, I., Pardo, L.M., 2019. Unraveling the multiple bottom-up supplies of an Antarctic nearshore benthic community. *Prog. Oceanogr.*, 174, 55–63.

Zhang, H., Chen, Y., Li, D., Yang, C., Zhou, Y., Wang, X., Zhang, Z., 2021. PAH residue and consumption risk assessment in four commonly consumed wild marine fishes from Zhoushan Archipelago, East China Sea. *Mar. Pollut. Bull.*, 170, 112670.

Zhang, L., Wang, L., Yin, K., Lü, Y., Yang, Y., Huang, X., 2014. Spatial and seasonal variations of nutrients in sediment profiles and their sediment–water fluxes in the Pearl River Estuary, Southern China. *J. Earth Sci.*, 25(1), 197–206.

Zhang, T., Hu, S., He, Y., You, S., Yang, X., Gan, Y., Liu, A., 2021. A fine-scale mangrove map of China derived from 2-meter resolution satellite observations and field data. *ISPRS Int. Geo-Inf.*, 10(2), 92.

Zhang, Y.E., Li, C., Yang, G., Wang, Y., Tao, Z., Zhang, Y., Wang, A., 2017. Ontogenetic diet shift in Antarctic krill (*Euphausia superba*) in the Prydz Bay: a stable isotope analysis. *Acta Oceanol. Sin.*, 36, 67–78.

Zhang, Z., Wang, Y., Zhu, Y., He, K., Li, T., Mishra, U., Peng, Y., Wang, F., Yu, L., Zhao, X., Zhu, L., Zhu, X., Qin, Z., 2022. Carbon sequestration in soil and biomass under native and non-native mangrove ecosystems. *Plant Soil*, 1–16.

Zhang, Z.W., Sun, Y.X., Sun, K.F., Xu, X.R., Yu, S., Zheng, T.L., Luo, X.J., Tian, Y., Hu, Y.X., Diao, Z.H., Mai, B.X., 2015. Brominated flame retardants in mangrove sediments of the Pearl River Estuary, South China: spatial distribution, temporal trend and mass inventory. *Chemosphere*, 123, 26–32.

Zhou, Q., Tu, C., Fu, C., Li, Y., Zhang, H., Xiong, K., Zhao, X., Li, L., Waniek, J.J., Luo, Y., 2020. Characteristics and distribution of microplastics in the coastal mangrove sediments of China. *Sci. Total Environ.*, 703, 134807.

Zhou, T., Liu, S., Feng, Z., Liu, G., Gan, Q., Peng, S., 2015. Use of exotic plants to control *Spartina alterniflora* invasion and promote mangrove restoration. *Sci. Rep.*, 5(1), 1–13.

Zhou, Z., Zhang, G.X., Xu, Y.B., Gu, J.D., 2018. Successive transitory distribution of Thaumarchaeota and partitioned distribution of Bathyarchaeota from the Pearl River estuary to the northern South China Sea. *Appl. Microbiol. Biotechnol.*, 102(18), 8035–8048.

Zuo, L., Sun, Y., Li, H., Hu, Y., Lin, L., Peng, J., Xu, X., 2020. Microplastics in mangrove sediments of the Pearl River Estuary, South China: Correlation with halogenated flame retardants' levels. *Sci. Total Environ.*, 725, 138344.

ABSTRACT (IN KOREAN)

연안에 집중된 인간 활동은 생태학적 가치가 높은 다양한 연안 서식지 환경을 변화시키고 기능을 감소시켰다. 그러나, 다양한 요인에 의해 발생된 연안 서식지 환경 변화에 대한 생물들의 생태학적 반응 연구는 여전히 부족한 실정이다. 서식지 환경 변화가 연안 생물에게 미치는 생태학적 영향은 연안 먹이망 구조와 기능의 평가를 통해 확인할 수 있다. 따라서 연안 먹이망 구조와 기능 연구는 생태학적 가치가 높은 다양한 연안 서식지의 보존과 관리에 사용될 수 있다. 본 연구는 탄소 및 질소 안정동위원소비 분석을 기반으로 한국 염습지 갯벌, 남중국 맹그로브 숲, 남극 연안에서 다양한 요인(퇴적물 특성, 식생 분포, 댐 방류수 영향, 빙하 및 해빙의 분포 변화)에 따른 시·공간적 서식지 환경 변화에 대해 먹이망 구조와 기능의 변화를 평가하였다. 본 연구의 목적은 1) 생태학적 가치가 높은 연안 서식지의 먹이망 구조와 기능을 밝히고, 2) 연안 서식지 환경 변화에 대한 생물의 시·공간적 생태 반응을 평가하는 것이다. 또한, 3) 연안 서식지에서 관찰된 탄소 및 질소 안정동위원소비 자료를 비교해 기후대별 연안 먹이망의 특성(먹이원 다양성 및 인위적 활동의 영향 정도)을 규명하는 것에 있다.

온대지역의 한국 염습지 갯벌과 열대지역의 남중국 맹그로브 숲은 지난 세기 동안 진행된 간척 사업으로 심각하게 훼손되었다. 따라서, 효율적인 연안 서식지 보존 관리를 위해 먹이망 구조와 기능에 대한 연구는 필수적이다. 이를 위해 한국의 대표적인 강화도 염습지에서 연구가 먼저 진행되었다. 강화도 염습지에 서식하는 저서생물의 탄소 안정동위원소비는 퇴적물 니질함량과 우점 염생식물(갈대, 칠면초)의 분포에 영향을 받는 것으로 나타났다. 퇴적물식자는 비식생 갯벌에서 저서미세조류 섭취가 증가했고, 염생식물 서식지에서는 ^{13}C 함량이 적은 유기물 섭취가 증가했다. 결과적으로, 서식지 환경의 특성(퇴적물 또는 염생식물)별로 다양한 유기물 분포가 한국 갯벌 먹이망 내 국소적 영양 흐름 변화를 야기함을 확인하였다. 세계 최장 방조제가 위치한 한국 새만금 갯벌에서는 방조제 배수갑문을 통해 배출되는 부영양 하수가 시·공간적 먹이망 역학에 미치는 영향을 확인하였다. 부영양 방류수 배출은 외측 갯벌 수·저층 환경의 영양염과 유기입자의 질소안정동위원소비 분포에 영향을 미쳤다. 이에 따라 배수갑문 근처 증가된 총질소 농도는 저서미세조류의 생물량 증가를 야기했으며, 저서생물의 저서미세조류 활용을 증가시켰다. 본 결과를 통해 인간

활동에 의한 환경 변화가 갯벌 먹이망 구조와 기능 변화에 영향을 준다는 것을 확인했다. 열대 지역 맹그로브 생태계 보전 및 관리를 위해 주장 하구에서 맹그로브 숲의 먹이망 구조와 기능을 평가한 결과, 우기에 주장 하구에서 서식하는 어류의 영양 지위가 증가하는 것을 확인했다. 저서동물은 모든 계절에 지속적으로 좁은 영양 지위를 나타냈다. 두 소비자는 모두 계절에 따른 먹이원 활용 변화를 나타냈으며, 건기에 맹그로브 및 염생식물 기원의 유기물 활용이 증가했고, 우기에 수층 입자의 활용이 증가했다. 문헌 비교 결과 주장 하구 먹이망은 중국의 다른 염습지에 비해 가벼운 탄소 및 무거운 질소 안정 동위원소비 분포 특징을 보여 맹그로브 유래 유기물과 대도시 하수의 유입이 많다는 것을 확인하였다.

남극 연안 생태계는 기후변화에 따른 다양한 변화를 겪고 있으며, 특히 장기간에 걸쳐 나타나는 빙하와 해빙의 변화가 먹이망 역학에 미치는 영향은 대부분 파악되지 않은 실정이다. 따라서, 지구온난화에 따른 빙하 후퇴가 가장 심각한 남극 반도에 위치한 마리안 소만에서 먹이망 영양역학을 평가하였다. 마리안 소만 빙벽으로부터 거리에 따른 5개 정점에서 저서 및 표영성 소비자와 먹이원을 채집하였다. 빙벽 근처에서 먹이원부터 소비자까지 무겁게 나타난 탄소 안정동위원소비는 마리안 소만 환경이 빙벽과의 거리에 따라 이질성을 가진다는 것을 보여주었다. 또한, 마리안 소만 삿갓조개의 현재 먹이원 활용을 10년 전과 비교한 결과, 주요 먹이원이 저서미세조류에서 해조류로 변화함을 확인하였다. 문헌 비교 결과 서·동남극 연안에서 10년 이상 장기간 나타난 해빙 면적 감소 및 증가가 두 지역의 대조적인 먹이망 영양역학 변화를 만드는 것을 확인하였다. 따라서, 남극 연안 먹이원의 다양성 감소는 계속되는 기후 변화 상황에서 남극 해양생태계 전체에 위협을 가할 수 있음을 시사하였다.

기후대별 주요 연안 서식지 환경 변화에 대해 먹이망 내 저서 및 표영성 생물의 생태학적 반응(먹이원 활용 및 생태적 지위)을 종합 평가하였다. 열대 및 남극 연안 먹이망에서 관찰된 먹이원의 넓은 탄소 안정동위원소비 분포는 다양한 기원의 유기물이 유입되는 것을 확인시켜 주었으며, 이는 온대지역과 대조되는 특징을 보였다. 기후대별 연안 서식지 먹이망 구조 및 기능을 비교한 결과, 각 기후대에서 생산력이 높은 먹이원(식물플랑크톤, 저서미세조류, 맹그로브 등)이 연안 소비자의 먹이 활동에 크게 영향을 주는 것을 확인하였다. 반면, 각 연안 서식지 내에서는 계절적인 강우량 변화가 다른 요인(퇴적물 특성 및 식생의 분포 등)에 비해 생물의 먹이활동에 큰 영향을 주었다. 온대 및 열대

연안 서식지 먹이망에서 무겁게 (> 10 %) 관찰된 질소 안정동위원소비의 분포는 인간활동에 따른 하수 영향을 확인시켜 주었다. 반면 남극 먹이망은 가벼운 질소 안정동위원소비 분포를 보여, 남극 연안환경에서 인간활동 영향은 크지 않았다는 것을 확인시켜 주었다. 본 연구는 기후대별 다양한 연안 서식지 먹이망 영양역학의 변화 예측에 대한 통찰력을 제공하며 향후 연안 생태계 기반 관리 및 보존에 활용될 수 있음에 의의를 가진다.

주제어: 연안 먹이망, 탄소 및 질소 안정동위원소비 분석, 한국, 중국, 남극

학 번: 2018-30803